Imperial College of Science, Technology and Medicine
Faculty of Medicine
Department of Infectious Disease

Molecular mechanisms of antibiotic tolerance in mycobacteria

Andrea Majstorovic

Submitted in part fulfilment of the requirements for the degree of
Doctor of Philosophy in Clinical Medicine Research of the University of London and
the Diploma of Imperial College. This thesis is entirely my own work, and,
except where otherwise indicated, describes my own research

Abstract

Antimicrobial resistance (AMR) has emerged as a critical global health issue requiring comprehensive research to understand its underlying mechanisms and to provide potential mitigation strategies. AMR can manifest as either bacterial growth in the presence of an antibiotic, leading to an increase in the concentration of antibiotic required to inhibit bacterial growth (resistance), or as an ability of a subpopulation (persistence) or a whole population (tolerance) to transiently withstand otherwise lethal concentrations of a drug. Both tolerance and persistence complicate the treatment of many bacterial infections, including tuberculosis; they prolong treatment, lead to treatment failure and disease recurrence, and foster the emergence of resistance. Thus, targeting tolerant and persistent cells would improve treatment outcomes, yet the molecular mechanisms underlying tolerance and persistence remain elusive.

To study the mechanisms behind the development of tolerant and persistent mycobacteria, the Vaubourgeix laboratory developed a robust method to isolate mutants that display tolerance or high persistence. The lab applied this method to the non-pathogenic species *Mycobacterium smegmatis*, and isolated 30 mutants that displayed tolerance and/or high persistence upon exposure to kanamycin. My thesis consists of studying two of these mutants, which contain mutations related to a gene encoding the tRNA m^1A58 methyltransferase MsTrmI. I found that these *mstrmI* mutants display increased survival to aminoglycosides and resistance to macrolides because of a lack of tRNA A58 methylation and further tRNA degradation. I identified that both resistance and tolerance are mediated by increased expression of a transcriptional regulator *whiB7* and members of its regulon. Finally, I proposed a potential mechanism by which *whiB7* expression could be maintained during exposure to ribosome-inhibitory antibiotics despite the deployment of rescue mechanisms antagonistic to *whiB7* expression. Understanding bacterial resilience to exposure to antibiotics will have implications for developing new antibacterials to be combined with existing drugs. Such combinations would have the potential to shorten antibiotic treatment, curb the rate of infection relapse and prevent the emergence of resistance.

Acknowledgements

I would like to thank my supervisor, Dr Julien Vaubourgeix, for the opportunity to work on this project and for everything he taught me throughout the last four years. I am grateful for your support, always having your doors open to discuss the results (the good and the bad!), and for your guidance throughout my PhD.

I would like to thank Dr Hélène Botella, for always having time for me and all my many cloning questions. Thank you for your patience, your company and positivity, and all the chats and funny stories we shared while working in our lab and in the CL3 – it was so nice to work together. Finally, thank you for taking over the experiments during my writing-up stage.

I would like to extend my gratitude to Dr David Holden and Dr Peter Hill, for your help, kind and wise words, and motivation when I needed it the most. I have learned so much from you, and cannot wait to continue to do so during my next position! Special thank you also goes to Dr Sophie Helaine and Dr Teresa Thurston, for being such inspirations for me.

Thank you to everyone who helped and collaborated with me on this project: Dr Sarah Schrader, for establishing the ground of this project and all your feedback when things went south; Dr Teresa Cortez; Dr Kristine Arnvig - for teaching me the art of Northern blots; Dr Przemyslaw Plocinski for RNA- and small RNA-seq, Dr Sandra Wolin and Dr Xinguo Chen for your work on tRNA stability and charging - the project grew so much with all of your help. To all my students: Ruta Prakapaite, Enkai Jin, Beatrice Ward, Jason Taslim, Rugha Maniam, Jade Pizzato, and Zhaolin Lu - it was my pleasure teaching you all and thank you for sharing the lab bench with me.

To all the present and past members of the Thurston, Holden, and Helaine groups: my office neighbours Camilla Godlee and Magda Szczesna, Alison Heggie, Xiujun Yu, Mei Liu, Ada Aleksandrowicz, Romina Tocci, Mitchell Pallett, Lisa Blundell, Megan Winterbotham, Cullum Stones, Teresa Thurston, Ines Diaz del Olmo, Yizhou Huang, Paul O'Sullivan, Charlotte Michaux, Severin Ronneau, Alexander Hall, Gregorz Grabe, Ondrej Cerny, and many many students that visited us over the years. Thank you for making our floor such an amazing environment to work in, and for all your feedback and ideas. I will especially miss all the cakes and sweets in the usual space!

Thank you to the most amazing people who entered my life through this PhD - now all doctors Ioanna Panagi, Ana Laura Moldoveanu, Vivian Tounta, and Mery Shahin - you made everyday lab life so so much better and funnier. Thank you for all the lunches, Carpo walks, and wine nights. The friendships we got are very precious to me and your help was immense. Thank you to my friends, back in Croatia and here in London, for always being there for me: Ana, Sara, Tihana, Elena, Tena, Manos, Tatiana, Eleni, Liza, Despoina, Giorgos, Evripides, Vangelis, Konstantinos, Catrin, Ella, and Cordelia.

Most importantly, I would like to thank my family. My parents, Mara and Zeljko Majstorović, and my brother and sister Antonio and Ivana, for all of your support, empathy, numerous trips to the airport you did for me, and for always having your home (and phone) open for me. Finally, the dearest and biggest thank you goes to my partner Alex, and our cat Mochi, who both spent numerous nights next to me working on this thesis. Thank you, Alex, for sharing this big journey with me, for being my safe harbour, for always reminding me what we can achieve, and for always dreaming bigger dreams with me. This work is dedicated to you.

Statement of Originality

I hereby declare that the work presented in this thesis is my own original work. Any work produced by collaborators or other's published or unpublished work shown here is fully recognized in the text, acknowledgments, or references.

Copyright Declaration

"The copyright of this thesis rests with the author. Unless otherwise indicated, its contents are licensed under a Creative Commons Attribution-Non Commercial 4.0 International Licence (CC BY-NC).

Under this licence, you may copy and redistribute the material in any medium or format. You may also create and distribute modified versions of the work. This is on the condition that: you credit the author and do not use it, or any derivative works, for a commercial purpose.

When reusing or sharing this work, ensure you make the licence terms clear to others by naming the licence and linking to the licence text. Where a work has been adapted, you should indicate that the work has been changed and describe those changes.

Please seek permission from the copyright holder for uses of this work that are not included in this licence or permitted under UK Copyright Law."

List of Abbreviations

Table 1: Abbreviations

AMs	alveolar macrophages
ATc	anhydrotetracycline
bp	Base pair
DCs	dendritic cells
DOT	directly observed therapy
EF-Tu	elongation factor thermos unstable
Eis	enhanced intracellular survival protein
Erm	erythromycin ribosomal methylase
IGRA	interferon-γ release assays
KD	knock-down
KO	knock-out
LTBI	latent TB infection
MDR-TB	Multi-drug resistant tuberculosis
MIC	Minimum inhibitory concentration
Msm	*Mycobacterium smegmatis*
MsTrmI	*Msm* tRNA A58 methyltransferase
Mtb	*Mycobacterium tuberculosis*
MTBC	Mycobacterium tuberculosis complex
MtTrmI	*Mtb* tRNA A58 methyltransferase
MRSA	Methicillin-resistant *Staphylococcus aureus*
ncRNA	non-coding RNA
NP	native promoter
OD_{600}	Optical density at 600 nm
ORF	open reading frame
PNPase	polynucleotide phosphorylase
PTM	post-translational modification
qRT-PCR	Real-Time Quantitative Reverse Transcription PCR
RD1	Region of interest

ROS	Reactive oxygen species
RNS	Reactive nitrogen species
RR-TB	Rifampicin resistant tuberculosis
Rsr	Ro-sixty related protein
RYPER	Ro-60/Y RNA/PNPase exoribonuclease ribonucleoprotein
SAM	S-adenosyl-L-methionine
SmpB	Small protein B
SNP	single nucleotide polymorphism
sRNAs	small trans-acting regulatory RNAs
TB	Tuberculosis
TetON	Tetracycline-inducible regulator
TLRs	Toll-like receptors
tmRNA	Transfer messenger RNA
TrmI	tRNA A58 methyltransferase
tRNA	Transfer RNA
TSS	transcription start site
TST	Tuberculin skin test
uORF	upstream open reading frame
WHO	World Health Organisation
XDR-TB	Extreme drug resistant tuberculosis
YrlAB	Y RNA-like A and B

Contents

Abstract **2**

Acknowledgements **3**

1 Introduction **19**

1.1 Tuberculosis 20

1.1.1 Global impact of tuberculosis 21

1.1.2 Pathogenesis 23

1.1.3 Diagnosis of TB 27

1.1.4 Treatment of tuberculosis 28

1.2 Antibiotic resistance 32

1.2.1 MIC-shifted resistance, tolerance and persistence 33

1.2.2 Triggers of phenotypic tolerance to antibiotics 37

1.2.3 Genetic alterations leading to tolerance and high persistence 44

1.2.4 Persisters and tolerant cells are harbingers of MIC-shifted resistance . . 50

1.3 Motivation and Objectives 53

2 Results I: Loss of *mstrmI* causes antibiotic tolerance and resistance in *Mycobacterium smegmatis* 54

2.1 Introduction . . . 55

2.2 Results . . . 55

2.2.1 Two mutants recovered in the screen contain mutations related to a gene encoding a tRNA methyltransferase . . . 55

2.2.2 The *mstrmI* mutants display increased survival to the aminoglycoside kanamycin . . . 59

2.2.3 Expression of *mstrmI* in both mutants restores sensitivity to aminoglycosides . . . 61

2.2.4 The *mstrmI* mutants exhibit MIC-shifted resistance to macrolides . . . 64

2.2.5 AG mutant, but not GS, has a growth defect . . . 66

2.2.6 The effect of the A-to-G mutation on *mstrmI* transcripts . . . 68

2.2.7 The G128S mutation affects the protein abundance of MsTrmI . . . 69

2.2.8 $MsTrmI^{G128S}$ is not post-translationally modified . . . 73

2.3 Summary . . . 76

3 Results II: Deletion mutant of *mstrmI* presents with mutations in an exoribonuclease 77

3.1 Introduction . . . 78

3.2 Results . . . 78

3.2.1 Construction of the *mstrmI* deletion mutant . . . 78

3.2.2 Phenotypes of Δ*mstrmI*_C1 deletion mutant . . . 80

3.2.3 The mutation in a gene encoding a PNPase diminishes increased survival of the deletion mutant Δ*mstrmI*_C1 to aminoglycosides 84

3.2.4 The second clone, Δ*mstrmI*_C2, also bears a *pnpase*-related mutation . . 88

3.2.5 The 29 bp deletion in the *pnpase* upstream region decreases *pnpase* expression 90

3.2.6 Mtb *trmI* deletion mutant does not have an increased survival to gentamicin 91

3.3 Summary 93

4 Results III: The transcriptional regulator WhiB7 mediates the AMR phenotypes of the *mstrmI* mutants 94

4.1 Introduction 95

4.2 Results 96

4.2.1 The AG and GS mutants have increased levels of *whiB7* and members of the WhiB7 regulon 96

4.2.2 Deletion of *whiB7* or *eis* in the *mstrmI* mutants abolishes increased survival to aminoglycosides 99

4.2.3 Deletion of *whiB7* abolishes resistance phenotype to macrolides 101

4.2.4 What is the relationship between the loss of MsTrmI and the activation of *whiB7*? 104

4.2.5 MsTrmI methylates *Msm* tRNAs 105

4.2.6 The impact of the loss of m^1A58 modification on the abundance and charging of tRNAs 108

4.2.7 The *mstrmI* mutants have increased levels of Y RNA and Rsr 112

4.2.8 The role of trans-translation in increased survival of the *mstrmI* mutants 117

4.3 Summary 126

5 Discussion **128**

5.1 The transcriptional regulator WhiB7 mediates AMR phenotypes of the *mstrmI* mutants 129

5.2 Is *whiB7* insensitive to rescue by trans-translation? 131

5.3 MsTrmI methylates *Msm* tRNAs 133

5.4 Δ*mstrmI* presents with *pnpase* mutations 135

5.5 What is the relationship between Y RNA, Rsr, and hypomethylated tRNA? . . 137

5.6 Concluding remarks 137

6 Materials and Methods **139**

6.1 Bacterial strains and culture conditions 140

6.2 Plasmid construction 140

6.3 Knocking-out genes in mycobacteria 140

6.4 Filter-based method 142

6.5 Determination of minimum inhibitory concentration 142

6.6 Growth curves 143

6.7 Kanamycin kill curves 143

6.8 RNA extraction 144

6.9 RNA sequencing 144

6.10 Small RNA sequencing 145

6.11 qRT-PCR 145

6.12 WGS and single nucleotide polymorphism identification 146

6.13 CRISPRi 146

6.14 Flow cytometry 147

6.15 SYBR green RNA staining 147

6.16 Northern blotting 148

6.17 Co-immunoprecipitation (Co-IP)/Mass spectrometry 149

6.18 Western blot 150

6.19 Statistical analysis 150

References **151**

Appendix **188**

A Plasmids, primers, and strains used in this study 188

B *Mtb* clinical isolates harbour mutations in *mttrmI* 201

List of Tables

1 Abbreviations 7

3.1 Δ*mstrmI*_C1 strain contains two additional mutations 83

3.2 Δ*mstrmI*_C2 strain has 29 bp deletion 263 bp upstream of the *pnpase* start codon 88

3.3 SNPs identified in the Δ*mttrmI* strain 92

4.1 List of genes that belong to the *whiB7* regulon and their expression levels in the WT *Msm*, AG and GS mutants, and the AG::NP *mstrmI* strains. 98

6.1 Primers used in this study 188

6.2 Bacterial strains used in this study. 196

6.3 Plasmids used in this study 199

List of Figures

1.1 Incidence of tuberculosis (TB) per 100,000 people in 2022 21

1.2 Top causes of death worldwide in 2019 based on WHO. 22

1.3 WHO End TB Strategy 2025 milestones 23

1.4 *Mtb* infection 26

1.5 Antibiotics used to treat tuberculosis and their mode of action 29

1.6 Types of AMR. 34

2.1 Experimental setup of the filter-based method to evaluate the fraction of survivors 57

2.2 Two mutants isolated in the screen contained mutations related to a tRNA A58 methyltransferase *mstrmI*. 58

2.3 The *mstrmI* mutants display increased survival upon exposure to aminoglycosides kanamycin, amikacin, and gentamicin 60

2.4 The *mstrmI* mutants display decreased killing to kanamycin in liquid media . . 61

2.5 The expression of *mstrmI* in both mutants restores WT sensitivity to aminoglycosides 63

2.6 Minimum inhibitory concentrations of *Msm* AG and GS mutants 65

2.7 *mstrmI* mutants exhibit MIC-shifted resistance to macrolides 66

2.8 Characterization of the growth rate of *mstrmI* mutants in 7H9 media 67

2.9 A-to-G mutation, but not G128S, strongly reduces *mstrmI* transcription 68

2.10 G128 residue of MsTrmI is predicted to be on the protein surface. 69

2.11 Expression of G128S *mstrmI* complements the increased survival phenotype of AG and GS mutants 70

2.12 G128S mutation affects the stability of MsTrmI 72

2.13 Confirmation of expression of different *mstrmI* G128 mutants. 74

2.14 Expressing 128A, but not 128D *mstrmI*, diminishes the increased survival phenotype of *mstrmI*-related mutants 75

3.1 The process of generating and curing a knockout of *mstrmI* 80

3.2 Δ*mstrmI*_C1 does not phenocopy the increased survival phenotype of *mstrmI* mutants 81

3.3 A time-kill curve of Δ*mstrmI*_C1 deletion mutant to kanamycin in liquid 82

3.4 The *pnpase* mutation decreases the survival of the Δ*mstrmI*_C1 deletion mutant 85

3.5 The deletion mutant Δ*mstrmI*_*pnpase*^{A167D} phenocopies both isolated tRNA methyltransferase mutants when a wild-type copy of the *pnpase* is expressed. . . 86

3.6 Minimum inhibitory concentrations of Δ*mstrmI*_*pnpase*^{A167D}, Δ*mstrmI*_*pnpase*^{A167D}::NP *pnpase*, and Δ*mstrmI*_*pnpase*^{A167D}::NP *pnpase*::NP *mstrmI* strains. 87

3.7 A 29 bp deletion upstream of the *pnpase* mutation decreases the survival of the Δ*mstrmI*_C2 deletion mutant 89

3.8 The 29 bp deletion 263 bp upstream of *pnpase* affects the *pnpase* transcript levels. 91

3.9 The survival of the WT *Mtb*, Δ*mttrmI* and complemented strain upon exposure to gentamicin. 92

4.1 *mstrmI* mutants have increased levels of the transcriptional regulator *whiB7* and members of its regulon 97

4.2 The level of *whiB7* in the AG mutant measured by a fluorescent reporter. 99

4.3 *whiB7* and *eis* mediate increased survival of *mstrmI* mutants to kanamycin. . . 100

4.4 WhiB7 mediates increased survival of the AG mutant to the aminoglycosides amikacin and gentamicin. 101

4.5 *whiB7* mediates MIC-shifted resistance to macrolides in the *mstrmI* mutants . . 103

4.6 *whiB7* expression is regulated via the translation rate of an open reading frame upstream of *whiB7*. 104

4.7 Analysis of tRNA A58 methylation status in *mstrmI* AG and deletion mutants. 107

4.8 SYBR-gold staining of tRNA upon rifampicin treatment 109

4.9 Loss of the A58 methylation affects tRNA levels and gel mobility. 111

4.10 *mstrmI* mutants contain increased levels of *rsr* and *yrlAB*, components of the degradation machinery RYPER 113

4.11 A schematic of the RYPER machinery. 114

4.12 YrlAB and Rsr are not essential for mediating the increased survival of the AG mutant upon exposure to kanamycin. 116

4.13 The *whiB7* uORF peptide contains a high percentage of alanine residues. 118

4.14 Trans-translation is an alanine-demanding process that resolves stalled ribosomes.119

4.15 Fail-safe rescue mechanism model from proteotoxic stress 120

4.16 Knocking down trans-translation abolishes increased survival of the *mstrmI* mutants 122

4.17 Alignment of mutated uORF of *whiB7* used in this study 124

4.18 Mutating GCC codons of the uORF of *whiB7* abolishes the increased survival of the AG mutant. 124

6.1 Mutations in *mttrmI* are found in *Mtb* clinical isolates. 201

Chapter 1

Introduction

Contents

1.1 Tuberculosis 20

1.1.1 Global impact of tuberculosis 21

1.1.2 Pathogenesis 23

1.1.3 Diagnosis of TB 27

1.1.4 Treatment of tuberculosis 28

1.2 Antibiotic resistance 32

1.2.1 MIC-shifted resistance, tolerance and persistence 33

1.2.2 Triggers of phenotypic tolerance to antibiotics 37

1.2.3 Genetic alterations leading to tolerance and high persistence 44

1.2.4 Persisters and tolerant cells are harbingers of MIC-shifted resistance . 50

1.3 Motivation and Objectives 53

1.1 Tuberculosis

Mycobacterium tuberculosis (*Mtb*) is a human pathogen and a causative agent of tuberculosis (TB), a communicable disease that is estimated to infect one-quarter of the world and that has collectively killed more people than any other bacteria in human history. As such, prior to the emergence of the SARS-CoV-2 pandemic, TB was the primary cause of mortality due to a single infectious agent (WHO, 2022).

Mtb was discovered in 1882 by Robert Koch, who demonstrated that TB is caused by an infection with tubercle bacillus *Mtb* (Barberis, Bragazzi, Galluzzo, & Martini, 2017). *Mtb* belongs to the *Mycobacterium tuberculosis* complex (MTBC), a group of mycobacteria that cause TB diseases in humans and animals. While *Mtb* and its close relative *Mycobacterium africanum* are responsible for the majority of TB cases in humans, zoonotic infections are caused by *Mycobacterium caprae* and *Mycobacterium bovis* (Sinha et al., 2016). *Mtb* is an obligate human intracellular pathogen and has no environmental reservoirs other than humans. The earliest findings of tuberculosis disease are as old as 70,000 B.C., allowing *Mtb* to become an extremely well-adapted human pathogen (Barberis et al., 2017).

Mycobacterial species are rod-shaped bacilli that are surrounded by a thick cell wall responsible for their extremely low permeability (Forrellad et al., 2013). From the outer to the inner layer, *Mtb*'s cell wall consists of a capsule composed predominantly of polysaccharides and glycoproteins, an outer membrane made of glycolipids and mycolic acids esterified by a polymer of arabinogalactan, a peptidoglycan layer, a periplasm, and a cytoplasmic membrane (Gengenbacher & Kaufmann, 2012). Grown at 37°C and in a rich medium, *Mtb* has a doubling time of 20 to 24 h and forms colonies on an agar within three to four weeks. *Mtb* has a 4.4 million base pair long GC-rich (65.6%) genome that encodes around 4000 predicted proteins, of which 27% are of an unknown function (Yang, Zeng, & Tsui, 2019).

1.1.1 Global impact of tuberculosis

TB stands as a prominent global health concern. According to data from the World Health Organization (WHO), there were 10.6 million new TB cases in both 2021 and 2022, showing an increase for the first time in several decades. The incidence rate, which is the number of new cases per 100,000 individuals annually, mirrored this trend: it increased by 3.6% to 133 incident cases after an overall 2% decrease over 20 years (WHO, 2022, 2023) (Fig. 1.1).

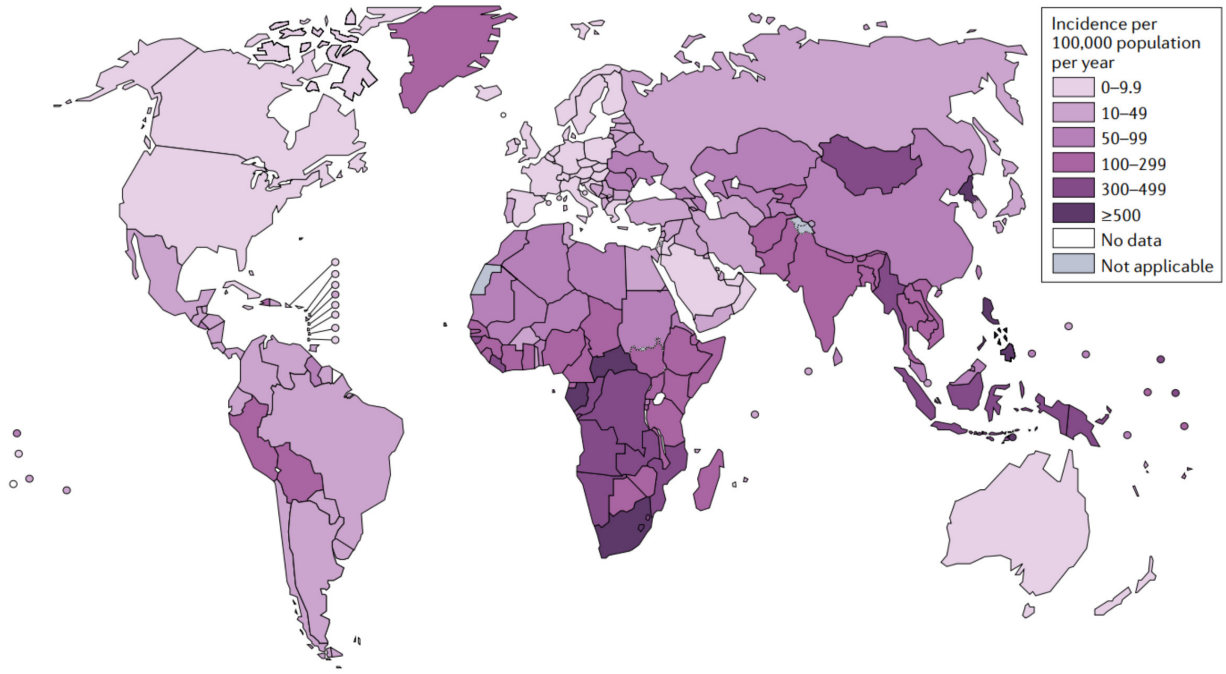


Figure 1.1: **Incidence of tuberculosis (TB) per 100,000 people in 2020**. Obtained from (WHO, 2022)

This increase in the incidence rate can largely be attributed to the ongoing SARS-CoV-2 pandemic. The pandemic led to the disruption of various aspects of TB health care, including the lack of diagnostic tools, reduced healthcare capacity, and heightened risks associated with hospital visits (WHO, 2022). As a result of these challenges, the estimated mortality rate for TB increased between 2019 and 2021, effectively reversing the declining trend in the number of TB-related deaths that had been observed between 2005 to 2019. The WHO estimated that TB was responsible for 1.4 million deaths among individuals who were HIV-negative in 2021 and 1.13 million deaths in 2022, with an additional 187,000 and 167,000 deaths, respectively, occurring among HIV-positive individuals who are at risk of developing TB. These combined

figures brought the total number of deaths attributable to TB to 1.6 million, making TB the 13th leading cause of death worldwide (WHO, 2022, 2023) (Fig. 1.2).

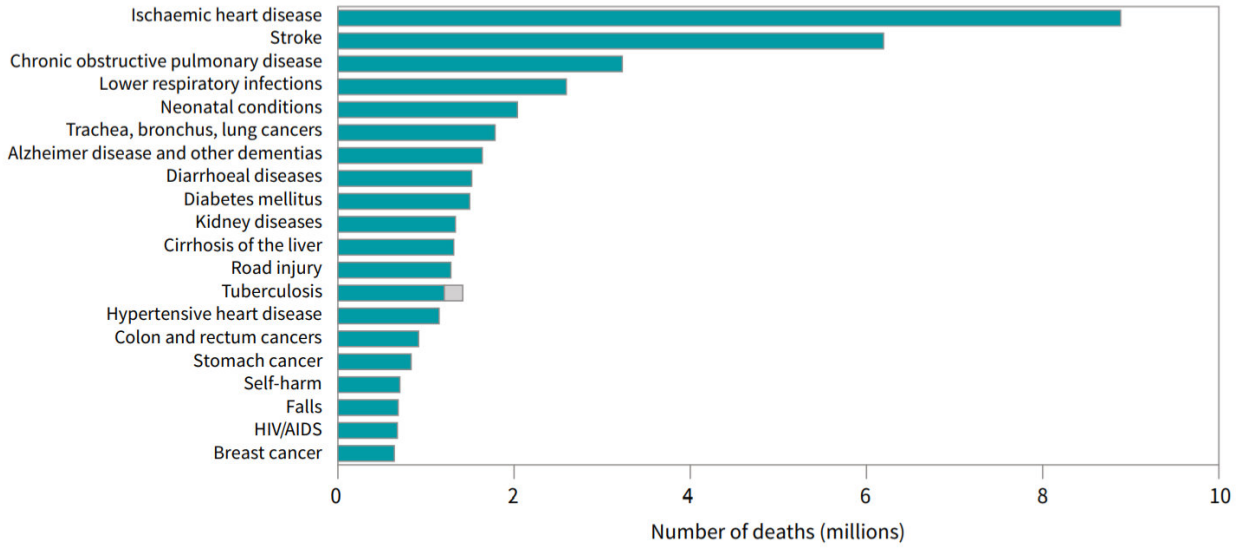


Figure 1.2: **Top causes of death worldwide in 2019 based on WHO.** The number of deaths from TB of HIV-positive people is indicated in grey, which are officially classified as caused by HIV/AIDS.

In addition, geographical and economic features impact the TB incidence rate. Most TB cases are reported in developing countries, including in Southeast Asia (43%), Africa (25%), and the Western Pacific (18%) (WHO, 2022). 30 high-TB-burden countries account for 87% of all estimated incident cases; eight of these countries account for almost two-thirds of the global total incident cases: India, Indonesia, China, the Philippines, Pakistan, Nigeria, Bangladesh, and South Africa. Low-income countries have the highest rate of active TB, while high-income countries have the lowest (WHO, 2022).

To decrease the TB health crisis, WHO and the United Nations (UN) in 2014 and 2015 established a set of strategies to end the TB epidemic: WHO End TB Strategy and the UN Sustainable Development Goals (WHO, 2022). The strategies aim to decrease the TB incidence rate and TB mortality by 80 and 90%, respectively. Furthermore, the strategies aim to prevent catastrophic costs (that account for more than 20% of household income) of TB treatment of all impacted families by 2030. Unfortunately, current trends suggest that these objectives will likely not be met. For instance, one of the key targets is to reduce TB deaths by 75% between 2015 and 2025, yet the progress between 2015 and 2021 amounted to only a

modest 5.9% decline (Fig. 1.3).

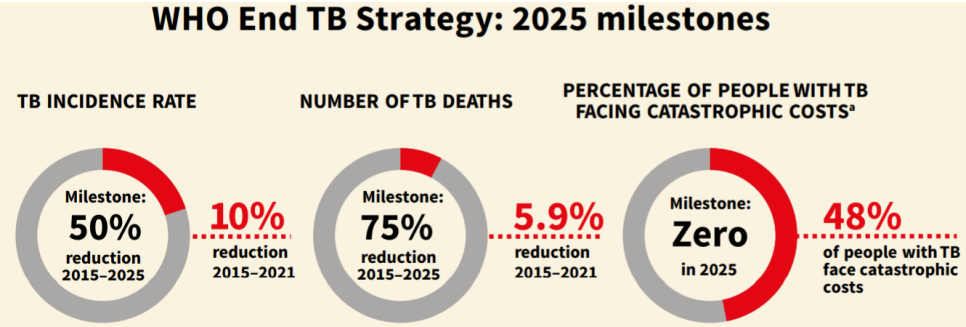


Figure 1.3: **WHO End TB Strategy 2025 milestones.** Obtained from (WHO, 2022), indicating milestones for TB incidence rate, number of deaths and percentage of people with TB facing catastrophic costs by 2025 milestone.

1.1.2 Pathogenesis

Mtb bacillus is transmitted almost exclusively via aerosol from an individual with an active pulmonary infection, through inhalation of aerosolized 1-5 μm particles that contain 1-10 *Mtb* bacilli (Patterson & Wood, 2019). Upon inhalation, *Mtb* is translocated to the lower respiratory tract where *Mtb* are phagocytosed by alveolar macrophages (AMs), a dominant type of immune cells *Mtb* infects (Cohen et al., 2018) (Fig. 1.4). Phagocytosis is initiated through pattern recognition receptors, which include Toll-like receptors, C-type lectin receptors, nucleotide-binding domain, and leucine-rich repeat-containing receptors (O'Garra et al., 2013). The detection of *Mtb*'s pathogen-associated molecular pattern molecules activates the NF-κB signalling and production of inflammatory cytokines such as IL-1β, TNF, and IL-6 (Chandra, Grigsby, & Philips, 2022). Immune cells could cause cessation of the infection at this stage, leading to so-called "early clearance" before the development of the adaptive immune response.

If the innate immune response fails to clear the infection, *Mtb* utilises its virulence mechanisms to spread further and establish a primary infection site. *Mtb* actively blocks the fusion of the lysosome with the phagosome that contains the bacilli to avoid killing by the cell (Hart, Armstrong, Brown, & Draper, 1972). Furthermore, it can disrupt the phagosomal membrane through the expression of its type VII secretion system ESX-1, causing the release of bacteria and bacterial products into the AMs' cytoplasm (Houben et al., 2012). In the cytoplasm, *Mtb*

is exposed to minimal oxidative and nitrosative stress but is also found to be able to replicate and access AMs nutrients (Pisu, Huang, Grenier, & Russell, 2020). If not killed by the AMs, *Mtb* migrates to the lung interstitium, where bacteria can infect other types of phagocytotic cells such as monocyte-derived macrophages, dendritic cells (DCs), inflammatory monocytes, and neutrophils - establishing the primary infection site (Wolf et al., 2008; Chackerian, Alt, Perera, Dascher, & Behar, 2002). At this stage, some *Mtb* can survive neutrophil-secreted ROS through an expression of enzymes such as KatG catalase-peroxidase and can cause necrosis of infected cells (Lamichhane, 2011). Release of *Mtb* from infected immune cells causes further recruitment of immune cells, their infection, and further *Mtb* replication within these cells.

As the primary infection site develops, infected DCs and/or monocytes are key in transporting *Mtb* antigens to the pulmonary lymph node to present them to naïve T cells, causing their activation and differentiation into Th1 $CD4^+$ T cells. Primed T cells traffic back to the infection site, release interferon-γ to activate an anti-inflammatory response of macrophages, and initiate recruitment of B and T cells to surround infected immune cells. Recruited cells form a multicellular structure called granuloma - which will be described below. *Mtb* can actively delay the migration of immune cells to the lymph node, T cell priming as well as migration of the T cells back to the infection site (Wolf et al., 2008; Chackerian et al., 2002). *Mtb*-induced delayed T cell priming and migration leads to the appearance of antigen-specific T cells in the lungs only a few weeks following the infection (Ankley, Thomas, & Olive, 2020). To delay adaptive immune response, *Mtb* for example utilizes Hip1 serine protease to cleave highly immunogenic GroEL2 chaperone, thus inhibiting its presentation by the DCs (Georgieva, Sia, Bizzell, Madan-Lala, & Rengarajan, 2018). Of special importance at this stage are $CD4^+$ T cells since their depletion is a significant risk factor for progression to active TB disease. As such, HIV-positive patients, who have a reduced number of $CD4^+$ T cells, are estimated to be 24-fold more prone to develop active TB, and 12% of all new cases are indeed HIV-positive patients (WHO, 2022). This fact highlights that $CD4^+$ T cell responses are vital for the control of *Mtb* infection. In fact, individuals with dysfunctive $CD4^+$ T cell response fail to form coherent granulomas, causing quicker *Mtb* dissemination (Caruso et al., 1999). Despite this, studies are unclear whether enhanced T cell response could improve the outcome of the *Mtb* infection as attempts to enhance CD4

T cell response to combat *Mtb* infection were unsuccessful in providing better outcomes in TB patients. Furthermore, mice with an increased number of $CD4^+$ T cells are more susceptible to developing active TB – pointing towards the importance of a balanced immune response (Barber, Mayer-Barber, Feng, Sharpe, & Sher, 2011; Chandra et al., 2022).

Prevention of the infection dissemination depends on the next steps of the adaptive immune response. In that vein, granuloma, a complex of immune cells, is a key component of *Mtb* containment. Granulomas are the defining pathology of TB disease. The organisation of granuloma is heterogeneous, with the centre exhibiting pro-inflammatory, and the periphery anti-inflammatory components - for example containing the $CD4^+$ killer T cells on the outer layer. In immunocompetent individuals with an effective adaptive immune response, granuloma sterilises or contains the infection without causing further tissue damage in 90-95% of the cases. Such patients are considered to be latently infected and do not develop symptoms or become infectious. It is estimated that a quarter of the world's population is latently infected with *Mtb* (LTBI), defined by WHO as "a state of persistent immune response to stimulation by *Mtb* antigens without evidence of clinically manifested active TB and with the absence of bacterial replication or below a detectable threshold due to immunological control" (Dartois & Rubin, 2022; WHO, 2022). Reactivation of TB can be avoided through preventive therapy to target the surviving bacteria in the granuloma; LTBI therapy reduces the reactivation rate by 60 to 90% and consists of nine months of daily isoniazid course (Magombedze, Dowdy, & Mulder, 2013). Within the granuloma core, *Mtb* may remain in a metabolically active but non-growing quiescent state, continuously adapting to the dynamic environment of the granuloma. Eventually, if the opportunity arises, such as in a subset of patients whose immune system is waning, *Mtb* may start to replicate and infect surrounding cells. Increased bacterial load over time could cause rupture of the granuloma and *Mtb* dissemination (Abel, El-Baghdadi, Bousfiha, Casanova, & Schurr, 2014) (Fig. 1.4). Among others, major risk factors contributing to the development of active TB disease include HIV co-infection, alcohol abuse, smoking, and diabetes.

Progression of *Mtb* infection from the LTBI to the active TB disease was shown to mostly occur within two years of the infection in 5-10% of the patients for reasons that largely remain

unclear (Vynnycky & Fine, 1997; Andrews et al., 2012). As much as the granuloma protects the host from the further spreading of the pathogen, it also is a source of nutrients for *Mtb*. The progression of granulomas is non-linear and varies within and between patients - it was shown in macaque studies that granulomas display heterogeneous lesions (P. L. Lin et al., 2014). This adds complexity to TB treatment because the penetration of antibiotics varies across different tissue structures (Zhu, Liu, & Fortune, 2023). In 15-20% of all TB cases, *Mtb* disseminates and can access the lymphatic system and the bloodstream, leading to extrapulmonary TB disease (Chandra et al., 2022). The patients transmit the *Mtb* if it reaches the airways and is aerosolized by cough.

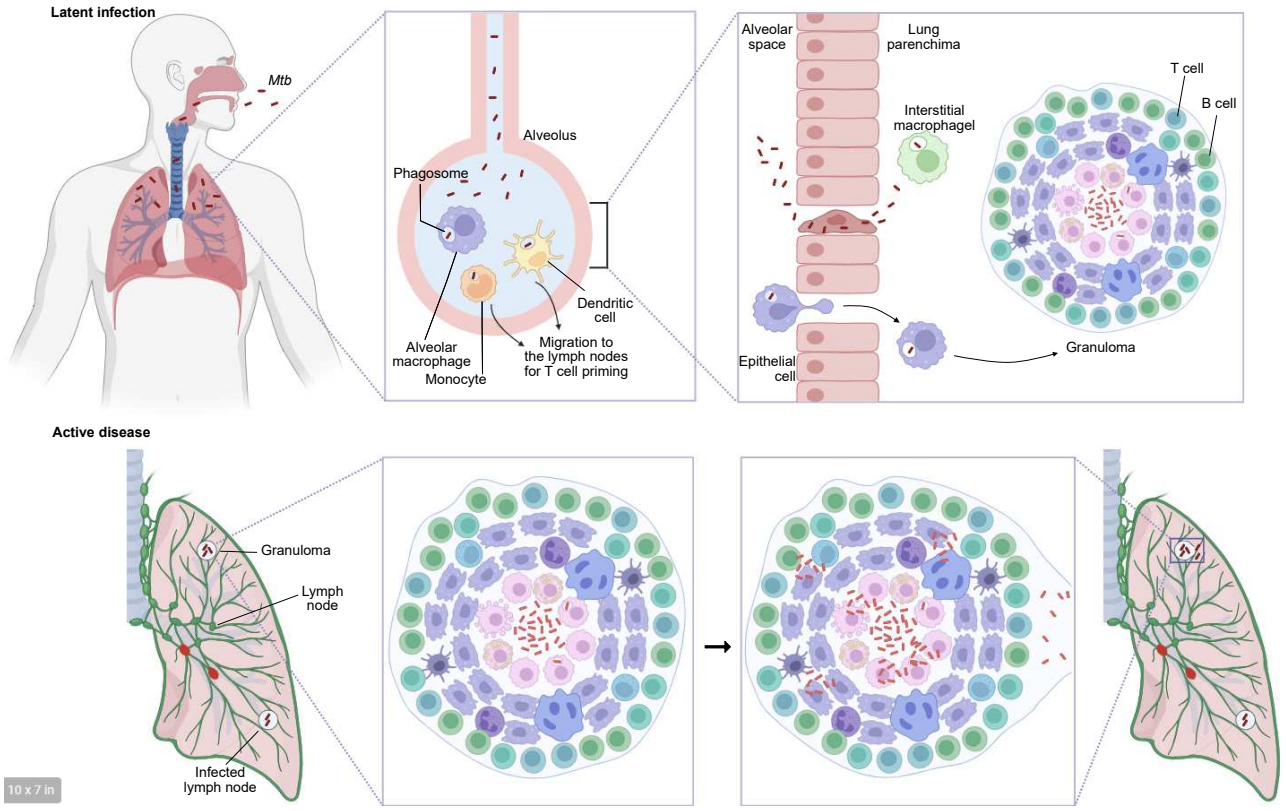


Figure 1.4: ***Mtb* infection**. The infection begins through inhalation of *Mtb*. *Mtb* translocates into the lower respiratory system, where it encounters monocytes, alveolar macrophages, and dendritic cells. If not eliminated, *Mtb* infection progresses to the lung parenchyma through infection of epithelial cells or migration of infected macrophages. At the same time, dendritic cells or inflammatory monocytes migrate to lymph nodes for T cell priming, leading to the recruitment of immune cells to the lung parenchyma and the formation of granuloma. Increased bacterial load over time could cause rupture of the granuloma and *Mtb* dissemination into other organs, leading to symptomatic infection and infectious host. Adapted from (Pai et al., 2016).

Generally, patients with active TB present with symptoms such as fever, fatigue, and weight

loss, and those with pulmonary TB have a persistent cough that can lead to coughing up blood (haemoptysis). Extrapulmonary TB mimics many diseases, as it can occur anywhere in the body, with the most common types in the lymph nodes, the pleura, the genitourinary system, bones and joints, the gastrointestinal system, the central nervous system, and the spine (Baykan et al., 2022). The most serious forms present as hematogenous TB, which often infects the bone marrow, and meningitis TB. Meningitis TB has a 50% mortality in HIV-positive patients and a 20% mortality rate if affecting children younger than 5 years of age. While the BCG vaccination poorly protects against pulmonary TB in adults, it provides up to 80% protection against meningitis TB in children (WHO, 2022).

1.1.3 Diagnosis of TB

The diagnostic tool that will be used to detect TB will be chosen based on whether the patient is suspected to have LTBI, active TB or drug resistance. For suspected LTBI patients, two diagnostic tests exist: the Mantoux tuberculin skin test (TST) and interferon-γ release assay (IGRA). The TST consists of the intradermal injection of purified protein derivatives of *Mtb* - an individual who previously developed cell-mediated immunity towards mycobacterial antigens will develop a skin test reaction within 48-72 hours. Although this method is inexpensive and easy to perform, it has the disadvantage that it is not specific to *Mtb* antigens; as such, the BCG vaccination can cause positive TST tests. The IGRA was introduced to replace the TST. It consists of an in vitro blood test to measure T cell release of IFN-γ after stimulation with antigens encoded by genes in the region of difference 1 (RD1), which contains genes encoding for the ESX-1 secretion system. The main limitation of IGRA is reduced sensitivity in immunocompromised patients that do not develop a strong adaptive immune response and no possibility of distinguishing between LTBI, re-infection and cleared infection (for example, patients that eliminated the infection might be positive due to memory T cell responses) (Pai et al., 2016). Diagnosis of active TB is done using imaging, microscopy, culturing, and molecular tests. X-rays and PET-CT are the established methods for screening TB, and suspected cases are followed with sputum smears and other microbiological and molecular methods such as

Xpert *Mtb*/RIF (Albert et al., 2016).

1.1.4 Treatment of tuberculosis

History of TB treatment

Over the centuries, efforts to treat TB have been largely "tales of frustration" (Iseman, 2002; Riva, 2014). Prior to the discovery of antibiotics, TB treatment ranged from herbal solutions, dietary interventions, aerotherapy, and heliotherapy to bleeding and purging, which mainly accelerated the progression and mortality of the disease (Diacon, Von Groote-Bidlingmaier, & Donald, 2012). Subtle improvements were made in TB treatment as the understanding of *Mtb* transmission, clinical practice, and preventive care developed. However, it was not until the discovery of the antibiotic streptomycin in the 1940s that mortality and morbidity in TB patients finally decreased.

Streptomycin became the first drug used to treat TB patients successfully. This was followed by the discovery of para-aminosalicyclic acid (PAS). Both streptomycin and PAS were effective but had significant side effects and caused the development of antibiotic resistance when administered as a monotherapy. As a response, the British Medical Research Council conducted a clinical trial using both drugs to treat TB. Indeed, combinatory treatment for active TB exhibited increased effectiveness and lowered the rates of antibiotic resistance ("Treatment of Pulmonary Tuberculosis with Streptomycin and Para-Amino-Salicylic Acid: A Medical Research Council Investigation", 1950). In 1951, the discovery of isoniazid and the many trials that showed its potential led to the development of "triple therapy", consisting of isoniazid with streptomycin and/or PAS, and this combination remained as the standard tuberculosis treatment for nearly 15 years ("Various combinations of isoniazid with streptomycin or with P.A.S. in the treatment of pulmonary tuberculosis; seventh report to the Medical Research Council by their Tuberculosis Chemotherapy Trials Committee.", 1955) . Soon after its discovery in 1961, ethambutol replaced PAS in combination with isoniazid, and the combination of those two with rifampin enabled the therapy to be shortened to "just" 9 months (Doster, Murray, Newman, &

Woolpert, 1973). The next decade led to the development of more antibiotics to treat TB, such as cycloserine, ethionamide, kanamycin, pyrazinamide, and capreomycin, gradually shaping the different regimes used today (Fig. 1.5).

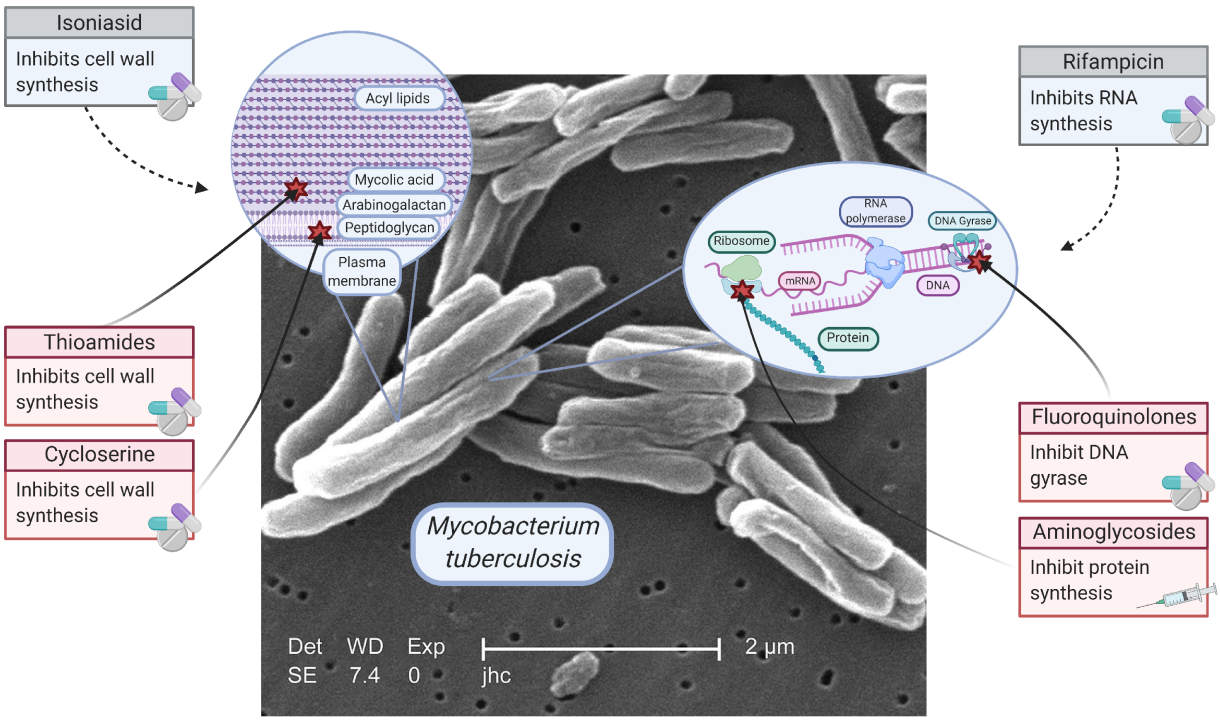


Figure 1.5: **Antibiotics used to treat tuberculosis and their mode of action**. Schematic generated using BioRender.

Current treatment for TB

In the complete absence of treatment, around 50% of individuals with active TB will die from the disease. Current TB treatment is 85% successful if administered promptly, and the standard regimen consists of four antibiotics: it consists of daily administration of isoniazid, rifampicin, ethambutol, and pyrazinamide for two months (so-called the intensive phase), followed by daily administration of isoniazid and rifampicin for four additional months (the continuation phase) – bringing the treatment duration to six months. This can be extended up to 12 months in cases of severe disease such as TB meningitis. Treatment progress is monitored through culturing,

sputum smear and X-ray (Pai et al., 2016).

Even though the treatment fails in only around 15% of the patients presented with drug-susceptible TB, major limitations in the treatment of TB are the toxicity of the drugs used, medical costs associated with the disease, and poor patient compliance. Directly observed therapy (DOT), where a medical professional observes dose uptake, aims to respond to the latter issue. Unfortunately, DOT is not always available and poor patient compliance occurs even when it is, leading to a lack of treatment, treatment failure, relapse, and the emergence of drug resistance.

Drug-resistant TB

Treatment of drug-resistant TB is significantly more intricate than drug-susceptible TB, and it has become a major concern. In 2021, drug resistance affected 450,000 TB patients, including 3.6% of new cases and 18% of previously treated patients (WHO, 2022). Therapies for active, drug-resistant TB are lengthy (at least 9–20 months), are highly toxic, and have a low compliance rate due to numerous complications. *Mtb* can develop resistance to all drugs used for the TB treatment. Resistance to rifampicin is termed RR-TB; resistance to both rifampicin and izoniazid is defined as multidrug-resistant TB (MDR-TB). Additionally, while pre-XDR-TB refers to *Mtb* resistant to rifampicin and any of the second-line fluoroquinolones; extreme drug-resistant TB (XDR-TB) refers to the *Mtb* resistant to bedaquiline and linezolid. RR-TB treatment includes fluoroquinolones instead of rifampicin, which is then administered in combination with isoniazid, pyrazinamide, and ethambutol for two months (the intensive phase), with the final continuation phase (isoniazid, ethambutol, fluoroquinolones) recommended for 18 additional months. MDR-TB and XDR-TB regimes vary depending on the resistance, and drugs in general are administered for 20 months. They may include fluoroquinolones, bedaquiline, injectable aminoglycosides (such as capreomycin, amikacin, and kanamycin), ethionamide, cycloserine, terizidone, and linezolid. Close monitoring is required due to serious side effects, and even when treated, MDR-TB patients have approximately a 30 to 50% success rate. In comparison, pre-XDR/XDR-TB treatments are only around 35% successful (WHO, 2023).

Shorter, safer, and more effective treatment regimens are urgently needed. Recent advances have been made to shorten the treatment and through the use of new compounds. For example, dose optimisation of rifamycins showed increased early bactericidal activity, and a rifamycin with a longer half-life - rifampentine - was in a clinical trial showed to decrease treatment length to four months in combination with moxifloxacin, isonazid, and pyrazinamide (Dorman et al., 2021). In addition, following 40 years of stagnation, new compounds have been authorised as anti-TB drugs - bedaquiline, delamanid, and pretomanid - and trials such as SimpliciTB for drug-sensitive TB (bedaquiline-pretomanid-moxifloxacin-pyrazinamide for four months) and ZeNIX for MDR-TB (bedaquiline-pretomanid-linezolid regimen with linezolid at a lower dose of 600 mg for 26 weeks) showed promising results, including a lower incidence of side effects (Conradie et al., 2022; Motta et al., 2023).

Prevention of the development of *Mtb* resistance, through either targeting the pathogen with novel combinations of existing drugs or novel antimicrobials, is essential to decrease the burden of TB. Antibiotic resistance is a major obstacle in getting to this goal, as the long duration of treatment is enough time for the surviving bacteria to select for mutations that render them resistant and shift their minimum inhibitory concentration (MIC). Ironically, this ability of bacteria to survive in the first place is the reason the long treatment is required. Exposure to the host's immune response, harsh environments such as low pH of the phagosome and even exposure to sub-inhibitory concentrations of antibiotics (such as in the low-permissive granuloma) render the bacteria transiently insensitive to killing. This ability does not require genetic changes in the bacterium but leads to decreased killing by one or more antibiotics due to changes in the expression of certain genes, growth decrease, ATP level changes or redox changes, among others. As such, it is a perfect "switch" that allows the bacteria to survive during unfavourable conditions and can be reversed upon more favourable opportunities. Understanding the mechanisms behind developing such forms of resistance and finding targets that could prevent their occurrence could also prevent the occurrence of antibiotic MIC-shifted resistance. The next pages will focus on describing different types of AMR and understanding the mechanisms by which they develop, focusing on *Mycobacterium tuberculosis*.

1.2 Antibiotic resistance

Antibiotic resistance, in a broad sense, is defined as the ability of bacteria to survive otherwise lethal concentrations of an antibiotic, regardless of the molecular mechanisms involved (Schrader, Botella, & Vaubourgeix, 2023). It is arguably one of the most important challenges that our healthcare faces today - in 2019, 4.95 million bacterial infections were associated with antibiotic resistance (Murray et al., 2022). Bacteria have become increasingly resistant to existing antibiotics, and there is an urgent need to discover new ones. Unfortunately, if AMR remains unaddressed, the death toll from antibiotic-resistant infections could reach 10 million per year by 2050 (O'Neill, 2014).

The AMR phenomenon has been an evolving challenge since the discovery of antibiotics. Resistance to arsphenamine, introduced in 1910 as the first widely used antibiotic to treat syphilis and trypanosomiasis, was described as early as 1917 (Zaffiri, Gardner, & Toledo-Pereyra, 2012). In a study that described this resistance, Akatsu and Noguchi investigated if exposure of spirochetes to increasing doses of arsphenamine in vitro would render them more resistant and discovered that resistance evolved over rounds of treatment (Akatsu & Noguchi, 1917). Decreased susceptibility to arsphenamine was further observed in the clinic just seven years after those findings (Stekel, 2018). Similarly, resistance to penicillin and sulfonamides was reported following their discovery in the 1930s and 1940s, underscoring a recurring theme in a fight against bacterial infections (Davies, 1996; Abraham & Chain, 1940; Hobby, Meyer, & Chaffee, 1942; Bigger, 1944). In the case of streptomycin, introduced in 1944 for the treatment of tuberculosis, the resistance was observed within four years of its clinical use (Crofton & Mitchison, 1948). These early observations laid the groundwork for understanding that bacteria can develop resistance to an antimicrobial following exposure by acquiring de novo mutations or by acquiring resistance genes via horizontal gene transfer.

1.2.1 MIC-shifted resistance, tolerance and persistence

Three phenomena that allow bacteria to survive exposure to bactericidal antibiotics are MIC-shifted resistance, persistence and tolerance (Balaban et al., 2019; van den Bergh, Fauvart, & Michiels, 2017; Schrader et al., 2023). MIC-shifted resistance (previously termed just "resistance") is defined as the ability of bacteria to survive and replicate in the presence of the drug, leading to an increase in the concentration of an antibiotic needed to prevent bacterial replication (minimum inhibitory concentration, MIC) (Schrader, Vaubourgeix, & Nathan, 2020; Schrader et al., 2023; Balaban et al., 2019). On the other hand, tolerance and persistence describe the ability of bacteria to survive exposure to a bactericidal concentration of an antibiotic (Balaban et al., 2019). The main distinguishing factor between tolerance and persistence is the penetrance within the population, such that tolerance manifests at the level of the whole population, while persistence transiently affects a subpopulation of the cells through phenotypic switching (Balaban et al., 2019; Schrader et al., 2020; Gollan, Grabe, Michaux, & Helaine, 2019; van den Bergh et al., 2017). The hallmark of persistence is biphasic killing upon exposure to an antibiotic, consisting of the initial killing of the antibiotic-sensitive subpopulation followed by a slower killing kinetics of antibiotic persisters (Balaban, Merrin, Chait, Kowalik, & Leibler, 2004; Schrader et al., 2021; Verstraeten et al., 2019; Gollan et al., 2019). Conversely, in the case of tolerance, bacterial counts over time decrease linearly, and it can be quantified by measuring the minimum duration of killing (MDK); for example, the MDK_{99} corresponds to the time needed to kill 99% of the population. For tolerant populations, the ability of bacteria to withstand killing for a prolonged period leads to an increase in the MDK_{99}. Upon regrowth of persistent and tolerant bacteria in the absence of an antibiotic, both tolerant and persistent bacteria give rise to populations that can be killed in the same proportion by the same antibiotic in the same conditions (Fig. 1.6). In addition to these types of AMR, another manifestation - heteroresistance - describes a phenomenon by which a fraction of the population displays a transient increase in the MIC value; the underlying heritability of the increased MIC is unstable and reversible (Dewachter, Fauvart, & Michiels, 2019; Balaban et al., 2019) (Fig. 1.6).

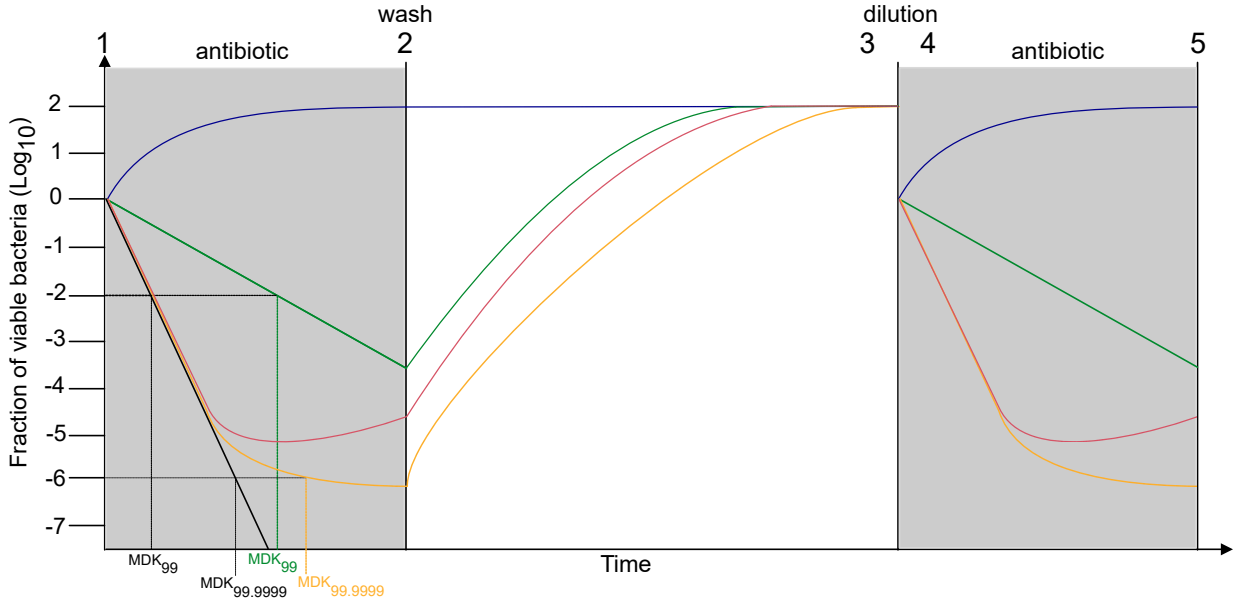


Figure 1.6: **Types of AMR.** AMR can manifest as MIC-shifted resistance (purple), tolerance (green), persistence (yellow) and heteroresistance (pink). The antibiotic-sensitive population is shown as a full black line. The killing kinetics is shown upon (1) exposure to an antibiotic (grey zone), (2) followed by a wash step to remove an antibiotic, (3) dilution of the cultures to the same OD as at the beginning of the experiment, and (4) upon second exposure to an antibiotic. MDK_{99} and $MDK_{99.9999}$ are indicated with dashed lines. Adapted from (Schrader et al., 2023)

Genetic and phenotypic AMR

Each of the manifestations of AMR - MIC-shifted resistance, tolerance, persistence, and heteroresistance - can be genetic and phenotypic in origin. Genetic AMR arises due to the acquisition of resistance genes or the development of *de novo* mutations. While genetic AMR is passed onto the progeny of resistant cells, phenotypic AMR is transient (with exceptions such as *hipQ* mutant (Balaban et al., 2004), which will be discussed later on) and arises upon activation of intrinsic resistance mechanisms triggered by environmental factors. Notably, the progeny of phenotypically resistant bacteria is genetically identical to susceptible populations - the resistance in the case of phenotypically resistant bacteria is passed onto the progeny in the form of the same endogenous resistance mechanisms, which could be triggered in the same manner in the progenitor cells (Schrader et al., 2023; Balaban et al., 2019). Both phenotypic and genetic forms have been identified for each AMR manifestation. For instance, persistence is inherently phenotypic. However, both environmental triggers and genetic mutations can impact

the proportion of persistent cells within a population, leading to what is termed "high persistence". A classic example of this is the mutation in the *hipA* gene, which was first reported by Moyed and Bertrant in 1983 as a cause of increased survival of *Escherichia coli* upon exposure to bactericidal antibiotics (Moyed & Bertrand, 1983). The following sections will dive deeper into the intricate mechanisms underlying these different manifestations of bacterial survival to antibiotics.

The initial observations of antibiotic tolerant cells

The first observations of persistence occurred shortly after the introduction of penicillin. In a seminal study published in 1942, Hobby and colleagues observed that a small fraction of streptococci survived 48 hours of exposure to penicillin at 37°C. Intriguingly, they observed that the proportion of surviving bacteria increased from 10^{-4} to 10^{-1} at 18°C and to 10^{0} at 4°C. This study also revealed that penicillin was less effective against bacteria in the stationary phase, concluding that penicillin primarily targeted dividing cells (Hobby et al., 1942). Building upon these observations, Bigger, in 1944, further elucidated the nature of these resilient bacterial cells when he noted that approximately one in a million cells survived 72 hours of exposure to penicillin at 37°C. When he outgrew these surviving cells, termed "persisters", in an antibiotic-free media and re-exposed them again to penicillin, he noted that the same proportion of bacteria survived - indicating that their resistance was not due to the emergence of genetic mutations. Bigger's work was pivotal in characterising the key features of persisters, as he outlined that (1) persisters are identical to their progeny and do not have genetic changes that render them resistant, (2) persistence is transient and can be reversed upon removal of the antibiotic, (3) persistence is stochastic or can be induced by environmental stresses, and that (4) persisters could arise in clinical practice in patients treated with penicillin and cause treatment failure (Bigger, 1944). In addition, Bigger noted that more bacteria survived if subjected to different growth-inhibitory conditions, thereby tying a bacterium's absence of growth with the inefficacy of a drug (Bigger, 1944).

In a pivotal study in 1956, Chabbert characterised another inducer of increased survival of

bacteria. He observed that *Staphylococcus* exposed to sub-MIC concentrations of erythromycin displayed decreased susceptibility to another antibiotic, spiramycin. In this case, growth in the presence of an antibiotic was not due to genetic alterations, as the same strain exposed to spiramycin alone was as susceptible as staphylococci would be. This priming effect of exposure to sub-MIC concentration of an antibiotic on MIC-shifted resistance to another antibiotic was found to apply to other macrolides and two other types of antibiotics that bind to the 23S rRNA of the 50S ribosomal subunit. The underlying mechanism was later found to involve the methylation of 23S rRNA in the macrolide binding pocket (Skinner, Cundliffe, & Schmidt, 1983; Gaynor & Mankin, 2003; Stsiapanava & Selmer, 2019). Chabbert's findings represent a seminal example of how MIC-shifted resistance can have a phenotypic origin, underscoring the complexity of bacteria's response to antibiotics.

Building on this work, further research in the field revealed that the host environment significantly impacts persistence. A study by Tompsett demonstrated this phenomenon, showing that staphylococci showed increased survival to penicillin when cultured in leukocytes compared to laboratory media. Additionally, McCune and colleagues reported that bacteria isolated from the kidneys of infected mice exhibited a biphasic killing pattern when exposed to a combination of antibiotics (McCune, Dineen, & Batten, 1956). These findings established the first blocks of evidence on the impact of host immunity on bacterial survival to antibiotics.

Work that followed brought to light more granularity to the phenomena described above, including the fact that a decreased rate of killing by an antibiotic - that manifests as either tolerance or high persistence - could also have a genetic background. In this vein, a study in 1983 showed that selected mutants of *E. coli* displayed high persistence upon exposure to ampicillin due to a gain-of-function mutation in the gene *hipA* (Moyed & Bertrand, 1983). *hipA* mutants, first selected in vitro, were further isolated from cystic fibrosis patients infected with *Pseudomonas aeruginosa* and who underwent multiple rounds of antibiotic treatment, as well as in uropathogenic *Escherichia coli* isolates from patients with recurrent urinary tract infections (Goneau et al., 2014). This study also provided evidence that such mutants emerged in clinical settings, suggesting increased survival upon antibiotic exposure could be a harbinger of treatment failure and relapse of infection. Finally, it was demonstrated later that mutations

that confer tolerance foster the development of MIC-shifted resistance *in vitro* and in treated patients, emphasising the importance of preventing the formation of persistent and tolerant cells (Levin-Reisman et al., 2017; Windels et al., 2019).

1.2.2 Triggers of phenotypic tolerance to antibiotics

Persistence refers to the transient ability of a subpopulation of bacteria called persisters to survive antibiotic exposure in an isogenic population (Verstraete, Van den Bergh, Verstraeten, & Michiels, 2022). Following Bigger and Hobby's initial observations, the frequency at which persisters arise in a population has been shown to increase in response to numerous stimuli such as nutrient starvation, host infection, change in oxygen level, and exposure to reactive oxygen species (Helaine & Kugelberg, 2014; Van Den Bergh et al., 2016; Gollan et al., 2019; Verstraeten et al., 2019). In addition, persisters can also appear in unstressed conditions. For example, *E. coli* persisters have been shown to survive exposure to ampicillin due to stochastic fluctuations in the abundance of energy-generating components (Manuse et al., 2021).

Nutrient limitation

Bacteria often reside in harsh environments such as biofilms and granulomas, and phenotypic switches aid them in coping with scarce nutrient availability. Under nutrient-deprived conditions, bacteria are shown to undergo a series of physiological and metabolic adaptations that prime them for survival in these hostile environments - such as changes in growth rate or entry into a dormant state and activation of stress responses (Amato et al., 2014; Amato & Brynildsen, 2014; D. Nguyen et al., 2011). In fact, it is known that when nutrients become limited, these adaptations effectively render bacteria less susceptible to antibiotic killing and lead to an increase in persistence (Keren, Shah, Spoering, Kaldalu, & Lewis, 2004; Willenborg, Willms, Bertram, Goethe, & Valentin-Weigand, 2014; Goneau et al., 2014; Jubair, Morris, & Ali, 2012). Moreover, the switch from one nitrogen source to another was also shown to contribute to antibiotic persistence development, indicating how even media components can impact the survival of bacteria (Amato, Orman, & Brynildsen, 2013). For instance, Amato and colleagues

observed that *E. coli* persisted in the presence of a fluoroquinolone due to a switch to another carbon source available in the culture medium (Amato et al., 2013). The same group identified that persistence in nutrient-scarce conditions is predominantly driven by RelA, a component of the stringent response (Amato & Brynildsen, 2014).

Stringent response

The stringent response is a stress signalling system that enables bacteria to respond to nutrient starvation, coupling nutrient availability and growth rate (Brown, 2019). This adaptive response is characterised by the accumulation of signal molecules guanosine tetraphosphate ppGpp and pentaphosphate pppGpp, which are produced by members of the protein family RSH (RelA/SpoT homologue) (Atkinson, Tenson, & Hauryliuk, 2011; Irving, Choudhury, & Corrigan, 2020). The impact of (p)ppGpp is rather broad and affects key cellular pathways such as protein translation and RNA metabolism. As such, the stringent response can change several aspects of bacterial metabolism and physiology. For instance, the stringent response was shown to decrease *E. coli* DNA replication through binding of (p)ppGpp to the RNA polymerase (Kraemer, Sanderlin, & Laub, 2019); it was also shown that (p)ppGpp inhibits the synthesis of purine nucleotides (Kriel et al., 2012) and induces changes of the bacterial transcriptional profile (Irving et al., 2020). In addition, the stringent response can also reduce translation through binding of (p)ppGpp to the initiator factor IF2 and via inhibition of elongation factors (Vinogradova et al., 2020; Rojas, Ehrenberg, Andersson, & Kurland, 1984; Y. Zhang, Zborníková, Rejman, & Gerdes, 2018).

Given the extensive influence of the stringent response on bacterial physiology, it was almost unsurprising to find that it has a role in persistence. For example, the studies where the stringent response was activated through amino acid or nitrogen starvation showed that the upregulation of (p)ppGpp production increased the level of persisters (Helaine & Kugelberg, 2014; D. Nguyen et al., 2011; Verstraeten et al., 2015; Prusa, Zhu, & Stallings, 2018). In addition, deletion of the enzymes responsible for the synthesis of (p)ppGpp, RelA and SpoT, was shown to cause a significant reduction in the number of persisters both *in vitro* and *in vivo*

(D. Nguyen et al., 2011; Helaine et al., 2014; Salzer & Wolz, 2023; Hansen, Lewis, & Vulić, 2008; Viducic et al., 2006). For example, *Salmonella* deficient in both *spoT* and *relA* were shown to have a decreased level of persisters upon infection of macrophages (Helaine et al., 2014). In mycobacteria, the stringent response is regulated through a single RSH enzyme, *rel*, which synthesises (p)ppGpp, and deletion of *rel* in *Mtb* was shown to decrease *Mtb* virulence in mice models, decrease growth in nutrient-limiting conditions and to increase its susceptibility to antibiotic killing (Karakousis et al., 2004; Dutta et al., 2019). For instance, deletion of *rel* was shown to increase the susceptibility of *Mtb* to isoniazid and decrease survival in the lungs of infected mice (Dutta et al., 2019). These studies underscored the role of the stringent response in bacterial survival and persistence.

ROS and RNS exposure

In addition to the nutrient starvation and stringent response, persisters were reported to increase in response to exposure to reactive oxygen species (ROS) and reactive nitrogen species (RNS), such as superoxide ions and nitrogen monoxide, molecules which are highly important for host cells' ability to control intracellular bacteria (Y. Wu, Vulić, Keren, & Lewis, 2012; Wang, El Meouche, & Dunlop, 2017; Ronneau, Michaux, & Helaine, 2023). In an example of *Salmonella*-macrophage interplay, recognition of bacteria by host cells activates a pro-inflammatory response, including the activity of NADPH oxidase that catalyses the reduction of oxygen to the superoxide anion, setting off a cascade that leads to the production of hydrogen peroxide and hydroxyl radicals, both of which are known to cause DNA damage in bacteria (Kohanski, Dwyer, & Collins, 2010; G. T. Nguyen, Green, & Mecsas, 2017). Following the respiratory burst mediated by NADPH oxidase, there is a sequential production of RNS, which further damages bacterial proteins and lipids (Rhen, 2019; Hill et al., 2021). Bacteria possess various mechanisms to counteract the exposure to ROS and RNS, such as superoxide dismutases and the catalase-peroxidase (e.g. KatG); lacking either of these enzymes leads to decreased persistence (Van Acker et al., 2013). In addition, in response to ROS, bacteria activate a DNA-damage response - namely the SOS response - that modulates bacterial genes through the interplay of a repressor and inducer pair LexA and RecA, which have been exten-

sively associated with persistence (Y. Wu et al., 2012; Dörr, Lewis, & Vulić, 2009; Dörr, Vulić, & Lewis, 2010).

Studies have shown that exposure to ROS and RNS can induce a state of persistence in various bacterial species, enhancing their ability to withstand antibiotic treatment. For instance, salicylate-induced ROS was shown to increase the persistence of *E. coli* by decreasing *E. coli* membrane potential, thus reducing its metabolic rate and leading to increased survival to antibiotics ciprofloxacin and ampicillin (Wang et al., 2017). Furthermore, exposure to ROS was shown to induce tolerance of *S. aureus* during macrophage infection (Rowe et al., 2020). In one study, Rowe and colleagues showed that ROS inactivated the TCA cycle, causing reduced respiration and ATP production that led to tolerance to rifampicin (Rowe et al., 2020). In addition, the induction of the SOS response was shown to be responsible for *E. coli* persistence to fluoroquinolones (Dörr et al., 2009).

Recently, Ronneau and colleagues presented evidence that RNS is a major driver of *Salmonella* persistence in macrophages - they showed that the RNS, produced by macrophages, locks *Salmonella* persisters in a non-growing state by corrupting their TCA cycle (Ronneau et al., 2023). Interestingly, they showed that a decline in RNS levels allows the regrowth of persisters, emphasising how understanding the temporal changes of the host immune response could aid in eradicating persisters (Ronneau et al., 2023). In addition, they also showed that RNS is essential for persister formation, as mice lacking the gene *nos2*, encoding the NO synthase, generated fewer persisters (Ronneau et al., 2023). Similarly, *Mtb* infecting *Nos2*-defective macrophages were more sensitive to isoniazid and rifampicin than those infecting WT cells, indicating the importance of RNS in drug tolerance of *Mtb* (Y. Liu et al., 2016).

Growth and antibiotic tolerance

Because some of the described mechanisms that trigger persistence were observed in cells that had reduced growth, the notion that growth inhibition is a mechanism by which bacteria achieve persistence stood for a long time as the main mechanism of antibiotic survival in the absence of genetic alterations. Some of the studies mentioned below abundantly supported

this notion. This includes a study by Tuomanen and colleagues, who documented that *E. coli* growth and killing by β-lactams were directly correlated - the less *E. coli* grew, the more it became resistant to treatment with β-lactams, corroborating Hobby and Bigger's earlier results (Tuomanen, Cozens, Tosch, Zak, & Tomasz, 1986). Similarly, in 2004, Balaban and colleagues used time-lapse microscopy to show that *E. coli* persisters were cells in the population with a slower growth rate (Balaban et al., 2004). More recently, slow growth was described as the sole mechanism by which *Salmonella* persisters form because persisters arose even without TA modules or (p)ppGpp production upon exposure to antibiotics (Pontes & Groisman, 2019). In addition, slow growth or no growth leading to persistence was argued to be due to metabolic slowdown and associated with low levels of ATP; in this vein, it was shown that *Staphylococcus aureus* persisters form through stochastic entry into a stationary phase followed by a drop in ATP levels (Conlon et al., 2016).

However, slowly-growing or non-growing bacteria are not necessarily metabolically inactive; rather, their transcriptome and proteome were found to differ from actively dividing bacteria (D. Nguyen et al., 2011; Rittershaus, Baek, & Sassetti, 2013; Radzikowski et al., 2016), indicating that halted replication or slowed metabolism are not necessary for tolerance or persistence. For instance, upon internalisation by host cells, bacteria were shown to reprogram their transcriptome and proteome or alter their metabolic state and growth, leading to decreased killing by both immune cells and antibiotics (Bumann & Schothorst, 2017; Helaine et al., 2014). In *Salmonella*, Helaine and colleagues showed that internalisation by macrophages induced a non-growing, antibiotic-tolerant state in a proportion of bacteria; however, the cells remained metabolically active during infection (Helaine et al., 2014). Similarly, non-growing but metabolically active persisters were observed in macrophages infected with *Mtb*, indicating that host immunity enhances bacterial phenotypic heterogeneity (Manina, Dhar, & McKinney, 2015; Mouton, Helaine, Holden, & Sampson, 2016). It is anticipated to find bacteria metabolically active during stress conditions since intracellular pathogens rely on the expression of certain effectors to avoid killing by immune cells. For example, *Salmonella* persisters were found to reprogram macrophage state to a more permissive anti-inflammatory state through secretion of its type 3 secretion system effectors (Stapels et al., 2018).

In the same vein, Gefen and colleagues showed that growth-arrested *E. coli* maintain a constant protein expression level over several days after cessation of growth (Gefen, Fridman, Ronin, & Balaban, 2014). Likewise, *S. aureus* and *Mtb* non-growing persister cells were shown to be transcriptionally active (Manina et al., 2015). However, mutants of *Mtb* and *Msm* that displayed increased survival to antibiotics were found to retain the same growth rate as the WT, demonstrating that a growth defect is not necessarily a mechanistic explanation for increased survival (Torrey, Keren, Via, Lee, & Lewis, 2016; Schrader et al., 2021). In this vein, another study in isoniazid-exposed *Msm* showed no correlation between pre-exposure growth rate and persistence. Instead, they observed that *Msm* susceptibility to isoniazid was inversely correlated with the stochastic expression of a catalase KatG, an enzyme required to activate isoniazid (Wakamoto et al., 2013). They showed that individual cells stochastically expressed *katG* and that such pulses were negatively correlated with antibiotic survival (Wakamoto et al., 2013).

Of note, these findings pointed towards the metabolism of bacteria as a mediator of antibiotic survival (Zheng et al., 2022). In line with this, metabolic dormancy was found to protect bacteria from antibiotic killing (Lopatkin et al., 2019; Stokes, Lopatkin, Lobritz, & Collins, 2019; Arnaud Gutierrez et al., 2017). To investigate the dependency of metabolic activity and antibiotic killing, Zheng and colleagues went on to determine which antibiotics are weakly or strongly dependent on the active metabolism of bacteria. They showed that more persister cells are killed by antibiotics which are weakly dependent on metabolism - such as gentamicin and colistin (Zheng, Stokes, & Collins, 2020). Promisingly, combinatory administration of strongly and weakly dependent antibiotics ampicillin and colistin was shown to maximise the efficacy in *E. coli* killing by these antibiotics; the authors proposed that using such combination therapy could reduce antibiotic toxicity and prevent recurrent infections (Zheng et al., 2020). In addition to this study, stimulating metabolism was shown to sensitise *E. coli, S. aureus,* and *Msm* to quinolone antibiotics (Arnaud Gutierrez et al., 2017; Ehrt, Schnappinger, & Rhee, 2018; Zheng et al., 2020), offering a promising avenue for developing more efficient treatment protocols against persistent bacteria.

Mycobacterial heterogeneity contributes to antibiotic tolerance

One of the reasons for prolonged TB treatment is the ability of *Mtb* to generate phenotypically distinct subpopulations during pathogenesis, with some of these subpopulations being tolerant to antibiotics (Chung, Johnson, & Aldridge, 2022). Some of the features that contribute to this heterogeneity are asymmetric growth and division patterns, environmental factors, and proteins that intrinsically reduce *Mtb* susceptibility to antibiotics, contributing to the persistence of bacteria even under antibiotic pressure.

Mycobacteria divide asymmetrically from the poles, producing daughter cells with differential size and growth rates. Aldridge et al. (Aldridge et al., 2012; Logsdon et al., 2017) and others (Joyce et al., 2012; Mouton et al., 2016; Botella et al., 2017) showed that cell division in mycobacteria is asymmetric, producing daughter cells that differ in size, growth rate, and susceptibility to antibiotics. Deletion of a key mediator of this phenotype, LamA, which inhibits growth from the new pole, was shown to sensitise *Mtb* to rifampicin and vancomycin - reinforcing a role for asymmetric division in the ability of different mycobacterial subpopulations to survive exposure to antibiotics (Hesper Rego, Audette, & Rubin, 2017). Additionally, it was shown that the new pole has a lag phase of variable duration prior to growth and variable cell wall composition, further contributing to the heterogeneity of mycobacteria (Hannebelle et al., 2020).

In addition to asymmetric growth patterns, variations at the transcriptional, translational and post-translational levels have been found to contribute to mycobacterial diversity within the population. Apart from the above-mentioned expression of *katG*, drug tolerance in *Mtb* was also found due to reversible phenotypic errors during translation. For instance, glutamate to glutamine and aspartate to aspargine substitution in the β-subunit of RNA polymerase were reported under nutrient-rich conditions, which led to tolerance to rifampicin (Javid et al., 2014).

Furthermore, *Mtb* possesses an ability to readily use different lipids as a carbon source, which was shown to affect cell morphology, growth state, and antibiotic susceptibility (Chung et al., 2022). Upon infection, *Mtb* was shown to induce the formation of so-called foamy macrophages, which accumulate lipid droplets that *Mtb* can use as a source of energy in vivo. To do so, it

uses enzymes, the isocitrate lyase 1 and 2, to metabolise lipids via the glyoxylate shunt (Peyron et al., 2008; Daniel, Maamar, Deb, Sirakova, & Kolattukudy, 2011). *Mtb* cells found in foamy macrophages were shown to be tolerant to rifampicin and isoniazid and were found to upregulate genes involved in dormancy and lipid metabolism, indicating how nutrient shifts can induce such states (Daniel et al., 2011).

In addition to these molecular adaptations, one of the factors that contributes to mycobacterial survival to antibiotics is a transcriptional regulator WhiB7. WhiB7 is a member of the WhiB family specific for Actinobacteria. In mycobacteria, WhiB7 was found to be involved in numerous cellular functions such as stress response, division, and pathogenesis (Geiman, Raghunand, Agarwal, & Bishai, 2006; Poulton et al., 2023; Reeves et al., 2013). *whiB7* expression is induced in response to diverse environmental stressors, including exposure of cells to antibiotics that inhibit protein synthesis (such as aminoglycosides, tetracyclines, and macrolides) and to compounds that interfere with DNA homeostasis (such as DNA topoisomerase inhibitors), entry into a stationary phase, heat shock, infection of macrophages and hypoxia (Morris et al., 2005; Burian, Ramón-García, Howes, & Thompson, 2012; Geiman et al., 2006; Larsson et al., 2012; Rustad, Harrell, Liao, & Sherman, 2008; Schrader et al., 2021). *whiB7* expression activates the expression of members of its regulon; this includes an efflux pump encoded by the gene *tap* and an aminoglycoside-modifying enzyme encoded by the gene *eis*; the latter reduces sensitivity to aminoglycosides (Burian et al., 2012). Such activation of *whiB7* and its regulon allows a temporary state of tolerance to aminoglycosides, while genetic mutations in the promoter of *whiB7* lead to MIC-shifted genetic resistance. In addition to these, genetic mutations in genes involved in the arginine biosynthesis pathway were found to induce increased expression of *whiB7*, leading to high persistence and increased tolerance to aminoglycosides of *Msm* and *Mtb* (Schrader et al., 2021).

1.2.3 Genetic alterations leading to tolerance and high persistence

Although persistence is always phenotypic in origin, tolerance and high persistence, which refers to an increase in the number of persisters in a bacterial population, can be induced

by mutations. The term "genetic tolerance" was introduced by Tomasz and colleagues to distinguish the tolerant populations Hobby and Bigger obtained upon switching bacteria to lower temperatures and the *Streptococcus* mutants they obtained. These mutants displayed a slower rate of killing at the whole population level when exposed to penicillin in contrast to biphasic killing exhibited by persisters (Tomasz, Albino, & Zanati, 1970).

Increased survival of the *hipA7* mutant

Adding to the notion that genetic mutations could drive decreased bacterial killing by an antibiotic, Moyed and Bertrand went on - in 1983 - to isolate mutants for which the mutation led to an increased fraction of persisters. To do so, they mutagenized *E. coli* K-12 with ethyl methanesulfonate before exposure to ampicillin. After successive cycles of exposure to the drug followed by a period of recovery - that is growth in the absence of the drug - they selected two mutants that displayed persistence at higher frequency and called them high persister or hip mutants. Gain-of-function mutations in the *hipA* loci conferred the ability of the two mutants, *hipA7* and *hipA9*, to have a 10,000-fold increase in survivors upon exposure to ampicillin (Moyed & Bertrand, 1983). In further studies, it was shown that *hipA* mutants displayed increased survival to numerous other stressors, including cycloserine, diaminopimelic acid starvation, phosphomycin, a DNA gyrase inhibitor, and nalidixic acid (Scherrer & Moyed, 1988).

The *hipA7* mutant has been extensively studied since its discovery. In 2004, as discussed previously, Balaban and colleagues showed that *hipA7* persisters have a reduced growth rate, allowing them to survive exposure to ampicillin (Balaban et al., 2004). They described *hipA7* persisters as a pre-existent population of nongrowing cells that are generated in a stationary phase, which resume replication after an extended time lag upon inoculation into fresh medium - characteristics of what they called "type I persistence" (Balaban et al., 2004). They also described another mutant, *hipQ*, and showed it differed from *hipA7* persisters as *hipQ* mutant was able to grow in the presence of the drug, but at a much slower rate - which they defined as characteristics of "type II persistence" (Balaban et al., 2004). Further research on the *hipA7* mutant revealed that HipA is part of the HipAB toxin-antitoxin (TA) system and that one of

the two mutations in the *hipA7* mutant - D291A - weakens the binding of the HipA with HipB (Schumacher et al., 2009). In fact, it was shown later that HipA is a toxin kinase that inhibits growth in the absence of a sufficient amount of the HipB antitoxin via phosphorylation of the glutamyl-tRNA synthetase GltX (Kaspy et al., 2013). Phosphorylation of GltX at Ser239, its ATP-binding site, leads to the accumulation of uncharged $tRNA^{Glu}$ in the cell, which results in the inhibition of translational processes, the activation of the stringent response, synthesis of (p)ppGpp and persister formation (Kaspy et al., 2013).

The role of TA modules in increased survival to antibiotics

As suggested above, TA modules have two elements: a stable toxin that interferes with an essential process and an unstable antitoxin that neutralises it without an activating signal (Ronneau & Helaine, 2019; Harms, Brodersen, Mitarai, & Gerdes, 2018). Although TA modules are widely distributed in bacteria, their distribution can vary even among closely related species. For example, while *Msm* possesses only three TA modules (MazEF, VapBC and Phd/Doc), *Mtb* possesses at least 79 (Sala, Bordes, & Genevaux, 2014). Major stress responses that regulate TA modules are the SOS and the stringent response, as summarised in (Ronneau & Helaine, 2019).

Research on the *hipA7* mutant linked TA modules with bacterial persistence for the first time, and TA systems were proposed as a mechanistic explanation of bacterial survival to antibiotics. However, the following years brought both supporting and contradicting findings on the importance of TA systems in persistence. Specifically, studies by Etienne Maisonneuve and Elsa Germain (Maisonneuve, Castro-Camargo, & Gerdes, 2013; Germain, Roghanian, Gerdes, & Maisonneuve, 2015) - which showed that deletion of 10 TA modules in *E. coli* (*mazF, chpB, relBE, dinJ/jafQ, jefM/joeB, higBA, prlF/jhaV, yafNO, mqsRA, hicAB)* led to decreased persistence as a result of increased (p)ppGpp, accumulation of polyphosphate and degradation of antitoxins by Lon protease - proved to be due to the presence of the ϕ80 bacteriophage in the deletion strains (Germain, Roghanian, Gerdes, & Maisonneuve, 2019). Hence, the hypothesis that TA modules have a central role in spontaneous persister formation was disproved in *E.*

coli. However, this result did not address whether the role of these TA systems could induce, e.g. growth inhibition under stress conditions, hence leading to decreased killing by antibiotics (Ronneau & Helaine, 2019).

For example, overexpression of RelE or MazF was shown to increase survival of *E. coli* upon antibiotic exposure, suggesting that these toxins contribute to increased survival to antibiotics in conditions when their antitoxin might be absent (Tripathi, Dewan, Siddique, & Varadarajan, 2014; Keren et al., 2004). Further, mutations in the YafN and VapB antitoxins led to an extended lag phase and thus increased persistence, suggesting a role of their cognate toxins in antibiotic survival (Winther & Gerdes, 2011; Levin-Reisman et al., 2017). In addition, mutations in the VapB antitoxin led to increased activity of the toxin VapC, which cleaves $tRNA^{fMet}$ and causes inhibition of translation and increased survival (Winther & Gerdes, 2011) - this mechanism was observed in both *E. coli* and *Msm* (Robson, McKenzie, Cursons, Cook, & Arcus, 2009). Furthermore, in *Salmonella* Typhimurium, a nonsense mutation in the *shpB* locus induced a 3- to 4-fold increase in survival following exposure to ampicillin (Slattery, Victorsen, Brown, Hillman, & Phillips, 2013; Helaine & Kugelberg, 2014) via a mechanism that remains unknown (Ronneau & Helaine, 2019). In addition to the role of the ShpAB system in *Salmonella* antibiotic tolerance, it was also shown that 13 other TA modules contribute to its survival during macrophage infection (Helaine et al., 2014). For example, overexpression of the toxins TacT, TacT2, and TacT3, which acetylate aminoacyl-tRNAs, contributes to an increase in the proportion of persister cells - and deletion mutants of these TA systems in *Salmonella* presented with a decreased level of persisters upon macrophage infection (Cheverton et al., 2016; Helaine et al., 2014; Ronneau & Helaine, 2019). Similarly, it was shown that overexpression of TisB, a membrane-disrupting toxin which is part of the SOS response regulon, induces membrane depolarisation and decreases ATP levels of a fraction of cells upon prolonged fluoroquinolone ciprofloxacin exposure, leading to an increase in *E. coli* persistence up to 100-fold. Importantly, TisB-induced depolarisation from its native locus is only observed in around 20% of the cells upon prolonged exposure to ciprofloxacin even though *tisB* transcript is found within a few minutes of the treatment initiation (Vogel, Argaman, Wagner, & Altuvia, 2004). In addition, membrane depolarisation is only observed in the later stages of the exposure, sug-

gesting a delay in the translation and/or accumulation of TisB (Berghoff, Hoekzema, Aulbach, & Wagner, 2017; Edelmann & Berghoff, 2022). Hence, it was proposed that the actual function of TisB in persistence is the prevention of premature awakening, which would lead to increased survival probability beyond the duration of the antibiotic treatment (Edelmann & Berghoff, 2022). Further studies will answer whether other toxins are also involved in bacterial persister stabilisation and reawakening.

Evolution of mutations conferring genetic tolerance and high persistence

Studying mutants that confer increased survival to antibiotics has proved useful in obtaining information on how persistence develops. Hence, research turned to evolution and selection experiments under exposure to antibiotics or mutagens to characterise evolved strains, and to study if such phenomena could lead to the development of mutations that cause increased survival in patients during antibiotic treatment.

In a paper published by Fridman and colleagues, it was shown that exposure to intermittent high concentrations of antibiotic selects for mutations conferring increased survival (Fridman, Goldberg, Ronin, Shoresh, & Balaban, 2014). In this study, Friedman and colleagues exposed *E. coli* to 15xMIC ampicillin and observed that bacteria evolved mutations conferring tolerance through increased lag time before regrowth (tolerance by lag), wherein an increased lag time before division helped bacteria evade antibiotic-induced killing (Fridman et al., 2014). Another study in *E. coli* showed that high levels of multidrug tolerance were obtained by a single or a few base pair mutations upon exposure to three to ten cycles of antibiotic exposure. These mutants displayed increased survival to the antibiotic they were exposed to (auto-resistance to amikacin), and to other antibiotics (allo-resistance to gentamicin, kanamycin, and ofloxacin fluoroquinolone) (Van Den Bergh et al., 2016). Concerningly, the authors noted that these findings also indicate that the emergence of high persistence could occur during patient treatment (Van Den Bergh et al., 2016).

In fact, high persistence and tolerant mutants were indeed identified in clinical isolates. For example, Mulcahy and colleagues identified an isolate of *P. aeruginosa* that displayed high

persistence due to a loss-of-function mutation in *mexZ*, a repressor of the MexXY-OprM efflux pump, leading to a 100-fold increase in survivors upon exposure to ofloxacin (Mulcahy, Burns, Lory, & Lewis, 2010). Furthermore, in a genome-wide association study of *Mtb* isolates from China, Hicks and colleagues identified that mutations in a transcriptional factor *prpR* - which regulates propionate catabolism that induce tolerance of *Mtb* upon exposure to ofloxacin, rifampicin, and isoniazid in culture medium and in human macrophages (Hicks, Carey, Yang, Zhao, & Fortunea, 2019). Tolerance of *prpR* mutants occurred through altered metabolism of propionyl-CoA in the absence of vitamin B_{12}, leading to propionyl-CoA accumulation and growth inhibition. In addition, the authors noted that *prpR* mutations - that are found in 5% of drug-susceptible isolates in China - might therefore contribute to TB treatment failure (Hicks et al., 2019). In addition, Safi et al. identified in *Mtb* clinical isolates transient frameshift mutations in the homopolymeric tracts (regions with repetitive DNA bases) of the *glpK* gene involved in glycerol catabolism that led to the formation of small colony variants tolerant to isoniazid, rifampicin, and moxifloxacin (Safi et al., 2019). Interestingly, the mutations were lost upon removal of the drug, indicating that mutations causing genetic tolerance could be transiently heritable (Safi et al., 2019).

Finally, studies such as those done by Torrey and colleagues and Schrader and colleagues (Torrey et al., 2016; Schrader et al., 2021), who identified mutants of *Mtb* and an *Mtb* model organism *Mycobacterium smegmatis* (*Msm*) displayed increased survival to antibiotics, further contributed to identifying mutations causing antibiotic tolerance. They showed that identified mutants had mutations in genes involved in lipid biosynthesis, carbon metabolism, toxin-antitoxin systems, metabolic pathways, and transcriptional regulators, suggesting that persister formation involves multiple pathways in mycobacteria as documented in other bacterial species. Finally, it was also shown that mutations that confer high persistence could provoke collateral damage: in this vein, Schrader and colleagues isolated mutants in the arginine biosynthesis pathway, whereby overexpression of the transcriptional factor *whiB7* and members of its regulon led to high persistence to kanamycin and rifampicin and also MIC-shifted resistance to macrolides (Schrader et al., 2021).

1.2.4 Persisters and tolerant cells are harbingers of MIC-shifted resistance

Persistence and tolerance have clinical consequences: they require prolonged treatment and/or multiple rounds of antibiotic treatment for relapsing infections. Unfortunately, prolonged antibiotic exposure also provides a reservoir of bacteria that can develop mutations leading to MIC-shifted resistance. This was proposed back in 1988 by Moreillon and Tomasz, who suggested that repeated antibiotic courses in patients, which select for tolerant mutants, might generate a pool of viable cells that could become resistant to the antibiotic (Moreillon, Tomasz, & Tomasz, 1988).

The link between tolerant strains and the development of resistance was experimentally shown in 2017, when Levin Reisman and colleagues showed that mutations that cause tolerance precede the development of MIC-shifted resistance. They reported in *E. coli* that daily, intermittent exposure to ampicillin fostered the development of mutations that caused tolerance by lag and further MIC-shifted resistance (Levin-Reisman et al., 2017). In fact, they observed that resistance mutations occurred at higher rates in already tolerant bacterial cells. The authors suggested that one of the reasons for this might be the fact that tolerance mutations arise more frequently in the population owing to a larger target size; indeed, while MIC-shifted resistance to ampicillin is restricted to mutations in the *ampC* gene promoter, mutations in more than one gene can cause tolerance (Levin-Reisman et al., 2017).

The evolution of tolerance to MIC-shifted resistance was further shown *in vivo* in a clinical setting. In this vein, Liu and colleagues investigated isolates from patients infected with methicillin-resistant *S. aureus* (MRSA), in which infection persisted for at least two weeks despite antibiotic treatment. The treatment consisted of five days of vancomycin, the addition of rifampicin on day four, and the replacement of vancomycin with daptomycin on day eight. The authors reported the rapid emergence of mutations conferring tolerance to vancomycin and daptomycin, followed by the emergence of MIC-shifted resistance to rifampicin at day nine, even though the patient received combination treatment (J. Liu, Gefen, Ronin, Bar-Meir, & Balaban, 2020). To confirm these results, the authors conducted evolution experiments *in vitro*

with the parental strain, following the same antibiotic regime used in the clinic. They confirmed that tolerance to vancomycin and daptomycin allowed the development of resistance to rifampicin only under combination therapy. Rather paradoxically, the combination treatment killed rifampicin-resistant mutants in the wild-type background. Hence, the authors concluded that the combinatory treatment might have been effective in the patients if it had been administered before the emergence of genetic tolerance, indicating the importance of diagnosing tolerance before designing antibiotic therapy (J. Liu et al., 2020).

The development of resistance from tolerant mutants was further supported by the studies showing that high persistence mutants more often acquire mutations that cause MIC-shifted resistance, establishing a positive association between persistence and mutation rates (Windels et al., 2019). Similarly, it was shown that MIC-shifted resistance developed *de novo* from the pool of persistent *Mtb* upon prolonged exposure to lethal concentrations of rifampicin and moxifloxacin (Sebastian et al., 2017). Because exposure to these antibiotics increases the level of ROS, rifampicin-induced persisters carried increased levels of hydroxyl radicals that generated genome-wide mutations, including mutations in *gyrA* or *rpoB* that caused MIC-shifted resistance (Sebastian et al., 2017). Building on this, Wilmaerts and colleagues demonstrated that persisters accumulate oxidative DNA damage when subjected to fluoroquinolone treatment. They showed that activating a specific transcription-coupled repair pathway led to an increased mutation rate and the emergence of resistant bacteria (Wilmaerts, Focant, Matthay, & Michiels, 2022). In essence, these studies linked cells displaying a decreased rate of killing by an antibiotic to increased mutagenesis.

Both tolerance and resistance provide bacteria survival advantages under antibiotic pressure, though their benefits vary depending on environmental conditions and treatment regimes. Resistance mutations enable bacteria growth during prolonged exposure to an antibiotic but often at a fitness cost in the absence of the drug, suggesting that continuous exposure to antibiotics favours the selection of resistance (Q. Zhang et al., 2011; Baym et al., 2016; Toprak et al., 2011; Drlica, 2003). Conversely, tolerance emerges as a favourable strategy when bacteria are exposed to high concentrations of an antibiotic in growth-inhibitory conditions. As such, tolerance might evolve under antibiotic concentrations that challenge the development of resistance,

requiring cyclical high-dose treatments intermittent with growth periods for the selection of tolerant mutants (Van Den Bergh et al., 2016; Mulcahy et al., 2010; Stepanyan et al., 2015; Michiels, Van den Bergh, Verstraeten, & Michiels, 2016). Then, such mutations were shown to even accelerate the evolution of resistance in conditions that favour the emergence of resistance (J. Liu et al., 2020; Levin-Reisman et al., 2017; Windels et al., 2019). This interplay suggests that while tolerance and resistance might be seen as distinct strategies, their co-evolution is highly intertwined (Windels, Van Den Bergh, & Michiels, 2020).

In summary, the observations made by Moreillon and Tomasz in 1988 have proved to be true over further research. Not only is the link between persistence and development of MIC-shifted resistance based on an increased pool of viable cells able to mutate, but more data is pointing towards persistent and tolerant cells having an increased probability of developing mutations that could render them resistant to the antibiotic (Windels et al., 2019; Bollen, Louwagie, Verstraeten, Michiels, & Ruelens, 2023). The choice of coping mechanisms in response to antibiotics seems to also depend on both the environment and the concentration of the drug. Low and continuous doses of antibiotics were shown to favour the development of MIC-shifted resistance, while tolerance and persistence mechanisms are favoured during irregular exposures to high concentrations of a drug (van den Bergh et al., 2017; Fridman et al., 2014; Charlebois, 2023; Sulaiman & Lam, 2021).

To conclude, the intricate relationship between bacterial tolerance, persistence, and their role in the development of MIC-shifted resistance highlights the challenges we face in the fight against infectious diseases. As the incidence of MIC-shifted resistance increases, we are just starting to grasp the role of tolerance and persistence in their development. Therefore, understanding the mechanisms behind bacterial survival to antibiotics through tolerance and persistence has become paramount to prevent MIC-shifted resistance. Investigating these phenomena is essential for developing novel targeted approaches and improving existing therapeutics, with the ultimate goal of eradicating AMR.

1.3 Motivation and Objectives

With a broad aim of identifying novel targets to prevent antibiotic tolerance and resistance, the main goal of this project was to gain insight into the mechanisms of mycobacterial mutants that display high persistence and/or genetic tolerance, which previously provided a powerful route of studying mechanisms of phenotypic resistance. By exposing the wild-type *Msm* to antibiotics, the previous members of the lab isolated the mutants using the methodology described in the next Chapter 2 (Schrader et al., 2021). In comparison to a class 3 pathogenic *Mtb*, *Msm* is a non-pathogenic class 1, fast-growing mycobacteria (doubling time of 3-4 hours compared to 24 hours for *Mtb*) and it shares more than 50% amino acid sequence identity and the same function with *Mtb* proteins (Etienne et al., 2005; Lelovic et al., 2020; Sparks, Derbyshire, Jacobs, & Morita, 2023; Judd et al., 2021). Hence, it is used as the model mycobacterium species, and we used it in this project intending to also translate the findings to *Mtb*.

The work presented here is divided into three sections. First, I aimed to characterise the phenotypes of two of the isolated *Msm* mutants upon exposure to different classes of antibiotics, which contained mutations related to a gene encoding for a tRNA m^1A58 tRNA methyltransferase MsTrmI. I aimed to understand how identified mutations impact this enzyme, with a starting hypothesis that the increased survival phenotype to antibiotics of these mutants was due to identified genetic mutations. Second, I aimed to investigate whether deletion of *mstrmI* mimics identified phenotypes of the *mstrmI* mutants. Furthermore, I aimed to investigate whether the findings in *Msm* would pertain to *Mtb*, by generating an *Mtb mstrmI* homologue. Finally, I aimed to investigate the molecular mechanisms behind increased survival upon antibiotic exposure due to loss of tRNA m^1A58 methylation.

Chapter 2

Results I: Loss of *mstrmI* causes antibiotic tolerance and resistance in *Mycobacterium smegmatis*

Contents

2.1 Introduction 55

2.2 Results 55

2.2.1 Two mutants recovered in the screen contain mutations related to a gene encoding a tRNA methyltransferase 55

2.2.2 The *mstrmI* mutants display increased survival to the aminoglycoside kanamycin 59

2.2.3 Expression of *mstrmI* in both mutants restores sensitivity to aminoglycosides 61

2.2.4 The *mstrmI* mutants exhibit MIC-shifted resistance to macrolides . . 64

2.2.5 AG mutant, but not GS, has a growth defect 66

2.2.6 The effect of the A-to-G mutation on *mstrmI* transcripts 68

2.2.7 The G128S mutation affects the protein abundance of MsTrmI 69

2.2.8 MsTrmI^{G128S} is not post-translationally modified 73

2.3 Summary 76

2.1 Introduction

Isolation and studying of mutants that display tolerance and/or high persistence due to specific mutations is a powerful tool to investigate mechanisms of tolerance, persistence, and high persistence (Moyed & Bertrand, 1983; Schrader et al., 2021; Fisher, Gollan, & Helaine, 2017). To isolate increased survival mutants, Schrader and colleagues - from the Vaubourgeix laboratory - developed a four-step method that allows for spatiotemporal separation of MIC-shifted resisters from survivors that display non-canonical resistance; this includes increased survival mutants and WT persisters (Schrader et al., 2021). The screen was conducted using the model mycobacterium *Mycobacterium smegmatis* (*Msm*) to extend the results to *Mtb*. This chapter describes my investigations into the AMR phenotypes of two isolated mutants that contain mutations related to a tRNA methyltransferase. The chapter begins by describing the screen that was previously done to obtain the two mutants in order to clarify the methodology used to obtain them and test their phenotypes.

2.2 Results

2.2.1 Two mutants recovered in the screen contain mutations related to a gene encoding a tRNA methyltransferase

To isolate mutants that display increased survival phenotype, 10^7 *Msm* were seeded onto a filter and then positioned on an agar plate containing an antibiotic of choice at a concentration of 10x MIC. The exposure time was determined to kill approximately 99.9999% of the wild-type population for each antibiotic (Schrader et al., 2021). During the exposure to an antibiotic, MIC-shifted resisters with more than a 10xMIC shift were able to grow and appear as colonies. Following the exposure, the filter was transferred to an agar plate containing 2x MIC of the

same antibiotic, allowing genetic MIC-shifted resisters with MIC change between 2- and 10-fold to grow and appear as colonies. Finally, the filter was transferred to an agar plate containing 0.4% charcoal for 24 hours to absorb any residual antibiotic and then to an agar plate without any antibiotic (recovery stage). At this last stage, all non-MIC-shifted survivors grew, allowing spatial separation of potential increased survival mutants and MIC-shifted resisters.

During the second stage of the method, all the colonies that grew during the recovery stage were isolated and outgrown in the liquid medium, and the MIC to the drug they were isolated from was measured to confirm there was no increase compared to the WT *Msm*. Those candidates that did not have a shift in MIC were further tested, as they can be WT persisters of increased survival mutants. To distinguish between those two cases, the third step involved testing each picked colony for the fraction of survivors relative to the WT.

To test the fraction of survivors, the third step involved seeding each isolated candidate onto a filter and, as in the first step, exposing it to 10x MIC of an antibiotic. Following exposure, filters were transferred onto a plate with charcoal for 24 hours to remove residual antibiotics and then to an agar plate for recovery - until the appearance of the colonies. As the exposure time was determined to kill most of the WT population, the WT strain following the exposure only formed a few colonies, and the number of surviving bacteria of the potential increased survival mutants was compared to this strain. Any candidate with an increased number of survivors compared to the WT qualified as an increased survival mutant, with the strongest phenotypes having a lawn of bacteria on the filter (Fig. 2.1). Finally, in the fourth step, each increased survival mutant was sent for whole genome sequencing to identify mutations that arose during the screen and which might be responsible for the increased survival phenotype.

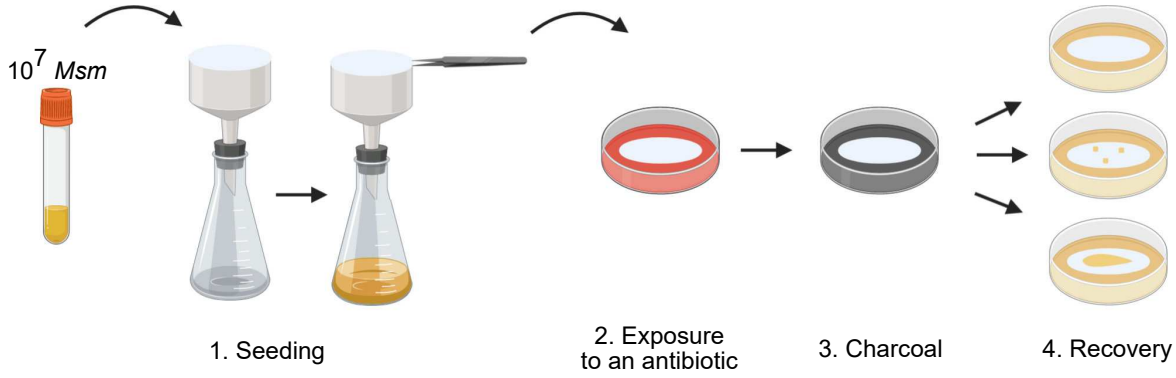


Figure 2.1: **Experimental setup of the filter-based method to evaluate the fraction of survivors**. (1) *Msm* grown to an exponential phase is diluted to 10^7 and seeded onto a filter. (2) The filter with *Msm* is transferred onto a plate containing 10x MIC of an antibiotic against the fraction of survivors is assessed. (3) Following the exposure, the filter is transferred onto a plate containing charcoal to absorb residual antibiotics and incubated for 25 hours. (4) After 24 hours on the charcoal plate, the filter is transferred to a recovery plate and incubated until the colonies appear. Shown are examples of testing outcomes, with no survivors, few colonies as survivors, or increased survival observed as a lawn of colonies.

The screen published in (Schrader et al., 2021) led to the selection and isolation of 28 mutants, of which 21 exhibited reproducible increased survival to the aminoglycoside kanamycin. Of those, two contained mutations related to the gene encoding for a tRNA methyltransferase (TrmI), thereafter dubbed *mstrmI* (*Mycobacterium smegmatis trmI*). While one of the *mstrmI* mutants had a mutation in the promoter region of the gene (an A-to-G small nucleotide polymorphism 15 bp before the open reading frame (ORF) start codon), the other mutant had a mutation that led to a glycine-to-serine substitution (G128S) (Fig. 2.2A). Based on these mutations, mutants were termed AG and GS, respectively. The gene *mstrmI* encodes for a tRNA m^1A58 methyltransferase, an enzyme that transfers methyl group onto tRNA(s) in the TΨC loop at the position A58 - the position that is present in all *Msm* tRNA species (Fig. 2.2B-D).

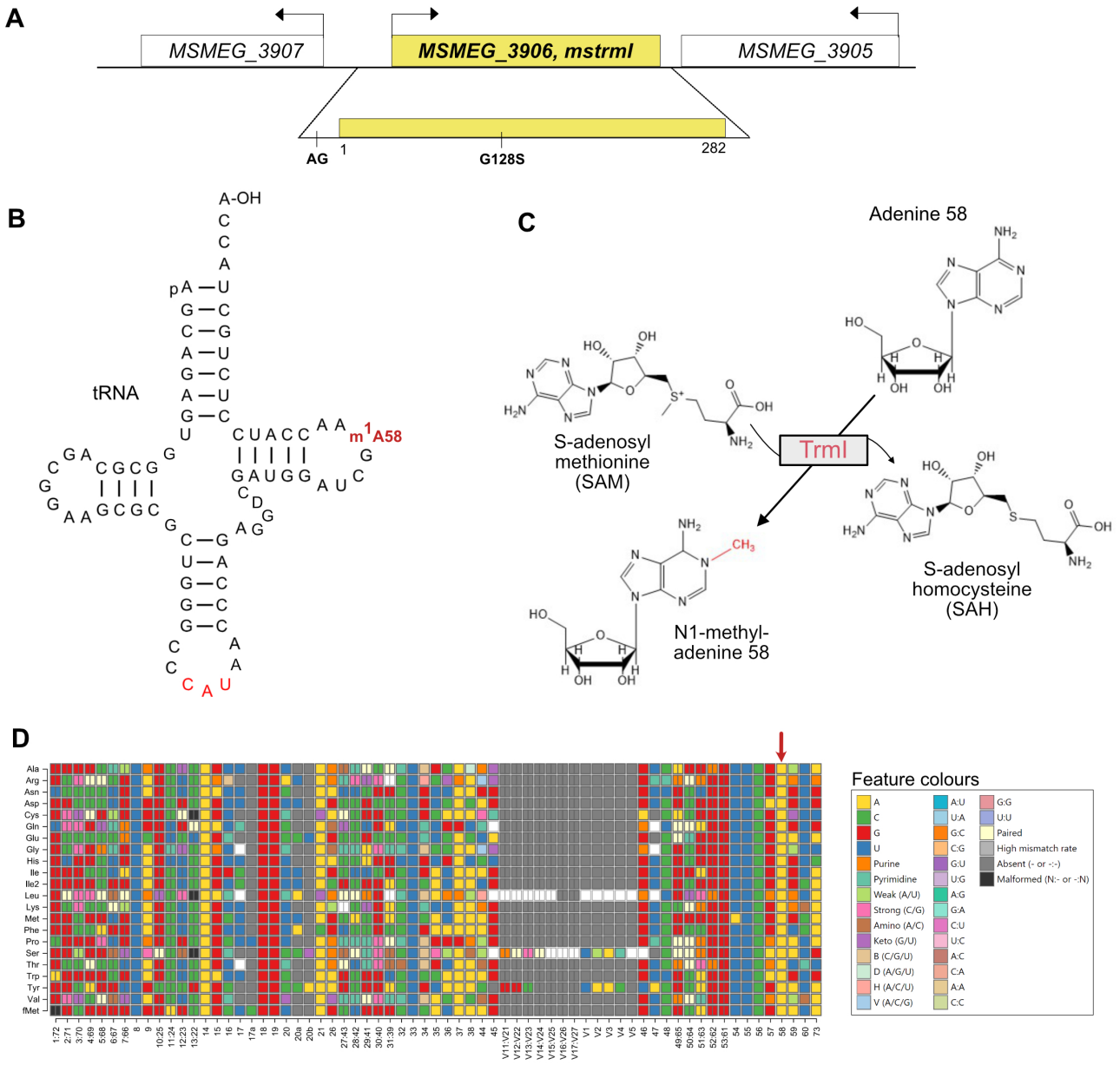


Figure 2.2: **Two mutants isolated in the screen contained mutations related to a tRNA A58 methyltransferase *mstrmI***. (A) Visual representation of A-to-G and G128S mutations related to *mstrmI*. (B) A schematic of a tRNA with indicated m^1A58 site. (C) A schematic of TrmI enzymatic activity. The schematic was generated using ChemDraw. (D) A tilemap displaying the consensus sequence of tRNA decoding twenty amino acids in *Msm*, corresponding to nucleotide colour legend. On the Y axis are marked amino acids which will be encoded by tRNAs, and on the X axis are positions in the tRNA. Created via tRNAviz (B. Y. Lin et al., 2019)

2.2.2 The *mstrmI* mutants display increased survival to the aminoglycoside kanamycin

I began by investigating if the two *mstrmI*-related mutants displayed increased survival upon exposure to kanamycin, the antibiotic used to isolate them. WT *Msm* and both mutants were seeded on filters and exposed for 12 hours to 10xMIC kanamycin. Filters were then transferred to charcoal plates for 24 hours prior to recovery on rich growth-permissive agar for approximately three days until the colonies appeared (Methods section 6.4). Both mutants displayed increased survival upon exposure to kanamycin as a lawn grew on filters rather than a few colonies (Figure 2.3, first row).

To investigate whether an increased survival of the *mstrmI* mutants was specific to kanamycin, I exposed both mutants to various antibiotics, including two other aminoglycosides (amikacin and gentamicin), a transcriptional inhibitor (rifampicin) and a DNA gyrase inhibitor (levofloxacin). In addition to increased survival to kanamycin, both mutants exhibited increased survival upon exposure to amikacin and gentamicin but not to rifampicin and levofloxacin (Fig. 2.3), suggesting that this phenotype might be specific to aminoglycosides. The two mutants in some of the experiments presented a decreased fraction of survival to rifampicin, which I did not follow up on as I focused on the mechanisms behind increased survival. Of note, no other drugs have been tested except macrolides, which is shown later on in this Chapter.

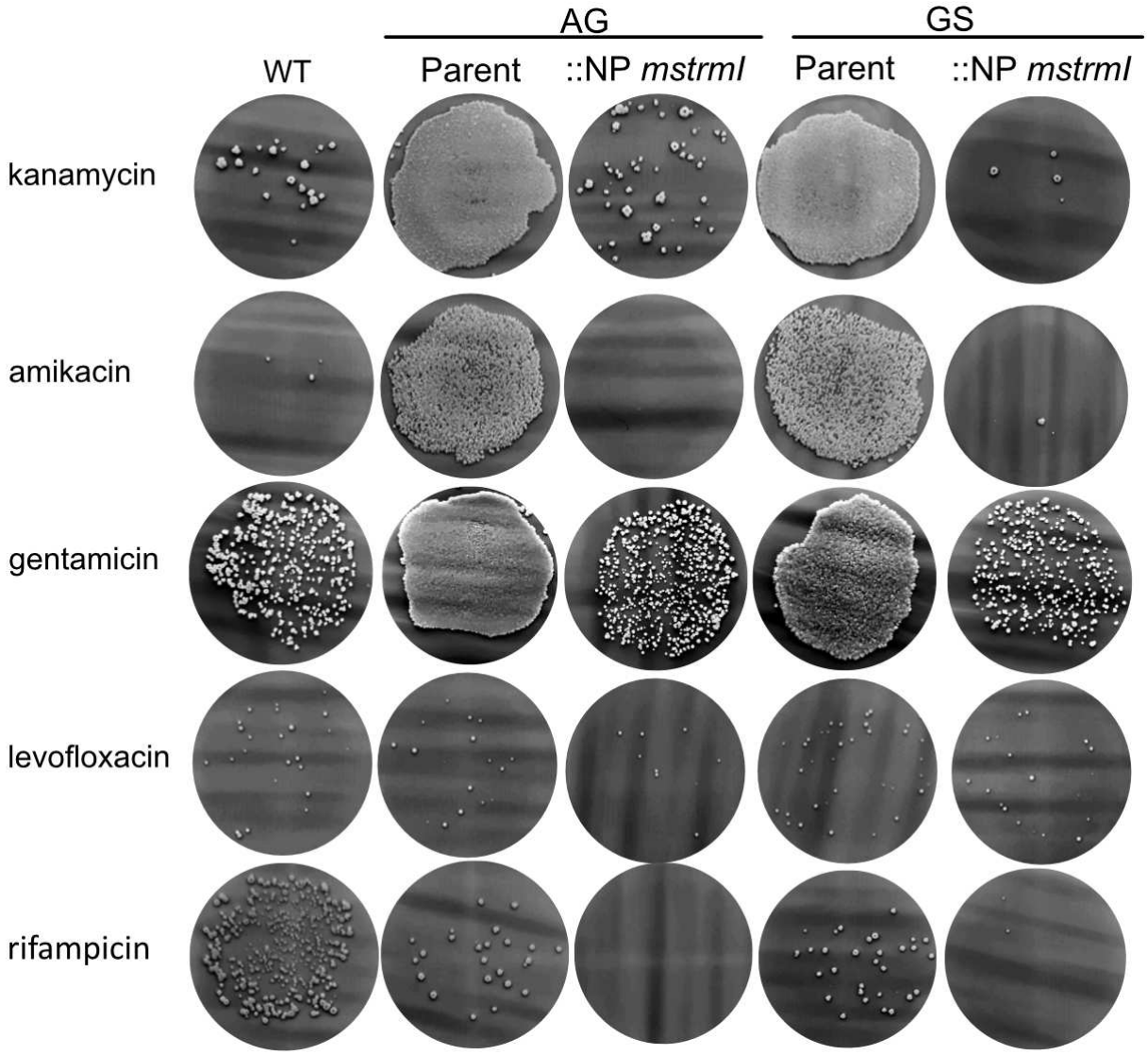


Figure 2.3: **The *mstrmI* mutants display increased survival upon exposure to aminoglycosides kanamycin, amikacin, and gentamicin**. WT *Msm*, AG and GS mutants and their complemented strains containing an integrated copy of *mstrmI* with its native promoter (NP *mstrmI*, described in Section 2.2.3) were exposed to 10x MICs of one of the six antibiotics presented here and transferred to charcoal and then recovery plate until the appearance of the colonies (as described in 6.4). Representative of at least three experiments.

To quantify the survival of both mutants, I exposed WT *Msm*, both mutants and the complemented strains to kanamycin at a concentration of 5-fold the MIC in a growth-permissive liquid medium for 60 hours. Compared to the WT *Msm* that displayed biphasic killing kinetics, both mutants exhibited a slower rate of killing at all times and a three to four-log increase in survival to kanamycin after 60 hours of exposure to kanamycin (Fig. 2.4). These killing kinetics might reflect both tolerance and high persistence to kanamycin.

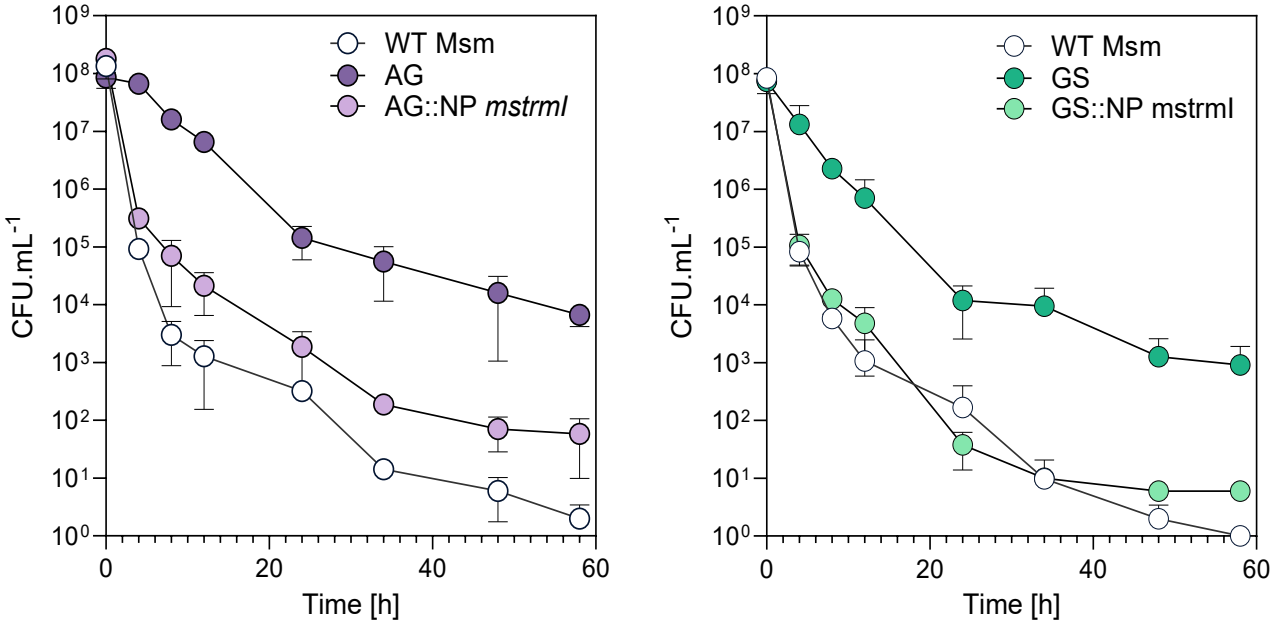


Figure 2.4: **The *mstrmI* mutants display decreased killing to kanamycin in liquid media.** Strains were exposed to 5xMIC (3.5 μg/mL) kanamycin and killing was observed as CFUs over the course of 60 h. Symbols, means of three independent experiments, with error bars +/- SD.

2.2.3 Expression of *mstrmI* in both mutants restores sensitivity to aminoglycosides

Given the nature of the mutations, it proved hard to predict whether they were loss-of-function or gain-of-function mutations. To gain some insights, I constructed plasmids that integrate into the chromosome and allow for the expression of either the WT or $mstrmI^{G128S}$ and expressed them in the AG and GS mutants. Expression was driven by either the native promoter (NP) of *mstrmI* or a strong promoter P1 (Ehrt et al., 2005) regulated by anhydrotetracycline (ATc)

(TetON). Both mutants were transformed with these constructs. Expression of *mstrmI* under both NP or TetON with sufficient ATc supplementation restored survival upon exposure to kanamycin to a WT level, in an ATc-dependent manner (Fig 2.3, 2.5A,B). Of note, the AG mutant that contained integrated TetON *mstrmI* showed a decrease in the increased survival even in the absence of ATc, which could be due to leakage of the construct (Fig 2.5A).

Finally, the expression of the $mstrmI^{G128S}$ in the WT *Msm* did not result in increased survival, indicating that the G128S mutation shows no dominant effect of mutations as a diplod, and that it is likely not a dominant gain-of-function mutation (Fig 2.5C). To have native regulation of the gene expression, the following experiments that required complementation were conducted with the WT allele of *mstrmI* expressed under its NP.

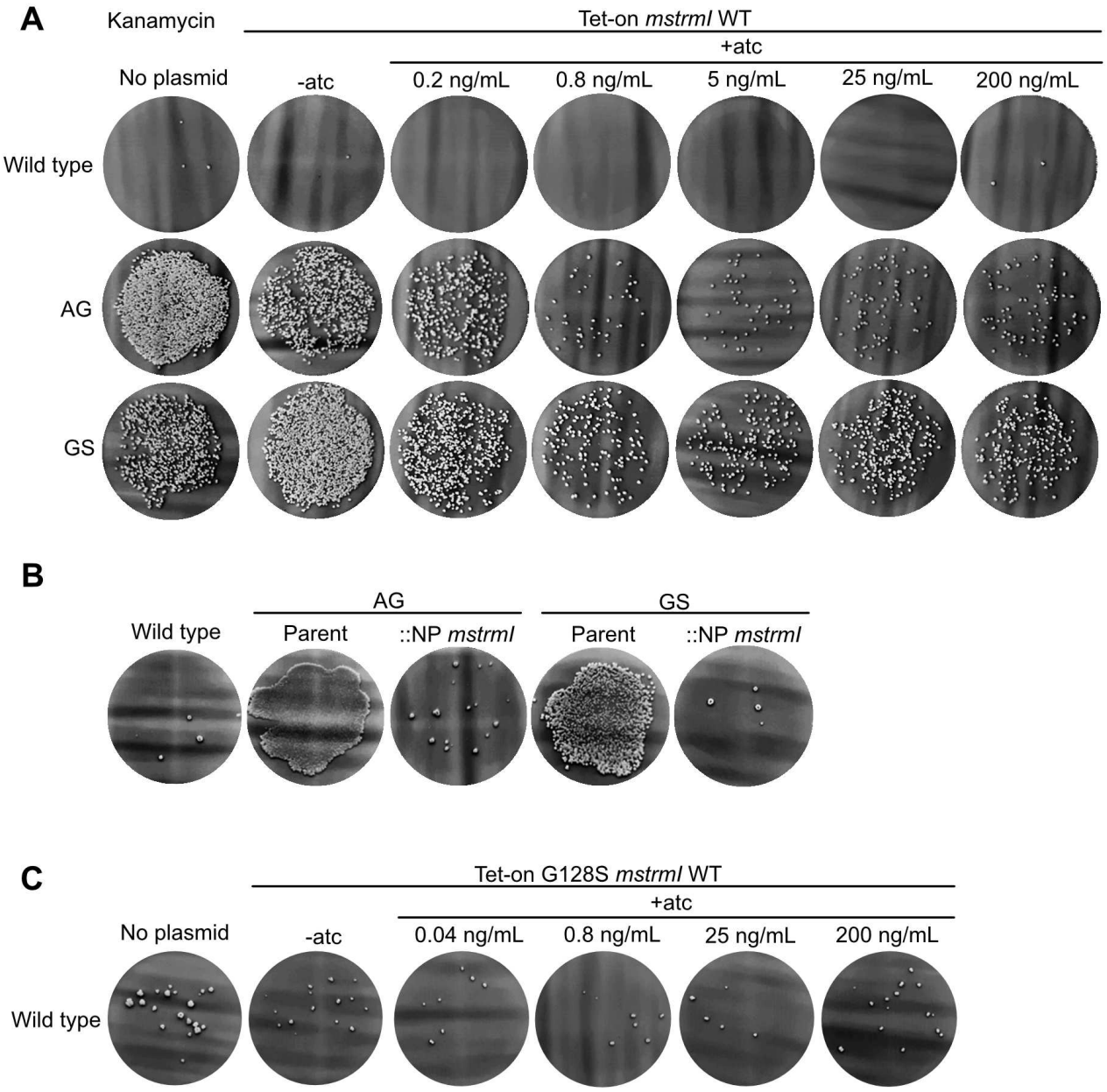


Figure 2.5: **The expression of *mstrmI* in both mutants restores WT sensitivity to aminoglycosides.** WT Msm, AG and GS mutants were transformed with TetON or NP-containing construct with copies of WT *mstrmI* or G128S mutated allele. (A) Survival upon exposure to kanamycin of the parental and transformed strains grown in the media containing no or indicated concentrations of ATc. Cultures were seeded onto filters, and filters were exposed to 10x the MIC of kanamycin. Survivors were recovered following filter transfer to charcoal and then to recovery plates. Representative of at least three independent experiments. (B) The WT, AG and GS strains were transformed with a WT allele containing an NP region of the gene. Representative of at least three experiments. (C) WT Msm was transformed to express the G128S *mstrmI* allele under the TetON regulation. Strains were grown in the media containing no or indicated concentrations of ATc to express G128S *mstrmI* prior to exposure to kanamycin. Representative of at least three independent experiments.

2.2.4 The *mstrmI* mutants exhibit MIC-shifted resistance to macrolides

To verify that increased survival to aminoglycosides was not due to MIC-shifted resistance, I measured the MIC of the *mstrmI* mutants to the antibiotics used to assess the fraction of survivors. To do so, I measured the growth of the WT *Msm*, AG and GS mutants and their complemented strains when exposed to nine concentrations of kanamycin, amikacin, gentamicin, levofloxacin and rifampicin; the optical density at 600 nm was measured at 72 hours of incubation with the drug. Both mutants displayed the same MIC as WT *Msm* for all tested antibiotics, ruling out that increased survival was caused by MIC-shifted resistance (Fig 2.6A-E).

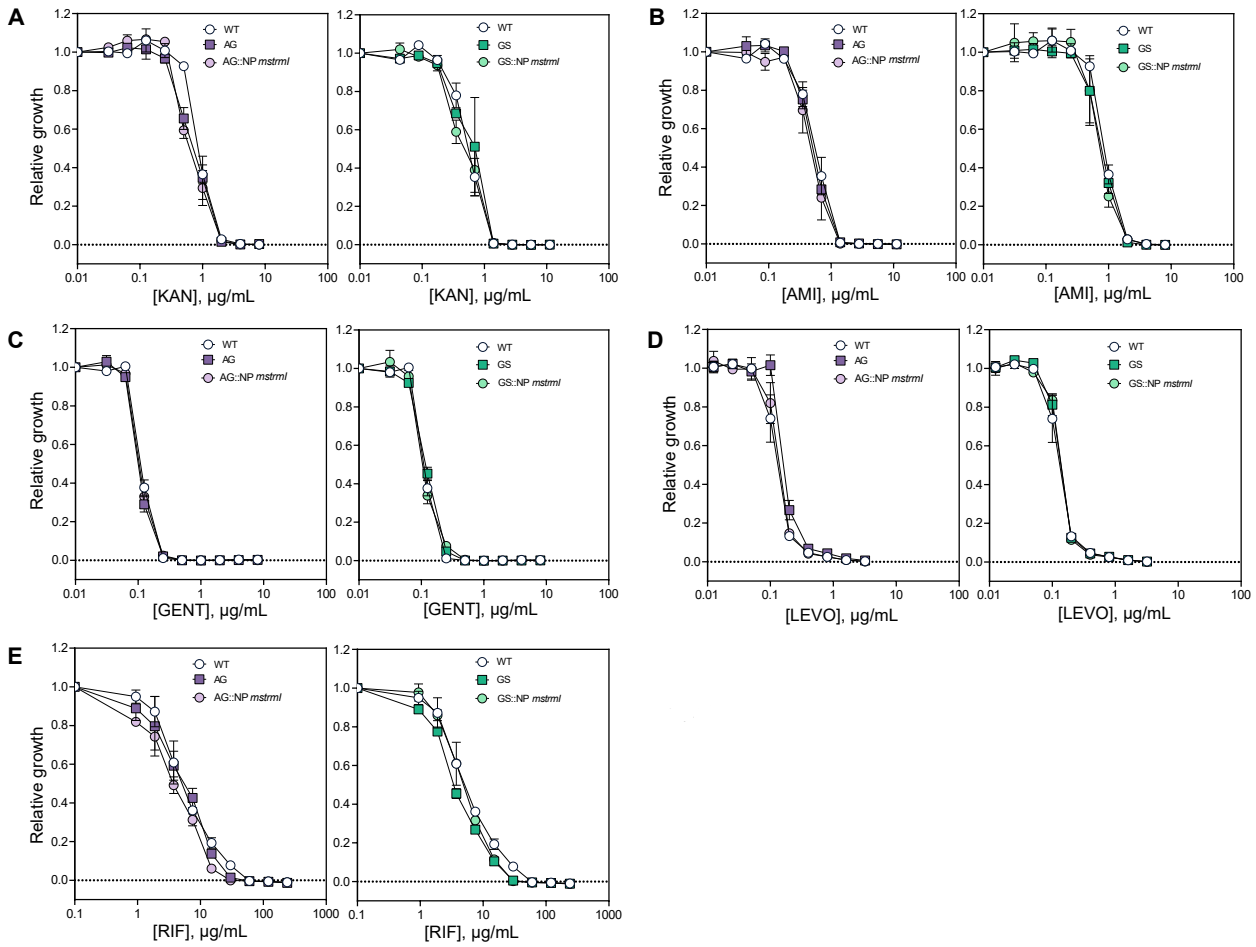


Figure 2.6: **Minimum inhibitory concentrations of *Msm* AG and GS mutants**. WT *Msm*, AG and GS mutants and their complementation strains were exposed to (A) kanamycin 0-11.2 μg/mL, (B) amikacin 0-8 μg/mL, (C) gentamicin 0-8 μg/mL, (D) levofloxacin 0-3.2 μg/mL, and (E) rifampicin 0-240 μg/mL and OD_{600} was measured. Graphs show growth relative to a no-antibiotic growth media, and each symbol is a mean of two technical repeats. Representative of at least three independent experiments.

In addition, I tested the MICs of both mutants to the macrolides clarithromycin and erythromycin, another type of protein synthesis inhibitors. Notably, macrolides inhibit protein synthesis by targeting the 50S ribosomal subunit and halt the formation of a polypeptide chain. Compared to the WT *Msm*, both mutants grew at higher concentrations of macrolides, suggesting that loss of *mstrmI* induces MIC-shifted resistance to macrolides (Fig. 2.7). This phenotype was complemented to the WT MIC level with the WT allele of *mstrmI* (Fig. 2.7). Collectively, these results demonstrate that the mutants for which the function of a tRNA methyltransferase is altered exhibit various forms of AMR: increased survival to aminoglycosides and MIC-shifted resistance to tested macrolides.

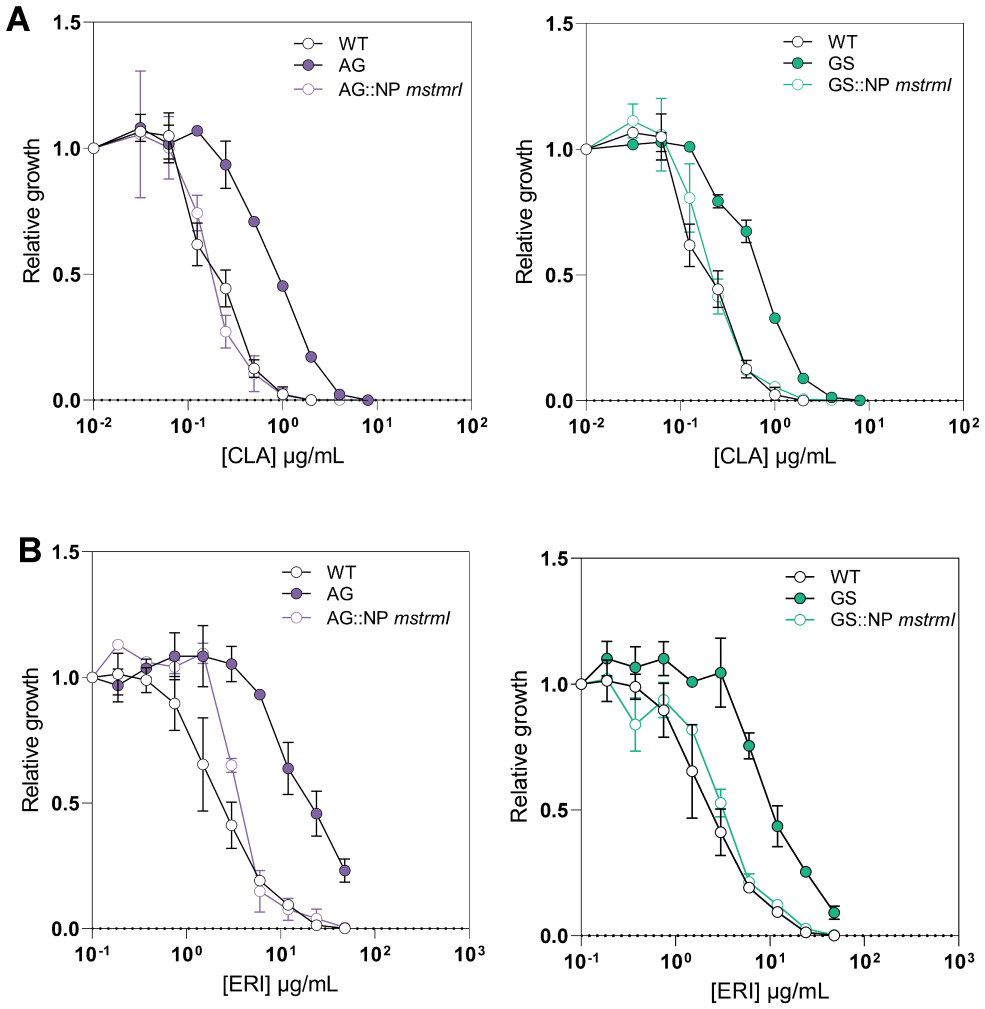


Figure 2.7: ***mstrmI* mutants exhibit MIC-shifted resistance to macrolides**. WT *Msm*, AG and GS mutants and their complementation strains were exposed to (A) clarithromycin 0-8 μg/mL or (B) erythromycin 0-48 μg/mL and grown in a 96 well plate for 48h. Graphs show growth relative to no antibiotic growth media, and each symbol is a mean of two technical repeats. Representative of three independent experiments.

2.2.5 AG mutant, but not GS, has a growth defect

Next, I wanted to assess whether the mutations of *mstrmI* impact the growth of these strains since slow growth has been observed as a mediator of decreased bacterial killing by antibiotics (Pontes & Groisman, 2019; Gollan et al., 2019; Tuomanen et al., 1986; Lopatkin et al., 2019). I measured the growth of WT *Msm* and *mstrmI* mutants as OD_{600} in media over the course of 30 hours and found that compared to the WT *Msm*, only one of the mutants, AG, displayed a decrease in the growth rate observed as around 0.9x of the growth rate of the WT *Msm*. On the other hand, the GS mutant retained the same growth rate as the WT *Msm*. Introducing

the WT *mstrmI* allele into the AG strain complemented the growth defect of the AG mutant (Fig. 2.8). Since only one of the *mstrmI* mutants presented with a slight growth defect, this suggested that slow growth is not the sole mediator of the increased survival of these two mutants upon exposure to antibiotics.

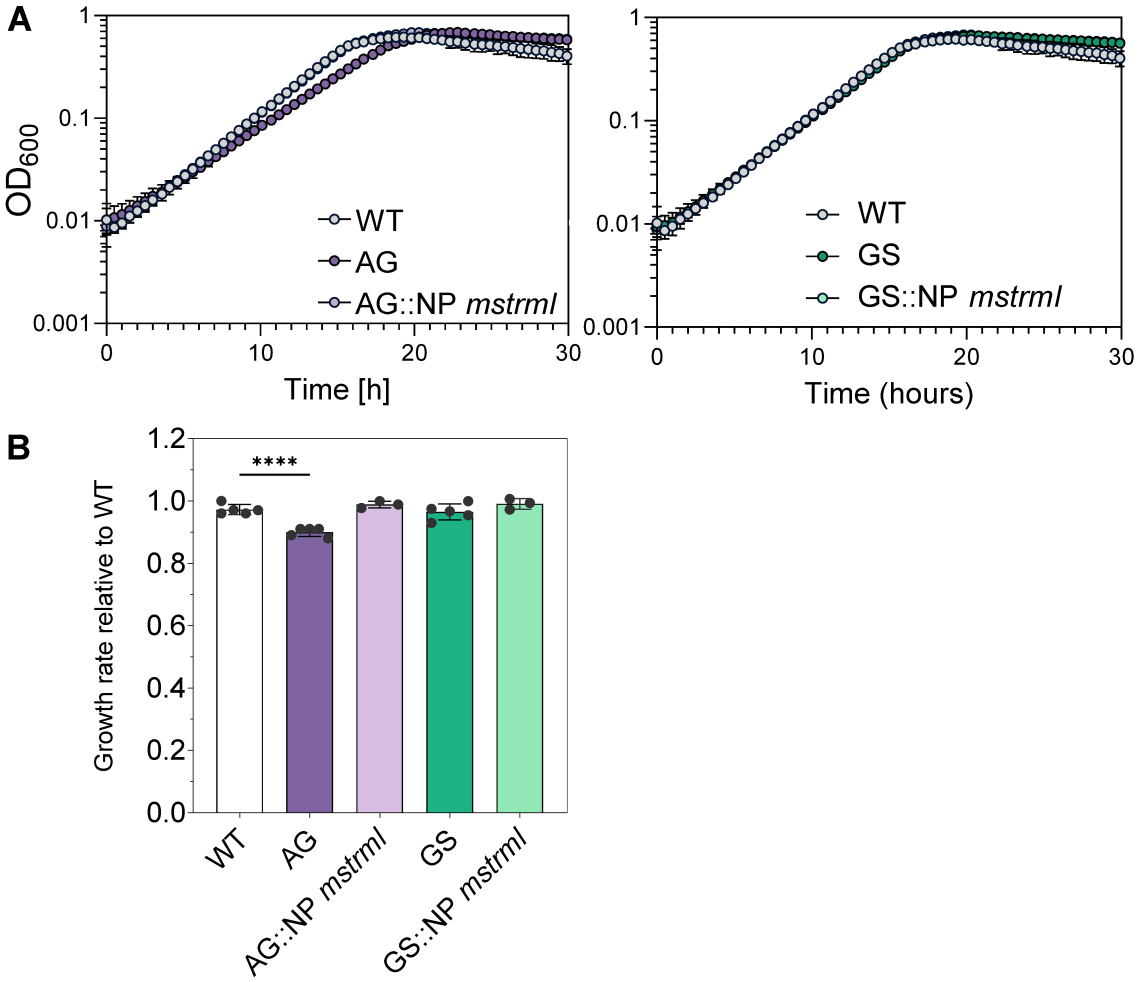


Figure 2.8: **Characterization of the growth rate of *mstrmI* mutants in 7H9 media**. WT *Msm*, AG and GS mutants and their complemented strains were grown in 7H9 media, and growth was measured as OD_{600} using a plate reader. (A) Symbols represent the mean of at least three replicate wells, and the results represent at least three independent experiments. (B) Growth rate relative to the WT *Msm* extracted from (A), with bars representing the mean generation times of at least three independent experiments and error bars representing +/- SD. Statistical analysis is done against the WT *Msm* using a one-way ANOVA test with multiple comparisons using a Dunnett test.

2.2.6 The effect of the A-to-G mutation on *mstrmI* transcripts

As the A-to-G single nucleotide polymorphism was found 15 base pairs (bp) upstream of the start codon of *mstrmI*, which is likely in the promoter of the gene, I hypothesized that this mutation led to decreased levels of *mstrmI* transcripts. Thus, I then used qRT-PCR to measure *mstrmI* levels and showed that the transcriptional level of *mstrmI* in the AG mutant was reduced by 90% relative to WT Msm (Fig. 2.9). This indicated that the A-to-G mutation located 15 bps upstream of the ORF of *mstrmI* interferes with the expression of the *mstrmI*. Of note, the mutation that leads to glycine to serine substation at position 128 did not affect transcript levels of *mstrmI* (Fig. 2.9).

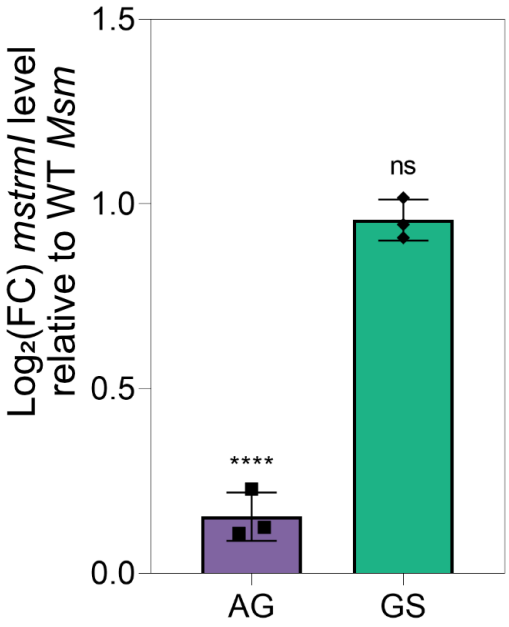


Figure 2.9: **A-to-G mutation, but not G128S, strongly reduces *mstrmI* transcription**. Transcript levels of WT *Msm*, AG, and GS mutant measured by qRT-PCR. RNA was extracted as described in the Methods section 6.8, and cDNA was prepared as described in the Methods section 6.11. Bars represent the mean of three replicates, with error bars representing +/- SD. Values were normalized to WT *Msm* transcript, and statistics were done using one-way ANOVA test (0.0001 (****)).

2.2.7 The G128S mutation affects the protein abundance of MsTrmI

To investigate the impact of the glycine-to-serine mutation on the tRNA methyltransferase, I used AlphaFold to generate a predicted structure of the WT and mutated G128S version of MsTrmI (Jumper et al., 2021). The structure of Rv2118c, which shares 81% amino acid identity with MsTrmI, has been previously resolved (Gupta & Chatterji, 2005) (Fig. 2.10A). In both WT MsTrmI and MsTrmI^{G128S} structures, the glycine residue at position 128 and the serine residue in the structure of the mutated version MsTrmI^{G128S} are exposed at the protein surface, are not involved in the binding of the cofactor SAM, and are not part of the interface where the protein dimerizes. This rendered complicated any attempt to rationalize how the glycine-to-serine substitution at position 128 impacted the protein structure so that the mutant displayed increased survival to aminoglycosides (Fig. 2.10B).

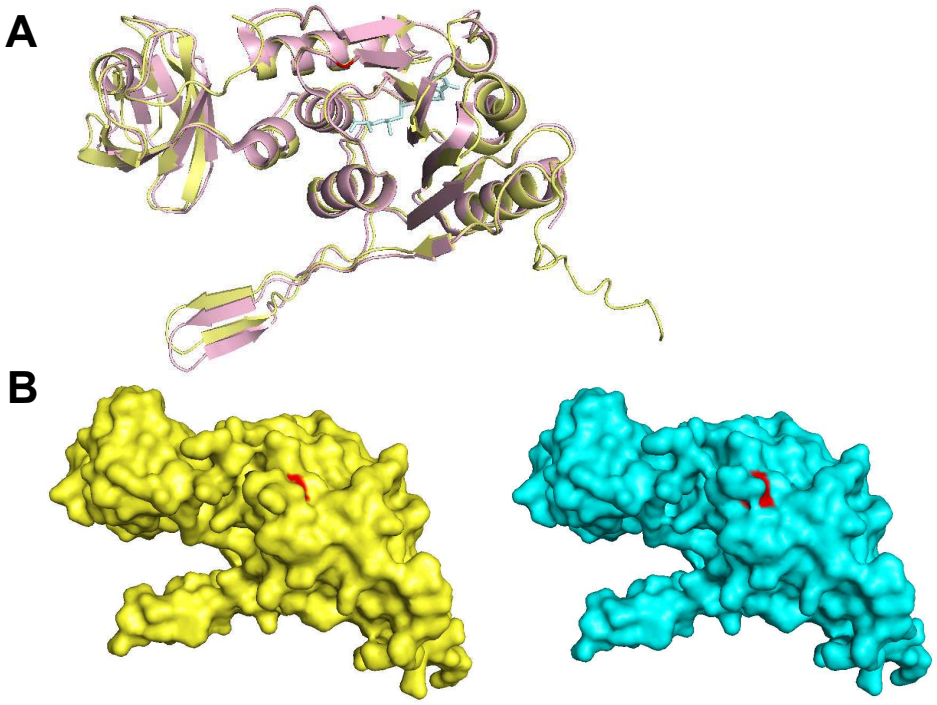


Figure 2.10: **G128 residue of MsTrmI is predicted to be on the protein surface.** (A) Alignment of MtTrmI (encoded by *Rv2118c)* in pink and MsTrmI in yellow, with SAM cofactor shown in blue. G128 of MsTrmI and G125 of MtTrmI (corresponding to G128) are shown in red. (B) The protein surface of MsTrmI (yellow) MsTrmI^{G128S} (cyan) with 128 residue shown in red. Figure generated using PyMol.

As mentioned earlier, the mutated allele *mstrmI*^{G128S} expression in WT *Msm* did not result in increased survival (Fig. 2.5). However, expression of the mutated allele complemented the increased survival in an ATc-dependant manner in both mutants (Fig. 2.11). A higher concentration of ATc - that is likely inducing higher expression of the mutated allele - was needed to restore the sensitivity to kanamycin of both mutants as compared to when complementation was done using the WT copy of *mstrmI*. This suggested that the glycine-to-serine mutation might lead to a decreased level of the MsTrmI, possibly due to lower stability and/or increased degradation.

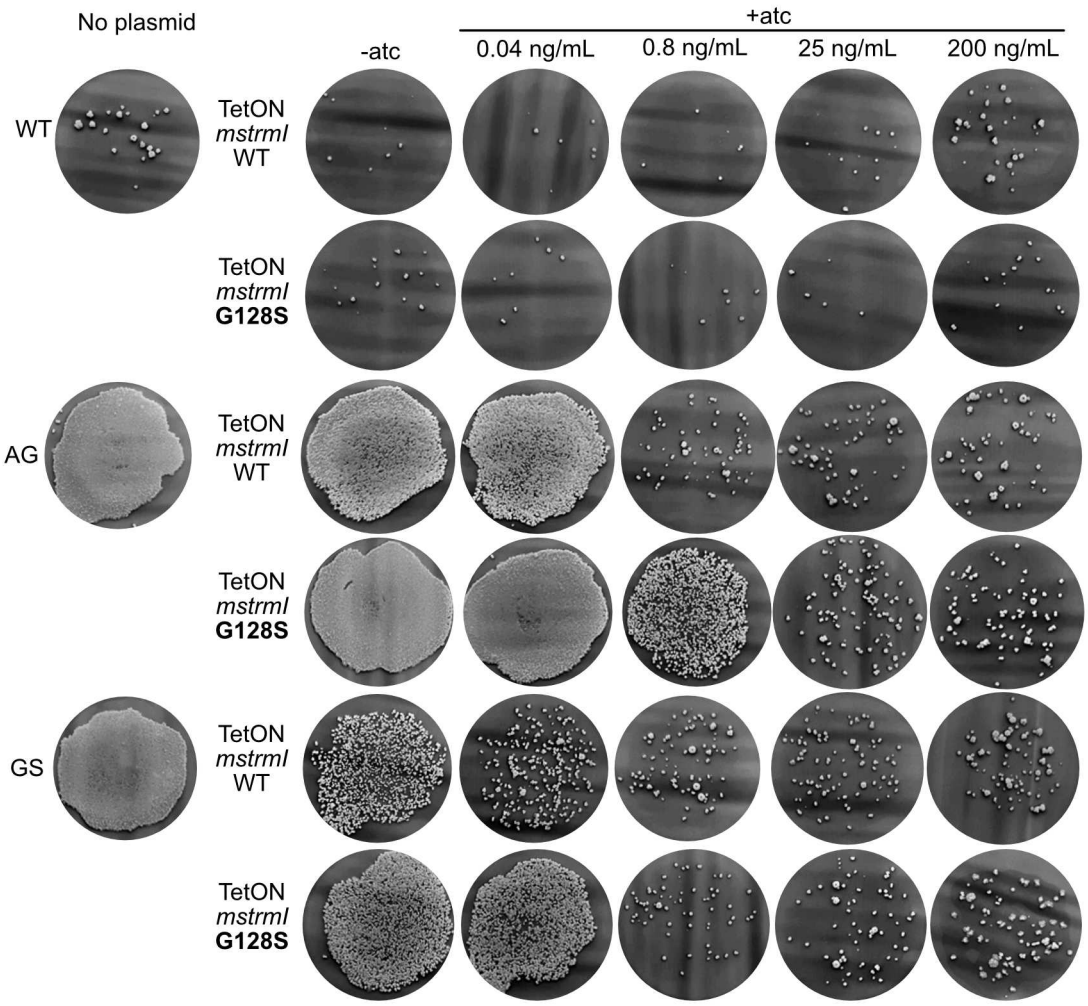


Figure 2.11: **Expression of G128S *mstrmI* complements the increased survival phenotype of AG and GS mutants**. Strains were grown in the absence or presence of indicated concentrations of ATc, and exposed to 10xMIC kanamycin, with survivors grown on recovery plate as described in 6.4. Representative of at least three independent experiments.

To assess this observation, I cloned an HA tag onto the C-terminus of *mstrmI* and *mstrmI*^{G128S}

and expressed them in WT *Msm*. Expression was induced with the addition of ATc overnight, and RNA was extracted to control whether the WT and mutated allele had the same level of the *mstrmI* transcript. Next, the cells were grown for an additional 12 hours after removing ATc before protein extractions. While the expression levels of *mstrmI*-HA measured by qRT-PCR were similar for WT and $mstrmI^{G128S}$ in the presence of ATc (Fig. 2.12C), the abundance of HA-tagged $MsTrmI^{G128S}$ was, on average, 37.9% that of the WT MsTrmI, as quantified by Western blot (Fig. 2.12A,B). Thus, the glycine-to-serine substitution seems to affect the levels of MsTrmI: it is likely that a lower abundance of the enzyme led to insufficient tRNA modification and further increased survival upon exposure to aminoglycosides. These results align with the observation that the overexpression of $mstrmI^{G128S}$ complemented the increased survival phenotype since increasing the abundance of MsTrmI in the mutant by expressing $mstrmI^{G128S}$ could rescue the levels of the protein to the WT level (2.11).

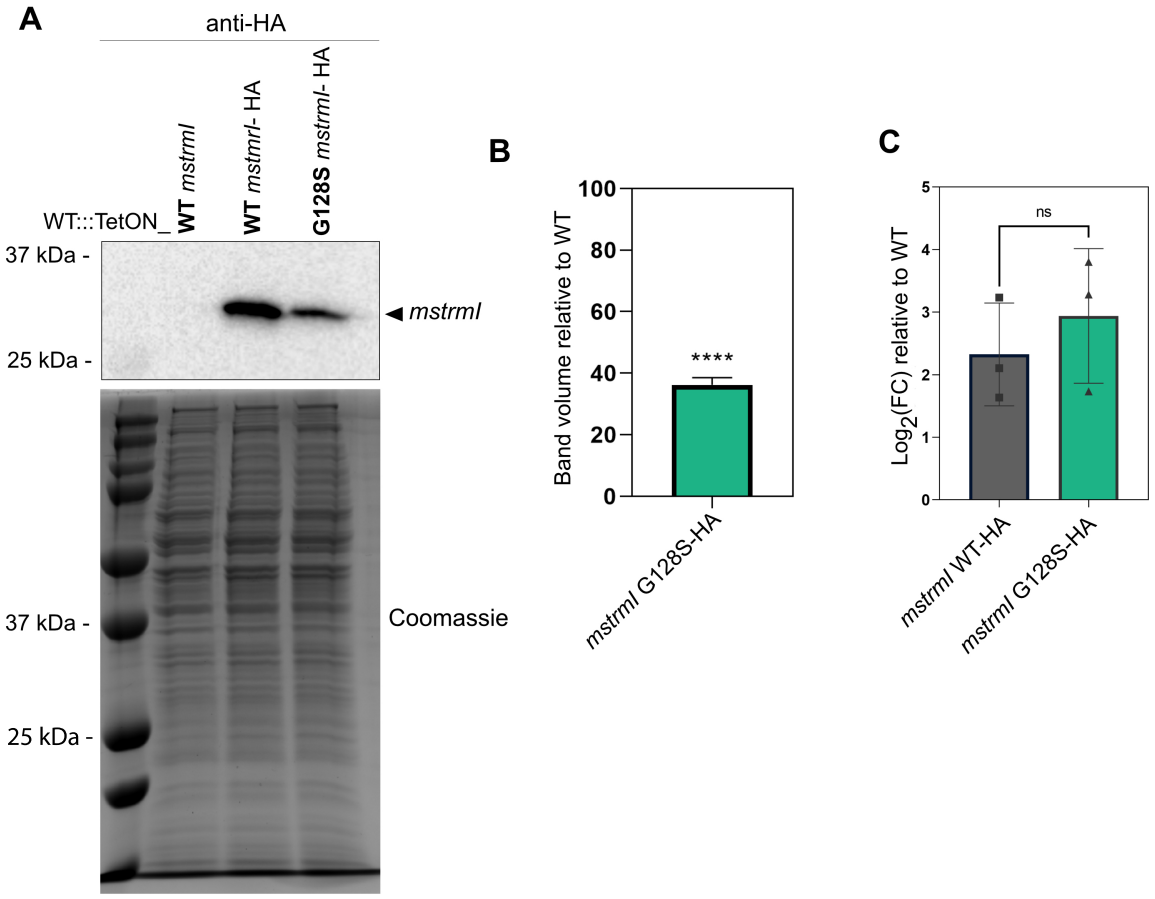


Figure 2.12: **G128S mutation affects the stability of MsTrmI**. HA-tagged WT and MsTrmI^{G128S} were overexpressed with 200 ng/mL ATc overnight, and the RNA of half the cells was isolated. The other half of the cells were washed to remove the inducer and then grown without ATc for a further 12h, followed by protein extraction. (A) Bacterial lysates were analysed by SDS-PAGE and immunoblotting with anti-HA to determine protein abundance. Gels were stained with Coomassie dye to control for equal loading of the samples. Representative of three independent experiments. (B) Quantification of band intensity of (A) three independent experiments. Statistical significance was calculated using an unpaired t-test. (C) Transcript levels of HA-tagged WT *mstrmI* and *mstrmI*^{G128S} measured by qRT-PCR. RNA was extracted as described in 6.8, and cDNA prepared as described in 6.11. Bars represent the mean of three replicates, with error bars being +/- SD. Values were normalised to WT, and statistics were done using unsupervised t tests.

2.2.8 MsTrmI^{G128S} is not post-translationally modified

Given the fact that 128S is predicted to be on the surface of MsTrmI (Fig. 2.10) and serine residues are prone to post-translational modifications (PTMs), including phosphorylation, I hypothesised that this mutation might affect the abundance of MsTrmI enzyme through PTMs of the 128S residue. Specifically, I hypothesised that expression of *mstrmI*^{G128S} might lead to the formation of phosphorylated (unstable) and non-phosphorylated (stable) *mstrmI*, possibly due to kinase saturation or phosphatase action. In that vein, I hypothesised I could complement the increased survival phenotype of the AG and GS mutants with *mstrmI*^{G128S} overexpression through the accumulation of non-phosphorylated MsTrmI^{G128S} in those cells.

First, to test if it would be possible to mimic a phosphorylated or a non-phosphorylated state of MsTrmI, I generated HA-tagged 128D *mstrmI* (chemically similar to phosphor-serine, phosphomimetic) or 128A *mstrmI* (non-phosphorylatable amino acid) under the TetON construct. I transformed the WT *Msm* with each of these constructs and expressed them in the absence or presence of a high concentration of ATc (200 ng/mL). Expression was confirmed via Western blot (Fig. 2.13).

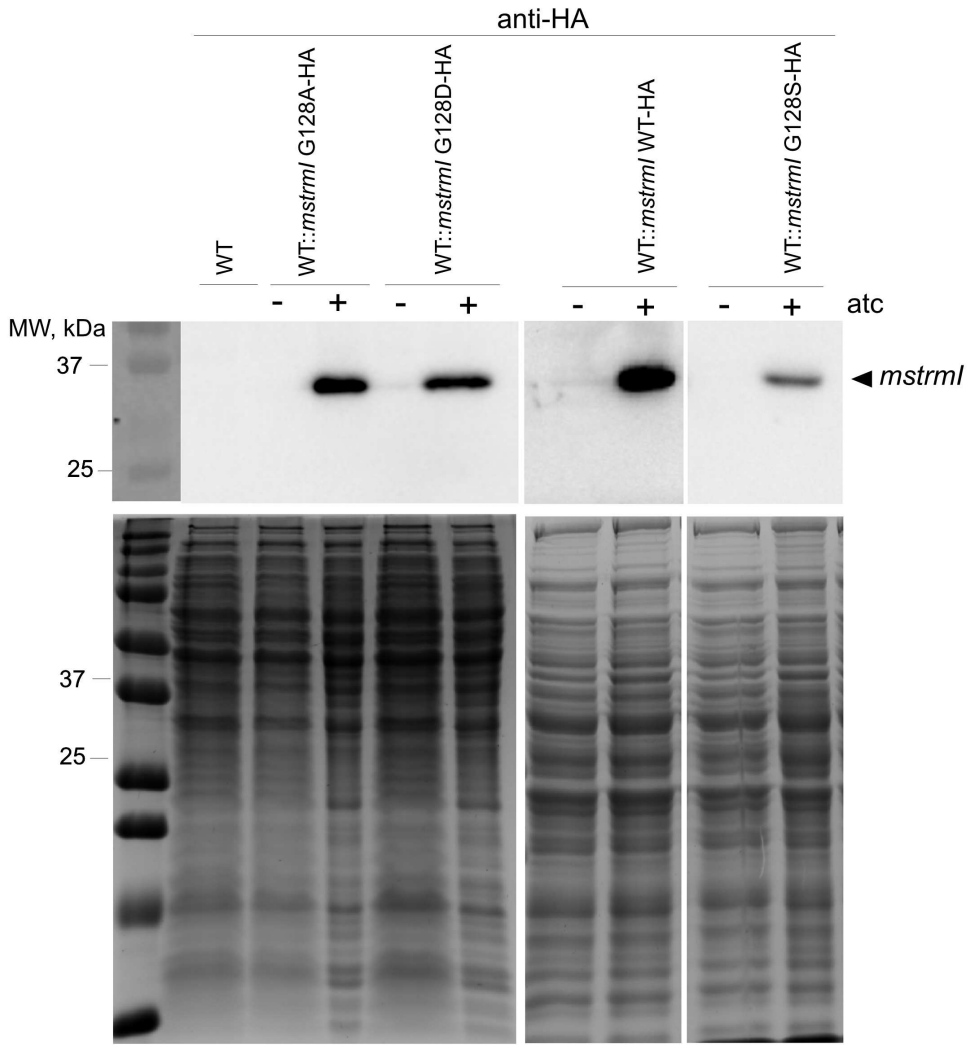


Figure 2.13: **Confirmation of expression of different *mstrmI* G128 mutants.** Expression was induced with 200 ng/μL ATc, proteins were isolated from the strains and the expression efficiency was determined by SDS-PAGE and immunoblotting against HA tag. Membranes were stained with Coomassie staining, which was used to control the loading of the proteins.

Expressing *mstrmI*^{128A} complemented the phenotype of the AG and GS mutants, while expressing *mstrmI*^{128D} phosphomimetic had no impact on the survival of AG and GS mutants (Fig. 2.14). This aligned with our hypothesis, as non-phosphorylatable MsTrmI^{128A} mimicked stable MsTrmI, while phosphomimetic MsTrmI^{128D} mimicked the unstable MsTrmI, and no complementation was observed. However, I could not conclude whether mutating glycine at position 128 interferes with protein folding and the enzyme's function. Thus, our next step was to assess the phosphorylation state of MsTrmI through mass spectrometry.

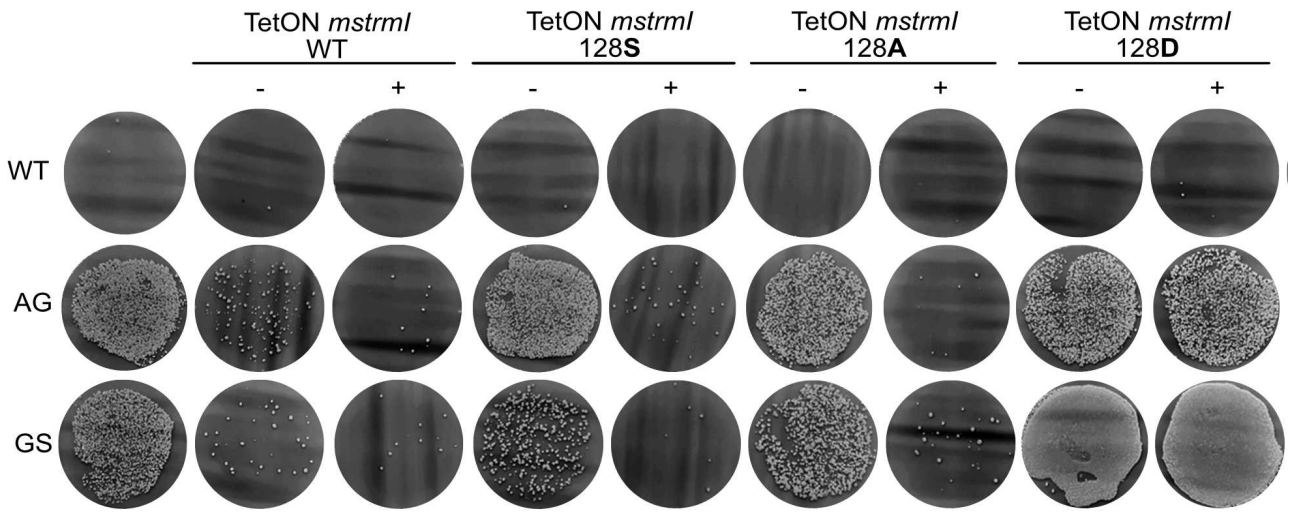


Figure 2.14: **Expressing 128A, but not 128D *mstrmI*, diminishes the increased survival phenotype of *mstrmI*-related mutants to kanamycin**. WT *Msm*, AG, and GS mutants were transformed with integrative TetON *mstrmI* WT, 128S, 128A (non-phosphorylatable amino acid), and 128D (phosphomimetic) constructs and the increased survival phenotype was assessed in the absence or presence of ATc (200 ng/mL). Representative of one repeat.

To analyse the phosphorylation status of MsTrmI^{G128S}, I expressed HA-tagged WT and G128S *mstrmI* with ATc in the WT background and pulled down WT and MsTrmI^{G128S} using HA-beads. Expression and elution were confirmed with a fraction of the sample via Western blot analysis, while the remaining pulled-down proteins were sent for mass spectrometry analysis. However, no phosphorylation or other PTMs have been identified in the protein region of interest, discarding the hypothesis that PTMs of 128S were responsible for the loss of MsTrmI^{G128S} activity.

Nevertheless, I have shown that the G128S mutation affects the protein abundance of MsTrmI, leading to decreased levels of this enzyme in the GS mutant. Other methods, such as crystallography, would be needed to assess the impact of G128S modification on the MsTrmI, but this has not been addressed in this work.

2.3 Summary

Taken together, these results show that the AG and GS mutants, recovered using the filter-based method upon exposure to kanamycin, display increased survival of *Msm* to other tested aminoglycosides and MIC-shifted resistance to macrolides (Fig. 2.3, 2.7). I show that the A-to-G and G128S mutations are loss-of-function mutations, since expressing the WT allele of *mstrmI* under either TetON or NP rescued the observed increased survival phenotypes to aminoglycosides (Fig. 2.3). Finally, I show that the A-to-G mutation decreases the transcript levels of *mstrmI* (Fig. 2.9), while the G128S mutation impacts the protein abundance of MsTrmI (Fig. 2.12). Together, these results reveal that even a partial loss of a tRNA m^1A58 methyltransferase can induce both MIC-shifted resistance and antibiotic tolerance.

Chapter 3

Results II: Deletion mutant of *mstrmI* presents with mutations in an exoribonuclease

Contents

3.1 Introduction 78

3.2 Results 78

3.2.1 Construction of the *mstrmI* deletion mutant 78

3.2.2 Phenotypes of Δ*mstrmI*_C1 deletion mutant 80

3.2.3 The mutation in a gene encoding a PNPase diminishes increased survival of the deletion mutant Δ*mstrmI*_C1 to aminoglycosides 84

3.2.4 The second clone, Δ*mstrmI*_C2, also bears a *pnpase*-related mutation 88

3.2.5 The 29 bp deletion in the *pnpase* upstream region decreases *pnpase* expression 90

3.2.6 Mtb *trmI* deletion mutant does not have an increased survival to gentamicin 91

3.3 Summary 93

3.1 Introduction

To further test whether the loss of MsTrmI was responsible for the phenotypes of the *mstrmI* mutants, my next step was to generate a knock-out (KO) strain Δ*mstrmI* and test if increased survival against aminoglycosides pertains to this strain. Several studies in other bacterial species investigated the impact of deleting *trmI* homologs, including bacterial survival to numerous stresses. For instance, loss of *trmI* in *Thermus thermophilus* results in a thermosensitive phenotype observed as a growth defect at 80°C (Droogmans et al., 2003). Furthermore, in yeast, *trmI* consists of two proteins encoded by genes essential for cell viability (Kadaba et al., 2004). In *S. cerevisiae*, that complex is encoded by *trm6* and *trm61*, and a mutation of *trm6* was found to cause initiator $tRNA^{Met}$ instability and their degradation (Anderson et al., 1998; Kadaba et al., 2004). Studies of mutated *trm6* identified spontaneous suppressor mutations within a 3'-5' exoribonuclease *DIS3/RRP44* and a DNA polymerase with poly(A) polymerase activity *TRF4* - and showed they function together to degrade aberrant initiator pre-$tRNA^{Met}$ lacking m^1A58 (Kadaba et al., 2004).

Notably, *Rv2118c*, encoding for Mtb *trmI* (*mttrmI*), was found to be non-essential (Minato et al., 2019; Dejesus et al., 2017; Sassetti, Boyd, & Rubin, 2003). Correspondingly, *mstrmI* was also classified as a non-essential gene (Dejesus et al., 2017; Bosch et al., 2021). However, certain CRISPRi-generated knock-downs of *mstrmI* displayed growth vulnerability (Bosch et al., 2021). To assess how the loss of a tRNA methyltransferase impacts survival to antibiotics in *Msm*, I went on to generate a deletion mutant of *mstrmI*.

3.2 Results

3.2.1 Construction of the *mstrmI* deletion mutant

As discussed in Chapter 2, both selected mutants - whose mutation affected the tRNA methyltransferase MsTrmI at the transcriptional or the protein level - exhibited increased survival

upon exposure to aminoglycosides. To investigate whether the complete loss of MsTrmI phenocopies the AG and GS mutants, I constructed a deletion mutant of *mstrmI* in *Msm* using homologous recombination (Murphy, Papavinasasundaram, & Sassetti, 2015). This method requires (1) the expression of RecE, an exoribonuclease, and RecT, a DNA annealing protein, from an episomal plasmid (pNIT RecET SacB KanR) in the WT *Msm*, and (2) electroporation of a single-stranded DNA oligo containing short flanking sequences homologous upstream and downstream sequences of the gene of interest, flanking a hygromycin cassette. Colonies, for which I used PCR to confirm that the gene of interest had been deleted, were plated on sucrose-containing plates to lose the pNIT RecET SacB KanR plasmid. Colonies were further streaked on plates without or containing kanamycin to confirm that the plasmid was lost (Fig. 3.1).

Although this method is well-established in *Msm* and usually yields several candidate mutants per experiment for non-essential genes, it required several tries and a longer incubation of the plates after electroporation to obtain colonies. After five rounds of the procedure described above, I obtained two clones which contained the hygromycin cassette between the upstream and downstream regions. These clones were named Δ*mstrmI*_C1 and _C2, in reference to the order of their recovery from the experiments that were carried out to do so.

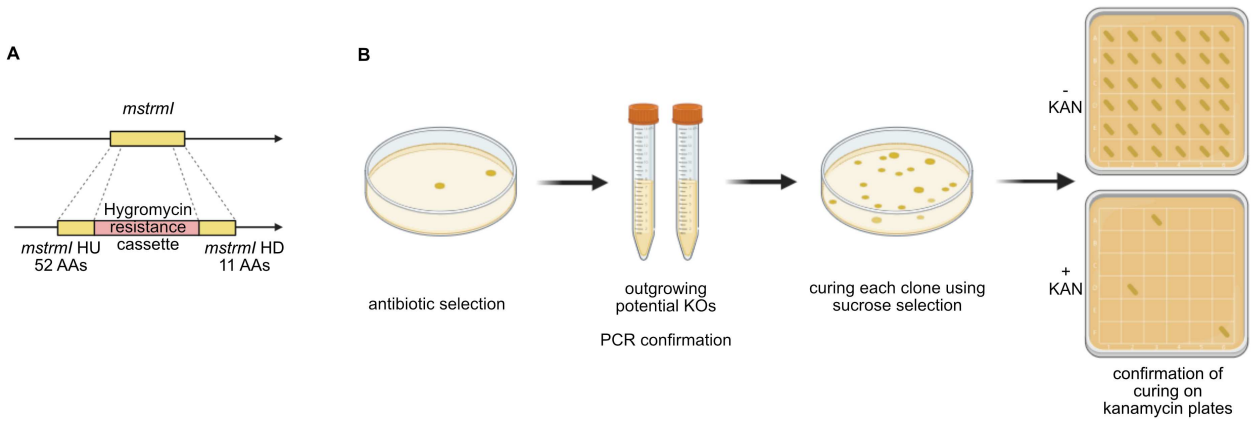


Figure 3.1: **The process of generating and curing Δ*mstrmI*** (A) Schematic of *mstrmI* before and following a homologous recombination event, during which the gene is exchanged with the hygromycin resistance cassette. (B) Schematic of the process of generating the KO of *mstrmI*. WT *Msm* transformed with the plasmid and oligonucleotide that contained a hygromycin cassette flanked by *mstrmI* homologous sequences were plated on plates containing hygromycin 50 μg/mL and the outgrown colonies were confirmed to be KOs using PCR. Then, each successful KO candidate was plated on sucrose plates to select negatively for the strains that lost the pNIT RecET SacB KanR plasmid. Finally, colonies from the sucrose plates were patched onto plates with/out kanamycin 25 μg/mL to proceed with a colony that did not grow on the kanamycin-containing plate since it lost the RecET plasmid. Those clones were sent for whole genome sequencing to confirm the successful removal of the gene.

3.2.2 Phenotypes of Δ*mstrmI*_C1 deletion mutant

To investigate the phenotypes of the deletion mutant Δ*mstrmI*_C1, I exposed to a set of antibiotics the WT *Msm*, Δ*mstrmI*_C1, and Δ*mstrmI*_C1 transformed with a WT *mstrmI* allele. The Δ*mstrmI*_C1 had an increase in survivors upon exposure to kanamycin and amikacin (Fig. 3.2AB). Still, the increase was minor compared to the fraction of survivors in the AG and GS mutants (Fig. 2.3). The increased survival was lost upon complementation with the WT allele of *mstrmI* (Fig. 3.2AB). The survival to levofloxacin and rifampicin remained the same as the survival of the WT *Msm* (Fig. 3.2AB). As with the AG and GS mutants, the MIC of the Δ*mstrmI*_C1 to investigated antibiotics remained unchanged from the WT MIC (Fig. 3.6A-E). Δ*mstrmI*_C1 had a statistically significant growth defect, with the growth rate being around 0.8 of that of the WT *Msm*. Expression of the WT *mstrmI* allele complemented the increased survival and partially the growth defect (Fig. 3.2A-D).

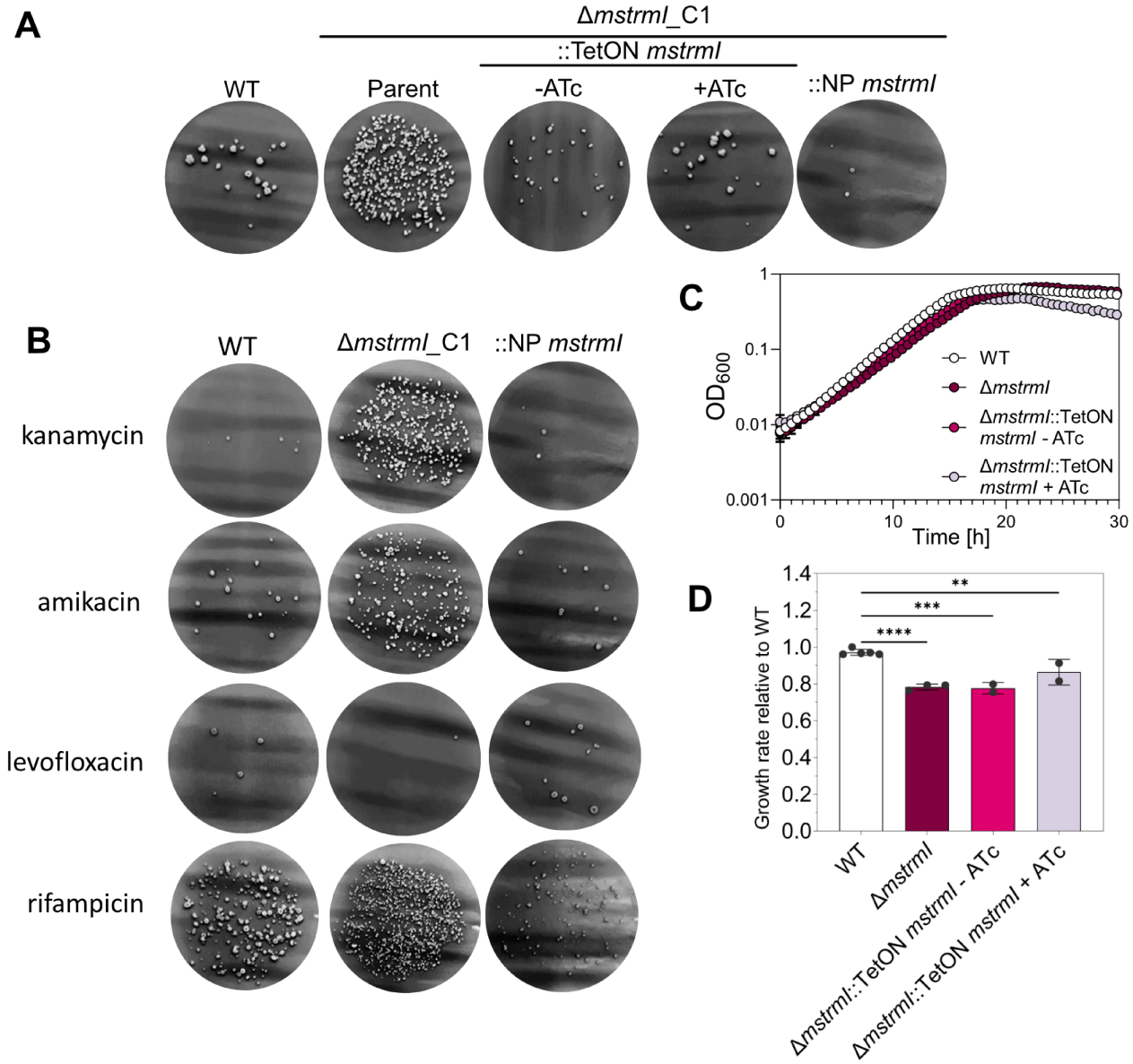


Figure 3.2: **Δ*mstrmI*_C1 does not phenocopy the increased survival phenotype of *mstrmI* mutants**. (A) The increased survival phenotype upon exposure to kanamycin of WT *Msm*, Δ*mstrmI*_C1, and complemented Δ*mstrmI*_C1 expressing WT allele of *mstrmI* under NP or TetON, grown in the absence or presence of ATc. Representative of at least three experiments. (B) The increased survival phenotype of WT *Msm*, Δ*mstrmI*_C1, and Δ*mstrmI*_C1::NP *mstrmI*. Representative of two independent experiments. (C) Growth curves of the WT *Msm*, the deletion mutant and complemented strains with a TetON-regulated expression of *mstrmI*, grown without or with 200 ng/mL ATc. Symbols represent the mean of at least three replicate wells +/- SD, and the results represent at least three independent experiments. (D) Growth rate relative to the WT *Msm* extracted from (C), with bars representing the mean of at least three independent experiments and error bars representing +/- SD. Statistical analysis is done against the WT *Msm* using a one-way ANOVA test with multiple comparisons using a Dunnett test.

To quantify the number of bacteria that survived exposure to antibiotics, I exposed the WT *Msm*, the deletion strain Δ*mstrmI*_C1 and the complemented strain to kanamycin at a concentration 5-fold of the MIC in liquid media. Compared to the WT *Msm*, which displayed an unambiguous biphasic killing, the deletion mutant Δ*mstrmI*_C1 exhibited a slower rate of killing during the course of antibiotic exposure. However, in comparison to both *mstrmI* mutants, which had a three to four-log increase in survival after 60 hours of exposure to kanamycin (Fig. 2.4), Δ*mstrmI*_C1 at 60 hours had only a one-log increase in the level of survivors compared to the WT *Msm* (Fig. 3.3). Complementation of the deletion mutant restored sensitivity to the WT level. Of note, the complemented strain grown without ATc had the same killing kinetics as the WT *Msm*, which I hypothesise is due to the leakage of *mstrmI* expression in the TetON construct (Fig. 3.3).

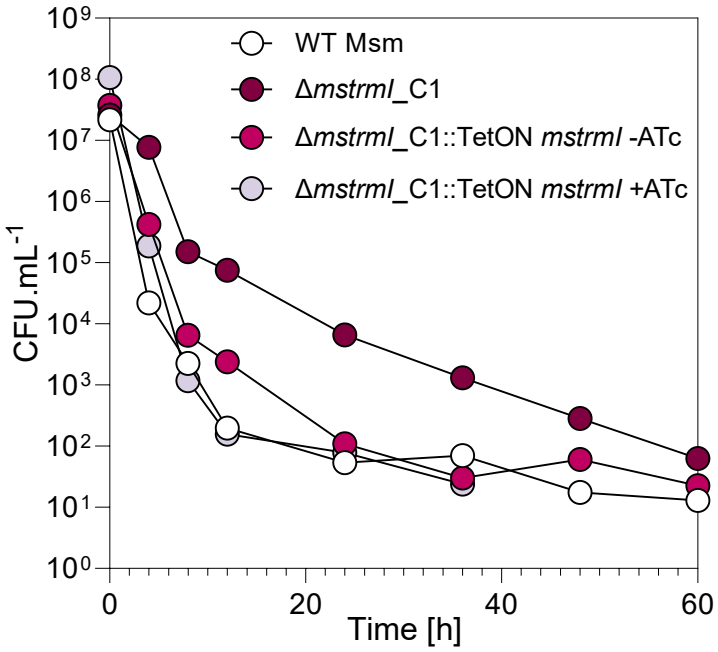


Figure 3.3: **A time-kill curve of Δ*mstrmI*_C1 deletion mutant to kanamycin in liquid**. Strains were exposed to 5xMIC (3.5 μg/mL) kanamycin, and killing was observed as CFUs over the course of 60 h. Result of one independent experiment.

As mentioned, the deletion mutant Δ*mstrmI*_C1 and the selected *mstrmI* mutants consistently did not survive lethal concentrations of aminoglycosides to the same extent. This prompted us to investigate whether additional genetic modifications accounted for these differences. To do so, the deletion mutant Δ*mstrmI*_C1 was sent for whole genome sequencing. Using a custom

pipeline to process the WGS data available in the laboratory, I identified that the deletion mutant Δ*mstrmI*_C1 had two additional mutations compared to the parental WT *Msm* strain that was used to generate the deletion mutant: the deletion mutant contained an A-to-G base mutation on the *Msm* genome (location 1808107), which led to a V1A substitution in MSMEG 1712, and it also contained a C-to-A base mutation on the *Msm* genome (location 2736496) that led to an A167D substitution of a polynucleotide phosphorylase (PNPase) - a 3'-5' exoribonuclease involved in RNA degradation (Tab. 3.1).

Table 3.1: **Δ*mstrmI*_C1 strain contains two additional mutations**. Whole genome sequencing results of Δ*mstrmI*_C1 strain SNPs, showing gene, mutation, and description of the gene.

Strain	Gene	Mutation	Description
Δ*mstrmI*_C1	*MSMEG_1712*	V1A	ABC transporter periplasmic-binding protein
Δ*mstrmI*_C1	*pnpase*	A167D	3'-5' exoribonuclease

PNPase is an enzyme involved in RNA decay and is highly conserved in bacteria and eukaryotes. In most organisms, PNPase functions as a 3'-5' exoribonuclease; it catalyses the degradation of single-stranded RNA by removing nucleotides from the 3' end (Mohanty & Kushner, 2000). As such, it is involved in the degradation and processing of tRNA, rRNA and sRNA. Deletion of *pnpase* leads to diverse phenotypes - from reduced virulence, growth defect, and differential survival to numerous stresses (Płociński et al., 2019; Quendera et al., 2023; Clements et al., 2002; J. Wu et al., 2009; Cameron, Matz, & De Lay, 2018; Henry, Shanks, van Hoof, & Rosenzweig, 2012; Haddad et al., 2009). Recently, PNPase was also identified as a factor in the biofilm production of *Listeria monocytogenes* - inactivation of the PNPase affected the regulation of pathways regulating metabolism of amino acids (Quendera et al., 2023).

In addition to its individual function, PNPase is associated with an RNA degradosome, a multiprotein complex involved in mRNA degradation (Tejada-Arranz, de Crécy-Lagard, & de Reuse, 2020). In mycobacteria, RNA degradasome consists of ribonucleases RNase J and E, and an RNA helicase RhlE (Płociński et al., 2019). Although PNPase, as part of the RNA degradosome, is involved in mRNA degradation, its main function is independent of the machinery. A deletion mutant in *Mtb* is not viable, and an *Mtb* strain with reduced *pnpase*

levels has destabilised many mRNAs (Płociński et al., 2019). In contrast, disruption of a degradosome has a moderate impact on transcriptional changes of *Mtb* (Płociński et al., 2019). Furthermore, PNPase is three to five times more abundant than RNase E, and the tRNA processing, rRNA degradation, and sRNA regulation functions of the PNPase are independent of the RNA degradosome (Mohanty & Kushner, 2007; Smith, Gupta, Denny, & Culver, 2018; Cameron et al., 2018; De Lay & Gottesman, 2011).

3.2.3 The mutation in a gene encoding a PNPase diminishes increased survival of the deletion mutant Δ*mstrmI*_C1 to aminoglycosides

To assess whether the mutations in *MSMEG_1712* and/or in the *pnpase* were responsible for decreased survival of the deletion mutant Δ*mstrmI*_C1 upon exposure to aminoglycosides – as compared to the AG and GS mutants – I expressed WT copies of *MSMEG_1712* or the *pnpase* in the deletion mutant Δ*mstrmI*_C1. While expression of *MSMEG_1712* did not affect the fraction of bacteria that survived exposure to aminoglycosides (Fig. 3.4), expression of the gene encoding for the PNPase restored increased survival to aminoglycosides of the deletion mutant to levels of those of the AG and GS mutants (Fig. 3.4).

Notably, expression of either *MSMEG_1712* or *pnpase* in the WT *Msm* did not lead to increased survival upon exposure to aminoglycosides, suggesting that the presence of an additional allele that allows for expression for either gene was not sufficient to confer increased survival (Fig. 3.4B).

Together, these data indicate that the A167D mutation in the PNPase is likely responsible for the decreased survival of the deletion mutant Δ*mstrmI*_C1 compared to the selected *mstrmI* mutants. From now on, Δ*mstrmI*_C1 will be annotated as Δ*mstrmI*_*pnpase*^{A167D}.

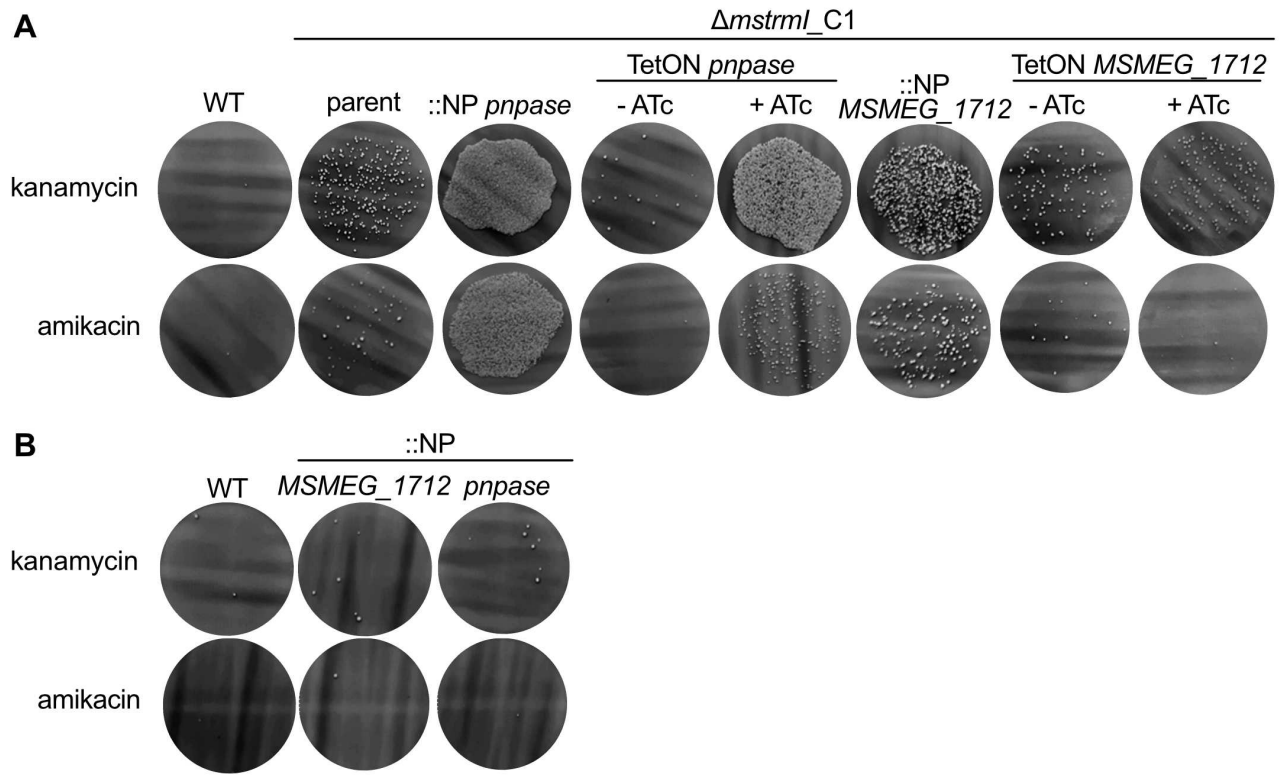


Figure 3.4: **The *pnpase* mutation decreases the survival of the Δ*mstrmI*_C1 deletion mutant**. (A) The increased survival phenotype upon exposure to kanamycin and amikacin of the WT *Msm*, Δ*mstrmI*_C1 deletion mutant, and the deletion mutant expressing TetON or NP-regulated WT alleles of *MSMEG_1712* or *pnpase*. TetON strains were grown in the absence or presence of 200 ng/mL ATc prior to exposure. Representative of three independent experiments. (B) The increased survival phenotype of the WT *Msm* expressing either TetON or NP-regulated WT alleles of *MSMEG_1712* or *pnpase*. TetON strains were grown in the absence or presence of 200 ng/mL ATc prior to exposure. One independent experiment.

In addition to increased survival to kanamycin, the deletion mutant Δ*mstrmI*_*pnpase*^{A167D} complemented with the *pnpase* displayed increased survival to other aminoglycosides but not to levofloxacin and rifampicin (Fig. 3.5A), MIC-shifted resistance to the macrolides (Fig. 3.6F-H), and 5-fold increase in survival upon exposure in liquid to kanamycin in comparison to the WT *Msm* (Fig. 3.5C). All phenotypes were complemented upon expression of *mstrmI* (Fig. 3.5A,B). Finally, Δ*mstrmI*_*pnpase*^{A167D}::NP *pnpase* had a statistically significant growth defect displayed as a growth rate of 0.7 of the WT *Msm*, which was complemented to the WT level upon expression of *mstrmI* (Fig. 3.5C,D). These results suggested that the *pnpase* mutation possibly emerged as a suppressor mutation upon deletion of *mstrmI*, and that the deletion mutant with the WT *pnpase* phenocopies the *mstrmI* mutants.

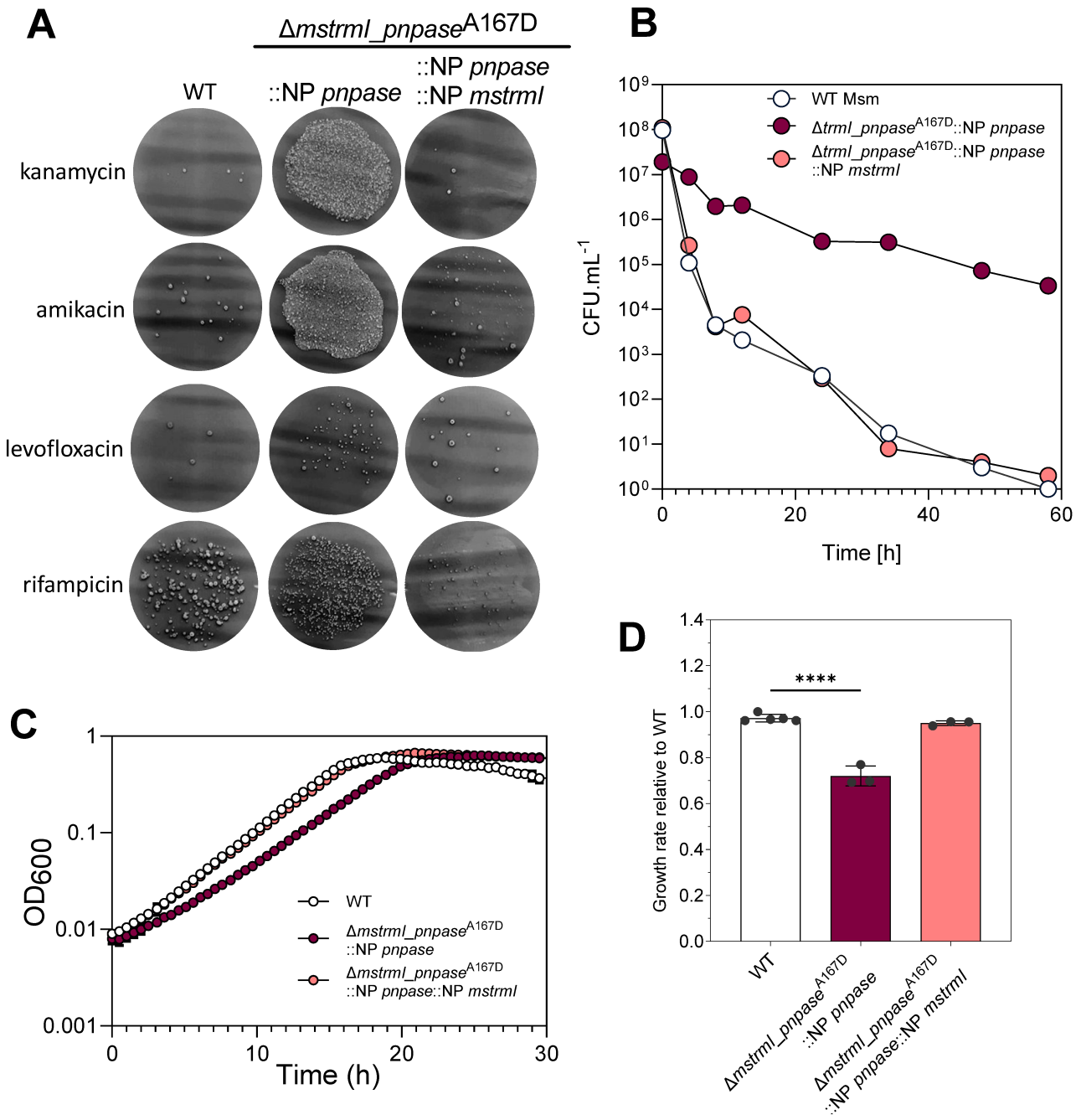


Figure 3.5: **Δ*mstrmI* expressing the WT *pnpase* phenocopies the AG and GS mutants**. (A) The increased survival phenotype upon exposure to kanamycin, amikacin, levofloxacin and rifampicin. Representative of three experiments. (B) Time-kill curve of investigated strains. Strains were grown in 7H9. To measure the killing, strains were exposed to 5xMIC kanamycin, and killing was observed as CFUs over the course of 60 hours. Representative of two independent experiments. (C) Growth of indicated strains in the 7H9 media. Symbols are the mean of 3-5 technical replicates, and the results represent at least three independent experiments. (D) Growth rate relative to the WT *Msm* extracted from (C), with bars representing the mean of at least three independent experiments and error bars representing +/- SD. Statistical analysis is done against the WT *Msm* using a one-way ANOVA test with multiple comparisons using a Dunnett test.

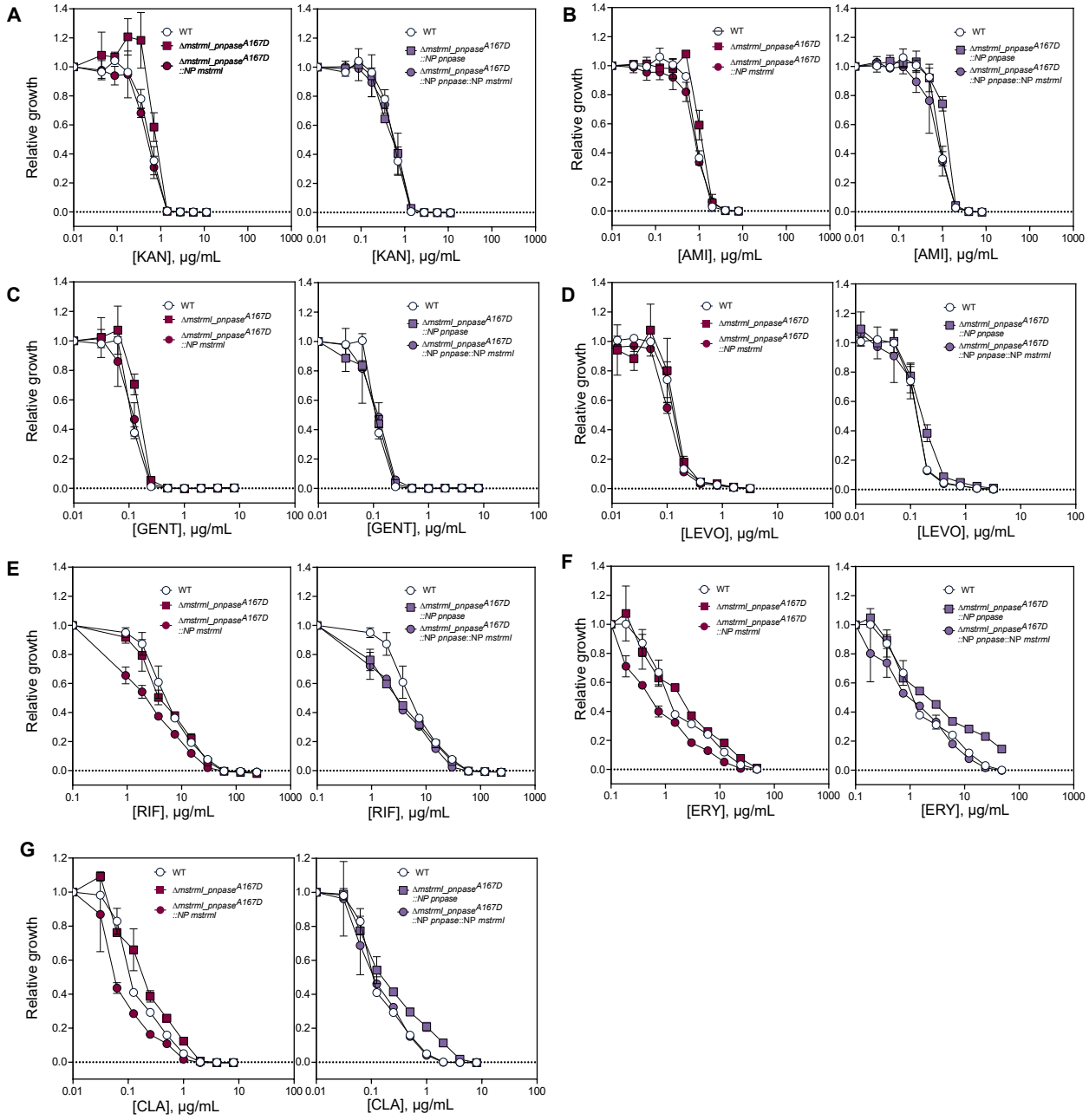


Figure 3.6: **Minimum inhibitory concentrations of Δ*mstrmI_pnpase*^{A167D}, Δ*mstrmI_pnpase*^{A167D}::NP *pnpase*, and Δ*mstrmI_pnpase*^{A167D}::NP *pnpase*::NP *mstrmI* strains**. The WT *Msm*, Δ*mstrmI_pnpase*^{A167D}, Δ*mstrmI_pnpase*^{A167D}::NP *pnpase*, and Δ*mstrmI_pnpase*^{A167D}::NP *pnpase*::NP *mstrmI* strains were exposed to (A) kanamycin 0-11.2 μg/mL, (B) amikacin 0-8 μg/mL, (C) gentamicin 0-8 μg/mL, (D) levofloxacin 0-3.2 μg/mL, (E) rifampicin 0-240 μg/mL, (F) erythromycin 0-48 μg/mL, and (G) clarithromycin 0-8 μg/mL and the OD_{600} was measured following incubation at 37°C for 72h. Graphs show growth relative to no antibiotic growth media, and each symbol is a mean of two technical repeats. Representative of two independent experiments.

3.2.4 The second clone, Δ*mstrmI*_C2, also bears a *pnpase*-related mutation

Next, I decided to study further the second clone of the deletion mutant, Δ*mstrmI*_C2, to investigate whether it also contained additional mutations and whether it recapitulated the phenotypes of the *mstrmI* mutant. I observed that this clone, too, did not have as increased survival as compared to the isolated *mstrmI* mutants (Fig. 3.7A). I whole genome sequenced this deletion clone and found it contained a 29 bp deletion 263 bp upstream of the *pnpase* start codon (*Msm* genome location 2735734).

Table 3.2: **Δ*mstrmI*_C2 strain has 29 bp deletion 263 bp upstream of the *pnpase* start codon**. Whole genome sequencing results of Δ*mstrmI*_C1 strain, showing gene, mutation, and description of the gene.

Strain	*Gene*	*Mutation*	*Description*
Δ*mstrmI*_C2	263 bp upstream of *pnpase*	29 bp deletion	3'-5'exoribonuclease

This 29 bp deletion leads to the loss of the first two bases of a small non-coding RNA (ncRNA) found upstream of the *pnpase*. This ncRNA is 77% identical to *Mtb ncRv127830*; it is found to share a transcriptional start site (TSS) with the *pnpase* ORF - and is suggested to regulate *pnpase* transcription (Fig.3.7B) (Dejesus et al., 2017). However, the regulation of *pnpase* transcription is suggested to be only partial from *ncRv127830*, as *ncRv127830* tolerated transposon insertions in one study, supporting the possibility that *Mtb pnpase* and *ncRv12783c* are independently essential RNA species (Dejesus et al., 2017). As I found this 29 bp deletion in the promoter region of the Δ*mstrmI*_C2 strain, the strain will be, from now on, annotated as Δ*mstrmI*_*pnpase*^{delNP}.

To assess whether this 29 bp deletion upstream of the *ncRv127830* was responsible for decreased survival of the deletion mutant Δ*mstrmI*_C2 upon exposure to aminoglycosides, I expressed the WT *pnpase* with the upstream region and assessed the survival. Expression of the WT allele of the *pnpase* in the Δ*mstrmI*_*pnpase*^{delNP} strain led to an increase in the fraction of bacteria that survived exposure to kanamycin, phenocopying the AG and GS mutants (Fig. 3.7C). In addition, complementation with the *pnpase* induced slow growth in the deletion mutant, indicating *pnpase*

is an intergenic suppressor mutation upon deletion of the *mstrmI* (Fig. 3.7D,E).

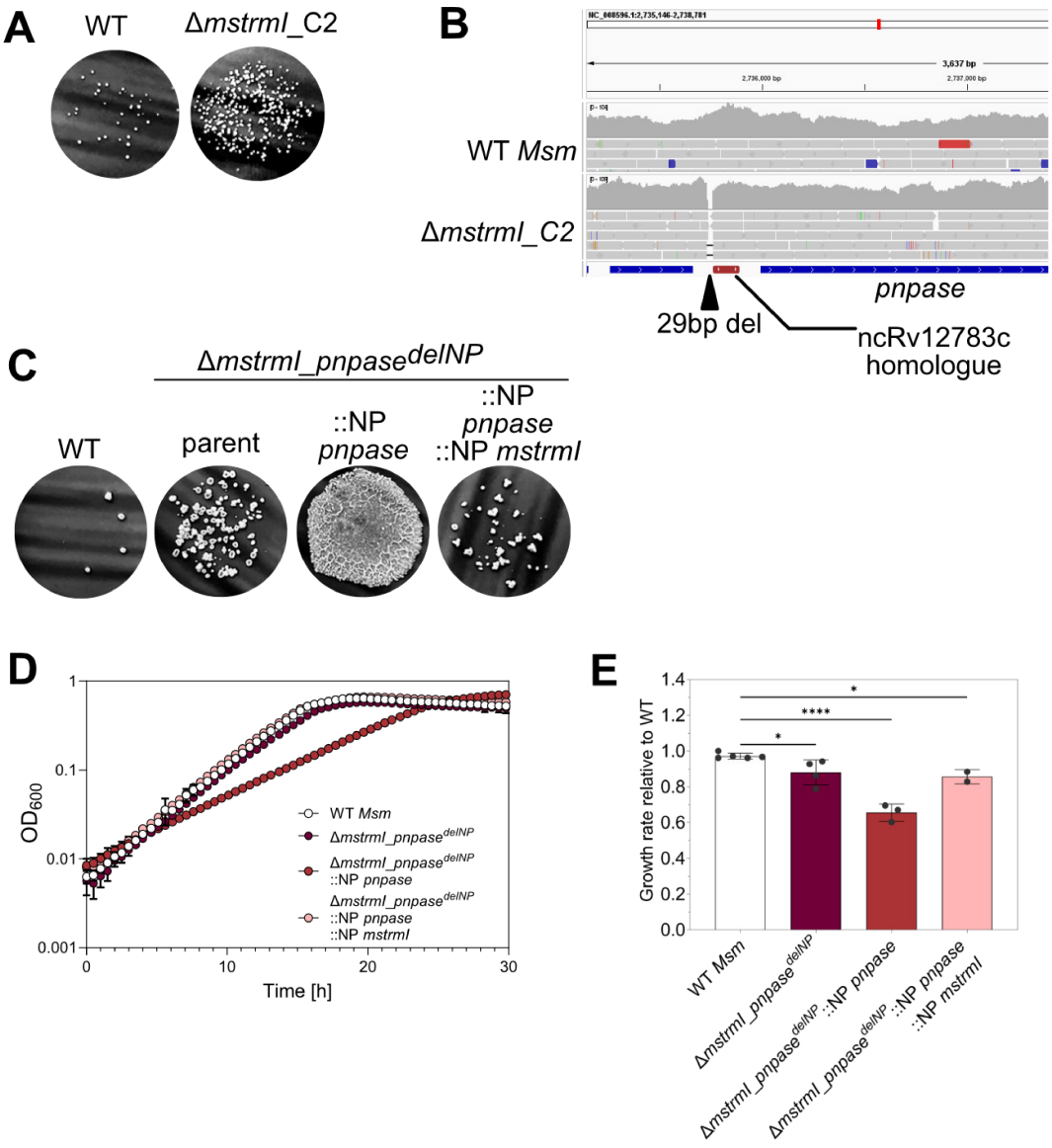


Figure 3.7: **A 29 bp deletion upstream of the *pnpase* mutation decreases the survival of the Δ*mstrmI*_C2 deletion mutant**. (A) The survival of the WT *Msm* and Δ*mstrmI*_C2 strain upon exposure to 10xMIC kanamycin (7 μg/mL). Representative of at least three replicates. (B) Graphical representation of whole genome sequencing of the WT *Msm* and Δ*mstrmI*_C2 strain, shown using IGV viewer. A black arrow indicates the 29 bp deletion upstream of the ncRv12783c and *pnpase*. (C) The survival upon exposure to 10xMIC kanamycin (7 μg/mL) of the WT *Msm* and Δ*mstrmI*_C2, and Δ*mstrmI*_C2 with integrated NP-regulated WT allele of *pnpase*, or both *pnpase* and *mstrmI*. Representative of at least three independent replicates. (D) Growth rate relative to the WT *Msm* extracted from (C), with bars representing the mean of at least three independent experiments and error bars representing +/- SD. Statistical analysis is done against the WT *Msm* using a one-way ANOVA test with multiple comparisons using a Dunnett test.

3.2.5 The 29 bp deletion in the *pnpase* upstream region decreases *pnpase* expression

The *pnpase* is essential in *Msm* and *Mtb*, and it has been shown that a knockdown of the *pnpase*, which reduces its levels by 20-fold, results in a growth defect in *Mtb* (Płociński et al., 2019). This led us to hypothesise that the PNPase^{A167D} mutation and the 29 bp deletion upstream of the *pnpase* could not lead to a complete loss of the PNPase activity. Because the non-coding RNA ncRv12783c is involved in the transcription of the *pnpase*, I hypothesised that 29 bp deletion might impact the levels of the *pnpase* transcript. To assess this, I measured *pnpase* levels using qRT-PCR. Aligning with our hypothesis, Δ*mstrmI_pnpase*^{delNP} strain lost 52% of the *pnpase* transcript compared to the WT *Msm pnpase* levels (Fig. 3.8).

Collectively, this indicated that: (1) Δ*mstrmI*_C2 contains suppressor mutations or deletion of *mstrmI* selected for pre-existing *pnpase* mutations in bacterial population that decreased the levels of the *pnpase*; (2) a partial loss of the PNPase decreases the ability of both Δ*mstrmI* clones to display increased survival upon exposure to aminoglycosides to the level of the AG and GS mutants; and that (3) the PNPase plays a role in the mechanism by which the deletion mutant of *mstrmI* survives better exposure to aminoglycosides. As mentioned, *pnpase* mutations appeared as suppressor mutations in the *Saccharomyces* tRNA A58 methyltransferase mutant, preventing initiator tRNA degradation (Kadaba et al., 2004). Interestingly, suppression mutations in a 3'-5' exoribonuclease also appeared in yeast *Schizosaccharomyces pombe* due to the loss of another tRNA m^{7}G46 methyltransferase, *trm8*, to restore the levels of tRNA^{Tyr} and tRNA^{Pro}, suggesting a role of the *pnpase* in the degradation of hypomodified tRNA (de Zoysa & Phizicky, 2020). Based on these findings, observed *pnpase*-related mutations could hypothetically help stabilise hypomethylated tRNA in the deletion mutant of *mstrmI*, which should not have any methyltransferase activity as compared to the AG and GS mutants - which retain a certain level of MsTrmI.

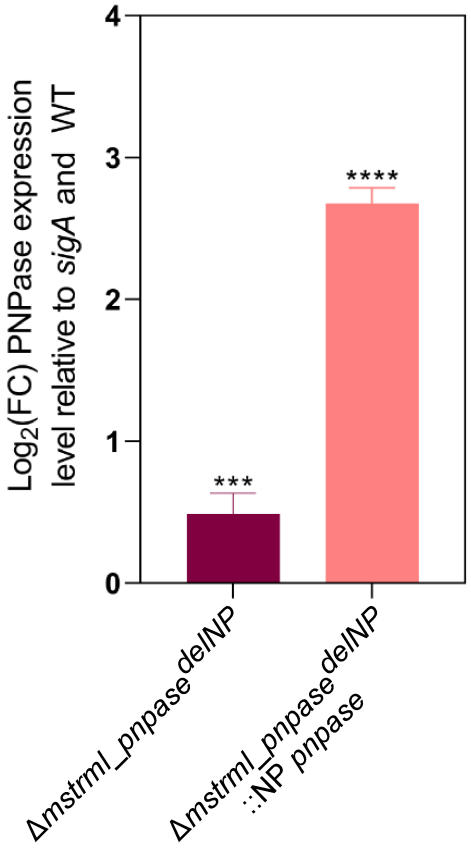


Figure 3.8: **The 29 bp deletion 263 bp upstream of *pnpase* affects the *pnpase* transcript levels**. Transcript levels of WT *Msm*, Δ*mstrmI*_delNP_*pnpase* and Δ*mstrmI*_delNP_*pnpase*::NP *pnpase* measured by qRT-PCR. RNA was extracted as described in 6.8, and cDNA was prepared as described in 6.11. Bars represent the mean of three replicates, with error bars being +/- SD. Values were normalised to WT=1, and statistics were done using a one-way ANOVA test (0.001 (***), 0.0001 (****)).

3.2.6 Mtb *trmI* deletion mutant does not have an increased survival to gentamicin

To investigate if deletion of a tRNA m^1A58 methyltransferase in *Mtb* would confer increased survival upon exposure to antibiotics, I constructed a deletion mutant of *Mtb mttrmI* (gene *rv2118c*) and complemented the deletion strain with the WT allele of *mttrmI*.

To test whether the deletion mutant has increased survival to aminoglycosides, I seeded the WT *Mtb*, Δ*mttrmI* and the complemented strain onto the filters and exposed them to gentamicin at a concentration equivalent to 15x the MIC for 14 days. Compared to the WT *Mtb*, Δ*mttrmI* strain did not have increased survival to gentamicin (Fig. 3.9). I did not observe *pnpase*

mutations in the deletion mutant; however, it did contain SNPs which are listed below (Tab. 3.3). Due to time constraints, the survival upon exposure to other antibiotics nor the impact of the uncovered SNPs were not investigated.

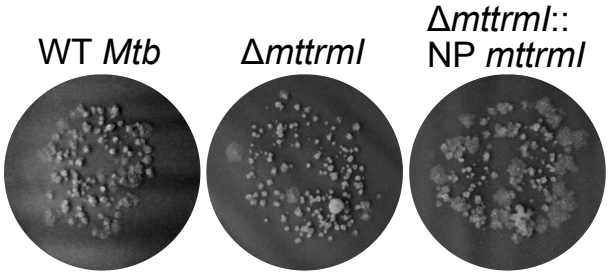


Figure 3.9: **The survival of the WT *Mtb*, Δ*mttrmI* and complemented strain upon exposure to gentamicin**. The WT *Mtb*, the deletion mutant Δ*mttrmI* and complemented strains were seeded onto filters and exposed to 15xMIC gentamicin for 14 days. Filters were switched to charcoal for 24 hours and then to recovery plate until the appearance of the colonies. Representative of two experiments.

Table 3.3: **Single nucleotide polymorphisms identified in Δ*mttrmI* deletion mutant.** Each SNP is annotated with a position in *Mtb* genome, reference and alternated base, the gene where the mutation is found, the effect of the mutation, and the product of this gene. Ref=reference base, Alt=modification found instead of the reference base.

Position	Ref.	Alt.	Gene	Protein	Product
14785	T	C	Rv0012	C233N	Probable conserved membrane protein
55533	TGCC	T	ponA1	P631del	Probable penicillin-binding protein PonA1
55553	C	T	ponA1	P631S	Probable penicillin-binding protein PonA1
990001	G	C	Rv0890c	P866A	Hypothetical protein
1010204	C	CG	Rv0907	C25fsX	Hypothetical protein
1025106	T	C	Rv0919	F141F	Probable N-acetyltransferase
1711627	C	T	Rv1520	Y200Y	Probable sugar transferase
2153410	A	G	Rv1907c	V158A	Hypothetical protein
2809621	T	C	bkdC	T107A	Probable keto acid dehydrogenase E2
2954439	T	C	Rv2627c	N104G	Hypothetical protein

3.3 Summary

Work in Chapter 3 characterised the deletion mutants Δ*mstrmI*_C1 and C2, and the impact of suppressor mutations related to the PNPase found in the Δ*mstrmI*_C1 and Δ*mstrmI*_C2 strains. I showed that both Δ*mstrmI*_C1 and Δ*mstrmI*_C2 strains have increased survival to kanamycin, however, to a lower extent than the AG and GS selected mutants (Fig. 3.2, 3.7). This trend was also observed in the time-kill curve experiment, where the deletion mutant had a different killing kinetics than the AG and GS mutants (3.3, 2.4). I discovered that mutations related to the *pnpase* were responsible for these diminished phenotypes, as complementation of the deletion mutants with the WT *pnpase* allele led to the same AMR phenotypes I observed in the AG and GS mutants (Fig. 3.4, 3.7).

I further showed that the 29 bp deletion upstream of the *pnpase* led to a partial loss of the *pnpase* transcript (Fig. 3.8). In addition, I observed that introducing the WT *pnpase* allele into Δ*mstrmI* strains with the *pnpase* mutations induced a growth defect in these strains (Fig. 3.5, 3.7). Based on these results and findings from Kadaba and colleagues that identified *pnpase* mutations in *trmI* loss-of-function mutant as suppressor mutations that stabilised tRNA from degradation (Kadaba et al., 2004), I propose that mutations related to the PNPase in our deletion mutants are likely preventing hypomodified tRNA degradation in *Msm*, too. This will be explored further in the next chapter.

Finally, work in this chapter revealed that the *Mtb* Δ*mttrmI* strain did not phenocopy the *Msm mstrmI* mutants upon exposure to gentamicin (Fig. 3.9) but did not identify additional AMR phenotypes. Testing the survival of *Mtb* Δ*mttrmI* strain to other antibiotics will be part of future work.

Chapter 4

Results III: The transcriptional regulator WhiB7 mediates the AMR phenotypes of the *mstrmI* mutants

Contents

4.1 Introduction 95

4.2 Results 96

4.2.1 The AG and GS mutants have increased levels of *whiB7* and members of the WhiB7 regulon 96

4.2.2 Deletion of *whiB7* or *eis* in the *mstrmI* mutants abolishes increased survival to aminoglycosides 99

4.2.3 Deletion of *whiB7* abolishes resistance phenotype to macrolides 101

4.2.4 What is the relationship between the loss of MsTrmI and the activation of *whiB7*? 104

4.2.5 MsTrmI methylates *Msm* tRNAs 105

4.2.6 The impact of the loss of m^1A58 modification on the abundance and charging of tRNAs 108

4.2.7 The *mstrmI* mutants have increased levels of Y RNA and Rsr 112

4.2.8 The role of trans-translation in increased survival of the *mstrmI* mutants117

4.3 Summary 126

4.1 Introduction

The data presented in the previous chapters revealed that loss of the MsTrmI tRNA A58 methyltransferase induces increased survival upon exposure to aminoglycosides and MIC-shifted resistance to macrolides. Next, I aimed to unravel the mechanism(s) responsible for these phenotypes.

Previous studies on the homologs of MsTrmI suggested that loss of A58 methylation could impact tRNA stability. The presence of the m^1A58 in tRNA was reported in *Msm* in 1979, when Vani and colleagues identified *Msm* contained this modification (Vani et al., 1979). Short after, Brahmachari and Ramakrishnan showed that MsTrmI methylates A58 of *E. coli* tRNAs, which naturally lack m^1A58 modification (Vani et al., 1979; Brahmachari & Ramakrishnan, 1984). In 2004, Varshney and colleagues documented that the homolog of MsTrmI in *Mtb* (MtTrmI) encoded by Rv2118c is a SAM-dependent methyltransferase that modifies initiator tRNAs at position A58 in *E. coli*, both *in vitro* and *in vivo* (Varshney et al., 2004). However, no study has yet investigated the physiologic substrate(s) of MsTrmI in Msm. Hence, I first aimed to characterise which tRNA(s) are modified by MsTrmI and what the impact of the loss of this enzyme is on *Msm* tRNAs.

4.2 Results

4.2.1 The AG and GS mutants have increased levels of *whiB7* and members of the WhiB7 regulon

I turned to transcriptomics to gain insight into the molecular mechanisms by which the isolated *mstrmI* mutants displayed increased survival to aminoglycosides and MIC-shifted resistance to macrolides. In collaboration with Dr Plocinski, we analysed the transcriptomes of the WT *Msm*, AG and GS mutants and the complemented AG strain by RNA sequencing[1]. Compared to the WT *Msm*, the AG mutant had more than a 4-fold increase of 75 genes, of which 11 had more than 8-fold, and one had more than a 16-fold increase (Fig. 4.1A). Furthermore, the AG mutant had 101 genes downregulated more than 8-fold compared to the WT *Msm* (Fig.4.1A). The GS mutant followed a similar trend; 61 genes had more than a 4-fold increase, of which eight were increased 8-fold, and one was 32-fold increased. Finally, 40 genes were downregulated more than 4-fold (Fig. 4.1B).

Among the 75 genes that were upregulated more than 4-fold in the AG mutant, I observed that 14 of them were part of the WhiB7 regulon (which contains 57 genes, (Hurst-Hess, Rudra, & Ghosh, 2017)) (Fig. 4.1D, Table 4.1). The same trend was observed in the GS mutant, with 15 out of 61 genes, whose expression increased more than 4-fold, belonging to the WhiB7 regulon - including *whiB7* itself (Fig. 4.1D). Members of the WhiB7 regulon include genes involved in intrinsic resistance to ribosome-targeting antibiotics, including *eis*, *tap*, and *erm*. I thus hypothesised that increased levels of *whiB7* might mediate increased survival to aminoglycosides and the MIC-shifted resistance to macrolides of the *mstrmI* mutants. Specifically, I hypothesised that the aminoglycoside-modifying enzyme Eis acting downstream of WhiB7 might mediate the increased survival of the *mstrmI* mutants by aminoglycosides.

[1]The GS complemented strain is still being processed for RNA sequencing due to loss of the RNA in the initial experiment. Dr Plockinski conducted experiments and processing of RNA-seq data, while I conducted the data analysis with the help of Dr Hill.

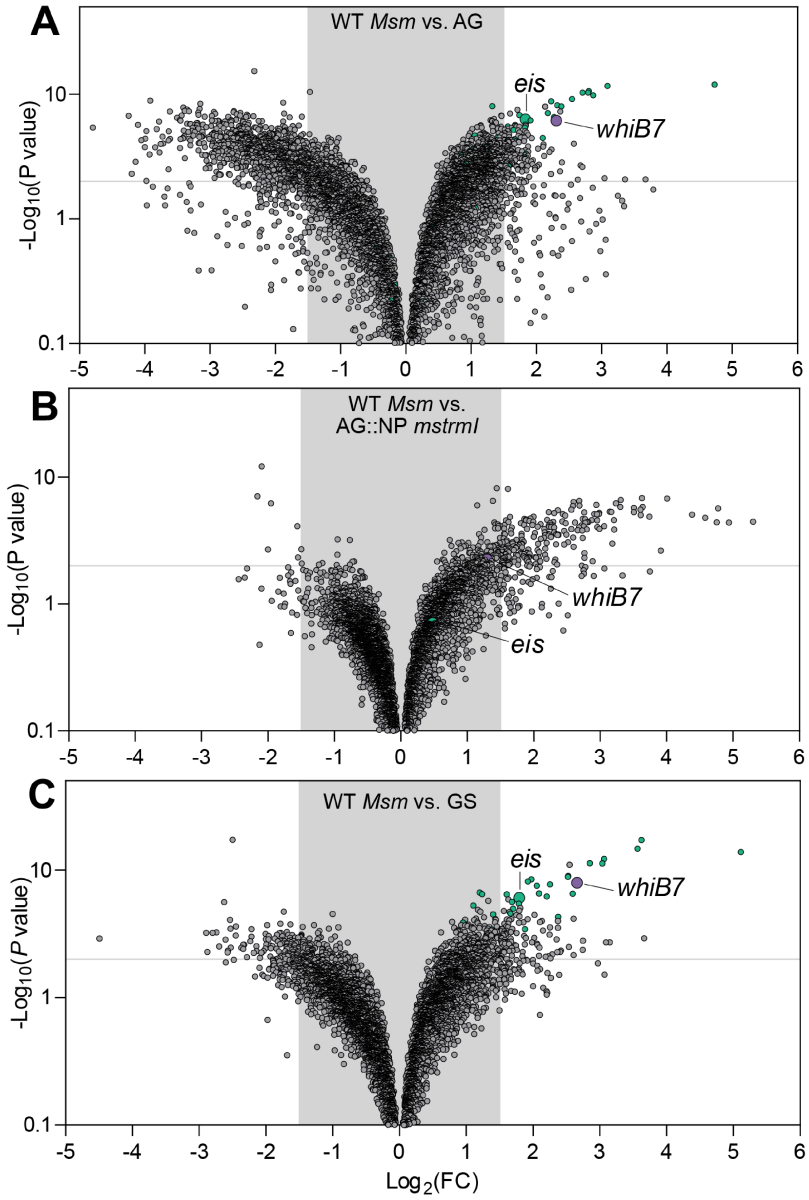


Figure 4.1: ***mstrmI* mutants have increased levels of the transcriptional regulator *whiB7* and members of its regulon**. RNA sequencing results are plotted as -Log_{10} of P value against Log_2 Fold Change (FC), with each gene representing one dot. *whiB7* in purple, and the members of its regulon in green, including an aminoglycoside-modifying enzyme *eis*. Grey zones are cutoffs for P value=0.5 and $\text{Log}_2\text{FC} \pm 1.5$. Average of three biological repeats.

Table 4.1: **List of genes that belong to the *whiB7* regulon and their expression levels in the WT *Msm*, AG and GS mutants, and the AG::NP *mstrmI* strains.** List of genes extracted from (Hurst-Hess et al., 2017). Genes with more than a 4-fold increase in transcript levels compared to the WT *Msm* are coloured in purple. Values are the average of three biological repeats.

Gene	Product	AG Log2(FC)	AG -Log10(P value)	AG::*mstrmI* Log2(FC)	AG::mstrmI -Log10(P value)	GS Log2(FC)	GS -Log10(P value)
MSMEG_0091	putative transcriptional regulator	1.66	4.26	0.33	0.37	1.43	3.27
MSMEG_0307	transcriptional regulator, AraC family protein	-0.72	0.79	-0.37	0.32	-0.05	0.04
MSMEG_0422	transferase	1.56	5.50	-0.08	0.09	1.97	8.42
MSMEG_0423	conserved hypothetical protein	0.90	2.64	0.12	0.16	1.08	3.56
MSMEG_0473	transcriptional regulator, LuxR family protein	0.35	0.42	-0.65	0.83	1.15	2.45
MSMEG_0476	chitin synthase	1.64	2.23	0.94	0.80	2.37	4.28
MSMEG_0546	hypothetical	2.80	10.58	0.17	0.15	3.62	17.19
MSMEG_0687	conserved hypothetical protein	0.74	2.61	-0.03	0.04	1.24	6.46
MSMEG_0688	alanine aminotransferase	2.09	4.45	1.23	1.80	2.59	6.51
MSMEG_1169	integral membrane transport protein	0.91	2.38	0.25	0.35	1.61	6.44
MSMEG_1193	Rsr	2.87	9.79	0.00	0.00	3.56	14.71
MSMEG_1419	hypothetical	2.27	6.54	-0.06	0.05	2.21	6.20
MSMEG_1515	two-component sensor histidine kinase	1.82	5.39	0.76	1.26	1.66	4.55
MSMEG_1516	thioredoxin reductase	1.83	5.69	0.60	0.91	1.70	4.98
MSMEG_1530	integral membrane protein	-0.25	0.48	-0.73	2.15	-0.13	0.22
MSMEG_1953	whiB7	2.31	6.12	1.30	2.24	2.66	7.94
MSMEG_2092	D-aminopeptidase	1.65	5.16	0.22	0.26	1.44	4.06
MSMEG_2188	integral membrane protein	2.55	9.10	0.08	0.07	2.53	8.96
MSMEG_2527	hypothetical	4.73	11.92	2.87	4.58	5.11	13.79
MSMEG_2542	integral membrane protein DUF6	2.32	8.14	-0.07	0.06	2.25	7.72
MSMEG_2736	GTP-binding protein	2.18	7.03	0.45	0.56	2.09	6.53
MSMEG_2795	transmembrane transport protein	-0.17	0.30	-0.14	0.24	0.10	0.16
MSMEG_2905	transcriptional regulator	1.82	3.09	2.44	5.11	1.37	1.90
MSMEG_3140	ABC transporter ATP-binding protein	1.67	4.36	0.80	1.29	1.61	4.09
MSMEG_3203	transporter, LysE family protein	1.28	3.38	0.07	0.07	1.56	4.77
MSMEG_3276	integral membrane protein	1.67	5.55	0.07	0.07	1.68	5.61
MSMEG_3306	zinc-binding alcohol dehydrogenase	1.00	3.00	-0.25	0.37	1.16	3.91
MSMEG_3512	competence damage-inducible protein A	1.14	5.62	0.31	0.66	1.11	5.26
MSMEG_3513	enhanced intracellular survival protein, eis	1.83	6.28	0.48	0.71	1.79	6.04
MSMEG_4141	conserved hypothetical protein	1.07	1.21	2.23	4.04	0.96	1.03
MSMEG_4303	methyltransferase	-0.11	0.08	-0.56	0.54	0.02	0.01
MSMEG_4539	alkanesulfonate monooxygenase	-0.88	1.19	-0.49	0.51	-0.30	0.28
MSMEG_4694	HNH endonuclease family protein	1.23	3.74	-0.29	0.40	0.91	2.21
MSMEG_4968	two-component system sensor kinase	-0.22	0.22	-0.36	0.39	-0.14	0.13
MSMEG_4969	two-component system response regulator	0.88	1.66	0.10	0.08	0.45	0.58
MSMEG_4970	hypothetical protein	-0.46	0.58	-0.44	0.53	-0.03	0.03
MSMEG_4971	oxidoreductase	1.40	4.51	0.26	0.35	1.40	4.49
MSMEG_4972	acetyltransferase	1.84	3.32	0.87	0.99	1.88	3.43
MSMEG_5047	drug resistance transporter Bcr/CflA subfamily protein	0.46	0.62	-0.10	0.09	0.80	1.39
MSMEG_5086	very-long-chain acyl-CoA synthetase	1.91	6.15	0.40	0.52	1.79	5.45
MSMEG_5087	conserved hypothetical protein	2.38	7.97	0.97	1.69	2.52	8.83
MSMEG_5102	ABC transporter ATP-binding protein	-0.06	0.07	0.72	1.53	0.60	1.18
MSMEG_5187	tetracycline-resistance determinant TetV	2.79	10.26	0.67	0.92	3.07	12.22
MSMEG_5292	hypothetical protein	1.58	2.65	0.87	1.03	1.67	2.91
MSMEG_5610	putative transcriptional regulator family protein	-1.59	2.30	-0.11	0.07	-1.02	1.15
MSMEG_5611	spore protein	0.25	0.22	-0.75	0.87	0.96	1.33
MSMEG_5612	amino-acid acetyltransferase	3.09	11.63	0.24	0.23	3.04	11.26
MSMEG_5613	probable conserved transmembrane protein	0.93	2.75	0.38	0.64	0.97	2.95
MSMEG_5659	ABC transporter, ATP-binding protein	0.86	3.22	-0.11	0.18	0.88	3.33
MSMEG_5660	ABC transporter ATP-binding protein	1.74	6.79	0.40	0.64	1.92	8.14
MSMEG_5753	serine/threonine specific protein phosphatase	2.23	8.74	-0.74	1.16	2.06	7.52
MSMEG_5816	conserved hypothetical protein	2.71	10.26	0.27	0.29	2.85	11.27
MSMEG_6245	chloramphenicol resistance protein	-0.55	1.39	-0.22	0.37	-0.26	0.46
MSMEG_6246	pyridoxal-phosphate-dependent transferase	1.06	4.66	0.00	0.00	0.95	3.87
MSMEG_6247	conserved hypothetical protein	0.35	0.83	-0.08	0.13	0.44	1.15
MSMEG_6248	conserved hypothetical protein	1.01	3.51	0.00	0.00	0.71	1.92
MSMEG_6249	conserved hypothetical protein	1.32	7.99	0.13	0.24	1.20	6.64
MSMEG_6250	glutamate--cysteine ligase	1.58	4.31	0.32	0.38	1.38	3.41
MSMEG_6922	transporter, major facilitator family protein	0.42	0.85	-0.33	0.58	0.31	0.56

To confirm that *whiB7* expression was increased in the *mstrmI* mutants, I measured the expression of *whiB7* in the WT *Msm*, the AG mutant and the corresponding complemented strain. To do so, I used a transcriptional reporter in which the expression of an mScarlet fluorescent reporter is regulated by the promoter of *whiB7* (Poulton et al., 2023). In line with the RNA-seq data, the AG mutant had increased *whiB7* expression - 46% of the bacterial population had increased expression of WhiB7 compared to WT *Msm* and the complemented strain (Fig .4.2).

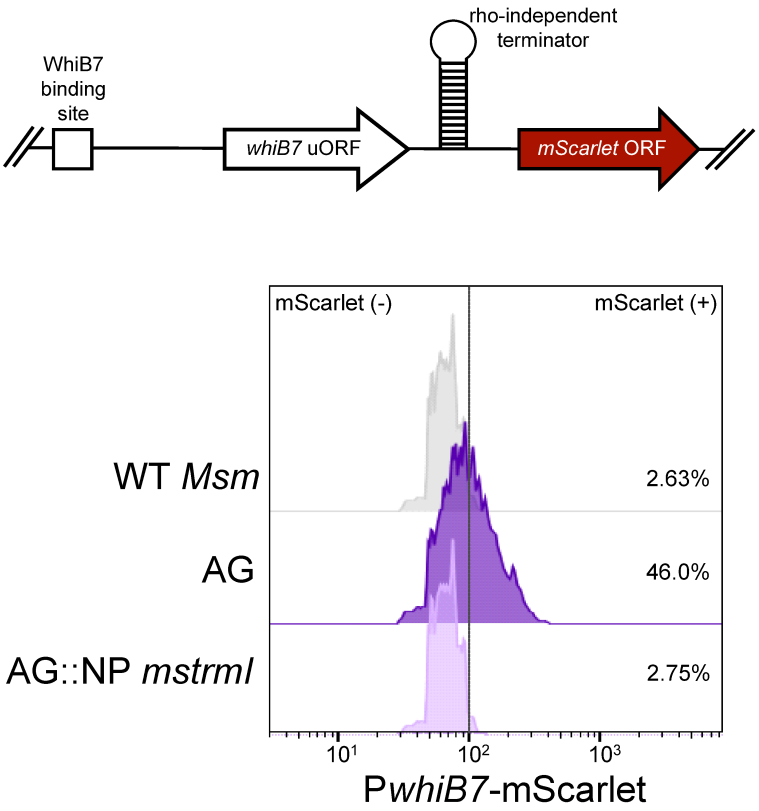


Figure 4.2: **The level of *whiB7* in the AG mutant measured by a fluorescent reporter.** The schematic of the P*whiB7-mScarlet* reporter, which was cloned into an integrative plasmid and transformed into the WT *Msm*, AG mutant and the complemented strain. The fluorescence of the strains with the reporter was measured using a flow cytometer with excitation and emission of 569 nm and 594 nm, respectively. Strains were gated for single cells, and the percentage of mScarlet-positive cells is indicated. Representative of three independent experiments. A part of the reporter plasmid was provided by Dr Poulton (Poulton et al., 2023).

4.2.2 Deletion of *whiB7* or *eis* in the *mstrmI* mutants abolishes increased survival to aminoglycosides

To investigate whether WhiB7 and Eis mediate increased survival of the *mstrmI* mutants, I deleted *whiB7* or *eis* in WT *Msm* and the *mstrmI* mutants, confirmed each KO using PCR and whole-genome sequencing and tested for a fraction of survivors upon exposure to kanamycin. In line with our hypothesis, deletion of either *whiB7* or *eis* abolished increased survival of the AG and GS mutants to WT level (Fig. 4.3A). I complemented the loss of increased survival by expressing either the *whiB7* or the *eis* allele in the deletion strains (Fig. 4.3A).

In addition, I tested the survival of Δ*whiB7* to investigate whether this strain displayed de-

creased survival to aminoglycosides as observed in the deletion strain of *whiB7* in the *mstrmI* mutants. Although the MIC of Δ*whiB7* was unchanged compared to WT Msm, Δ*whiB7* was more sensitive to kanamycin; however, the difference in survival between the WT and Δ*whiB7* strain was less as compared to the loss of survivors in the AG and GS mutants upon deletion of *whiB7* (Fig. 4.3B). Together, these results indicate that increased survival to kanamycin of the *mstrmI* mutants is mediated by increased expression of WhiB7 and Eis.

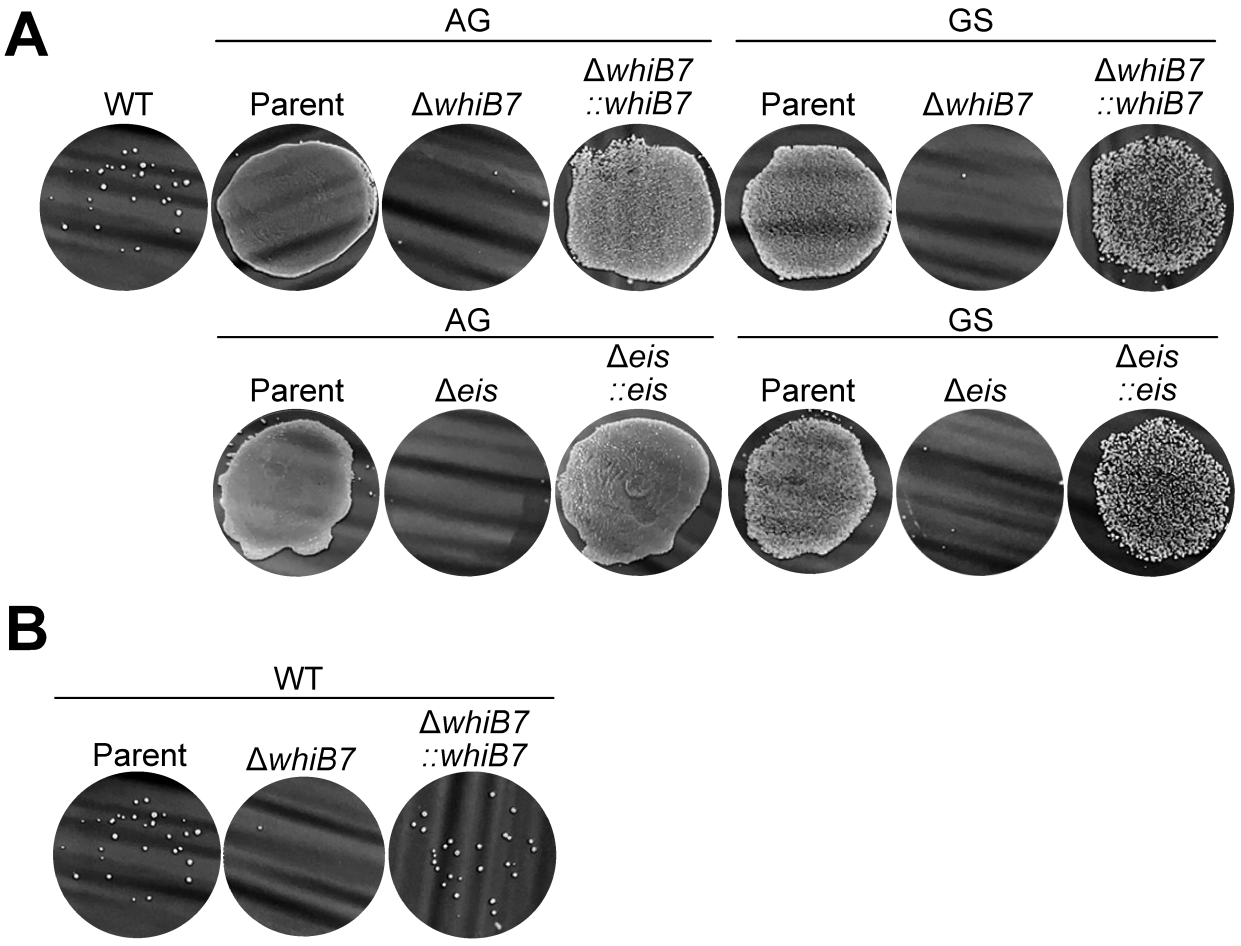


Figure 4.3: ***whiB7* and *eis* mediate increased survival of *mstrmI* mutants to kanamycin.** The fraction of survivors upon exposure to 10x MIC kanamycin of: (A) the WT *Msm*, AG and GS mutants, AG Δ*whiB7*, AG Δ*eis*, GS Δ*whiB7*, GS Δ*eis*, and their complemented strains containing WT alleles of either *whiB7* or *eis*; (B) WT, Δ*whiB7*, and Δ*whiB7* complemented with NP *whiB7*. Representative of at least three experiments.

Furthermore, I tested whether *whiB7* and/or *eis* mediated the increased survival of *mstrmI* mutants upon exposure to amikacin and gentamicin. Although deletion of *whiB7* abolished the increased survival upon exposure to both antibiotics, deletion of *eis* abolished increased survival to amikacin but not gentamicin. This was complemented (Fig. 4.4). This indicated

that WhiB7 also mediated increased survival to amikacin and gentamicin. However, although Eis was the mediator of increased survival to amikacin, other gene(s) from the *whiB7* regulon are likely responsible for increased survival to gentamicin in the *mstrmI* AG mutant (Fig. 4.4).

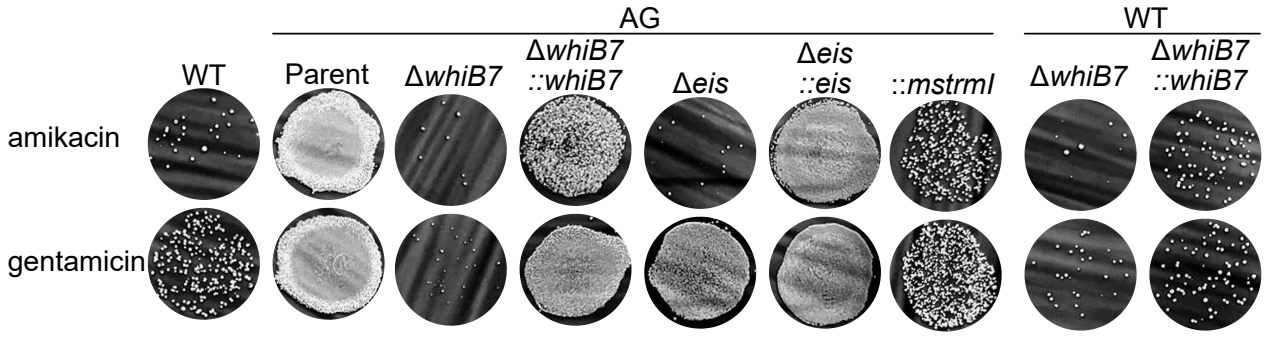


Figure 4.4: **WhiB7 mediates increased survival of the AG mutant to the aminoglycosides amikacin and gentamicin.** Survival upon exposure to 10xMIC amikacin or 10xMIC gentamicin was assessed for the WT *Msm*, AG mutant and complemented strain, and Δ*whiB7* and Δ*eis* and their complemented strains by seeding filters and exposing them to the indicated antibiotics. Results are representative of at least three independent experiments for the WT, AG mutant and complemented strain and of one experiment for the *whiB7* and *eis* deletion mutants and complemented strains.

4.2.3 Deletion of *whiB7* abolishes resistance phenotype to macrolides

In addition to increased survival to aminoglycosides, *mstrmI* mutants displayed MIC-shifted resistance to macrolides (Fig. 2.7). A large part of macrolide resistance in mycobacteria is linked to the presence of a functional Erythromycin Ribosomal Methylase (*erm*), an enzyme encoded by the gene that belongs to the whiB7 regulon that confers resistance to erythromycin and clarithromycin in *M. abscessus* (Brown-Elliott et al., 2015; Nash, Brown-Elliott, & Wallace, 2009). Therefore, I hypothesised that WhiB7 might mediate MIC-shifted resistance to macrolides in the *mstrmI* mutants.

To test this, I measured the MIC of erythromycin and clarithromycin of WT *Msm*, the *mstrmI* mutants in which Δ*whiB7* has been deleted, and the corresponding complemented strains. In line with our hypothesis, the MIC-shifted resistance to macrolides was abolished to the Δ*whiB7* level when I deleted *whiB7* in the *mstrmI* mutants (Fig. 4.5). I complemented the loss of the

MIC-shifted resistance with the *whiB7* allele (Fig. 4.5). Together, these data indicated that MIC-shifted resistance of *mstrmI* mutants to macrolides was mediated by *whiB7*.

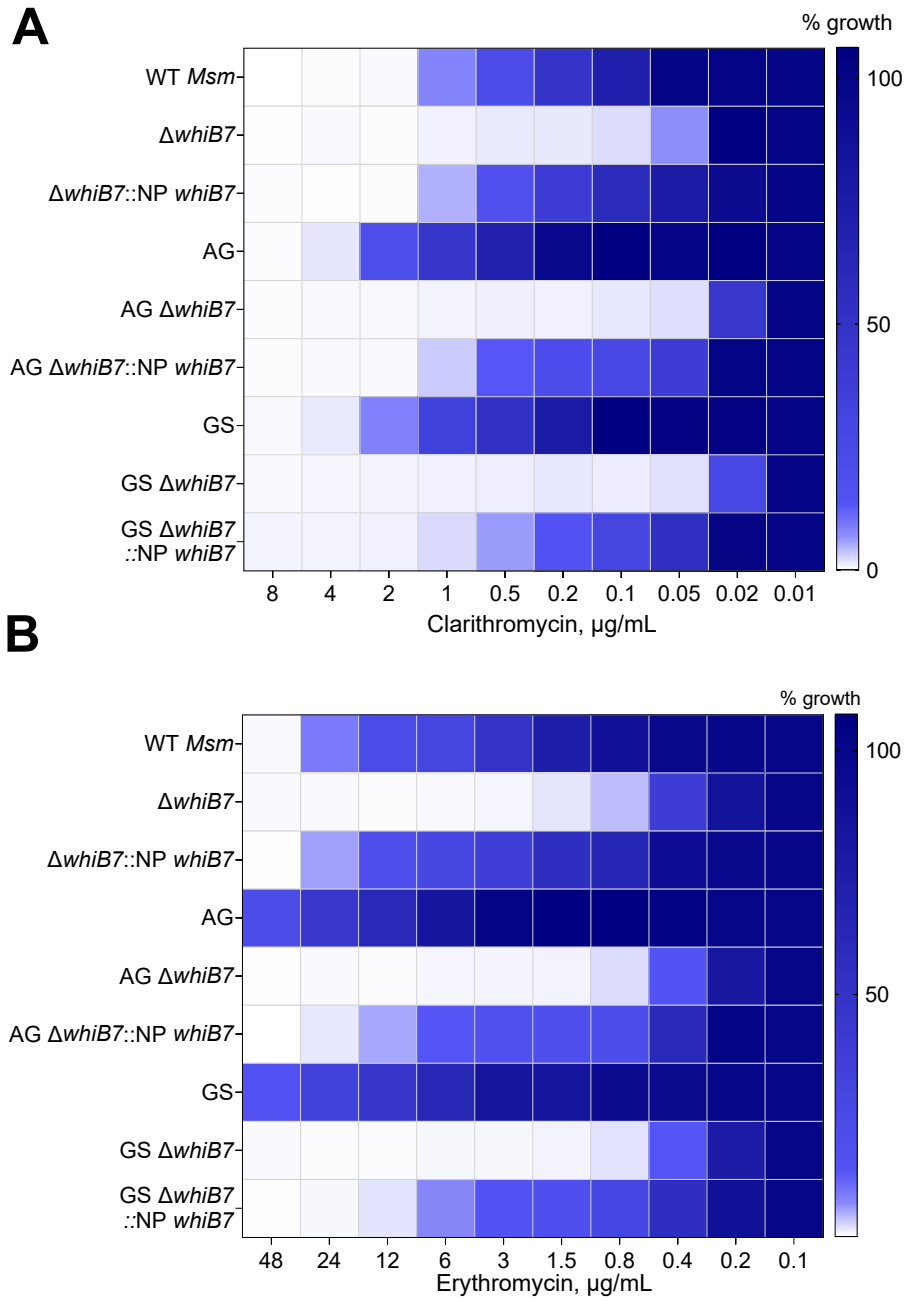


Figure 4.5: ***whiB7* mediates MIC-shifted resistance to macrolides in the *mstrmI* mutants.** Each strain was grown to an exponential phase and exposed to (A) 0-8 μg/mL clarithromycin or (B) 0-48 μg/mL erythromycin in a 96-well plate. OD_{600} was measured after a 72-hour incubation using a plate reader. Each square represents the relative growth of each strain at each concentration compared to the same strain in the absence of the antibiotic. Each measure was a mean of two technical repeats. The mean of at least two independent experiments with two technical replicates.

4.2.4 What is the relationship between the loss of MsTrmI and the activation of *whiB7*?

The expression of *whiB7* is regulated by the rate at which a small ORF upstream of whiB7 (uORF_*whiB7*) is translated. In the absence of stress, translation of the uORF_*whiB7* and the occupancy of the ribosome on the uORF stop codon promotes the formation of a Rho-independent transcriptional terminator, preventing transcription of *whiB7* (Lee, Lee, & Roe, 2022). However, upon exposure to various stresses that affect protein translation - such as aminoglycoside and macrolide exposure - the uORF is not efficiently translated, thus promoting the formation of an antiterminator and leading to transcriptional readthrough into *whiB7* (Lee et al., 2022). In a feedback loop, increased levels of WhiB7 activate further transcription of *whiB7*, leading to a several thousand-fold increase in expression upon exposure to translation-inhibitory antibiotics (Burian et al., 2012). An increase in *whiB7* expression was found in response to a myriad of stressors, such as mutations in arginine biosynthesis genes in *Msm* and in response to different stresses in the host environment (Schrader et al., 2021; Lee et al., 2022; Schnappinger et al., 2003; Poulton et al., 2023) (Fig. 4.6).

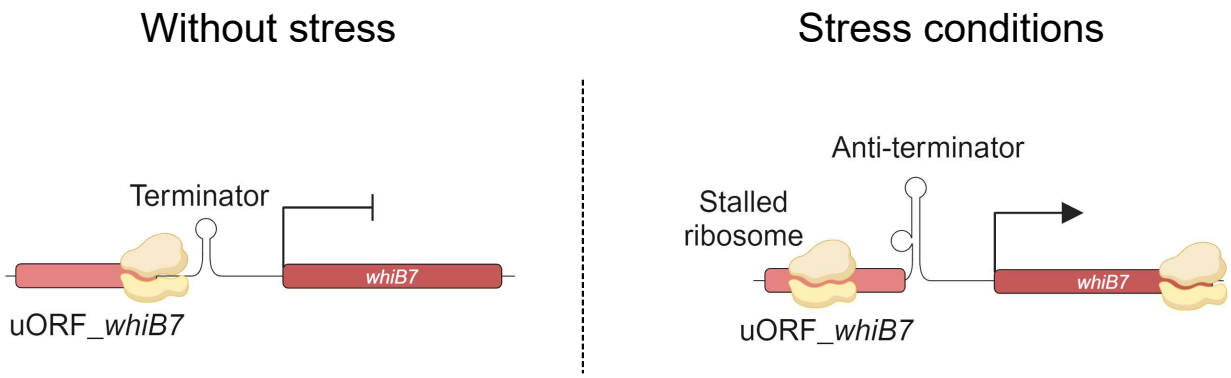


Figure 4.6: ***whiB7* expression is regulated via the translation rate of an open reading frame upstream of *whiB7*.** In the absence of stress, an upstream ORF (uORF) is being translated with the ribosome (yellow), promoting the formation of a transcriptional terminator and preventing transcription of *whiB7*. Upon exposure to stress, such as exposure to antibiotics, ribosomes will inefficiently translate the uORF, leading to ribosome stalling, which will promote the formation of an antiterminator and cause transcriptional readthrough into *whiB7*. Schematic generated via BioRender.

To understand the mechanistic relationship between the lack of the MsTrmI and *whiB7* ac-

tivation, I first aimed to understand better the function of MsTrmI, including the nature of its substrates and the impact of the loss of A58 methylation on *Msm* tRNAs. In *T. thermophilus*, tRNA m^1A58 methyltransferase is essential for this bacteria's adaptation to extreme temperatures (Droogmans et al., 2003). In yeast, tRNA m^1A58 methyltransferase was shown to methylate 16 tRNAs. However, the loss of this modification only affected the stability of the initiator $tRNA^{fMet}$; hypomethylated initiator $tRNA^{fMet}$ was shown to be polyadenylated and degraded by a 3'-5' exoribonuclease, a member of the multi-subunit exosome complex (Anderson et al., 1998; Kadaba et al., 2004; Anderson, Phan, & Hinnebusch, 2000). This literature led us to hypothesize that the loss of the tRNA A58 methyltransferase MsTrmI might impact tRNA stability - therefore, the level of tRNAs - and potentially their level of charging. Of note, charging refers to the aminoacylation of a tRNA with its cognate amino acid. This might, in turn, cause ribosome stalling on the uORF located upstream of *whiB7*, therefore activating WhiB7 expression.

4.2.5 MsTrmI methylates *Msm* tRNAs

First, I investigated if MsTrmI methylates tRNAs of *Msm*, and whether decreased methyltransferase expression in the AG mutant led to a reduced level of A58 modification. To assess this, in collaboration with Dr Plocinski, we sequenced small RNAs from the following strains: WT *Msm*, AG mutant, the AG mutant complemented with a wild-type allele of *mstrmI*, the Δ*mstrmI* with the $PNPase^{A167D}$ mutation and Δ*mstrmI* complemented with a wild-type allele of the *pnpase*[2]. Small RNA-seq has been used frequently to identify epitranscriptional modifications because the presence of methylation at a base leads to misincorporation of the expected nucleotide opposite of a chemically modified nucleotide by the reverse transcriptase rather than the formation of an RT stop, thus allowing us to identify a modification event (Siegfried, Busan, Rice, Nelson, & Weeks, 2014; Yamagami, Sieg, Assmann, & Bevilacqua, 2022). The methylation of A58 is observed as a substitution of A58 in RNA-sequencing reads by any other base (G, C, or T) (Yamagami et al., 2022).

[2] Δ*mstrmI* complemented with the WT alleles of the *pnpase* and *mstrmI* was not sequenced at the stage of thesis submission. The small RNA-seq was done by Dr Plocinski, while I conducted the data analysis.

I aligned small RNA-seq reads to the *Msm* genome and analysed each tRNA for modifications at the A58 site. I observed that MsTrmI methylates most of *Msm* tRNAs for which we had reads coverage (Fig. 4.7). Specifically, we obtained reads for 35 tRNAs, of which two were not modified at all - a $tRNA^{Val\ (CAC)}$ (*MSMEG_2836*) and a $tRNA^{Arg\ (ACG)}$ (*MSMEG_6349*). Furthermore, I found that deletion of *mstrmI* (precise name strain in Fig. 4.7) completely abolished A58 modification in the *Msm* tRNAs, suggesting that MsTrmI is the only m^1A58 tRNA methyltransferase in *Msm* (Fig. 4.7A). Of note, the deletion mutant of *mstrmI* that contains a single polymorphism in the *pnpase* and that has been complemented by both the genes encoding the PNPase and MsTrmI was not subjected to sequencing, preventing us from drawing solid conclusions. Finally, I observed that the A-to-G *mstrmI* mutation of the AG mutant leads to decreased levels of the A58 modification compared to both WT and the complemented strain (Fig. 4.7B). Together, these results indicate that the AG mutant partially loses tRNA methylation at position A58 and that MsTrmI might be the only enzyme responsible for tRNA methylation at position A58 in *Msm*.

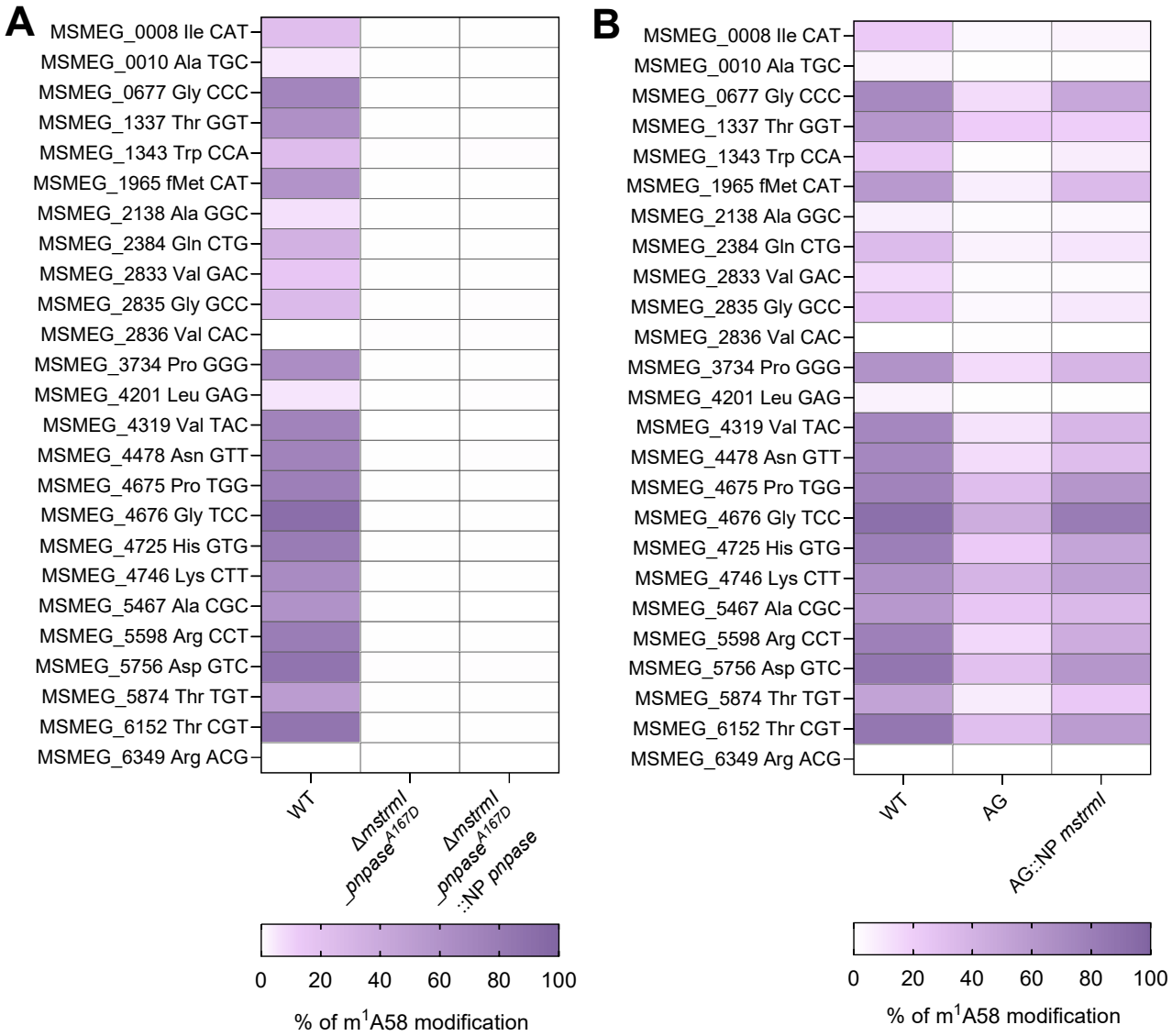


Figure 4.7: **Analysis of tRNA A58 methylation status in *mstrmI* AG and deletion mutants.** (A) Heatmap showing levels of m^1A58 modification of tRNAs in the WT *Msm*, $\Delta mstrmI\_pnpase^{A167D}$ and $\Delta mstrmI\_pnpase^{A167D}$ complemented with the WT *pnpase* allele. (B) Heatmap showing levels of m^1A58 modification of tRNA in the WT *Msm*, AG mutant and the complemented strain. Data was extracted from a small RNA-seq done by Dr Plocinski. Absent tRNAs had less than 100, or no sequencing reads. Average of three biological repeats.

4.2.6 The impact of the loss of m^1A58 modification on the abundance and charging of tRNAs

Hypomethylation of tRNAs at position A58 was shown to impact their stability and initiate their degradation (Kadaba et al., 2004). Thus, I hypothesized that, similarly, hypomethylated tRNAs in *Msm* might be less stable. To assess if tRNAs were less stable and degraded more quickly in the AG mutant, I treated WT *Msm* and the AG mutant with a high concentration of rifampicin to inhibit transcription, including transcription of tRNAs (as described in (Prossliner, Agrawal, Heidemann, Sørensen, & Svenningsen, 2023)). Next, I isolated RNAs at the indicated time points and separated them on a denaturing urea polyacrylamide gel before tRNA visualisation with SYBR Gold staining.

Using this method, I did not observe differences in the levels of tRNAs or any obvious difference in the degradation of tRNAs between WT *Msm* and the AG mutant at any of the time points (Fig. 4.8). This could be due to the fact that I probed for the stability of the tRNA pool, and not discrete subspecies, although it might be that only the most modified tRNAs were less abundant in the AG mutant. This further prompted us to probe for the abundance of individual tRNAs.

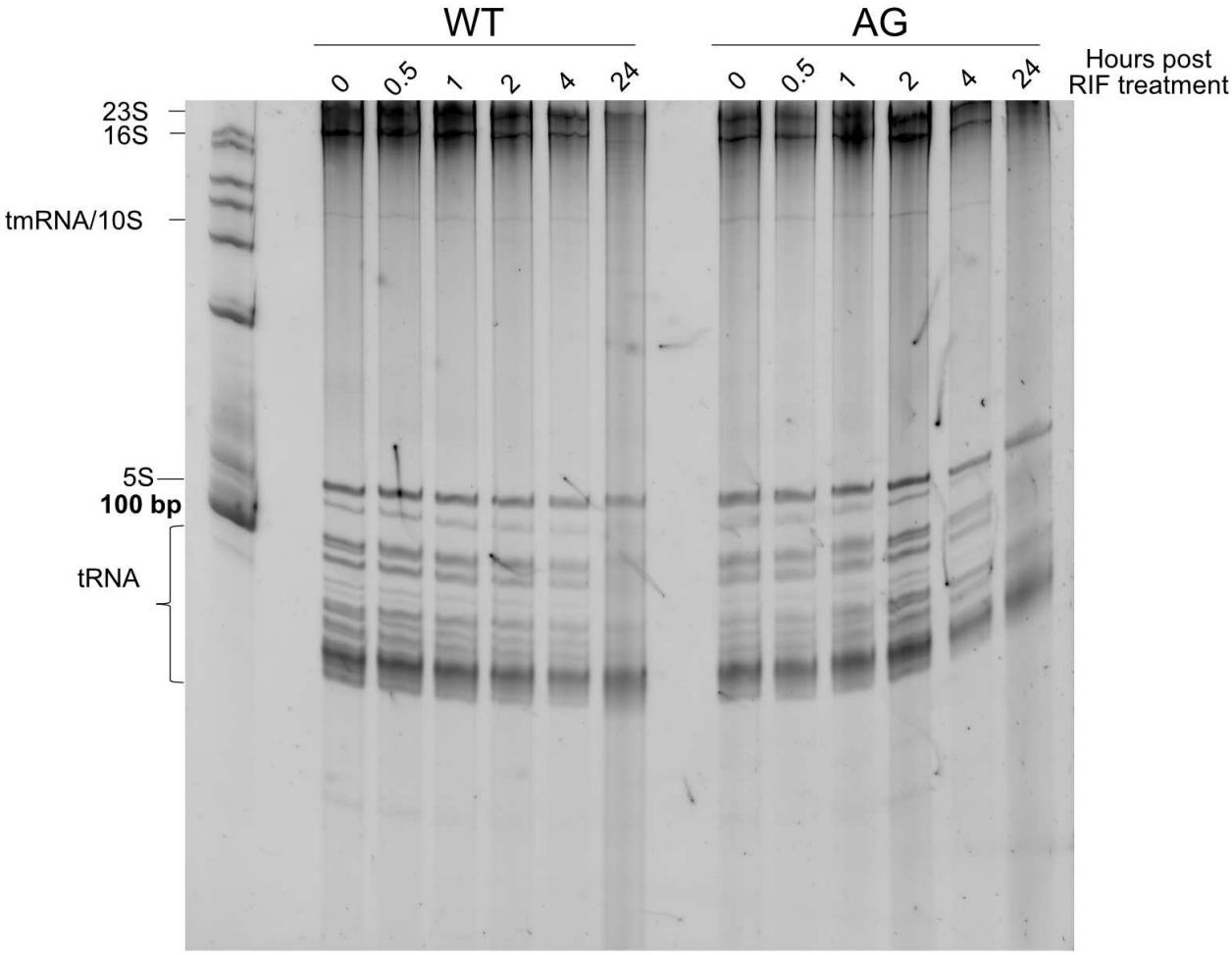


Figure 4.8: **SYBR-gold staining of tRNA upon rifampicin treatment.** WT *Msm* and AG mutant were subcultured into 200 mL of 7H9 medium, grown to OD_{600}=0.25 and treated with 200 μg/mL rifampicin. At indicated time points, 30 mL of each culture was taken and total RNA was isolated. Samples were run on Urea PAGE gel and visualised with SYBR Gold stain. Representative of two experiments.

Our collaborators, Drs Wolin and Chen at the NIH National Cancer Institute (USA) used radiolabeled probes in Northern blots experiments to measure the level of specific tRNA species and evaluate their abundance and charging, which is used as a proxy of correct folding (Chen & Wolin, 2023; Copela, Fernandez, Sherrer, & Wolin, 2008). This revealed that the AG mutant, compared to the WT *Msm* and the complemented AG strain, had decreased levels of the $tRNA^{Ala\ (CGC)}$, $tRNA^{Ala\ (GGC)}$, $tRNA^{Ala\ (TGC)}$, $tRNA^{Arg\ (TCT)}$, $tRNA^{Arg\ (TCT)}$, and $tRNA^{Arg\ (ACG)}$, $tRNA^{His\ (GTG)}$ and possibly $tRNA^{Val\ (CAC)}$. The latter was the tRNA for which we did not observe A58 modification, but more repeats are needed to evaluate the reproducibility of the obtained results (Fig. 4.9A).

To investigate charging, RNAs of the same strains were extracted under acidic conditions to preserve charged tRNA (Varshney, Lee, & RajBhandary, 1991; Copela et al., 2008); half of each sample was treated with a base to remove the amino acid as a control. For all tRNAs in all strains, we observed a mixture of charged and uncharged tRNAs. Overall, it appeared that the lack of A58 modification did not affect the aminoacylation of tRNAs, as we detected charged tRNAs in the mutant strains in proportion to that of WT *Msm* (Fig. 4.9B). Finally, we detected a shift in the mobility of the tRNAs extracted from the AG mutant in all but one tRNA: $tRNA^{Val\ (CAC)}$ - which is one of the tRNAs for which we did not detect A58 methylation in the small RNA seq experiment (Fig. 4.9B, 4.7B). Of note, I showed in Chapter 2 that the AG mutant retains around 10% of *mstrmI* transcripts; hence, the observed differences might be more obvious in the deletion mutant. However, I decided not to use the deletion mutants of *mstrmI* that I constructed because all had mutations in the *pnpase* that might affect the overall levels of tRNAs and provide confounding results.

Together, these results indicate that the loss of the A58 methylation affects the tRNA levels and - potentially - their folding as observed as a mobility shift in charging gel. Since hypomodification of tRNA was shown to induce ribosomal pausing during translation - and consequentially alter the cell's transcriptome (Morscher et al., 2018; Nedialkova & Leidel, 2015) - I hypothesised that such tRNA would cause ribosomal stalling in the uORF of *whiB7* and induce increased *whiB7* expression. Our current experiments involve ribosome profiling (Ribo-seq) of the WT, AG mutant and the complemented strain to provide further insight into ribosome occupancy at the codon level and establish the impact of the lack of A58 modification on codon translation rates in bacterial cells (Ingolia, Ghaemmaghami, Newman, & Weissman, 2009; Nedialkova & Leidel, 2015; Y. Li, Wang, & Liu, 2012; Sawyer, Grabowska, & Cortes, 2018).

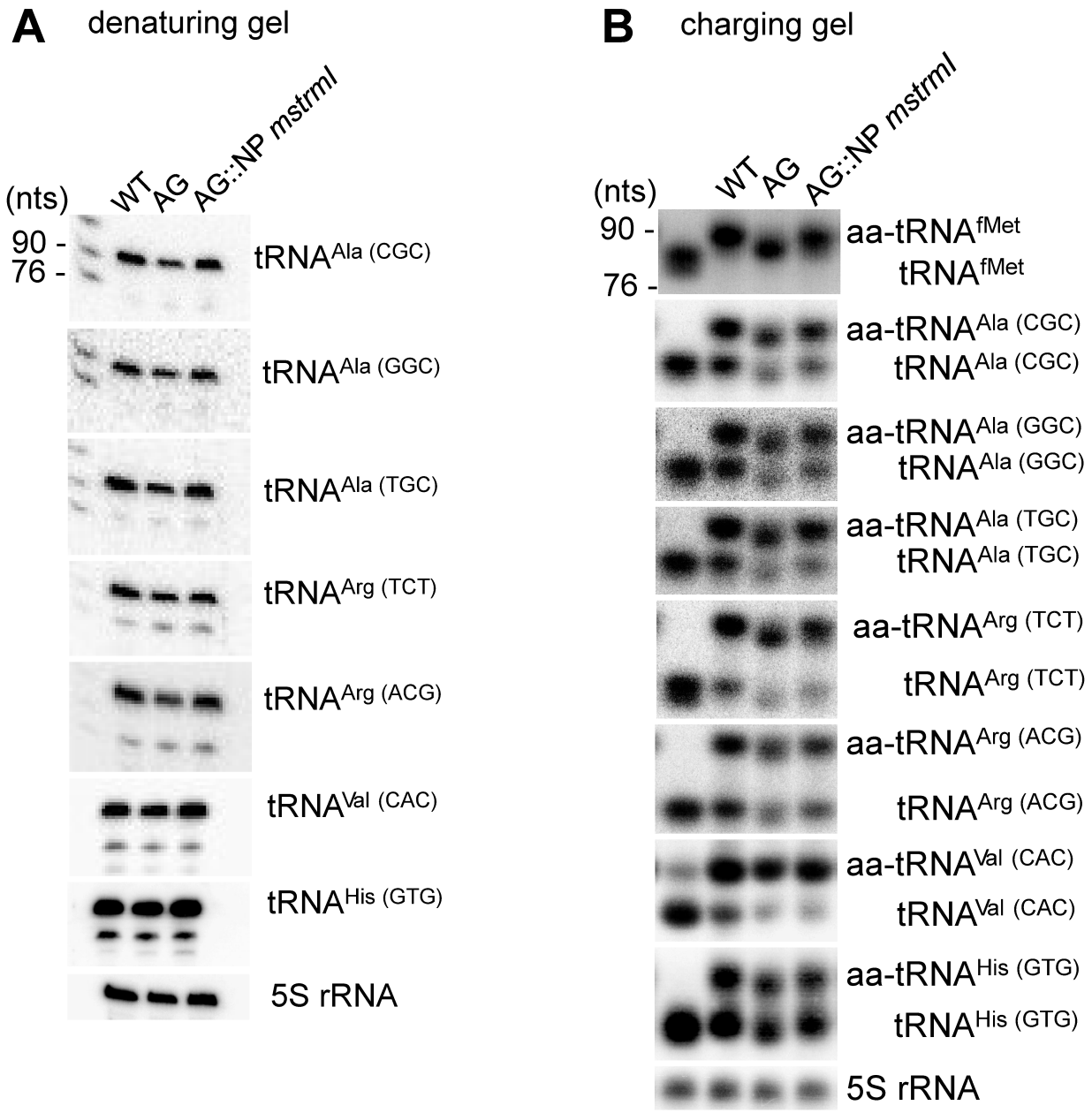


Figure 4.9: **Loss of the A58 methylation affects tRNA levels and gel mobility.** (A) RNA from the WT *Msm*, the AG mutant and complemented AG strain was subjected to northern blot analysis to detect the levels of tRNA fMet, Ala (CGC, GGC, TGC), Arg (TCT, ACG), Val (CAC), and His (GTG), with 5S probed as a loading control. (B) RNA was extracted under acidic conditions to preserve aminoacylation and probed for the same tRNA as described in (A). Lane 1 is deacylated WT *Msm* RNA. Result of one experiment.

4.2.7 The *mstrmI* mutants have increased levels of Y RNA and Rsr

Small RNA-seq data analysis also revealed that the *mstrmI* mutants and the deletions strain contained increased levels of a tRNA-mimicking RNA species termed Y RNA. Specifically, the AG mutant had a 6-fold increase in the levels of *y rna* compared to the WT *Msm* and the complemented AG mutant. The deletion mutants of Δ*mstrmI* with the A167D mutation in the PNPase - either complemented or not by a wild-type allele of the PNPase - had an 8-fold increase in the levels of *y rna* (Fig. 4.10A).

Y RNAs are 80 to 220 nucleotides-long, non-coding RNA that structurally mimic tRNAs. They contain a large stem-loop, a tRNA-like domain, including a TψC loop, and paired nucleotides at the 5' and 3' ends of the RNA (Chen et al., 2013). Y RNAs are found in eukaryotes and a subset of bacteria, and the number of Y RNAs varies between species (Sim & Wolin, 2018). *Msm* contains two Y RNAs termed Y RNA-like A and B (YrlAB), while none were identified in *Mtb* (Chen, Sim, Wurtmann, Feke, & Wolin, 2014).

The function of Y RNAs is tightly related to Ro60, its binding partner. This ring-shaped autoantigen is a major target of the immune system of patients suffering from systemic lupus erythematosus (Dieppe, Wollheim, & Schumacher, 2001). The binding of Ro60 to Y RNA stabilises Y RNA level; deletion of *ro60* significantly reduces the number of Y RNAs in bacteria (Chen et al., 2014; Labbé, Hekimi, & Rokeach, 1999). In metazoans, Ro60 was proposed to function in ncRNA quality control; it was proposed that Ro60 binds ncRNAs that fail to assemble with their corresponding RNA-binding partner and that Ro60 tethers the 3' end of these RNAs (Fuchs, Stein, Fu, Reinisch, & Wolin, 2006). In contrast to ncRNAs, the binding of Y RNAs to Ro60 is sequence-specific (Green, Long, Shi, & Wolin, 1998). Because the binding sites of the ncRNA and Y RNA to the Ro60 cavity overlap, it is thought that one of the functions of Y RNA is to regulate the access of ncRNAs to the Ro60 cavity and regulate ncRNAs binding to their cognate partners (Stein, Fuchs, Fu, Wolin, & Reinisch, 2005). Interestingly, I identified Rsr in our RNA-seq data annotated as a TROVE-containing protein based on one of its domains and found that the expression levels of *rsr* were increased in the *mstrmI* mutants

and the deletion mutants with the mutated or complemented *pnpase* (Fig. 4.10B).

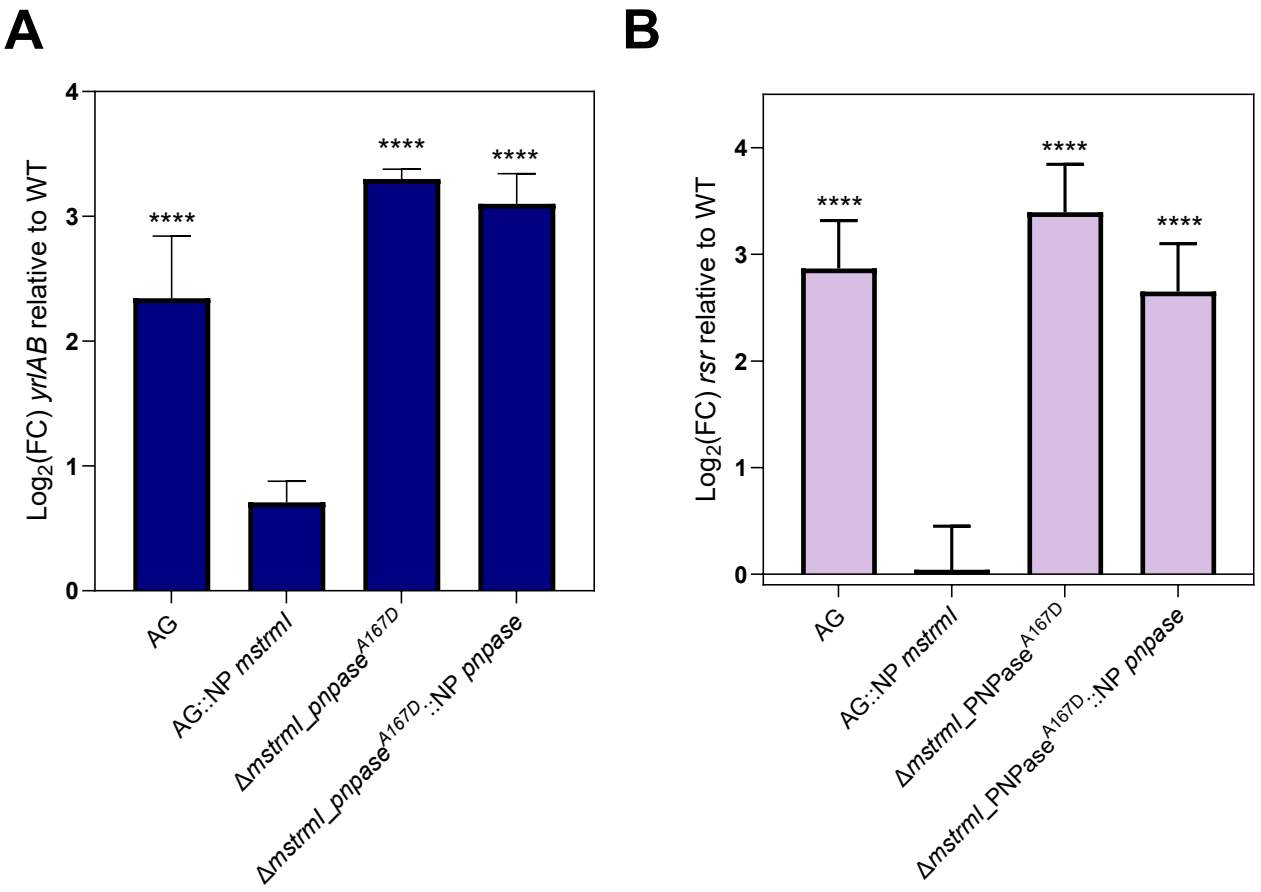


Figure 4.10: ***mstrmI* mutants contain increased levels of *rsr* and *yrlAB*, components of the degradation machinery RYPER**. (A) Log_2 fold-change difference of the levels of *rsr* relative to the WT *Msm* levels. Bars represent the mean and error bars +/- SD from three biological repeats. (B) Log2 fold-change difference of the levels of *yrlAB* relative to the WT *Msm* levels obtained from small RNA sequencing. Bars represent the mean and error bars +/- SD from three biological repeats. Statistical analysis was done using one-way ANOVA with Dunnett test to correct for multiple comparisons against the WT *Msm*.

Further exploring the functions of Y RNAs and Ro60 and Ro60-related proteins (Rsr) in bacteria, I found in the literature that Y RNAs and Rsr form a complex with the PNPase termed RYPER, that stands for Ro60/Y RNA/PNPase exoribonuclease ribonucleoprotein. RYPER is a double-ringed ribonucleoprotein specialised for the degradation of structured RNA (Chen et al., 2013) (Fig. 4.11). In fact, biochemical studies showed that the RYPER machinery degrades structured RNAs more efficiently, such as pre-5s rRNA and tRNA fragment-like substrates, than the PNPase alone (Chen et al., 2013; Evguenieva-Hackenberg, Hou, Glaeser, & Klug, 2014; Sim & Wolin, 2018; Chen et al., 2013; Górna, Carpousis, & Luisi, 2012).

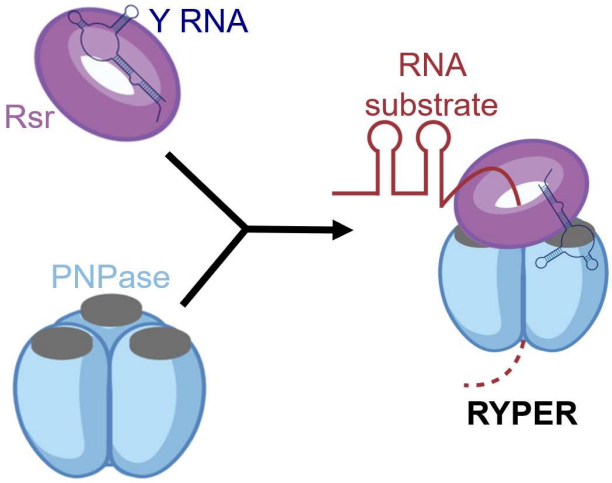


Figure 4.11: **A schematic of the RYPER machinery.** The PNPase is shown in light blue, Rsr is depicted in purple, and Y RNA in dark blue. The RNA substrate is shown in red. Made using BioRender.

Collectively, these findings prompted the following questions: a) do increased levels of Rsr and Y RNA help protect hypomethylated tRNAs from degradation by competing for access to the Ro60-related protein, or did the levels of Y RNA and Rsr increase in the mutants as a consequence of the increased requirement for RYPER to degrade such hypomethylated tRNA? Also, b) did mutations in the gene encoding the PNPase or its promoter occur to prevent the degradation of hypomodified tRNA through RYPER? To investigate the impact of Rsr and Y RNA in *mstrmI* mutants, I made deletion mutants of *rsr* or *yrlAB* in WT Msm and the AG mutant. I assessed if the survival of these strains depended on the other members of the RYPER machinery. In addition, I created strains that either overexpress *rsr* or *yrlAB* in the WT background and tested whether increased levels of *yrlAB* and *rsr* could induce increased survival to aminoglycosides.

Rsr and YrlAB are not essential to mediate increased survival of the *mstrmI* mutants

Since the *mstrmI* mutants had increased levels of *yrlAB* and *rsr*, I first investigated whether overexpressing *yrlAB* or *rsr* would impact the survival of WT *Msm*. I overexpressed *rsr*, *yrlAB*, or both *yrlAB* and *rsr* in WT *Msm* and measured the survival of these strains upon exposure

to kanamycin. None of these strains displayed increased survival upon exposure to kanamycin (Fig. 4.12A). Next, I tested whether the deletion of *yrlAB* or *rsr* alleles diminished the increased survival of the AG mutant. Surprisingly, deletion of either *yrlAB* or *rsr* did not affect the level of survivors of WT *Msm* and the AG mutant (Fig. 4.12B).

Overall, these results suggested that Rsr and YrlAB did not directly mediate the increased survival of the AG mutant upon exposure to kanamycin. Although the increased levels of *rsr* and *yrlAB* in the *mstrmI* mutants might contribute to the degradation of hypomodified tRNA, the main driver of hypomethylated tRNA degradation is likely the PNPase.

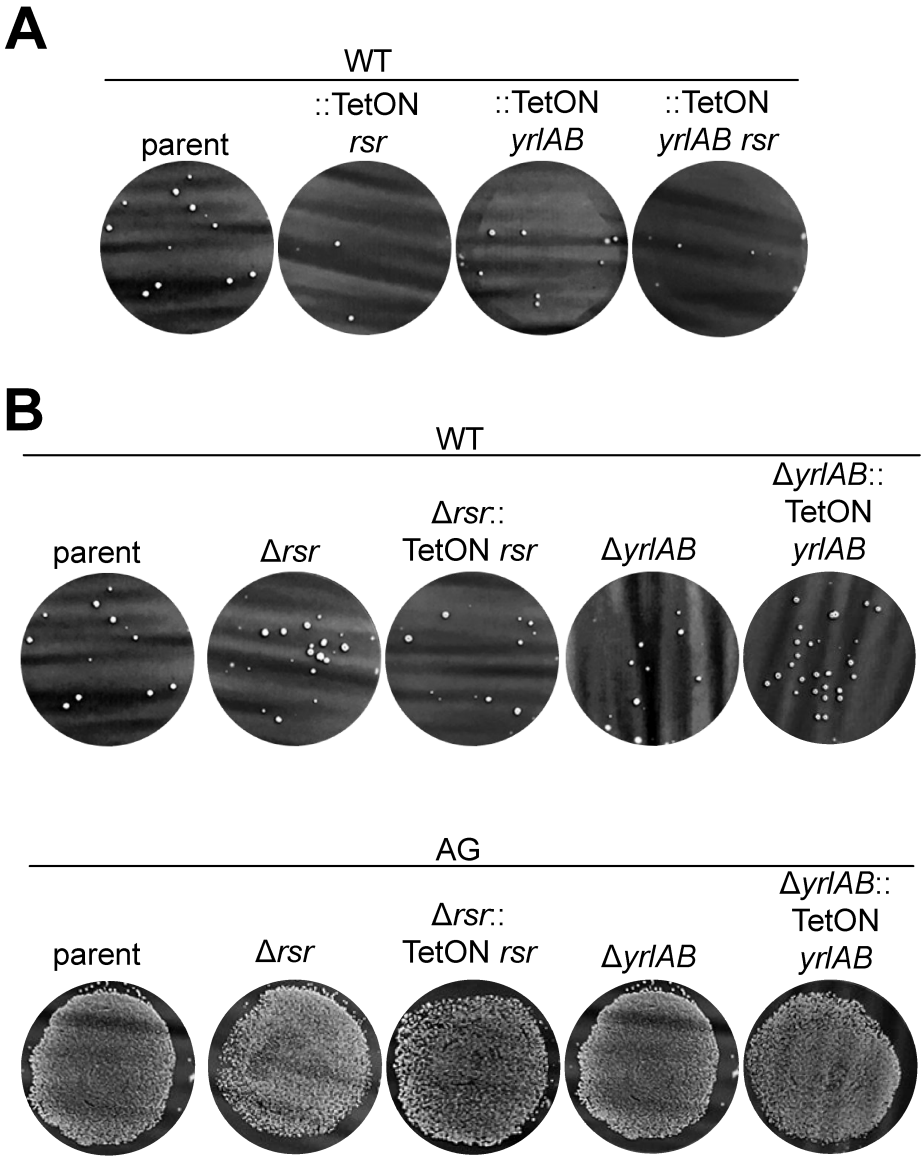


Figure 4.12: **YrlAB and Rsr are not essential for mediating the increased survival of the AG mutant upon exposure to kanamycin.** (A, B) The increased survival phenotype upon exposure to 10xMIC kanamycin for 12 hours. All strains containing the TetON complementation construct were grown in the presence of 200 ng/mL ATc. Representative of two biological repeats.

4.2.8 The role of trans-translation in increased survival of the *mstrmI* mutants

Since we found that hypomethylation of *Msm* impacts the levels of tRNAs, I wondered whether a decrease in the levels of specific tRNAs could be causing ribosome stalling on the *whiB7* uORF, which would, in turn, activate *whiB7* expression. Interestingly, the upstream ORF of *whiB7* of both *Msm* and *Mtb* encodes for a peptide with a high proportion of alanine residues, 24.1% and 22.5%, respectively. This is about 10% higher than the average alanine content in the *Msm* and *Mtb* proteome (Fig. 4.13A,B). In addition, alanine residues in the uORF are distributed on three polyalanine stretches (three or four subsequent alanine residues) (Fig. 4.13A). Such stretches, specifically polyproline stretches, were reported to cause ribosomal stalling in bacteria (Ude et al., 2013; Doerfel et al., 2013) (Fig. 4.13A).

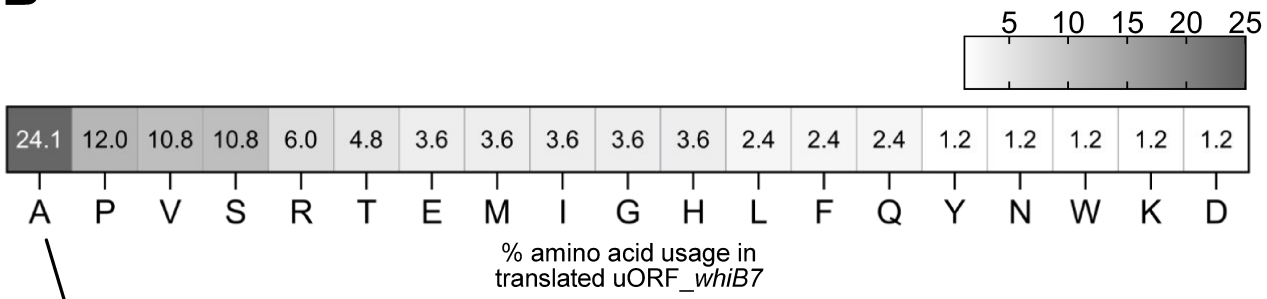
Four codons encode for alanine: GCC, GCA, GCG, and GCT. In *Msm*, there are three $tRNA^{Ala}$ with the corresponding anticodons (the GCA and GCT codons are likely read by the same $tRNA^{Ala}$ via a wobble base). Interestingly, I observed a discrepancy between codon usage in the uORF of *whiB7* and the overall *Msm* genome, with the GCC codon being enriched in the uORF of *whiB7* (Fig. 4.13C).

A

Species	uORF amino acid sequence	% alanines
Msm	VSREMISYVNLSEV**A**V**A**GMPGFIPSVVPV**A**VSSAPMPHQTPEL**A**H**A** **A**H**AAA**GWP**AAAA**I**A**PQPKRRRT**AAA**T**A**TS**A**SVDRSPF	24.1
Mtb	VIDNN**A**FGVG**AAAA**VPT**A**GTPHSKNRV**AAA**TDESVERGST	22.5

Msm	whole proteome	13.3
Mtb	whole proteome	12.9

B



C

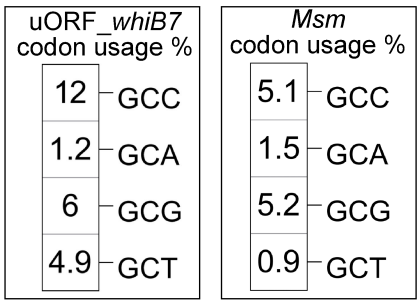


Figure 4.13: **The *whiB7* uORF peptide contains a high percentage of alanine residues.** (A) Amino acid sequences of *Msm* and *Mtb* uORF of *whiB7*, with the indicated proportion of alanine residues. Percentages of alanine in the proteome of *Msm* and *Mtb* (B) Percentage of each amino acid in the uORF of *whiB7*. (C) Codon usage in the uORF of *whiB7* and the *Msm* genome

.

To explore this further, I looked into how bacteria resolve stalled ribosomes. Bacteria primarily use a system called trans-translation. Trans-translation is a process ubiquitous in bacteria that prevents the accumulation of stalled ribosomes and defective toxic peptides. Trans-translation requires a tRNA and mRNA mimic called transfer-messenger RNA (tmRNA, also known as SsrA RNA) and a tmRNA-binding protein SmpB. The tmRNA encodes a 12-residue long, alanine-rich tag (ADSNQRDYALAA in *Msm* and ADSHQRDYALAA in *Mtb*) that allows for the degradation of aberrant nascent polypeptides (Fig. 4.14A). Surprisingly, three out of four alanine residues of the degradation tag in *Msm* are coded by a GCC codon. In addition, the tmRNA, which forms a complex with SmpB, is aminoacylated with alanine residues, making the trans-translation process avid for alanine residues.

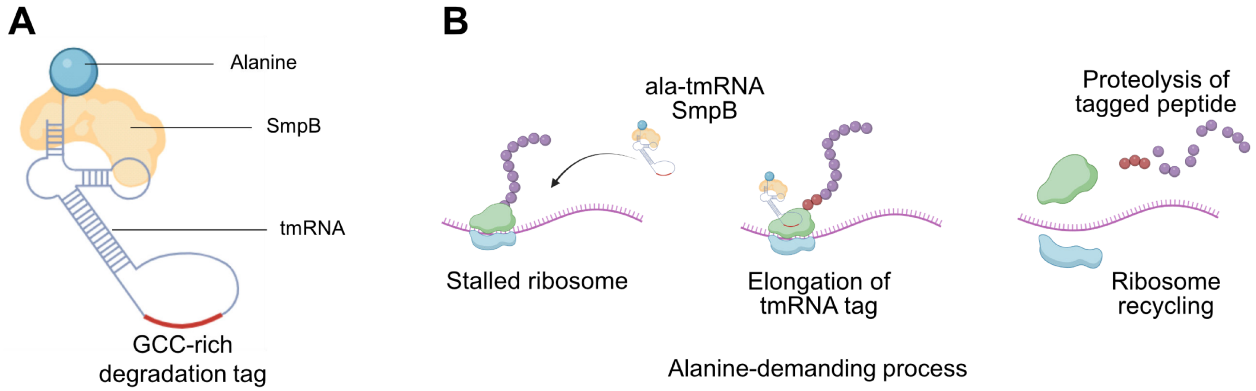


Figure 4.14: **Trans-translation is an alanine-demanding process that resolves stalled ribosomes.** (A) Schematic of tmRNA in complex with SmpB and charged with alanine. (B) Schematic of trans-translation even that results in degradation of a nascent polypeptide chain and recycling of the stalled ribosome. Generated using BioRender.

Upon ribosome stalling, EF-Tu delivers the alanyl-tmRNA-SmpB complex to the A site of the ribosome, and the nascent polypeptide is transferred to the alanine on tmRNA. Further, the polypeptide is tagged with a tmRNA/SsrA tag for further degradation by proteases. As a result, the aberrant nascent polypeptides are degraded and stalled ribosomes are released and recycled (Fig. 4.14B) (Campos-Silva et al., 2022; Andini & Nash, 2011; Moore & Sauer, 2007). Disrupting trans-translation was shown to increase susceptibility to ribosome-targeting antibiotics in *E. coli, Legionella pneumophila* and *S. Typhimurium* (De la Cruz & Vioque, 2001; Aboa, Ueda, Sunohara, Ogawa, & Aiba, 2002; Brunel & Charpentier, 2016; Luidalepp, Hallier, Felden, & Tenson, 2005; Personne & Parish, 2014).

Because of the commonalities in the alanine residue content and the enrichment in the use of GCC codons between tmRNA and the uORF of *whiB7*, I sought to investigate whether trans-translation might increase *whiB7* expression and have a role in the increased survival of the *mstrmI* mutants. Specifically, I wondered how *whiB7* activation - which occurs via ribosome stalling on the uORF - is maintained if trans-translation increases, which happens upon exposure to aminoglycoside (Andini & Nash, 2011).

I thus hypothesised that the expression of *whiB7* fostered by ribosome stalling might be maintained despite increased trans-translation because trans-translation depletes $tRNA^{Ala\text{-}GGC}$, further maintaining ribosome stalling on the polyalanine stretches on the uORF of *whiB7* that leads to *whiB7* expression (Fig. 4.15C).

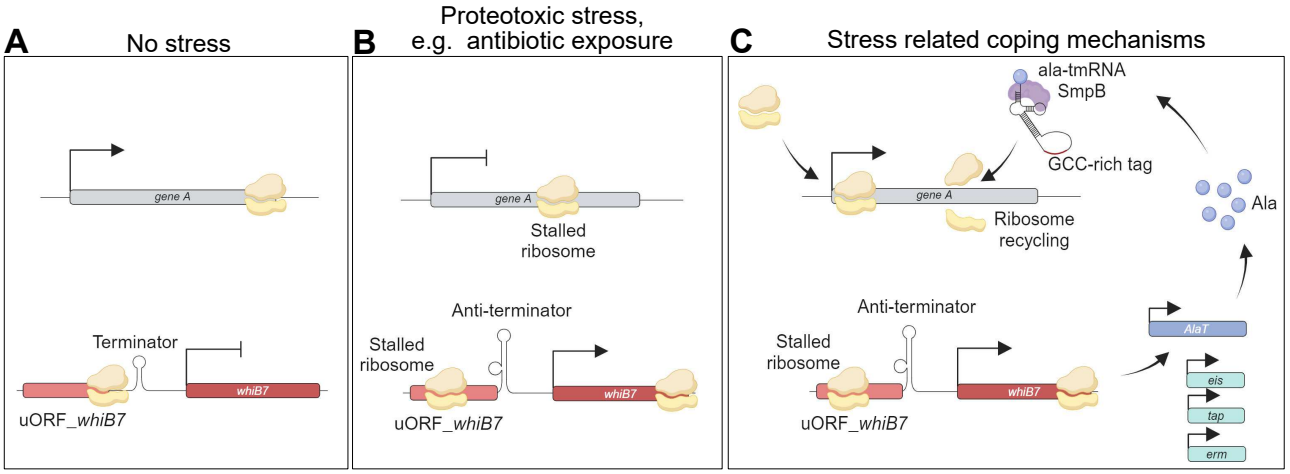


Figure 4.15: **Fail-safe rescue mechanism model from proteotoxic stress**. (A) During no stress conditions, ribosomes translate *gene A* and the uORF_*whiB7*. In the case of *whiB7*, translation of the uORF leads to the formation of a terminator, which prevents the expression of *whiB7*. (B) Upon proteotoxic stress, such as aminoglycoside exposure, ribosomes stall on *gene A* and the uORF_*whiB7*. In the case of *whiB7*, ribosome stalling promotes the formation of an anti-terminator, allowing the expression of *whiB7*. (C) We propose a model where stalling on the uORF_*whiB7* is maintained through the depletion of alanines and $tRNA^{Ala\text{-}GGC}$ by trans-translation. Expression of *whiB7* induces expression of its regulon, including the alanine aminotransferase (AlaT), which repletes the pool of alanine residues that will be further used for trans-translation. Trans-translation depletes the cell from alanine residues and $tRNA^{Ala\text{-}GGC}$, which maintains the stalling on the uORF_*whiB7* due to its high requirement for $tRNA^{Ala\text{-}GGC}$

.

To investigate this, I first used CRISPRi to deplete *smpB* levels and trans-translation[3]; I confirmed *smpB* depletion via qRT-PCR (Fig. 4.16A). Next, I measured the survival upon exposure

[3]We were advised not to target tmRNA due to inefficiency to knock it down using CRISPRi system in mycobacteria (Jeremy Rock, personal communication, 2023).

to amikacin of WT *Msm* and the AG mutant, and WT and AG *smpB*^{KD} strains grown using a range of ATc concentrations to induce the CRISPRi system at different levels. I exposed bacterial cells to amikacin because the CRISPRi system contains a kanamycin resistance cassette; we previously showed that the presence of the kanamycin resistance cassette does not interfere with the survival of *Msm* to other aminoglycosides (data not shown). Knocking down *smpB* led to the loss of increased survival of the AG mutant to amikacin in an ATc-dependent manner, meaning that the AG mutant survived less when trans-translation decreased (Fig. 4.16B). In addition, I measured the expression of *whiB7* using the P*whiB7*_mScarlet reporter, and observed that knocking down *smpB* led to decreased, but not completely abrogated expression of *whiB7* in the AG mutant (Fig. 4.16C).

Together, these results suggested that *trans*-translation might mediate - partially - increased survival of the *mstrmI* isolated mutants and that *whiB7* expression might be maintained despite engagement of trans-translational processes. However, since depleting trans-translation might have secondary effects on bacterial survival, I proceeded to investigate the relationship between trans-translation and maintaining ribosomal stalling on the uORF_*whiB7* by investigating the importance of the GCC codon, shared between the tmRNA and the uORF of *whiB7*.

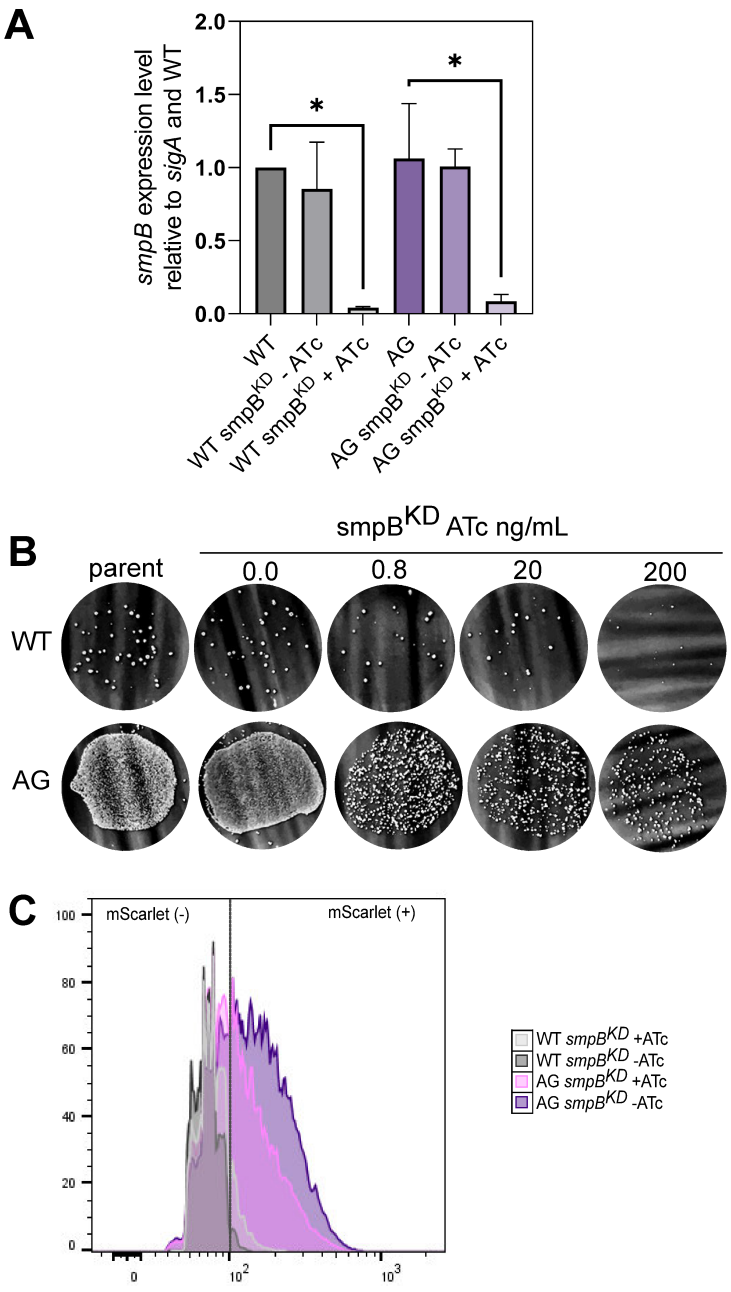


Figure 4.16: **Knocking down trans-translation abolishes increased survival of the *mstrmI* mutants**. (A) Transcript levels of the WT *Msm*, AG mutant and *smpB*^{KD} strains grown in the absence or presence of 200 ng/mL ATc measured by qRT-PCR. RNA was extracted as described in 6.8, and cDNA was prepared as described in 6.11. Representative of two biological repeats with three technical repeats. (B) Survival upon exposure to amikacin of WT, AG mutant, and WT and AG *smpB*^{KD} strains grown with a range of ATc. Representative of five biological repeats. (C) The fluorescence of the strains with the P*whiB7*_uORF reporter was measured using a flow cytometer with excitation and emission of 569 nm and 594 nm, respectively. Strains were gated for single cells, and the percentage of mScarlet-positive cells is indicated. Representative of two biological experiments. A part of the reporter plasmid was provided by Dr Poulton (Poulton et al., 2023).

To do so, I mutated the uORF of *whiB7* to either replace all alanine-encoding codons with GCC codons (all-to-GCC), all GCC codons to GCG (GCC-to-GCG), or mutate all alanine codons to encode for other amino acids (Ala-to-other). I integrated these constructs into the Δ*whiB7* WT and AG strains and measured the survival of these strains upon exposure to kanamycin in liquid (Fig. 4.17). I observed that removing the GCC codons from the uORF abrogated increased survival of the AG mutant upon exposure to kanamycin, while it did not affect the WT *Msm*. In addition, replacing all alanine-encoding codons with other amino acids also decreased the survival of the AG mutant, but not to the same level as replacing GCC codons with GCG codons did. This result indicated that increased survival depends on the presence of the GCC codon in the uORF of *whiB7*, however multiple repeats are needed to confirm these preliminary results.

```
WT              gtgtcccgcgaaatgatcagctacgtcaacttgagcgaagtcGCAgtgGCGggcatgccc    60
GCG-to-GCC      gtgtcccgcgaaatgatcagctacgtcaacttgagcgaagtcGCAgtgGCCggcatgccc    60
all-to-GCC      gtgtcccgcgaaatgatcagctacgtcaacttgagcgaagtcGCCgtgGCCggcatgccc    60
GCC-to-GCG      gtgtcccgcgaaatgatcagctacgtcaacttgagcgaagtcGCAgtgGCGggcatgccc    60
                ****************************************** ***   *********

WT              gggttcattccttccgttgtaccggtgGCTgtttcgtcgGCCcccatgccgcatcagacg    120
GCG-to-GCC      gggttcattccttccgttgtaccggtgGCTgtttcgtcgGCCcccatgccgcatcagacg    120
all-to-GCC      gggttcattccttccgttgtaccggtgGCCgtttcgtcgGCCcccatgccgcatcagacg    120
GCC-to-GCG      gggttcattccttccgttgtaccggtgGCTgtttcgtcgGCGcccatgccgcatcagacg    120
                ************************** ********** ******************

WT              cccgagctcGCGcatGCCGCTcacGCCGCCGCTggttggccgGCCGCCGCTGCCattGCG    180
GCG-to-GCC      cccgagctcGCCcatGCCGCTcacGCCGCCGCTggttggccgGCCGCCGCTGCCattGCC    180
all-to-GCC      cccgagctcGCCcatGCCGCCcacGCCGCCGCCggttggccgGCCGCCGCCGCCattGCC    180
GCC-to-GCG      cccgagctcGCGcatGCGGCTcacGCGGCGGCTggttggccgGCGGCGGCTGCGattGCG    180
                *********   ***** ** ***** ** ** ********** ** ** ** ***

WT              ccgcagcccaagcgtcgtcgcaccGCCGCCGCCaccGCGacaagcGCGtccgtggatcgg    240
GCG-to-GCC      ccgcagcccaagcgtcgtcgcaccGCCGCCGCCaccGCCacaagcGCGtccgtggatcgg    240
all-to-GCC      ccgcagcccaagcgtcgtcgcaccGCCGCCGCCaccGCCacaagcGCGtccgtggatcgg    240
GCC-to-GCG      ccgcagcccaagcgtcgtcgcaccGCGGCGGCGaccGCGacaagcGCGtccgtggatcgg    240
                ************************ ** ** ***   ********************

WT              agccccttctag    252
GCG-to-GCC      agccccttctag    252
all-to-GCC      agccccttctag    252
GCC-to-GCG      agccccttctag    252
                ************
```

Figure 4.17: **Alignment of the WT and mutated uORF of *whiB7* used in this study.** Codons encoding an alanine are highlighted in purple (GCA), blue (GCC), green (GCG), and yellow (GCT), while the codon encoding for a histidine is colored in orange (CAC). An alignment was generated using Clustal Omega.

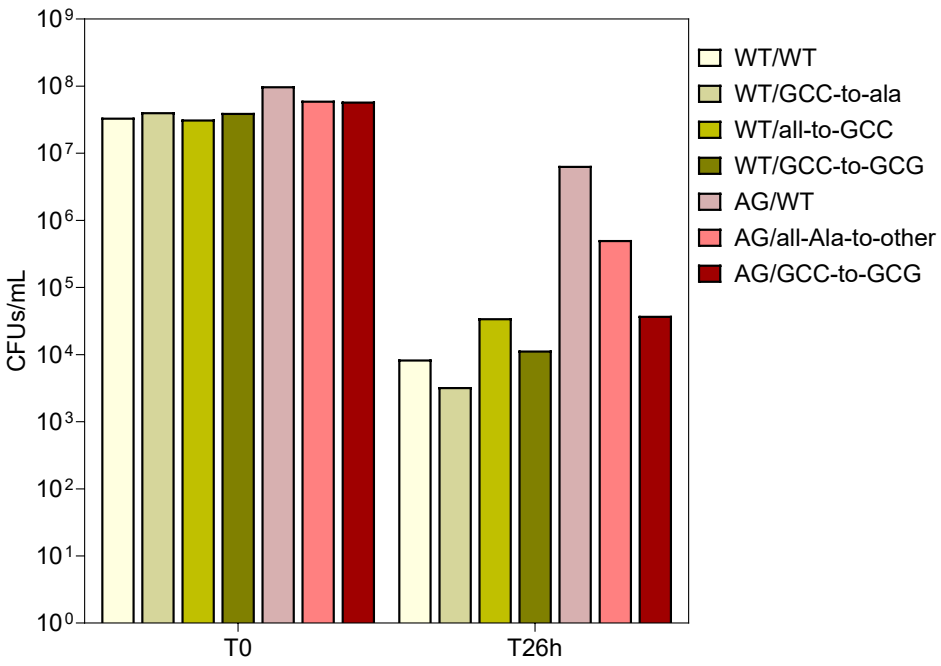


Figure 4.18: **Mutating GCC codons of the uORF of *whiB7* abolishes the increased survival of the AG mutant.** Strains were exposed to 5xMIC amikacin, and killing was observed as CFUs over the course of 60 h. Result of one experiment done by Dr Helene Botella.

Finally, we are currently working on investigating the relationship between trans-translation and *whiB7* expression by testing whether *whiB7* levels would be retained if GCC codons are not utilized during trans-translation. We are currently testing two scenarios:

1. Would the expression of *whiB7* be abolished if we overexpress a tmRNA with mutated GCC-to-GCG codons? This would prevent the consumption of $tRNA^{Ala\ (GGC)}$ and would decrease the levels of $tRNA^{Ala\ (CGC)}$ instead.

2. Would *whiB7* expression be maintained if the uORF of *whiB7* had all GCC codons replaced by GCG, and then a mutated $tmRNA^{GCC\text{-}to\text{-}GCG}$ is expressed? This experiment would allow us to test if we can obtain increased *whiB7* levels when the most abundant codons in the uORF of *whiB7* and in the SsrA tag are the same.

If both are confirmed, these results would establish that stalling on the uORF of *whiB7* is, rather counter-intuitively, maintained through the activity of trans-translation. In other words, this would mean that *whiB7* expression is insensitive to rescue by trans-translation and that the uORF of *whiB7* might have evolved to have this dependency.

4.3 Summary

In this chapter, I presented data showing that decreased killing to aminoglycosides and MIC-shifted resistance to macrolides of the *mstrmI* mutants is mediated by increased levels of *whiB7*. Specifically, I showed that decreased killing to kanamycin and amikacin depended on *whiB7* and its downstream effector *eis*, an aminoglycoside-modifying enzyme, whose levels were increased up to 8-fold in the *mstrmI* mutants.

To investigate the relationship between the increase of *whiB7* in the mutants lacking a tRNA A58 methyltransferase and WT *Msm*, I looked into the impact of the partial loss of a tRNA methyltransferase MsTrmI on the tRNA. I discovered that hypomethylated tRNA were less abundant and had different migration on the gel - pointing towards structural differences upon loss of m^1A58 modification. Since *whiB7* expression is induced upon stalling of the ribosomes on the uORF, I hypothesised that lack of sufficient functional tRNAs leads to a phenomenon akin to amino acid starvation, leading to ribosome stalling. To confirm this, we are currently doing Ribo-seq in collaboration with Dr Teresa Cortes at the Institute of Biomedicine Valencia, Spain, to uncover ribosomal occupancy in the *mstrmI* mutant versus WT *Msm* and complemented strain.

Finally, I observed that the uORF of *whiB7* encodes for a peptide with a high percentage of alanine residues. I also observed a discrepancy between the usage of codons encoding for alanine in the uORF and the *Msm* genome, with the GCC codon being highly used in the uORF of *whiB7*. I noticed that another process, trans-translation, which resolves stalled ribosomes upon stresses such as exposure to aminoglycoside, also requires high levels of alanine (for the charging of tmRNA) and tRNA encoding for the GCC codon (for the SsrA tag). This prompted us to seek whether *whiB7* expression might be influenced by the level of trans-translation.

I showed that knocking-down trans-translation led to reduced expression of *whiB7* and abolished increased survival of the AG mutant. Finally, some of our preliminary results suggest that decreased killing is also observed in the AG mutant that has a mutated uORF such that there are no more GCC codons. This might indicate that - although trans-translation resolves

stalled ribosomes and should reduce whiB7 expression - the reliance on GCC codons might provide a fail-safe mechanism that would allow to maintain stalling on certain genomic regions that are important to cope with stress, while trans-translation and ribosome recycling allow overall recovery of a bacterial cell from proteotoxic stress.

In other words, our model proposes that *whiB7* expression is maintained during antibiotic exposure through the depletion of $tRNA^{Ala\ (GGC)}$ and alanine by trans-translation. As such, the expression of *whiB7* is maintained due to the insensitivity of the uORF to ribosome rescue by trans-translation. Such a mechanism would allow bacteria to survive antibiotic exposure while preventing toxicity from incorrectly translated peptides and resolving ribosomes for another translation event. We propose that other genomic regions might also be insensitive to trans-translation rescue, allowing them to maintain the expression of genes required for stress survival. Our current investigation involves analysis of other genes whose expression is regulated via transcriptional attenuator and whether their expression also depends on trans-translation - in *Mtb* and other bacteria. Such findings would open the doors to understanding how bacteria maintain translation during exposure to translation-inhibitory antibiotics.

Chapter 5

Discussion

Contents

5.1 The transcriptional regulator WhiB7 mediates AMR phenotypes of the *mstrmI* mutants 129

5.2 Is *whiB7* insensitive to rescue by trans-translation? 131

5.3 MsTrmI methylates *Msm* tRNAs 133

5.4 Δ*mstrmI* presents with *pnpase* mutations 135

5.5 What is the relationship between Y RNA, Rsr, and hypomethylated tRNA? 137

5.6 Concluding remarks 137

Tolerance and persistence to antibiotics contribute to the relapse of bacterial infections and the development of MIC-shifted resistance under antibiotic pressure (J. Liu et al., 2019; Sebastian et al., 2017; Windels et al., 2019). Therefore, these phenomena threaten our capability to treat bacterial infections, and understanding the mechanisms behind their development can generate future strategies for combating persisting infections. In this work, I utilised the mutants isolated in the screen by our group members to unveil the mechanism behind their increased survival (Schrader et al., 2021). In addition to discovering that the mediator of increased survival of investigated mutants is a transcriptional regulator *whiB7*, this approach led us to develop a

model of a novel mechanism of bacteria's ability to maintain the expression of *whiB7* during exposure to ribosome-targeting antibiotics.

5.1 The transcriptional regulator WhiB7 mediates AMR phenotypes of the *mstrmI* mutants

I discovered that *Msm* with loss-of-function mutations in a gene encoding a tRNA m^1A58 methyltransferase present with increased survival to ribosome-inhibiting antibiotics aminoglycosides kanamycin, amikacin, and gentamicin, and MIC-shifted resistance to macrolides clarithromycin and erythromycin. While aminoglycosides inhibit translation through binding with high affinity to the A-site of the 16S rRNA of the 30S ribosomal subunit, promoting mistranslation of the translating peptide (Kotra, Haddad, & Mobashery, 2000), macrolides inhibit protein synthesis through interaction with the 23S rRNA of the 50S ribosomal subunit, blocking the nascent peptide chain exit and preventing the polypeptide chain elongation (Tenson, Lovmar, & Ehrenberg, 2003). Generally, the MIC-shifted resistance to aminoglycosides occurs due to several mechanisms, such as decreased permeability, increased efflux, modification of the 30S subunit, and enzymatic modification and inactivation of aminoglycosides by Eis. In the case of macrolides, the MIC-shifted resistance occurs due to mutations of the 23S rRNA and through the function of Erm ribosomal methylase. Since both Eis and Erm are in the WhiB7 regulon, it was not surprising that I found increased levels of *whiB7* in the *mstrmI* mutants.

Previous work in the Vaubourgeix lab for the first time linked tolerance and persistence of *Msm* upon exposure to kanamycin with increased levels of *whiB7* due to mutations in the arginine biosynthesis pathway (Schrader et al., 2021). Our work here further extends these findings and shows that both decreased killing by aminoglycosides and MIC-shifted resistance to macrolides are directly due to increased levels of *whiB7* - which, in our case, is overexpressed due to the loss of an m^1A58 modification on tRNAs. I show that *whiB7* and its downstream aminoglycoside-modifying enzyme *eis* are required for *mstrmI* mutants to have increased survival to kanamycin and MIC-shifted resistance to macrolides. This finding strongly highlights

that WhiB7 might act as a point of convergence in the regulation of multiple mechanisms of antibiotic survival in mycobacteria, consistent with the previous work published by (Schrader et al., 2020). Understanding this astonishing resilience could have implications for developing novel antimicrobials that could prevent the activation of *whiB7* in combination with existing antitubercular drugs.

WhiB7 has an important role in the intrinsic resistance of mycobacteria. Δ*whiB7* strains are more susceptible to antibiotics targeting ribosomes (Ramón-García et al., 2013; Morris et al., 2005; Burian et al., 2012; Warit et al., 2015; Bowman & Ghosh, 2014). For example, deletion of *whiB7* leads to a 32-fold decrease in MIC to erythromycin and decreased expression of *erm* in *Msm* (Ramón-García et al., 2013). In addition, overexpression of *whiB7*, due to mutations in the upstream region of the gene, induces MIC-shifted resistance to aminoglycosides in an *eis*-dependent manner (Reeves et al., 2013). Furthermore, the activation of WhiB7 is induced by a myriad of stressors, specifically ribosome-targeting antibiotics such as aminoglycosides, macrolides, and lincosamides, leading to a multiple-log increase in *whiB7* mRNA levels (Aziz, Go, & Dick, 2020). For example, exposure to clarithromycin induces up to a 4,000-fold increase in transcript levels of *whiB7* and up to a 70-fold increase in *erm* in *M. abscessus*. In addition, exposure to subinhibitory concentrations of macrolides was shown to induce resistance to these drugs in an *erm*-dependent manner (Nash et al., 2009).

In the case of *mstrmI* mutants, I observed a 6-8-fold increase in the levels of *whiB7* transcript even before antibiotic exposure - a small increase in comparison to the levels of *whiB7* that are found in mycobacteria exposed to ribosome-targeting antibiotics. I hypothesise that this small increase in the levels of *whiB7* before exposure to an antibiotic provides the initial tolerance to antibiotics and further drives decreased killing by aminoglycosides. Based on our findings, low induction of *whiB7* could have beneficial implications for the treatment of tuberculosis. In fact, I identified that clinical isolates of *Mtb* possess mutations in *Rv2118c*, *Mtb* homologue of *mstrmI*, leading to both sensitive and resistant phenotypes (Appendix 6.1). Unfortunately, no clinical isolate contained only *mttrmI* mutations, preventing us from drawing solid conclusions if such phenotypes were driven by *mttrmI* mutations. It would be interesting to investigate if these clinical isolates have increased levels of *whiB7* due to identified *Rv2118c* mutations.

It was surprising that *Mtb* deletion mutant of the *mttrmI* did not have an increased survival to gentamycin. Whole genome sequencing revealed that the KO strain did possess other SNPs, such as those in genes encoding for a peptidoglycan synthase PonA1 and a probable acetyl-transferase. I can speculate that such SNPs could abrogate the survival of this strain, especially since changes in PonA1 activity were shown to lead to lower susceptibility to rifampicin and peptidoglycan-targeting antibiotics, and changes in the physiology of the cells (Kieser et al., 2015). Due to time constraints, I did not test the growth of this strain nor survival upon exposure to other antibiotics, so it remains to be understood if Δ*mttrmI* strain without the above-mentioned mutations would reproduce other phenotypes of the *msttrmI* mutants - and whether this strain has increased levels of *whiB7*.

A few questions remain to be addressed regarding increased levels of *whiB7* in the *mstrmI* mutants. For example, it would be interesting to investigate if *mstrmI* mutants have less intracellular kanamycin than the WT *Msm* - since many efflux pumps are found in the regulon of *whiB7*. Next, it would be interesting to knock out *erm* and investigate if this would abrogate the MIC shift of the *mstrmI* mutants. Finally, one of the questions throughout our research was how *whiB7* expression is maintained during exposure to antibiotics that cause ribosome stalling. To answer this, I looked into the regulation of *whiB7* expression and the regulation of a ribosome-rescue system trans-translation - which are both activated upon proteotoxic stress exposure.

5.2 Is *whiB7* insensitive to rescue by trans-translation?

I am the first to report the dependency between the activity of trans-translation and *whiB7* expression. Specifically, I proposed a model which suggests that during exposure to kanamycin, *whiB7* activation is maintained (and not prevented through recycling of stalled ribosomes on the uORF) through depletion of alanine and $tRNA^{Ala\text{-}GGC}$ by trans-translation. In this regard, the uORF of *whiB7* works as an alanine sensor, supported by the fact that almost one-fourth of its codons encode for an alanine. In fact, during the course of these observations, the uORF

of *whiB7* was proposed in a pre-print by Poulton and colleagues to coordinate an adaptive response to alanine starvation (Poulton et al., 2023).

I show here that knocking down trans-translation abolishes the increased survival of the *mstrmI* mutants and partially decreases *whiB7* expression. However, due to possible secondary effects of accumulation of erroneous peptides that would not be degraded without trans-translation, we would carefully interpret these results as they are. Instead, we make our hypothesis based on the link between $tRNA^{Ala\ (GGC)}$ usage for the *ssrA* tag - and the high content of GCC codon in the uORF of *whiB7*. As mentioned in Chapter 4, we are currently investigating whether it is possible to abrogate the link between the $tRNA^{Ala\text{-}GGC}$ and the *ssrA* tag by overexpressing a tmRNA with mutated GCC-to-GCG codons in the tag. In addition, we are investigating if it is possible to restore the *whiB7* expression in these cells if a mutated tmRNA with GCC-to-GCG is overexpressed in *Msm* that contains a *whiB7*_uORF where a GCG replaces all the GCC codons. If the experiments show that the expression of *whiB7* depends on this link, the results would confirm that *whiB7* is insensitive to rescue by trans-translation. Following the experiments where would would test the survival fraction of these strains, we would also utilise the fluorescent reporter P*whiB7*_mScarlet to measure *whiB7* expression.

In the proposed model, I suggest that the feedback loop of trans-translation and *whiB7* activation is maintained through alanine aminotransferase, encoded by *MSMEG_0688*. *MSMEG_0688* is a member of the *whiB7* regulon, meaning that it will be expressed upon *whiB7* induction, but the expression of *MSMEG_0688* was also shown to increase *whiB7* expression (Jansen et al., 2020). As such, this dependency and the fact that disruption of arginine biosynthesis factors led to increased *whiB7* in the work from our lab indicates a link between amino acid biosynthesis and regulation of this transcriptional factor (Schrader et al., 2021; Poulton et al., 2023; Jansen et al., 2020; Burian et al., 2012). The model proposed in this work could be one explanation of how *MSMEG_0688* induces *whiB7* expression - through the activity of trans-translation. It remains to be investigated if *mstrmI* mutants have elevated levels of alanine, both prior to and following antibiotic exposure, and what are the levels of *MSMEG_0688* in the *mstrmI* mutants.

Finally, our model could suggest that targeting both *whiB7* and trans-translation could have

a synergistic effect in eradicating persisting bacteria. Trans-translation is a promising target for novel inhibitors as it is ubiquitous for bacteria and we could speculate that jointly targeting WhiB7 and trans-translation could abrogate the development of tolerance and persistence in mycobacteria. In fact, a small group of molecules were identified in a screen as effective inhibitors of trans-translation that showed broad-spectrum activity against *Bacillus anthracis*, *Msm*, and *Shigella flexneri* (Luidalepp et al., 2005; Campos-Silva et al., 2022; Aron et al., 2021; Alumasa et al., 2017; Marathe et al., 2023). (Ramadoss et al., 2013).

In addition to the work that will be done to investigate the direct link between trans-translation and *whiB7* expression, it would be of interest to investigate whether our model applies to other transcriptional attenuators and whether the genes they regulate are involved in the survival of bacteria to antibiotics. It would be highly interesting to investigate which other genes regulated in the same manner as *whiB7* would maintain their expression during proteotoxic stress exposure. This would provide an additional pool of genes that could potentially become novel antibiotic targets. In addition, it would be interesting to investigate if the model applies to *Mtb* and other bacterial species. Finally, we are currently working on repeats of the time-kill curve of Figure 4.18 to confirm the results and obtain the statistical significance of these experiments.

5.3 MsTrmI methylates *Msm* tRNAs

I am the first to show that the MsTrmI encoded from *MSMEG_3906* is indeed a tRNA m^1A58 methyltransferase in *Msm*. Furthermore, this research extended the scope of m^1A58 methyltransferase MsTrmI activity beyond just the initiator $tRNA^{Met}$ (Varshney et al., 2004), revealing its action on a range of tRNAs in *Msm*. However, due to limitations in capturing Illumina sequencing reads on all tRNAs, alternative methodologies could be employed for a more comprehensive analysis. Techniques such as high-performance liquid chromatography can be utilised to purify tRNA and assess their level. Additionally, methods such as recently-developed Nano-tRNAseq, a nanopore-based approach that provides quantitative estimates of

tRNA modifications and abundances, could be utilised to investigate other tRNA modifications that might be disrupted or added due to the loss of the m^1A58 (Lucas et al., 2023).

In addition to the methylation status, I have shown in a subset of tRNAs that the loss of m^1A58 modification impacts the abundance and folding of these species, in alignment with findings by (Kadaba et al., 2004; Ozanick et al., 2009). The impact on the folding is also indicated by the fact that it was shown m^1A58 reverse-Hoogsteen base pairs with modified U54 (m^5s^2U54); this base pair stacks with G53-C61 pair in the T stem-loop, and together, their interactions stabilise the T- and D-arms through further pairing with G18-ψ55 and G19-C56 pairs (Watanabe, Shinma, Oshima, & Nishimura, 1976; Yokoyama, Watanabe, & Miyazawa, 1987). Hence, the absence of the A58 methylation might impact tRNA stability by impacting these interactions.

Furthermore, since methylation of the N1 atom introduces a positive charge in the TψC loop of the tRNA, the absence of this modification could impact the binding of the tRNA to the ribosome, aminoacyl-tRNA synthetase or the elongation factor. Although our investigation has so far been limited to eight tRNAs, focusing on their charging and abundance, future research should aim to explore a wider array of tRNAs. This could specifically include those present in the uORF of *whiB7*, such as proline, which is found to be the second most prevalent after alanine. It would be particularly insightful to examine the same tRNAs we investigated in the AG mutant, in the deletion mutants strain - including those with mutated *pnpase* and those complemented with *pnpase* and *mstrmI*. Comparing the levels between those strains would provide further insight into the role of the PNPase and the *pnpase* mutations in hypomethylated *Msm*.

Interestingly, the lack of the m^1A58 modification in human cells was shown not to impact tRNA stability but rather decrease charging efficiency (Saikia, Fu, Pavon-Eternod, He, & Pan, 2010). This finding points to a species-specific functional diversity of the m^1A58 modification, as discussed by Schaffer and colleagues (Schaffer, Pinkard, & Coller, 2019), and paves the way for speculations that the m^1A58 modification might serve multiple roles in *Msm*. This could be further investigated through the analysis of other tRNA species in *Msm*. In addition, the

fact that certain tRNA species are being less modified may be linked to their usage in other genes encoding for proteins involved in stress responses, such as what we observe with $tRNA^{Ala}$ and WhiB7. Intriguingly, it was also shown that cells fragment tRNA and that such tRNA fragments can regulate gene expression - altering transcriptional and translational landscapes under stress conditions (Z. Li & Stanton, 2021). Hence, the lack of m^1A58 modification might influence the generation or abundance of such tRNA fragments in cells, suggesting a potential role in cellular response to environmental stresses (Z. Li & Stanton, 2021). This potential link between tRNA modification and stress response mechanisms offers a promising avenue for further research in *Msm*, potentially uncovering novel aspects of bacterial adaptation and survival strategies.

5.4 Δ*mstrmI* presents with *pnpase* mutations

Our work here showed that the A-to-G and the G128S mutations are loss-of-function mutations, with the A-to-G mutation abolishing 90% of the *mstrmI* transcript and the G128S mutation leading to loss of the MsTrmI protein. According to DeJesus and colleagues and Bosch and colleagues, *mstrmI* was classified as a non-essential gene (Dejesus et al., 2017). However, certain knock-downs of *mstrmI* generated through CRISPRi showed growth vulnerability. To evaluate the impact of the loss of a tRNA methyltransferase on the survival of Msm to antibiotics, I created deletion mutants and identified they did not recapitulate the increased survival phenotype to the level of the AG and GS mutants - due to mutations related to the *pnpase* - the $PNPase^{A167D}$ mutation and 29bp deletion upstream of the *pnpase*, respectively. I uncovered that the deletion upstream of the *pnpase* in the Δ*mstrmI*_C2 strain was directly upstream of the start codon of an uORF homologous to the *ncRv12783* - and I showed this mutation affects the *pnpase* transcription.

PNPase is an exoribonuclease that catalyzes phosphorolytic degradation of RNA from the 3' end (Briani, Carzaniga, & Dehò, 2016). PNPase participates in the maturation and quality control of stable RNA: tRNAs (Z. Li & Deutscher, 2002) and rRNAs (Cheng & Deutscher, 2003),

sRNAs (Andrade and Arraiano, 2008; De Lay and Gottesman, 2011; Andrade et al., 2012; Saramago et al., 2014) and affects the stability of numerous mRNAs (Mohanty & Kushner, 2010). Due to the direct role of the PNPase to degrade tRNAs, I hypothesise that these mutations in the *pnpase* prevent the degradation of hypomodified tRNA in the Δ*mstrmI* strains and lead to stabilisation of the levels of the hypomodified tRNAs in the deletion mutant. This aligns with the findings by Kadaba and colleagues that identified spontaneous suppressor mutations within a 3'-5' exoribonuclease *DIS3/RRP44* upon mutating *trm6* (Kadaba et al., 2004). They showed that the mutation led to stabilising levels of $tRNA^{Met}$ lacking m^1A58 that would have otherwise been degraded (Kadaba et al., 2004).

In addition, I report here that even a partial loss of the PNPase abolishes the growth defect observed in the Δ*mstrmI* with the WT *pnpase*. Due to time constraints, I could not study the exact mechanism behind this, but one can hypothesise that the loss of available tRNAs, which I found are all hypomethylated in the KO, could affect the translation of this strain. We will be able to determine the protein synthesis rates of these strains through analysis of currently ongoing ribosome sequencing experiments - as the density of ribosomes across an ORF can be used to determine protein synthesis rates (Y. Li et al., 2012). Using this method, we aim to compare ribosome occupancy on mRNAs of the WT, AG mutant and complemented strain and see whether ribosomes stall more frequently in the mutant. If proven correct, we would investigate if the stalling in those cases activates the expression of certain genes through the same or similar regulation mechanism observed with *whiB7*.

Regardless of the growth defect of the deletion mutant, a similar level of growth impairment was not evident in the *mstrmI* mutants. While both AG and GS mutants presented with increased survival to aminoglycosides, only one of the mutants - AG - had a slight growth defect. Since the GS mutant had the same growth rate as the WT *Msm* while presenting with increased survival to aminoglycoside, this work further supports the notion that slow growth is not required for antibiotic tolerance. Instead, the increased survival of the *mstrmI* mutants relied solely on the WhiB7 and Eis, which do not depend on bacterial replication.

5.5 What is the relationship between Y RNA, Rsr, and hypomethylated tRNA?

I have identified that *mstrmI* mutants have increased levels of *rsr* and *yrlAB*, which, together with the PNPase, form degradation machinery termed RYPER. Intriguingly, *rsr* was also found highly upregulated in the arginine biosynthesis mutants that had increased survival to kanamycin due to increased *whiB7*. Motivated by these findings, I sought to investigate whether *rsr* and *yrlAB* were involved in mediating increased survival of *mstrmI* mutants. I knocked out either *rsr* or *yrlAB* in the mutant and evaluated the increased survival phenotype. Contrary to expectations, the increased survival phenotype pertained even after *rsr* and *yrlAB* deletion, suggesting they are not responsible for the antibiotic tolerance of these strains.

I hypothesise that the upregulation of *rsr* and *yrlAB* may be a response to the accumulation of hypomethylated tRNAs, rather than a direct contributor to increased antibiotic survival. Hence, they do not contribute to the mechanism of increased survival but play a role in the hypomethylated tRNA degradation. To investigate this hypothesis, each component of the RYPER machinery in both the WT and *mstrmI* mutant strains could be pulled down and assessed if hypomodified tRNAs are found bound to the machinery. In addition, it could be tested in the *mstrmI* mutants if the deletion of *rsr* and *yrlAB* leads to the same tRNA levels as in the WT - which could indicate that RYPER is involved in the degradation of hypomodified tRNA. Studying this would provide deeper insight into the molecular mechanism governing tRNA stability and degradation in the context of A58 methylation.

5.6 Concluding remarks

Collectively, this research highlights the importance of WhiB7 and trans-translation for the survival of *Msm* upon exposure to ribosome-targeting antibiotics. While the involvement of WhiB7 in MIC-shifted resistance and tolerance has been previously documented, our study brings to light a novel pathway: these phenotypes can be achieved through the loss of an

enzyme methylating the m^1A58 site of tRNAs. Furthermore, this study is also the first to report on a relationship between *whiB7* expression and trans-translation, proposing a model through which *whiB7* expression is maintained through a "fail-safe" mechanism, driven by the depletion of alanine during trans-translation.

Given these findings, it is tempting to hypothesise that targeting *whiB7* and trans-translation would prevent the occurrence of tolerance and persistence in mycobacteria. Such an approach holds the potential to reduce treatment duration and aid in the eradication of TB. However, as highlighted by McDermott in 1956, the challenge of antibiotic therapy is a complex "three-body" problem, involving the interplay between the host, pathogen and drug (McDermott, McCune, & Tompsett, 1956). Advancement on these three fronts is essential to prevent a pandemic fuelled by antibiotic-resistant pathogens. With this project, we contribute to the pathogen and drug side of the problem, and future research should extend these findings by exploring the effects of identified mutations and *whiB7* activation during host infections.

Chapter 6

Materials and Methods

Contents

6.1 Bacterial strains and culture conditions 140

6.2 Plasmid construction 140

6.3 Knocking-out genes in mycobacteria 140

6.4 Filter-based method 142

6.5 Determination of minimum inhibitory concentration 142

6.6 Growth curves 143

6.7 Kanamycin kill curves 143

6.8 RNA extraction 144

6.9 RNA sequencing 144

6.10 Small RNA sequencing 145

6.11 qRT-PCR 145

6.12 WGS and single nucleotide polymorphism identification 146

6.13 CRISPRi 146

6.14 Flow cytometry 147

6.15 SYBR green RNA staining 147

6.16 Northern blotting 148

6.17 Co-immunoprecipitation (Co-IP)/Mass spectrometry 149

6.18 Western blot 150

6.19 Statistical analysis 150

6.1 Bacterial strains and culture conditions

All strains used in this study are listed in Table 6.2. *Msm* strains were grown at 37°C with 200 rpm shaking in Middlebrook 7H9 medium (BD Difco) supplemented with 0.5% bovine albumin serum (Roche), 0.2% glycerol, 0.2% dextrose (Sigma), 0.05% tyloxapol (Sigma), and 0.085% sodium chloride (Sigma) (referred from now on as just "7H9" media). *Mtb* strains were grown in the same conditions but without shaking. Appropriate antibiotics (hygromycin 50 μg/mL (Roche), zeocin 25 μg/mL (Thermo Fisher), streptomycin 25 μg/mL (Sigma-Aldrich), or kanamycin 25 μg/mL (Thermo Fisher)) were used during culturing strains bearing episomal or chromosomally integrating plasmids for the experiments.

6.2 Plasmid construction

Plasmids used in this study were made using primers listed in Table 6.1. Besides the CRISPRi plasmids, all plasmids were constructed using Invitrogen Gateway recombination cloning technology. The plasmids were transformed into DH5α chemically competent *E. coli* cells generated in the lab or into *E. coli* MACH1 cells (Thermo Fisher).

6.3 Knocking-out genes in mycobacteria

Msm competent cells were transformed with pNIT_RecET_SacB_KanR plasmid that expresses RecET in the presence of isovaleronitrile (IVN, Sigma Aldrich). Transformed strains were grown to OD_{600} 0.7 in a 75 cm^3 culture flask (Corning), and IVN was added at a concentration

of 12 μM to induce the expression of RecE, an exoribonuclease, and RecT, a DNA annealing protein, from an episomal plasmid. The culture was further incubated at 37°C with 120 rpm shaking for 3 h, and the competent cells were made by centrifuging for 10 min at 4°C 4,000 rpm and washing the pellet with ice-cold 10% glycerol four times. The final pellet was resuspended in 1 mL of 10% glycerol and electroporated with 1000 ng of PCR-amplified oligo containing upstream and downstream homologous regions of the gene of interest, with the middle of the gene exchanged with an antibiotic cassette (HYG or ZEO), that would be recombined with the targeted gene. Electroporation was done in a 2 mm gap electroporation cuvette (Molecular BioProducts) at 2.5 kV, 25 μF and 800 Ω settings. Recovery was done in 7H9 media at 37°C for 3 h with shaking at 250 rpm. The bacteria were plated on 7H10 agar plates with an antibiotic encoded in the oligo to select knock-out candidates. Colonies were screened using PCR and then outgrown and plated on 10% sucrose plates to select for bacteria cured from the episomal plasmid containing *sacB*. Grown colonies were patched on agar plates with/without kanamycin to confirm the loss of the plasmid, and those that did not grow on kanamycin were selected.

To KO *mttrmI* in *Mtb*, *Mtb* H37Rv cells were transformed with the pNIT_RecET_SacB_KanR plasmid and then grown to the exponential phase. RecET expression was induced by adding 1 μM IVN for 24 hours and 0.2 M glycin for 16 hours. Then, competent cells were made as described above, and 1 μg of homologous oligo with a HYG cassette between the flanking regions was transformed. Recovery was done in 7H9 media for 24 hours, followed by plating of the cultures on 7H10 agar plates supplemented with 10% OADC, 50 μg/mL HYG and 0.5% glycerol. Plates were incubated for 2-3 weeks at 37°C, cured on plates containing 8.5% sucrose and patched onto 7H10 plates supplemented with kanamycin. Colonies that grew on sucrose plates but not on kanamycin-containing plates were selected and tested using PCR, and KO was confirmed via WGS.

6.4 Filter-based method

Bacteria were seeded onto a Durapore membrane filter (Millipore Sigma, 0.22 μm pore) and placed onto a sterilised Swinnex 47 mm filter holder (Millipore Sigma) on top of a vacuum canister (Cardinal Health). Bacterial liquid cultures grown to the exponential phase were diluted to a final concentration of 10^7 bacteria per mL (OD=0.1, with approximation that OD=1 is equivalent to 1x10^8 CFU/mL), and prepared solutions were deposited onto the filter.

To test for the fraction of survivors, each filter seeded as in 6.4 was transferred onto 7H10 agar plates containing 10x the MIC of the antibiotic used to screen for the HS candidates, following which the plates were incubated at 37°C for an appropriate exposure time. After exposure, filters were transferred onto 7H10 plates containing charcoal and further incubated for 24 h at 37°C to absorb residual antibiotics from the filters. Then, the filters were placed onto growth-permitting 7H10 agar plates (recovery plates) and further incubated for the time needed (three to four days for *Msm*) to allow for the growth of survivors, following which the photographs were taken of the filters with a mobile phone camera. For *Mtb*, the procedure differed in that the 7H10 plates contained 10% oleic acid-albumin-dextrose-catalase (OADC), and photographs were taken with a camera following approximately 20 days of incubation on recovery plates. All the candidates with more than a 10-fold increase in survivors as compared to the WT control are considered HS mutants. To process the photographs of the filters, raw images were shown in grayscale with adjusted brightness and contrast.

6.5 Determination of minimum inhibitory concentration

The MICs of all strains were determined for antibiotics by the standard microdilution method. Bacterial cultures were subcultured into 7H9 and grown to exponential phase at 37°C with 200 rpm shaking. In a 96-well plate, 200 μL of cultures at OD_{600}=0.025 in triplicates were exposed to nine concentrations in a two-fold dilution series of each drug (kanamycin 4.35-

1,120 μg/mL; amikacin 3.13-800 μg/mL; levofloxacin 1.25-320 μg/mL; rifampicin 93.75-24,000 μg/mL; clarithromycin 3.13-800 μg/mL; erythromycin 18.75-4,800 μg/mL), with a control well with no antibiotic and the solvent used to solubilize the drug. Plates were incubated at 37°C with shaking at 80 rpm. OD_{600} was measured after 24, 48, and 72 hours using a plate reader.

6.6 Growth curves

Msm cultures were subcultured into 7H9 and grown overnight to the exponential phase. OD_{600} was measured using a spectrophotometer and adjusted to 0.05 in 200 μL of 7H9. If an effect of any compound was measured, these compounds were added to the 7H9, and each culture was seeded at least in triplicates in a 96-well plate. OD_{600} was measured every 30 min for 48 hours using Tecan Infinite M200 PRO, with shaking at 80 rpm between readings. The absorbance of 7H9 without/with any compound was subtracted from the measured values. Growth rates were calculated based on growth differences during the linear growth stage.

6.7 Kanamycin kill curves

Msm cultures were grown to the mid-log phase in 7H9. OD_{600} was measured, and cultures were adjusted in 10 mL 7H9 to OD_{600}=0.1 (approximately $1x10^7$ CFU/mL). Kanamycin was added to the cultures in a final concentration of 5xMIC (3.5 μg/mL). Cultures were incubated at 37°C with shaking at 100 rpm. To enumerate CFUs, aliquots were taken and serially diluted at time points 0, 4, 8, 12, 24, 36, 48, and 60 hours and 10 μL of at least three dilutions were plated on 7H10 agar plates containing 0.5% glycerol and 0.4% charcoal. Charcoal was added to plates to eliminate the need to wash the cultures as it absorbs the remaining antibiotic. To increase the detection range at later time points, 100 μL or 1 mL of cultures were centrifuged, pellet resuspended in 10 μL 7H9, and plated on plates.

6.8 RNA extraction

Cultures were grown to mid-log phase in 10 mL 7H9, resuspended in a fresh GTC (guanidium thiocyanate, N-lauryl sarcosine, sodium citrate) buffer and centrifuged for 10 min 3400 rpm in a 50 mL Falcon tube. The pellet was resuspended in 450 μL TRI reagent (Zymo Research, R2050) and bead beaten to extract the genomic material. Chloroform-extracted RNA was purified with a Direct-zol RNA miniprep kit (Zymo Research, R2052). Following washing and elution, RNA was treated with Turbo DNase (Thermo Fisher, AM2238) to eliminate DNA, and total samples were re-purified using Direct-zol RNA miniprep kit (for qRTPCR) or using RNA Clean and Concentrator 25-kit (Zymo Research, R1017) for RNA-seq samples. The concentration of RNA was measured before proceeding with RNA seq, small RNA seq or qRT-PCR.

6.9 RNA sequencing

Total RNA was extracted as described in Section 6.8. RNA was depleted from ribosomal RNA (rRNA) using RiboMinus Transcriptome Isolation Kit for bacteria (Thermo Fisher Scientific, K155004) and concentrated with RNA Clean and Concentrator-25 kit. Libraries were made from rRNA-depleted RNA using NEBNext Ultra II Directional RNA Library Prep Kit for Illumina (New England Biolabs, E7765S) with Illumina Index Primers Set 1 and 2 (NEB, E7335S and E7500S). Libraries were purified with NEBNext Sample Purification Beads from the Library Prep Kit (NEB, E7767S). The quality of each library was analysed on Bioanalyzer and the libraries were pooled together for Illumina sequencing on Illumina HiSeq4000 with 75 bp paired end sequencing. This work was done by Dr Plocinski at the University of Lodz, Poland.

To process the data, reads were trimmed using Trim galore! software version 0.6.5 (options -paired -illumina), and aligned to *Msm* genome (obtained from Mycobrowser) using Kallisto (version 0.46.1) with options –rf-stranded (Bray, Pimentel, Melsted, & Pachter, 2016). Differential expression analysis was done using DESeq2 (version 1.28.0) as previously described (Stapels et al., 2018) to obtain Log_2 fold-change (FC) and adjusted p-values between WT *Msm*

and the selected mutants KO strains, and their complemented strains. Log_2FC and adjusted p-values were plotted in Prism (version 10).

6.10 Small RNA sequencing

Total RNA was extracted as described in Section 6.8. To isolate small RNA, 2 μg of total RNA was processed using VAHTS Small RNA Library Prep Kit for Illumina with Universal Primer and Index primers (Vazyme, NR813-816) according to the kit protocol. Library selection was done using VAHTS DNA Clean Beads (Vazyme, N411). The libraries were quantified using qPCR to adjust for loading onto sequencing flowcell. The sequencing was done on NextSeq550 with a Midoutput flowcell. This work was done by Dr Plocinski at the University of Lodz, Poland.

6.11 qRT-PCR

RNA was extracted as described above. cDNA was prepared using 500 ng of RNA as a template with MuLV Reverse Transcriptase (RT) (Invitrogen, 28025-013) in the presence of an RNase inhibitor (Invitrogen, 10777-019) and random hexamers (Invitrogen, N8080127). RT was substituted with Ambion water to obtain a no-RT control of the presence of remaining genomic DNA. Transcribed cDNA was mixed with PowerTrack SYBR Green Master Mix (ThermoFisher) and cycled with quantification on StepOnePlusTM (ThermoFisher, 4376599). A second derivative analysis was done to obtain crossing points (Cp) for each sample using StepOne software (v2.2.2). $\Delta\Delta$Cp was calculated for each strain by subtracting the average ΔCp (subtracted mean of the internal control from the sample) of at least three technical replicates of wild-type from the ΔCp of tested strains. Data were presented as $\log_2$ fold change value relative to internal control, calculated as 2-$\Delta\Delta$Cp. All the primers used for qRT-PCR are in Table 6.1. For *Msm*, SigA (MSMEG_2758) was used as an internal control.

6.12 WGS and single nucleotide polymorphism identification

Strains were grown to mid-log to stationary phase in 20 mL 7H9, and genomic DNA was isolated by bead beating, phenol-chloroform extraction, and ethanol precipitation. Genomic DNA was whole genome sequenced at MicrobesNG (University of Birmingham). Gene KO was visually confirmed using IGV from the Broad Institute software. Single nucleotide polymorphisms (SNPs) were identified by aligning the sequences with NP_008596.1 for *Msm* or NZ_CM001515.1 for *Mtb* using the Variant Calling Pipeline for bacterial genomes developed at Applied Bioinformatics Core at Weill Cornell Medicine. The pipeline involved adapter trimming using cutadapt, read alignment using BWA package, duplicate marking using Picard's MarkDuplicates, haplotype caller using GATK HaplotypeCaller, and variant annotation using SnpEff.

6.13 CRISPRi

Msm-adapted ATc-regulated CRISPRi backbone (pLJR962) with a catalytically inactivated CRISPRi cas9 allele from *Streptococcus thermophilus*, which was kindly provided by Rock Lab (The Rockefeller University). sgRNA was designed to target the open reading frame of a gene of interest, with the protospacer adjacent motif (PAM) determined based on the published consensus to obtain the strongest gene silencing. To design the sgRNA, 20 nucleotides were added to the 5' of the PAM sequence, and 5'-GGGA-3' and 5'-AAAC-3' were added to the forward and reverse primer, respectively. The primers were annealed using an annealing buffer at 95°C for 2 minutes, followed by a decrease in temperature of 0.1°C/sec to 25°C. pLJR962 was BsmBI-digested for 4 hours at 55°C in a buffer 3.1, and 0.5 μL of annealed oligos were ligated overnight with 9 ng digested backbone using T4 DNA ligase and ligase buffer (NEB M0202T). The ligation mix was transformed into *E. coli* DH5α competent cells and plated on LB plates supplemented with kanamycin at 25 μg/mL. Each plasmid was sequenced to confirm sgRNA

using primer 1834 (5'-TTCCTGTGAAGAGCCATTGATAATG-3'). Confirmed plasmids were transformed into *Msm*, and the strains were grown on 7H10 agar plates supplemented with 25 μg/mL kanamycin.

For the CRISPRi experiment, strains containing pLJR962 CRISPRi plasmid with/without the sgRNA were grown from glycerol stock in 7H9 medium. ATc was added to subcultures the day before the experiment either at 200 ng/mL or in a range to determine the minimum concentration needed to KD the gene. To test the HS phenotype, filters were seeded and placed on 7H10 agar plates supplemented with 0.5% glycerol, 2 μg/mL amikacin, and none or the same concentration of ATc as in the liquid cultures. Filters were processed as described in the 6.4 section.

6.14 Flow cytometry

Cultures were grown to the exponential phase to prepare the samples for analysis. 500 μL of the culture was washed once with an equal volume of PBS with 0.02% tyloxapol and twice with just PBS. The final pellet was resuspended in 500 μL of PBS and centrifuged at 800 rpm for 3 minutes to obtain single-cell suspensions. 200 μL of the upper layer of the supernatant was transferred to polystyrene round bottom tubes for flow cytometry and analysed on BD Fortessa flow cytometer. To measure mScarlet fluorescence, excitation and emission were set to 569 nm and 594 nm, respectively. Cells were gated for single cells and 100,000 events were recorded. Data was visualised using FlowJo software.

6.15 SYBR green RNA staining

To detect RNA using SYBR green staining, *Msm* was grown to the exponential phase and treated with rifampicin 200 μg/mL, and total RNA was isolated at indicated time points using FASTRNA Pro Blue Kit (MP). RNA was separated on 15% denaturing acrylamide gels, the gel

was stained using SYBR Green II RNA gel stain (Sigma-Aldrich) for 30 minutes and illuminated using 300 nm ultraviolet transillumination.

6.16 Northern blotting

To probe for individual tRNA, the RNA from logarithmic-stage grown *Msm* was extracted with hot acid phenol as previously described (Copela et al., 2008). RNA was separated on an 8% polyacrylamide 8.3M urea gels and transferred onto Hybond N membrane (Amersham). To investigate the aminoacylation, RNA was extracted at low pH, separated on polyacrylamide 8M urea and 0.1M NaOAc gels in cold (Varshney et al., 1991). Membranes were hybridazed with [γ-^{32}P]ATP-labeled oligonucleotides as described previously (Copela et al., 2008). These experiments were done by Dr Xinguo Chen at the NIH National Cancer Institute, United States.

Oligonucleotide probes were:

$tRNA^{fMet}$: TGAGCCCAGCGAGCTACCGAGCTGCTCC

$tRNA^{Ala\ (CGC)}$: CTACTCGATGCGAACGAGTCGCGCTAC

$tRNA^{Ala\ (GGC)}$: CCCCACACTGCCAGTGTGGTGCGCTAC

$tRNA^{Ala\ (TGC)}$: ATCTGCCTTGCAAAGGCAGCGCTCTA

Msm 5S rRNA: CTTAGCTTCCGGGTTCGGGATGGGACCGGGCGTTTCC

$tRNA^{Arg\ (ACG)}$: CCCCTAACCTTCTGATCCGTAGTCAGAT

$tRNA^{Arg\ (TCT)}$: CCTGCAACCGTCGGATTAGAAGGCCGAT

$tRNA^{Val\ (CAC)}$: GAGGCGGACGCTCTCCCACTGAGCTACGAGACC

$tRNA^{His\ (GTG)}$: GGATCACAACCTGGTGCTCTACCAACTGAACTACAGCCAC

6.17 Co-immunoprecipitation (Co-IP)/Mass spectrometry

WT and G128S MsTrmI and their potential partners were isolated for mass-spectrometry by Co-IP. *Msm* were grown to exponential phase in 10 mL complete 7H9 medium with 0.02% tyloxapol and with or without 200 ng/mL atc to induce the expression of TetON *mstrmI*. Cells were pelleted via 1 minutes 4,000 rpm centrifugation and resuspended in 1x PBS with 0.05% tyloxapol, followed by 10 minutes 4,000 rpm centrifugation step. The pellet was resuspended in a 1 mL buffer composed of 10 mL PBS, 1 tablet of Protease Inhibitor (PI, Roche 4693116001), and PhosSTOP (PS, Roche 4906845001) to prevent phosphorylation of G128S site, followed by centrifugation 13,000 rpm 1 min. After the centrifugation, one-tenth of the supernatant was separated, denatured by SDS-loading buffer (125 mM Tris-Cl pH 6.8, 4% SDS, 10% glycerol, 5% 2-mercaptoethanol, bromphenol blue), and marked as an "Input" sample. The rest of the supernatant was mixed with prepared HA-agarose beads (Pierce HA epitope tag beads 26181). The beads were prepared by washing three times with the above-described buffer with PBS + PI + PS, with 4,000 rpm 1 min centrifugation in between. The final pellet of beads was resuspended in 550 μL PBS + 0.05% tyloxapol. Lysates were incubated with the HA-beads to enrich for HA-tagged proteins for 2 hours in the cold room on a roller, followed by centrifugation 4,000 rpm 1min. The supernatant was kept for the "Depleted" sample to control for the IP, and the supernatant was washed three times in lysis buffer PBS + 0.05% tyloxapol with 4,000 rpm 1 min centrifugation between washing. For western blot analysis, bound proteins were eluted by the addition of SDS loading buffer. The samples were boiled at 95 °C for 7 min, centrifuged for 1 min at 1,500 g, and subjected to SDS-PAGE and immunoblotting. For mass spectrometry, IP sample was shipped on dry ice to Poland to Institute of Biochemistry and Biophysics Mass Spectrometry Laboratory. The analysis was done by Drs Agata Malinowska and Bianka Swiderska as described in (Płociński et al., 2019).

6.18 Western blot

Samples were separated on a 12% SDS-PAGE gel by electrophoresis for 90-120 minutes until the samples reached the bottom of the gel, with 110 V constant voltage. Gels were transferred using the Trans-Blot Turbo Transfect System (Bio-Rad) onto Immobilon-P polyvinylidene difluoride membranes (Millipore), using 15 V constant voltage for 25 minutes. Blocking of the membranes was done for 1 hour in 5 mL solution containing 5% (w/v) BSA in TBS-T buffer (150 mM NaCl, 100 mM Tris pH 7.4, 1% Tween-20). Following blocking, the membranes were incubated with the blocking buffer containing a primary antibody mouse anti-HA (Bio Legend 901503, 1:2000) overnight at 4°C with rotation. The next day, membranes were washed three times in TBS-T, each wash following 10 min incubation at RT with rotation. Following washing, the membranes were incubated in 5 mL blocking buffer with a goat anti-mouse HRP-linked secondary antibody (Agilent, P0447, 1:2500) for 1 hour at RT with rotation. The membranes were then washed three times in TBS-T, and developed using ECL plus (Pierce, Thermo Scientific) chemiluminescence reagents. Detection was done using Bio-Rad ChemiDoc imaging system.

6.19 Statistical analysis

Statistical analysis was done with GraphPad Prism 10. Unless otherwise specified, data is presented as mean +/- standard deviation of at least three independent biological repeats per condition. Statistical significance was calculated with either student's t-test (two-tailed, unpaired) or one-way ANOVA (for multiple groups, one independent variable), as indicated where appropriate.

References

Abel, L., El-Baghdadi, J., Bousfiha, A. A., Casanova, J. L., & Schurr, E. (2014). *Human genetics of tuberculosis: A long and winding road* (Vol. 369) (No. 1645). Retrieved from http://dx.doi.org/10.1098/rstb.2013.0428 doi: 10.1098/rstb.2013.0428

Aboa, T., Ueda, K., Sunohara, T., Ogawa, K., & Aiba, H. (2002, 7). SsrA-mediated protein tagging in the presence of miscoding drugs and its physiological role in Escherichia coli. *Genes to Cells*, *7*(7), 629–638. doi: 10.1046/J.1365-2443.2002.00549.X

Abraham, E. P., & Chain, E. (1940). An Enzyme from Bacteria able to Destroy Penicillin. *Nature 1940 146:3713*, *146*(3713), 837–837. Retrieved from https://www.nature.com/articles/146837a0 doi: 10.1038/146837a0

Akatsu, S., & Noguchi, H. (1917, 3). The drug-fastness of spirochetes to arsenic, mercurial, and iodide compounds in vitro. *Journal of Experimental Medicine*, *25*(3), 349–362. doi: 10.1084/JEM.25.3.349

Albert, H., Nathavitharana, R. R., Isaacs, C., Pai, M., Denkinger, C. M., & Boehme, C. C. (2016, 8). Development, roll-out and impact of Xpert MTB/RIF for tuberculosis: what lessons have we learnt and how can we do better? *The European Respiratory Journal*, *48*(2), 516. Retrieved from /pmc/articles/PMC4967565//pmc/articles/PMC4967565/?report=abstracthttps://www.ncbi.nlm.nih.gov/pmc/articles/PMC4967565/ doi: 10.1183/13993003.00543-2016

Aldridge, B. B., Fernandez-Suarez, M., Heller, D., Ambravaneswaran, V., Irimia, D., Toner, M., & Fortune, S. M. (2012, 1). Asymmetry and aging of mycobacterial cells lead to variable growth and antibiotic susceptibility. *Science (New York, N.Y.)*, *335*(6064), 100–104. Retrieved from https://pubmed.ncbi.nlm.nih.gov/22174129/ doi: 10.1126/SCIENCE.1216166

Alumasa, J. N., Manzanillo, P. S., Peterson, N. D., Lundrigan, T., Baughn, A. D., Cox, J. S., &

Keiler, K. C. (2017, 9). Ribosome Rescue Inhibitors Kill Actively Growing and Nonreplicating Persister Mycobacterium tuberculosis Cells. *ACS Infectious Diseases*, *3*(9), 634–644. Retrieved from https://pubs.acs.org/doi/full/10.1021/acsinfecdis.7b00028 doi: 10.1021/ACSINFECDIS.7B00028/ASSET/IMAGES/MEDIUM/ID-2017-00028E{_}0012.GIF

Amato, S. M., & Brynildsen, M. P. (2014, 3). Nutrient Transitions Are a Source of Persisters in Escherichia coli Biofilms. *PLOS ONE*, *9*(3), e93110. Retrieved from https://journals.plos.org/plosone/article?id=10.1371/journal.pone.0093110 doi: 10.1371/JOURNAL.PONE.0093110

Amato, S. M., Fazen, C. H., Henry, T. C., Mok, W. W., Orman, M. A., Sandvik, E. L., ... Brynildsen, M. P. (2014). The role of metabolism in bacterial persistence. *Frontiers in Microbiology*, *5*(MAR). Retrieved from /pmc/articles/PMC3939429//pmc/articles/PMC3939429/?report=abstracthttps://www.ncbi.nlm.nih.gov/pmc/articles/PMC3939429/ doi: 10.3389/FMICB.2014.00070

Amato, S. M., Orman, M. A., & Brynildsen, M. P. (2013, 5). Metabolic Control of Persister Formation in Escherichia coli. *Molecular Cell*, *50*(4), 475–487. doi: 10.1016/J.MOLCEL.2013.04.002

Anderson, J., Phan, L., Cuesta, R., Carlson, B. A., Pak, M., Asano, K., ... Hinnebusch, A. G. (1998, 12). The essential Gcd10p–Gcd14p nuclear complex is required for 1-methyladenosine modification and maturation of initiator methionyl-tRNA. *Genes & Development*, *12*(23), 3650. Retrieved from /pmc/articles/PMC317256//pmc/articles/PMC317256/?report=abstracthttps://www.ncbi.nlm.nih.gov/pmc/articles/PMC317256/ doi: 10.1101/GAD.12.23.3650

Anderson, J., Phan, L., & Hinnebusch, A. G. (2000, 5). The Gcd10p/Gcd14p complex is the essential two-subunit tRNA(1-methyladenosine) methyltransferase of Saccharomyces cerevisiae. *Proceedings of the National Academy of Sciences of the United States of America*, *97*(10), 5173–5178. Retrieved from /pmc/articles/PMC25801//pmc/articles/PMC25801/?report=abstracthttps://www.ncbi.nlm.nih.gov/pmc/articles/PMC25801/ doi: 10.1073/pnas.090102597

Andini, N., & Nash, K. A. (2011, 9). Expression of tmRNA in mycobacteria is increased by antimicrobial agents that target the ribosome. *FEMS Microbiology Letters*, *322*(2), 172–179. Retrieved from https://academic.oup.com/femsle/article/322/2/172/481142

doi: 10.1111/J.1574-6968.2011.02350.X

Andrews, J. R., Noubary, F., Walensky, R. P., Cerda, R., Losina, E., & Horsburgh, C. R. (2012, 3). Risk of progression to active tuberculosis following reinfection with Mycobacterium tuberculosis. *Clinical infectious diseases : an official publication of the Infectious Diseases Society of America*, *54*(6), 784–791. Retrieved from https://pubmed.ncbi.nlm.nih.gov/22267721/https://pubmed.ncbi.nlm.nih.gov/22267721/?dopt=Abstract doi: 10.1093/CID/CIR951

Ankley, L., Thomas, S., & Olive, A. J. (2020, 7). Fighting Persistence: How Chronic Infections with Mycobacterium tuberculosis Evade T Cell-Mediated Clearance and New Strategies To Defeat Them. *Infection and immunity*, *88*(7). Retrieved from https://pubmed.ncbi.nlm.nih.gov/32094248/ doi: 10.1128/IAI.00916-19

Arnaud Gutierrez, A., Jain, S., Bhargava, P., Hamblin, M., Lobritz, M. A., & Collins Correspondence, J. J. (2017). Understanding and Sensitizing Density-Dependent Persistence to Quinolone Antibiotics Metabolic priming of OXPHOS reverses tolerance in diverse bacterial species In Brief. *Molecular Cell*, *68*. Retrieved from https://doi.org/10.1016/j.molcel.2017.11.012 doi: 10.1016/j.molcel.2017.11.012

Aron, Z. D., Mehrani, A., Hoffer, E. D., Connolly, K. L., Srinivas, P., Torhan, M. C., ... Keiler, K. C. (2021, 3). trans-Translation inhibitors bind to a novel site on the ribosome and clear Neisseria gonorrhoeae in vivo. *Nature Communications 2021 12:1*, *12*(1), 1–12. Retrieved from https://www.nature.com/articles/s41467-021-22012-7 doi: 10.1038/s41467-021-22012-7

Atkinson, G. C., Tenson, T., & Hauryliuk, V. (2011). The RelA/SpoT homolog (RSH) superfamily: distribution and functional evolution of ppGpp synthetases and hydrolases across the tree of life. *PloS one*, *6*(8). Retrieved from https://pubmed.ncbi.nlm.nih.gov/21858139/https://pubmed.ncbi.nlm.nih.gov/21858139/?dopt=Abstract doi: 10.1371/JOURNAL.PONE.0023479

Aziz, D. B., Go, M. L., & Dick, T. (2020, 2). Rifabutin Suppresses Inducible Clarithromycin Resistance in Mycobacterium abscessus by Blocking Induction of whiB7 and erm41. *Antibiotics*, *9*(2). Retrieved from /pmc/articles/PMC7168051//pmc/articles/PMC7168051/?report=abstracthttps://www.ncbi.nlm.nih.gov/pmc/articles/PMC7168051/ doi: 10.3390/ANTIBIOTICS9020072

Balaban, N. Q., Helaine, S., Lewis, K., Ackermann, M., Aldridge, B., Anders-

son, D. I., ... Zinkernagel, A. (2019, 7). Definitions and guidelines for research on antibiotic persistence. *Nature Reviews. Microbiology*, *17*(7), 441. Retrieved from /pmc/articles/PMC7136161//pmc/articles/PMC7136161/?report=abstracthttps://www.ncbi.nlm.nih.gov/pmc/articles/PMC7136161/ doi: 10.1038/S41579-019-0196-3

Balaban, N. Q., Merrin, J., Chait, R., Kowalik, L., & Leibler, S. (2004, 9). Bacterial persistence as a phenotypic switch. *Science*, *305*(5690), 1622–1625. doi: 10.1126/science.1099390

Barber, D. L., Mayer-Barber, K. D., Feng, C. G., Sharpe, A. H., & Sher, A. (2011, 2). CD4 T cells promote rather than control tuberculosis in the absence of PD-1-mediated inhibition. *Journal of immunology (Baltimore, Md. : 1950)*, *186*(3), 1598–1607. Retrieved from https://pubmed.ncbi.nlm.nih.gov/21172867/ doi: 10.4049/JIMMUNOL.1003304

Barberis, I., Bragazzi, N. L., Galluzzo, L., & Martini, M. (2017). The history of tuberculosis: from the first historical records to the isolation of Koch's bacillus. *Journal of Preventive Medicine and Hygiene*, *58*(1), E9. Retrieved from /pmc/articles/PMC5432783//pmc/articles/PMC5432783/?report=abstracthttps://www.ncbi.nlm.nih.gov/pmc/articles/PMC5432783/

Baykan, A. H., Sayiner, H. S., Aydin, E., Koc, M., Inan, I., & Erturk, S. M. (2022, 12). Extrapulmonary tuberculosıs: an old but resurgent problem. *Insights into Imaging*, *13*(1), 1–21. doi: 10.1186/S13244-022-01172-0/FIGURES/56

Baym, M., Lieberman, T. D., Kelsic, E. D., Chait, R., Gross, R., Yelin, I., & Kishony, R. (2016, 9). Spatiotemporal microbial evolution on antibiotic landscapes. *Science*, *353*(6304), 1147–1151. Retrieved from https://www.science.org/doi/10.1126/science.aag0822 doi: 10.1126/SCIENCE.AAG0822/SUPPL{_}FILE/BAYM.SM.PDF

Berghoff, B. A., Hoekzema, M., Aulbach, L., & Wagner, E. G. H. (2017, 3). Two regulatory RNA elements affect TisB-dependent depolarization and persister formation. *Molecular Microbiology*, *103*(6), 1020–1033. Retrieved from https://onlinelibrary.wiley.com/doi/full/10.1111/mmi.13607https://onlinelibrary.wiley.com/doi/abs/10.1111/mmi.13607https://onlinelibrary.wiley.com/doi/10.1111/mmi.13607 doi: 10.1111/MMI.13607

Bigger, J. W. (1944). The bactericidal action of penicillin on Staphylococcus pyogenes. *Irish Journal of Medical Science*, *19*(11), 553–568. doi: 10.1007/BF02948386

Bollen, C., Louwagie, E., Verstraeten, N., Michiels, J., & Ruelens, P. (2023, 8). Environ-

mental, mechanistic and evolutionary landscape of antibiotic persistence. *EMBO reports*, *24*(8). Retrieved from https://www.embopress.org/doi/10.15252/embr.202357309 doi: 10.15252/EMBR.202357309/ASSET/AD05556D-6A53-478C-9B67-06184CA06D17/ASSETS/GRAPHIC/EMBR202357309-FIG-0004-M.PNG

Bosch, B., DeJesus, M. A., Poulton, N. C., Zhang, W., Engelhart, C. A., Zaveri, A., ... Rock, J. M. (2021, 8). Genome-wide gene expression tuning reveals diverse vulnerabilities of M. tuberculosis. *Cell*, *184*(17), 4579–4592. Retrieved from https://pubmed.ncbi.nlm.nih.gov/34297925/ doi: 10.1016/J.CELL.2021.06.033

Botella, H., Yang, G., Ouerfelli, O., Ehrt, S., Nathan, C. F., & Vaubourgeix, J. (2017, 9). Distinct Spatiotemporal Dynamics of Peptidoglycan Synthesis between Mycobacterium smegmatis and Mycobacterium tuberculosis. *mBio*, *8*(5). Retrieved from https://pubmed.ncbi.nlm.nih.gov/28900018/https://pubmed.ncbi.nlm.nih.gov/28900018/?dopt=Abstract doi: 10.1128/MBIO.01183-17

Bowman, J., & Ghosh, P. (2014, 1). A complex regulatory network controlling intrinsic multidrug resistance in Mycobacterium smegmatis. *Molecular microbiology*, *91*(1), 121. Retrieved from /pmc/articles/PMC9297318//pmc/articles/PMC9297318/?report=abstracthttps://www.ncbi.nlm.nih.gov/pmc/articles/PMC9297318/ doi: 10.1111/MMI.12448

Brahmachari, V., & Ramakrishnan, T. (1984, 11). Studies on 1-methyl adenine transfer RNA methyltransferase of Mycobacterium smegmatis. *Archives of Microbiology*, *140*(1), 91–95. Retrieved from https://link.springer.com/article/10.1007/BF00409778 doi: 10.1007/BF00409778/METRICS

Bray, N. L., Pimentel, H., Melsted, P., & Pachter, L. (2016, 4). Near-optimal probabilistic RNA-seq quantification. *Nature Biotechnology 2016 34:5*, *34*(5), 525–527. Retrieved from https://www.nature.com/articles/nbt.3519 doi: 10.1038/nbt.3519

Briani, F., Carzaniga, T., & Dehò, G. (2016, 3). Regulation and functions of bacterial PNPase. *Wiley Interdisciplinary Reviews: RNA*, *7*(2), 241–258. Retrieved from https://onlinelibrary.wiley.com/doi/full/10.1002/wrna.1328https://onlinelibrary.wiley.com/doi/abs/10.1002/wrna.1328https://wires.onlinelibrary.wiley.com/doi/10.1002/wrna.1328 doi: 10.1002/WRNA.1328

Brown, D. R. (2019, 2). Nitrogen Starvation Induces Persister Cell Formation in Escherichia coli. *Journal of bacteriology*, *201*(3). Retrieved from https://pubmed.ncbi.nlm.nih

.gov/30420451/ doi: 10.1128/JB.00622-18

Brown-Elliott, B. A., Hanson, K., Vasireddy, S., Iakhiaeva, E., Nash, K. A., Vasireddy, R., ... Wallace, R. J. (2015, 3). Absence of a functional erm gene in isolates of Mycobacterium immunogenum and the Mycobacterium mucogenicum group, based on in vitro clarithromycin susceptibility. *Journal of clinical microbiology*, *53*(3), 875–878. Retrieved from https://pubmed.ncbi.nlm.nih.gov/25568437/ doi: 10.1128/JCM.02936-14

Brunel, R., & Charpentier, X. (2016, 11). Trans-translation is essential in the human pathogen Legionella pneumophila. *Scientific Reports*, *6*. Retrieved from /pmc/articles/PMC5124942//pmc/articles/PMC5124942/?report=abstracthttps://www.ncbi.nlm.nih.gov/pmc/articles/PMC5124942/ doi: 10.1038/SREP37935

Bumann, D., & Schothorst, J. (2017, 10). Intracellular Salmonella metabolism. *Cellular Microbiology*, *19*(10), e12766. Retrieved from https://onlinelibrary.wiley.com/doi/full/10.1111/cmi.12766https://onlinelibrary.wiley.com/doi/abs/10.1111/cmi.12766https://onlinelibrary.wiley.com/doi/10.1111/cmi.12766 doi: 10.1111/CMI.12766

Burian, J., Ramón-García, S., Howes, C. G., & Thompson, C. J. (2012, 9). WhiB7, a transcriptional activator that coordinates physiology with intrinsic drug resistance in Mycobacterium tuberculosis. *Expert Review of Anti-Infective Therapy*, *10*(9), 1037–1047. doi: 10.1586/ERI.12.90

Cameron, T. A., Matz, L. M., & De Lay, N. R. (2018, 10). Polynucleotide phosphorylase: Not merely an RNase but a pivotal post-transcriptional regulator. *PLoS Genetics*, *14*(10). Retrieved from /pmc/articles/PMC6181284//pmc/articles/PMC6181284/?report=abstracthttps://www.ncbi.nlm.nih.gov/pmc/articles/PMC6181284/ doi: 10.1371/JOURNAL.PGEN.1007654

Campos-Silva, R., D'urso, G., Delalande, O., Giudice, E., Macedo, A. J., & Gillet, R. (2022, 1). Trans-Translation Is an Appealing Target for the Development of New Antimicrobial Compounds. *Microorganisms*, *10*(1). Retrieved from /pmc/articles/PMC8778911//pmc/articles/PMC8778911/?report=abstracthttps://www.ncbi.nlm.nih.gov/pmc/articles/PMC8778911/ doi: 10.3390/MICROORGANISMS10010003

Caruso, A. M., Serbina, N., Klein, E., Triebold, K., Bloom, B. R., & Flynn, J. L. (1999, 5). Mice Deficient in CD4 T Cells Have Only Transiently Diminished Levels of IFN-γ, Yet Succumb to Tuberculosis. *The Journal of Immunology*, *162*(9), 5407–5416. Retrieved

from https://dx.doi.org/10.4049/jimmunol.162.9.5407 doi: 10.4049/JIMMUNOL.162.9.5407

Chackerian, A. A., Alt, J. M., Perera, T. V., Dascher, C. C., & Behar, S. M. (2002). Dissemination of Mycobacterium tuberculosis is influenced by host factors and precedes the initiation of T-cell immunity. *Infection and Immunity*, *70*(8), 4501–4509. doi: 10.1128/IAI.70.8.4501-4509.2002

Chandra, P., Grigsby, S. J., & Philips, J. A. (2022). Immune evasion and provocation by Mycobacterium tuberculosis. *Nature Reviews Microbiology*. Retrieved from www.nature.com/nrmicro doi: 10.1038/s41579-022-00763-4

Charlebois, D. A. (2023, 9). Quantitative systems-based prediction of antimicrobial resistance evolution. *npj Systems Biology and Applications 2023 9:1*, *9*(1), 1–6. Retrieved from https://www.nature.com/articles/s41540-023-00304-6 doi: 10.1038/s41540-023-00304-6

Chen, X., Sim, S., Wurtmann, E. J., Feke, A., & Wolin, S. L. (2014, 11). Bacterial noncoding Y RNAs are widespread and mimic tRNAs. *RNA*, *20*(11), 1715. Retrieved from /pmc/articles/PMC4201824//pmc/articles/PMC4201824/?report=abstracthttps://www.ncbi.nlm.nih.gov/pmc/articles/PMC4201824/ doi: 10.1261/RNA.047241.114

Chen, X., Taylor, D. W., Fowler, C. C., Galan, J. E., Wang, H. W., & Wolin, S. L. (2013, 3). An RNA Degradation Machine Sculpted by Ro Autoantigen and Noncoding RNA. *Cell*, *153*(1), 166. Retrieved from /pmc/articles/PMC3646564//pmc/articles/PMC3646564/?report=abstracthttps://www.ncbi.nlm.nih.gov/pmc/articles/PMC3646564/ doi: 10.1016/J.CELL.2013.02.037

Chen, X., & Wolin, S. L. (2023, 5). Transfer RNA halves are found as nicked tRNAs in cells: evidence that nicked tRNAs regulate expression of an RNA repair operon. *RNA*, *29*(5), 620. Retrieved from /pmc/articles/PMC10159003//pmc/articles/PMC10159003/?report=abstracthttps://www.ncbi.nlm.nih.gov/pmc/articles/PMC10159003/ doi: 10.1261/RNA.079575.122

Cheng, Z. F., & Deutscher, M. P. (2003, 5). Quality control of ribosomal RNA mediated by polynucleotide phosphorylase and RNase R. *Proceedings of the National Academy of Sciences of the United States of America*, *100*(11), 6388. Retrieved from /pmc/articles/PMC164456//pmc/articles/PMC164456/?report=

abstracthttps://www.ncbi.nlm.nih.gov/pmc/articles/PMC164456/ doi: 10.1073/PNAS.1231041100

Cheverton, A. M., Gollan, B., Przydacz, M., Wong, C. T., Mylona, A., Hare, S. A., & Helaine, S. (2016). A Salmonella Toxin Promotes Persister Formation through Acetylation of tRNA. *Molecular cell*, *63*(1), 86–96. Retrieved from http://www.ncbi.nlm.nih.gov/pubmed/27264868http://www.pubmedcentral.nih.gov/articlerender.fcgi?artid=PMC4942678 doi: 10.1016/j.molcel.2016.05.002

Chung, E. S., Johnson, W. C., & Aldridge, B. B. (2022, 9). Types and functions of heterogeneity in mycobacteria. *Nature reviews. Microbiology*, *20*(9), 529–541. Retrieved from https://pubmed.ncbi.nlm.nih.gov/35365812/ doi: 10.1038/S41579-022-00721-0

Clements, M. O., Eriksson, S., Thompson, A., Lucchini, S., Hinton, J. C., Normark, S., & Rhen, M. (2002, 6). Polynucleotide phosphorylase is a global regulator of virulence and persistency in Salmonella enterica. *Proceedings of the National Academy of Sciences of the United States of America*, *99*(13), 8784–8789. Retrieved from https://www.pnas.org/doi/abs/10.1073/pnas.132047099 doi: 10.1073/PNAS.132047099/SUPPL{_}FILE/0470TABLE2.XLS

Cohen, S. B., Gern, B. H., Delahaye, J. L., Adams, K. N., Plumlee, C. R., Winkler, J. K., ... Urdahl, K. B. (2018, 9). Alveolar Macrophages Provide an Early Mycobacterium tuberculosis Niche and Initiate Dissemination. *Cell host & microbe*, *24*(3), 439–446. Retrieved from https://pubmed.ncbi.nlm.nih.gov/30146391/ doi: 10.1016/J.CHOM.2018.08.001

Conlon, B. P., Rowe, S. E., Gandt, A. B., Nuxoll, A. S., Donegan, N. P., Zalis, E. A., ... Lewis, K. (2016). Persister formation in Staphylococcus aureus is associated with ATP depletion. *Nature Microbiology*, *1*(5). doi: 10.1038/nmicrobiol.2016.51

Conradie, F., Bagdasaryan, T. R., Borisov, S., Howell, P., Mikiashvili, L., Ngubane, N., ... Spigelman, M. (2022, 9). Bedaquiline-Pretomanid-Linezolid Regimens for Drug-Resistant Tuberculosis. *The New England journal of medicine*, *387*(9), 810–823. Retrieved from https://pubmed.ncbi.nlm.nih.gov/36053506/ doi: 10.1056/NEJMOA2119430

Copela, L. A., Fernandez, C. F., Sherrer, R. L., & Wolin, S. L. (2008, 6). Competition between the Rex1 exonuclease and the La protein affects both Trf4p-mediated RNA quality control and pre-tRNA maturation. *RNA*, *14*(6), 1214–1227. doi: 10.1261/RNA.1050408

Crofton, J., & Mitchison, D. A. (1948). Streptomycin resistance in pulmonary tuberculosis. *British Medical Journal*, *2*(4588), 1009–1015. doi: 10.1136/bmj.2.4588.1009

Crook, D. W., Peto, T. E., Hoosdally, S. J., Cruz, A. L. G., Walker, A. S., Walker, T. M., ... Grazian, C. (2022, 8). A data compendium associating the genomes of 12,289 Mycobacterium tuberculosis isolates with quantitative resistance phenotypes to 13 antibiotics. *PLOS Biology*, *20*(8), e3001721. doi: 10.1371/JOURNAL.PBIO.3001721

Daniel, J., Maamar, H., Deb, C., Sirakova, T. D., & Kolattukudy, P. E. (2011, 6). Mycobacterium tuberculosis Uses Host Triacylglycerol to Accumulate Lipid Droplets and Acquires a Dormancy-Like Phenotype in Lipid-Loaded Macrophages. *PLoS Pathogens*, *7*(6). Retrieved from /pmc/articles/PMC3121879//pmc/articles/PMC3121879/?report=abstracthttps://www.ncbi.nlm.nih.gov/pmc/articles/PMC3121879/ doi: 10.1371/JOURNAL.PPAT.1002093

Dartois, V. A., & Rubin, E. J. (2022, 11). Anti-tuberculosis treatment strategies and drug development: challenges and priorities. *Nature Reviews. Microbiology*, *20*(11), 685. Retrieved from /pmc/articles/PMC9045034//pmc/articles/PMC9045034/?report=abstracthttps://www.ncbi.nlm.nih.gov/pmc/articles/PMC9045034/ doi: 10.1038/S41579-022-00731-Y

Davies, J. (1996). Origins and evolution of antibiotic resistance. *Microbiología (Madrid, Spain)*, *12*(1), 9–16. doi: 10.1128/MMBR.00016-10

Dejesus, M. A., Gerrick, E. R., Xu, W., Park, S. W., Long, J. E., Boutte, C. C., ... Ioerger, T. R. (2017, 1). Comprehensive essentiality analysis of the Mycobacterium tuberculosis genome via saturating transposon mutagenesis. *mBio*, *8*(1). Retrieved from https://journals.asm.org/doi/10.1128/mBio.02133-16 doi: 10.1128/MBIO.02133-16/SUPPL{_}FILE/MBO002173137ST6.XLSX

De la Cruz, J., & Vioque, A. (2001). Increased sensitivity to protein synthesis inhibitors in cells lacking tmRNA. *RNA*, *7*(12), 1708. Retrieved from /pmc/articles/PMC1370211/?report=abstracthttps://www.ncbi.nlm.nih.gov/pmc/articles/PMC1370211/

De Lay, N., & Gottesman, S. (2011, 6). Role of polynucleotide phosphorylase in sRNA function in Escherichia coli. *RNA*, *17*(6), 1172. Retrieved from /pmc/articles/PMC3096048//pmc/articles/PMC3096048/?report=abstracthttps://www.ncbi.nlm.nih.gov/pmc/articles/PMC3096048/ doi: 10.1261/RNA.2531211

Dewachter, L., Fauvart, M., & Michiels, J. (2019, 10). Bacterial Heterogene-

ity and Antibiotic Survival: Understanding and Combatting Persistence and Heteroresistance. *Molecular Cell*, *76*(2), 255–267. Retrieved from http://www.cell.com/article/S1097276519307336/fulltexthttp://www.cell.com/article/S1097276519307336/abstracthttps://www.cell.com/molecular-cell/abstract/S1097-2765(19)30733-6 doi: 10.1016/J.MOLCEL.2019.09.028

de Zoysa, T., & Phizicky, E. M. (2020, 8). Hypomodified tRNA in evolutionarily distant yeasts can trigger rapid tRNA decay to activate the general amino acid control response, but with different consequences. *PLOS Genetics*, *16*(8), e1008893. doi: 10.1371/JOURNAL.PGEN.1008893

Diacon, A. H., Von Groote-Bidlingmaier, F., & Donald, P. R. (2012, 8). From magic mountain to table mountain. *Swiss medical weekly*, *142*. Retrieved from https://pubmed.ncbi.nlm.nih.gov/22915310/https://pubmed.ncbi.nlm.nih.gov/22915310/?dopt=Abstract doi: 10.4414/SMW.2012.13665

Dieppe, P., Wollheim, F. A., & Schumacher, H. R. (2001, 12). Characterization of a soluble cytoplasmic antigen reactive with sera from patients with systemic lupus erythematosus : Clark G, Reichlin M, Tomasi TB. *Classic Papers in Rheumatology*, 224–225. doi: 10.3109/9780203214237-110

Doerfel, L. K., Wohlgemuth, I., Kothe, C., Peske, F., Urlaub, H., & Rodnina, M. V. (2013, 1). EF-P is essential for rapid synthesis of proteins containing consecutive proline residues. *Science (New York, N.Y.)*, *339*(6115), 85–88. Retrieved from https://pubmed.ncbi.nlm.nih.gov/23239624/ doi: 10.1126/SCIENCE.1229017

Dorman, S. E., Nahid, P., Kurbatova, E. V., Phillips, P. P., Bryant, K., Dooley, K. E., ... Chaisson, R. E. (2021, 5). Four-Month Rifapentine Regimens with or without Moxifloxacin for Tuberculosis. *New England Journal of Medicine*, *384*(18), 1705–1718. Retrieved from http://www.nejm.org/doi/10.1056/NEJMoa2033400 doi: 10.1056/NEJMoa2033400

Dörr, T., Lewis, K., & Vulić, M. (2009, 12). SOS Response Induces Persistence to Fluoroquinolones in Escherichia coli. *PLoS Genetics*, *5*(12), 1000760. Retrieved from /pmc/articles/PMC2780357//pmc/articles/PMC2780357/?report=abstracthttps://www.ncbi.nlm.nih.gov/pmc/articles/PMC2780357/ doi: 10.1371/JOURNAL.PGEN.1000760

Dörr, T., Vulić, M., & Lewis, K. (2010, 2). Ciprofloxacin causes persister formation by inducing the TisB toxin in Escherichia coli. *PLoS biology*, *8*(2). Retrieved from https://pubmed

.ncbi.nlm.nih.gov/20186264/ doi: 10.1371/JOURNAL.PBIO.1000317

Doster, B., Murray, F. J., Newman, R., & Woolpert, S. F. (1973, 2). Ethambutol in the initial treatment of pulmonary tuberculosis. U.S. Public Health Service tuberculosis therapy trials. *The American review of respiratory disease*, *107*(2), 177–190. Retrieved from https://pubmed.ncbi.nlm.nih.gov/4567069/ doi: 10.1164/ARRD.1973.107.2.177

Drlica, K. (2003, 7). The mutant selection window and antimicrobial resistance. *Journal of Antimicrobial Chemotherapy*, *52*(1), 11–17. Retrieved from https://dx.doi.org/10.1093/jac/dkg269 doi: 10.1093/JAC/DKG269

Droogmans, L., Roovers, M., Bujnicki, J. M., Tricot, C., Hartsch, T., Stalon, V., & Grosjean, H. (2003, 4). Cloning and characterization of tRNA (m1A58) methyltransferase (TrmI) from Thermus thermophilus HB27, a protein required for cell growth at extreme temperatures. *Nucleic Acids Research*, *31*(8), 2148. Retrieved from /pmc/articles/PMC153742//pmc/articles/PMC153742/?report=abstracthttps://www.ncbi.nlm.nih.gov/pmc/articles/PMC153742/ doi: 10.1093/NAR/GKG314

Dutta, N. K., Klinkenberg, L. G., Vazquez, M. J., Segura-Carro, D., Colmenarejo, G., Ramon, F., ... Karakousis, P. C. (2019). Inhibiting the stringent response blocks Mycobacterium tuberculosis entry into quiescence and reduces persistence. *Science advances*, *5*(3). Retrieved from https://pubmed.ncbi.nlm.nih.gov/30906866/ doi: 10.1126/SCIADV.AAV2104

Edelmann, D., & Berghoff, B. A. (2022, 3). A Shift in Perspective: A Role for the Type I Toxin TisB as Persistence-Stabilizing Factor. *Frontiers in Microbiology*, *13*, 871699. Retrieved from /pmc/articles/PMC8969498//pmc/articles/PMC8969498/?report=abstracthttps://www.ncbi.nlm.nih.gov/pmc/articles/PMC8969498/ doi: 10.3389/FMICB.2022.871699

Ehrt, S., Guo, X. V., Hickey, C. M., Ryou, M., Monteleone, M., Riley, L. W., & Schnappinger, D. (2005). Controlling gene expression in mycobacteria with anhydrotetracycline and Tet repressor. *Nucleic Acids Research*, *33*(2), e21. Retrieved from /pmc/articles/PMC548372//pmc/articles/PMC548372/?report=abstracthttps://www.ncbi.nlm.nih.gov/pmc/articles/PMC548372/ doi: 10.1093/NAR/GNI013

Ehrt, S., Schnappinger, D., & Rhee, K. Y. (2018, 4). Metabolic principles of persistence and

pathogenicity in Mycobacterium tuberculosis. *Nature Reviews Microbiology 2018 16:8*, *16*(8), 496–507. Retrieved from https://www.nature.com/articles/s41579-018-0013-4 doi: 10.1038/s41579-018-0013-4

Etienne, G., Laval, F., Villeneuve, C., Dinadayala, P., Abouwarda, A., Zerbib, D., ... Daffé, M. (2005, 6). The cell envelope structure and properties of Mycobacterium smegmatis mc2155: Is there a clue for the unique transformability of the strain? *Microbiology*, *151*(6), 2075–2086. doi: 10.1099/mic.0.27869-0

Evguenieva-Hackenberg, E., Hou, L., Glaeser, S., & Klug, G. (2014). Structure and function of the archaeal exosome. *Wiley interdisciplinary reviews. RNA*, *5*(5), 623–635. Retrieved from https://pubmed.ncbi.nlm.nih.gov/24789718/ doi: 10.1002/WRNA.1234

Fisher, R. A., Gollan, B., & Helaine, S. (2017, 5). Persistent bacterial infections and persister cells. *Nature Reviews Microbiology*, *15*(8), 453–464. Retrieved from http://www.ncbi.nlm.nih.gov/pubmed/28529326http://www.nature.com/doifinder/10.1038/nrmicro.2017.42 doi: 10.1038/nrmicro.2017.42

Forrellad, M. A., Klepp, L. I., Gioffré, A., García, J. S., Morbidoni, H. R., de la Paz Santangelo, M., ... Bigi, F. (2013). *Virulence factors of the mycobacterium tuberculosis complex* (Vol. 4) (No. 1). Retrieved from http://dx.doi.org/10.4161/viru.22329 doi: 10.4161/viru.22329

Fridman, O., Goldberg, A., Ronin, I., Shoresh, N., & Balaban, N. Q. (2014, 9). Optimization of lag time underlies antibiotic tolerance in evolved bacterial populations. *Nature*, *513*(7518), 418–421. Retrieved from https://pubmed.ncbi.nlm.nih.gov/25043002/ doi: 10.1038/NATURE13469

Fuchs, G., Stein, A. J., Fu, C., Reinisch, K. M., & Wolin, S. L. (2006, 11). Structural and biochemical basis for misfolded RNA recognition by the Ro autoantigen. *Nature structural & molecular biology*, *13*(11), 1002–1009. Retrieved from https://pubmed.ncbi.nlm.nih.gov/17041599/ doi: 10.1038/NSMB1156

Gaynor, M., & Mankin, A. (2003, 3). Macrolide antibiotics: binding site, mechanism of action, resistance. *Current topics in medicinal chemistry*, *3*(9), 949–960. Retrieved from https://pubmed.ncbi.nlm.nih.gov/12678831/ doi: 10.2174/1568026033452159

Gefen, O., Fridman, O., Ronin, I., & Balaban, N. Q. (2014, 1). Direct observation of single stationary-phase bacteria reveals a surprisingly long period of constant protein production activity. *Proceedings of the National Academy of Sciences of the United*

States of America, *111*(1), 556–561. Retrieved from /pmc/articles/PMC3890821//pmc/articles/PMC3890821/?report=abstracthttps://www.ncbi.nlm.nih.gov/pmc/articles/PMC3890821/ doi: 10.1073/PNAS.1314114111/-/DCSUPPLEMENTAL

Geiman, D. E., Raghunand, T. R., Agarwal, N., & Bishai, W. R. (2006, 8). Differential Gene Expression in Response to Exposure to Antimycobacterial Agents and Other Stress Conditions among Seven Mycobacterium tuberculosis whiB-Like Genes. *Antimicrobial Agents and Chemotherapy*, *50*(8), 2836. Retrieved from /pmc/articles/PMC1538666//pmc/articles/PMC1538666/?report=abstracthttps://www.ncbi.nlm.nih.gov/pmc/articles/PMC1538666/ doi: 10.1128/AAC.00295-06

Gengenbacher, M., & Kaufmann, S. H. (2012, 5). *Mycobacterium tuberculosis: Success through dormancy* (Vol. 36) (No. 3). doi: 10.1111/j.1574-6976.2012.00331.x

Georgieva, M., Sia, J. K., Bizzell, E., Madan-Lala, R., & Rengarajan, J. (2018, 2). Mycobacterium tuberculosis GroEL2 Modulates Dendritic Cell Responses. *Infection and Immunity*, *86*(2). Retrieved from /pmc/articles/PMC5778359//pmc/articles/PMC5778359/?report=abstracthttps://www.ncbi.nlm.nih.gov/pmc/articles/PMC5778359/ doi: 10.1128/IAI.00387-17

Germain, E., Roghanian, M., Gerdes, K., & Maisonneuve, E. (2015, 4). Stochastic induction of persister cells by HipA through (p)ppGpp-mediated activation of mRNA endonucleases. *Proceedings of the National Academy of Sciences of the United States of America*, *112*(16), 5171–5176. Retrieved from https://pubmed.ncbi.nlm.nih.gov/25848049/ doi: 10.1073/PNAS.1423536112

Germain, E., Roghanian, M., Gerdes, K., & Maisonneuve, E. (2019, 5). Retraction for Germain et al., Stochastic induction of persister cells by HipA through (p)ppGpp-mediated activation of mRNA endonucleases. *Proceedings of the National Academy of Sciences*, *116*(22), 11077–11077. Retrieved from https://www.pnas.org/doi/abs/10.1073/pnas.1906160116 doi: 10.1073/PNAS.1906160116

Gollan, B., Grabe, G., Michaux, C., & Helaine, S. (2019). Bacterial Persisters and Infection: Past, Present, and Progressing. *Annual Review of Microbiology*, *73*(1), 359–385. doi: 10.1146/annurev-micro-020518-115650

Goneau, L. W., Yeoh, N. S., MacDonald, K. W., Cadieux, P. A., Burton, J. P., Razvi, H., & Reid, G. (2014). Selective Target Inactivation Rather than Global Metabolic Dormancy

Causes Antibiotic Tolerance in Uropathogens. *Antimicrobial Agents and Chemotherapy*, *58*(4), 2089. Retrieved from /pmc/articles/PMC4023725//pmc/articles/PMC4023725/?report=abstracthttps://www.ncbi.nlm.nih.gov/pmc/articles/PMC4023725/ doi: 10.1128/AAC.02552-13

Górna, M. W., Carpousis, A. J., & Luisi, B. F. (2012, 5). From conformational chaos to robust regulation: the structure and function of the multi-enzyme RNA degradosome. *Quarterly Reviews of Biophysics*, *45*(2), 105–145. doi: 10.1017/S003358351100014X

Green, C. D., Long, K. S., Shi, H., & Wolin, S. L. (1998, 7). Binding of the 60-kDa Ro autoantigen to Y RNAs: evidence for recognition in the major groove of a conserved helix. *RNA (New York, N.Y.)*, *4*(7), 750–765. Retrieved from https://pubmed.ncbi.nlm.nih.gov/9671049/ doi: 10.1017/S1355838298971667

Gupta, S., & Chatterji, D. (2005, 3). *Stress responses in mycobacteria* (Vol. 57) (No. 3). doi: 10.1080/15216540500090611

Haddad, N., Burns, C. M., Bolla, J. M., Prévost, H., Fédérighi, M., Drider, D., & Cappelier, J. M. (2009, 12). Long-term survival of Campylobacter jejuni at low temperatures is dependent on polynucleotide phosphorylase activity. *Applied and Environmental Microbiology*, *75*(23), 7310–7318. Retrieved from https://journals.asm.org/doi/10.1128/AEM.01366-09 doi: 10.1128/AEM.01366-09/ASSET/2248D157-136A-4314-9D88-A90D9EEBD878/ASSETS/GRAPHIC/ZAM0230904620004.JPEG

Hannebelle, M. T., Ven, J. X., Toniolo, C., Eskandarian, H. A., Vuaridel-Thurre, G., McKinney, J. D., & Fantner, G. E. (2020, 1). A biphasic growth model for cell pole elongation in mycobacteria. *Nature Communications 2020 11:1*, *11*(1), 1–10. Retrieved from https://www.nature.com/articles/s41467-019-14088-z doi: 10.1038/s41467-019-14088-z

Hansen, S., Lewis, K., & Vulić, M. (2008, 8). Role of global regulators and nucleotide metabolism in antibiotic tolerance in Escherichia coli. *Antimicrobial Agents and Chemotherapy*, *52*(8), 2718–2726. doi: 10.1128/AAC.00144-08

Harms, A., Brodersen, D. E., Mitarai, N., & Gerdes, K. (2018, 6). Toxins, Targets, and Triggers: An Overview of Toxin-Antitoxin Biology. *Molecular Cell*, *70*(5), 768–784. Retrieved from http://www.cell.com/article/S1097276518300030/fulltexthttp://www.cell.com/article/S1097276518300030/abstracthttps://www.cell.com/molecular-cell/abstract/S1097-2765(18)30003-0 doi: 10.1016/J.MOLCEL.2018.01.003

Hart, P. D., Armstrong, J. A., Brown, C. A., & Draper, P. (1972, 5). Ultrastructural study of the behavior of macrophages toward parasitic mycobacteria. *Infection and immunity*, *5*(5), 803–807. Retrieved from https://pubmed.ncbi.nlm.nih.gov/4629254/ doi: 10.1128/IAI.5.5.803-807.1972

Helaine, S., Cheverton, A. M., Watson, K. G., Faure, L. M., Matthews, S. A., & Holden, D. W. (2014, 1). Internalization of salmonella by macrophages induces formation of nonreplicating persisters. *Science*, *343*(6167), 204–208. Retrieved from https://www.science.org/doi/10.1126/science.1244705 doi: 10.1126/SCIENCE.1244705/SUPPL{_}FILE/HELAINE-SM.PDF

Helaine, S., & Kugelberg, E. (2014, 7). Bacterial persisters: formation, eradication, and experimental systems. *Trends in Microbiology*, *22*(7), 417–424. Retrieved from https://www.sciencedirect.com/science/article/pii/S0966842X14000705?via%3Dihub doi: 10.1016/J.TIM.2014.03.008

Henry, A., Shanks, J., van Hoof, A., & Rosenzweig, J. A. (2012, 11). The Yersinia pseudotuberculosis degradosome is required for oxidative stress, while its PNPase subunit plays a degradosome-independent role in cold growth. *FEMS Microbiology Letters*, *336*(2), 139–147. Retrieved from https://dx.doi.org/10.1111/j.1574-6968.12000.x doi: 10.1111/J.1574-6968.12000.X

Hesper Rego, E., Audette, R. E., & Rubin, E. J. (2017, 6). Deletion of a mycobacterial divisome factor collapses single-cell phenotypic heterogeneity. *Nature*, *546*(7656), 153–157. Retrieved from https://pubmed.ncbi.nlm.nih.gov/28569798/ doi: 10.1038/NATURE22361

Hicks, N. D., Carey, A. F., Yang, J., Zhao, Y., & Fortunea, S. M. (2019, 3). Bacterial Genome-Wide Association Identifies Novel Factors That Contribute to Ethionamide and Prothionamide Susceptibility in Mycobacterium tuberculosis. *mBio*, *10*(2). Retrieved from https://pubmed.ncbi.nlm.nih.gov/31015328/ doi: 10.1128/MBIO.00616-19

Hill, P. W., Moldoveanu, A. L., Sargen, M., Ronneau, S., Glegola-Madejska, I., Beetham, C., ... Helaine, S. (2021, 12). The vulnerable versatility of Salmonella antibiotic persisters during infection. *Cell host & microbe*, *29*(12), 1757–1773. Retrieved from https://pubmed.ncbi.nlm.nih.gov/34731646/ doi: 10.1016/J.CHOM.2021.10.002

Hobby, G. L., Meyer, K., & Chaffee, E. (1942, 6). Observations on the Mechanism of Action of Penicillin.. *https://doi.org/10.3181/00379727-50-13773*, *50*(2), 281–285. Retrieved

from https://journals.sagepub.com/doi/abs/10.3181/00379727-50-13773 doi: 10.3181/00379727-50-13773

Houben, D., Demangel, C., van Ingen, J., Perez, J., Baldeón, L., Abdallah, A. M., ... Peters, P. J. (2012, 8). ESX-1-mediated translocation to the cytosol controls virulence of mycobacteria. *Cellular microbiology*, *14*(8), 1287–1298. Retrieved from https://pubmed.ncbi.nlm.nih.gov/22524898/ doi: 10.1111/J.1462-5822.2012.01799.X

Hurst-Hess, K., Rudra, P., & Ghosh, P. (2017, 11). Mycobacterium abscessus WhiB7 regulates a species-specific repertoire of genes to confer extreme antibiotic resistance. *Antimicrobial Agents and Chemotherapy*, *61*(11). doi: 10.1128/AAC.01353-17

Ingolia, N. T., Ghaemmaghami, S., Newman, J. R., & Weissman, J. S. (2009, 4). Genome-Wide Analysis in Vivo of Translation with Nucleotide Resolution Using Ribosome Profiling. *Science (New York, N.Y.)*, *324*(5924), 218. Retrieved from /pmc/articles/PMC2746483//pmc/articles/PMC2746483/?report=abstracthttps://www.ncbi.nlm.nih.gov/pmc/articles/PMC2746483/ doi: 10.1126/SCIENCE.1168978

Irving, S. E., Choudhury, N. R., & Corrigan, R. M. (2020). The stringent response and physiological roles of (pp)pGpp in bacteria. *Nature Reviews Microbiology*, *19*, 256–271. Retrieved from www.nature.com/nrmicro doi: 10.1038/s41579-020-00470-y

Iseman, M. D. (2002, 7). Tuberculosis therapy: past, present and future. *European Respiratory Journal*, *20*(36 suppl), 87S-94s. Retrieved from https://erj.ersjournals.com/content/20/36_suppl/87Shttps://erj.ersjournals.com/content/20/36_suppl/87S.abstract doi: 10.1183/09031936.02.00309102

Jansen, R. S., Mandyoli, L., Hughes, R., Wakabayashi, S., Pinkham, J. T., Selbach, B., ... Rhee, K. Y. (2020, 12). Aspartate aminotransferase Rv3722c governs aspartate-dependent nitrogen metabolism in Mycobacterium tuberculosis. *Nature Communications*, *11*(1). doi: 10.1038/s41467-020-15876-8

Javid, B., Sorrentino, F., Toosky, M., Zheng, W., Pinkham, J. T., Jain, N., ... Rubin, E. J. (2014, 1). Mycobacterial mistranslation is necessary and sufficient for rifampicin phenotypic resistance. *Proceedings of the National Academy of Sciences of the United States of America*, *111*(3), 1132–1137. doi: 10.1073/pnas.1317580111

Joyce, G., Williams, K. J., Robb, M., Noens, E., Tizzano, B., Shahrezaei, V., & Robertson, B. D. (2012, 9). Cell division site placement and asymmetric growth in mycobacteria.

PloS one, *7*(9). Retrieved from https://pubmed.ncbi.nlm.nih.gov/22970255/ doi: 10.1371/JOURNAL.PONE.0044582

Jubair, M., Morris, J. G., & Ali, A. (2012, 9). Survival of Vibrio cholerae in Nutrient-Poor Environments Is Associated with a Novel "Persister" Phenotype. *PLOS ONE*, *7*(9), e45187. Retrieved from https://journals.plos.org/plosone/article?id=10.1371/journal.pone.0045187 doi: 10.1371/JOURNAL.PONE.0045187

Judd, J. A., Canestrari, J., Clark, R., Joseph, A., Lapierre, P., Lasek-Nesselquist, E., ... Derbyshire, K. M. (2021). A Mycobacterial Systems Resource for the Research Community. *mBio*, *12*(2), 1–15. Retrieved from https://pubmed.ncbi.nlm.nih.gov/33653882/ doi: 10.1128/MBIO.02401-20

Jumper, J., Evans, R., Pritzel, A., Green, T., Figurnov, M., Ronneberger, O., ... Hassabis, D. (2021, 7). Highly accurate protein structure prediction with AlphaFold. *Nature 2021 596:7873*, *596*(7873), 583–589. Retrieved from https://www.nature.com/articles/s41586-021-03819-2 doi: 10.1038/s41586-021-03819-2

Kadaba, S., Krueger, A., Trice, T., Krecic, A. M., Hinnebusch, A. G., & Anderson, J. (2004). Nuclear surveillance and degradation of hypomodified initiator tRNA Met in S. cerevisiae. *Genes & Development*, *18*(11), 1227–1240. Retrieved from http://www.genesdev.org/cgi/doi/10.1101/gad.1183804. doi: 10.1101/gad.1183804

Karakousis, P. C., Yoshimatsu, T., Lamichhane, G., Woolwine, S. C., Nuermberger, E. L., Grosset, J., & Bishai, W. R. (2004, 9). Dormancy Phenotype Displayed by Extracellular Mycobacterium tuberculosis within Artificial Granulomas in Mice. *The Journal of Experimental Medicine*, *200*(5), 647. Retrieved from /pmc/articles/PMC2212740//pmc/articles/PMC2212740/?report=abstracthttps://www.ncbi.nlm.nih.gov/pmc/articles/PMC2212740/ doi: 10.1084/JEM.20040646

Kaspy, I., Rotem, E., Weiss, N., Ronin, I., Balaban, N. Q., & Glaser, G. (2013, 12). HipA-mediated antibiotic persistence via phosphorylation of the glutamyl-tRNA-synthetase. *Nature Communications*, *4*. doi: 10.1038/ncomms4001

Keren, I., Shah, D., Spoering, A., Kaldalu, N., & Lewis, K. (2004, 12). Specialized persister cells and the mechanism of multidrug tolerance in Escherichia coli. *Journal of Bacteriology*, *186*(24), 8172–8180. doi: 10.1128/JB.186.24.8172-8180.2004

Kieser, K. J., Boutte, C. C., Kester, J. C., Baer, C. E., Barczak, A. K., Meniche,

X., ... Rubin, E. J. (2015, 6). Phosphorylation of the Peptidoglycan Synthase PonA1 Governs the Rate of Polar Elongation in Mycobacteria. *PLoS Pathogens*, *11*(6). Retrieved from /pmc/articles/PMC4483258//pmc/articles/PMC4483258/?report=abstracthttps://www.ncbi.nlm.nih.gov/pmc/articles/PMC4483258/ doi: 10.1371/JOURNAL.PPAT.1005010

Kohanski, M. A., Dwyer, D. J., & Collins, J. J. (2010). How antibiotics kill bacteria: from targets to networks. *Nat Rev Microbiol.*, *8*(6), 423–435. Retrieved from www.nature.com/reviews/micro doi: 10.1038/nrmicro2333

Kotra, L. P., Haddad, J., & Mobashery, S. (2000). Aminoglycosides: perspectives on mechanisms of action and resistance and strategies to counter resistance. *Antimicrobial agents and chemotherapy*, *44*(12), 3249–3256. Retrieved from https://pubmed.ncbi.nlm.nih.gov/11083623/ doi: 10.1128/AAC.44.12.3249-3256.2000

Kraemer, J. A., Sanderlin, A. G., & Laub, M. T. (2019, 7). The Stringent Response Inhibits DNA Replication Initiation in E. coli by Modulating Supercoiling of oriC. *mBio*, *10*(4). Retrieved from https://pubmed.ncbi.nlm.nih.gov/31266875/https://pubmed.ncbi.nlm.nih.gov/31266875/?dopt=Abstract doi: 10.1128/MBIO.01330-19

Kriel, A., Bittner, A. N., Kim, S. H., Liu, K., Tehranchi, A. K., Zou, W. Y., ... Wang, J. D. (2012, 10). Direct regulation of GTP homeostasis by (p)ppGpp: a critical component of viability and stress resistance. *Molecular cell*, *48*(2), 231–241. Retrieved from https://pubmed.ncbi.nlm.nih.gov/22981860/ doi: 10.1016/J.MOLCEL.2012.08.009

Labbé, J. C., Hekimi, S., & Rokeach, L. A. (1999, 1). The levels of the RoRNP-associated Y RNA are dependent upon the presence of ROP-1, the Caenorhabditis elegans Ro60 protein. *Genetics*, *151*(1), 143–150. Retrieved from https://pubmed.ncbi.nlm.nih.gov/9872955/ doi: 10.1093/GENETICS/151.1.143

Lamichhane, G. (2011). Mycobacterium Tuberculosis Response to Stress from Reactive Oxygen and Nitrogen Species. *Frontiers in Microbiology*, *2*(AUG), 105. Retrieved from /pmc/articles/PMC3163289/https://www.ncbi.nlm.nih.gov/pmc/articles/PMC3163289/ doi: 10.3389/FMICB.2011.00176

Larsson, C., Luna, B., Ammerman, N. C., Maiga, M., Agarwal, N., & Bishai, W. R. (2012, 7). Gene expression of Mycobacterium tuberculosis putative transcription factors whiB1-7 in redox environments. *PloS one*, *7*(7). Retrieved from https://pubmed.ncbi.nlm.nih.gov/22829866/ doi: 10.1371/JOURNAL.PONE.0037516

Lee, J. H., Lee, E. J., & Roe, J. H. (2022, 1). uORF-mediated riboregulation controls transcription of whiB7/wblC antibiotic resistance gene. *Molecular microbiology*, *117*(1), 179–192. Retrieved from https://pubmed.ncbi.nlm.nih.gov/34687261/ doi: 10.1111/MMI.14834

Lelovic, N., Mitachi, K., Yang, J., Lemieux, M. R., Ji, Y., & Kurosu, M. (2020, 11). Application of Mycobacterium smegmatis as a surrogate to evaluate drug leads against Mycobacterium tuberculosis. *Journal of Antibiotics*, *73*(11), 780–789. doi: 10.1038/S41429-020-0320-7

Levin-Reisman, I., Ronin, I., Gefen, O., Braniss, I., Shoresh, N., & Balaban, N. Q. (2017). Antibiotic tolerance facilitates the evolution of resistance. *Science*, *355*(6327), 826–830. doi: 10.1126/science.aaj2191

Li, Y., Wang, Y., & Liu, X. (2012). The Role of Airway Epithelial Cells in Response to Mycobacteria Infection. *Clinical and Developmental Immunology*, *2012*, 11. Retrieved from /pmc/articles/PMC3337601//pmc/articles/PMC3337601/?report=abstracthttps://www.ncbi.nlm.nih.gov/pmc/articles/PMC3337601/ doi: 10.1155/2012/791392

Li, Z., & Deutscher, M. P. (2002). RNase E plays an essential role in the maturation of Escherichia coli tRNA precursors. *RNA (New York, N.Y.)*, *8*(1), 97–109. Retrieved from https://pubmed.ncbi.nlm.nih.gov/11871663/ doi: 10.1017/S1355838202014929

Li, Z., & Stanton, B. A. (2021, 5). Transfer RNA-Derived Fragments, the Underappreciated Regulatory Small RNAs in Microbial Pathogenesis. *Frontiers in Microbiology*, *12*, 17. Retrieved from /pmc/articles/PMC8166272//pmc/articles/PMC8166272/?report=abstracthttps://www.ncbi.nlm.nih.gov/pmc/articles/PMC8166272/ doi: 10.3389/FMICB.2021.687632

Lin, B. Y., Chan, P. P., & Lowe, T. M. (2019, 7). tRNAviz: explore and visualize tRNA sequence features. *Nucleic acids research*, *47*(W1), W542-W547. Retrieved from https://pubmed.ncbi.nlm.nih.gov/31127306/ doi: 10.1093/NAR/GKZ438

Lin, P. L., Ford, C. B., Coleman, M. T., Myers, A. J., Gawande, R., Ioerger, T., ... Flynn, J. L. (2014, 1). Sterilization of granulomas is common in active and latent tuberculosis despite within-host variability in bacterial killing. *Nature Medicine*, *20*(1), 75–79. Retrieved from http://www.ncbi.nlm.nih.gov/pubmed/24336248http://www.pubmedcentral.nih.gov/articlerender.fcgi?artid=PMC3947310 doi: 10.1038/nm.3412

Liu, J., Gefen, O., Ronin, I., Bar-Meir, M., & Balaban, N. Q. (2020, 1). Effect of tolerance on the evolution of antibiotic resistance under drug combinations. *Science*, *367*(6474), 200–204. doi: 10.1126/science.aay3041

Liu, J., Shi, W., Zhang, S., Hao, X., Maslov, D. A., Shur, K. V., ... Zhang, Y. (2019). Mutations in Efflux Pump Rv1258c (Tap) Cause Resistance to Pyrazinamide, Isoniazid, and Streptomycin in M. tuberculosis. *Frontiers in Microbiology*, *10*(FEB). Retrieved from `/pmc/articles/PMC6389670//pmc/articles/PMC6389670/?report=abstracthttps://www.ncbi.nlm.nih.gov/pmc/articles/PMC6389670/` doi: 10.3389/FMICB.2019.00216

Liu, Y., Tan, S., Huang, L., Abramovitch, R. B., Rohde, K. H., Zimmerman, M. D., ... Russell, D. G. (2016). Immune activation of the host cell induces drug tolerance in Mycobacterium tuberculosis both in vitro and in vivo. *Journal of Experimental Medicine*, *213*(5), 809–825. doi: 10.1084/jem.20151248

Logsdon, M. M., Ho, P. Y., Papavinasasundaram, K., Richardson, K., Cokol, M., Sassetti, C. M., ... Aldridge, B. B. (2017, 11). A Parallel Adder Coordinates Mycobacterial Cell-Cycle Progression and Cell-Size Homeostasis in the Context of Asymmetric Growth and Organization. *Current biology : CB*, *27*(21), 3367–3374. Retrieved from `https://pubmed.ncbi.nlm.nih.gov/29107550/` doi: 10.1016/J.CUB.2017.09.046

Lopatkin, A. J., Stokes, J. M., Zheng, E. J., Yang, J. H., Takahashi, M. K., You, L., & Collins, J. J. (2019, 12). Bacterial metabolic state more accurately predicts antibiotic lethality than growth rate. *Nature microbiology*, *4*(12), 2109–2117. Retrieved from `https://pubmed.ncbi.nlm.nih.gov/31451773/` doi: 10.1038/S41564-019-0536-0

Lucas, M. C., Pryszcz, L. P., Medina, R., Milenkovic, I., Camacho, N., Marchand, V., ... Novoa, E. M. (2023, 4). Quantitative analysis of tRNA abundance and modifications by nanopore RNA sequencing. *Nature Biotechnology 2023*, 1–15. Retrieved from `https://www.nature.com/articles/s41587-023-01743-6` doi: 10.1038/s41587-023-01743-6

Luidalepp, H., Hallier, M., Felden, B., & Tenson, T. (2005). tmRNA Decreases the Bactericidal Activity of Aminoglycosides and the Susceptibility to Inhibitors of Cell Wall Synthesis. *http://dx.doi.org/10.4161/rna.2.2.2020*, *2*(2), 70–74. Retrieved from `https://www.tandfonline.com/doi/abs/10.4161/rna.2.2.2020` doi: 10.4161/RNA.2.2.2020

Magombedze, G., Dowdy, D., & Mulder, N. (2013). Latent Tuberculosis: Models, Computational Efforts and the Pathogen's Regulatory Mechanisms during Dormancy. *Frontiers in*

Bioengineering and Biotechnology, *1*. doi: 10.3389/fbioe.2013.00004

Maisonneuve, E., Castro-Camargo, M., & Gerdes, K. (2013, 8). (p)ppGpp controls bacterial persistence by stochastic induction of toxin-antitoxin activity. *Cell*, *154*(5), 1140. Retrieved from https://pubmed.ncbi.nlm.nih.gov/23993101/ doi: 10.1016/J.CELL.2013.07.048

Manina, G., Dhar, N., & McKinney, J. D. (2015). Stress and host immunity amplify mycobacterium tuberculosis phenotypic heterogeneity and induce nongrowing metabolically active forms. *Cell Host and Microbe*, *17*(1), 32–46. Retrieved from http://dx.doi.org/10.1016/j.chom.2014.11.016 doi: 10.1016/j.chom.2014.11.016

Manuse, S., Shan, Y., Canas-DuarteID, S. J., BakshiID, S., Sun, W.-S., MoriID, H., ... LewisID, K. (2021). Bacterial persisters are a stochastically formed subpopulation of low-energy cells. *PLOS Biology*, *19*(4), e3001194. doi: 10.1371/journal.pbio.3001194

Marathe, N., Nguyen, H. A., Alumasa, J. N., Kuzmishin Nagy, A. B., Vazquez, M., Dunham, C. M., & Keiler, K. C. (2023, 10). Antibiotic that inhibits trans -translation blocks binding of EF-Tu to tmRNA but not to tRNA . *mBio*, *14*(5). Retrieved from https://journals.asm.org/doi/10.1128/mbio.01461-23 doi: 10.1128/MBIO.01461-23/SUPPL{_}FILE/MBIO.01461-23-S0010.DOCX

McCune, R. M., Dineen, P. A., & Batten, J. C. (1956). The effect of antimicrobial drugs on an experimental staphylococcal infection in mice. *Annals of the New York Academy of Sciences*, *65*(3), 91–102. Retrieved from https://pubmed.ncbi.nlm.nih.gov/13363203/ doi: 10.1111/J.1749-6632.1956.TB36627.X

McDermott, W., McCune, R. M., & Tompsett, R. (1956, 8). Dynamics of antituberculous chemotherapy. *American review of tuberculosis*, *74*(2 Part 2), 100–108. Retrieved from https://pubmed.ncbi.nlm.nih.gov/13340169/ doi: 10.1164/ARTPD.1956.74.2-2.100

Michiels, J. E., Van den Bergh, B., Verstraeten, N., & Michiels, J. (2016, 11). Molecular mechanisms and clinical implications of bacterial persistence. *Drug Resistance Updates*, *29*, 76–89. doi: 10.1016/J.DRUP.2016.10.002

Minato, Y., Gohl, D. M., Thiede, J. M., Chacón, J. M., Harcombe, W. R., Maruyama, F., & Baughn, A. D. (2019, 6). Genomewide Assessment of Mycobacterium tuberculosis Conditionally Essential Metabolic Pathways . *mSystems*, *4*(4). Retrieved from /pmc/articles/PMC6593218//pmc/articles/PMC6593218/

?report=abstracthttps://www.ncbi.nlm.nih.gov/pmc/articles/PMC6593218/ doi: 10.1128/msystems.00070-19

Mohanty, B. K., & Kushner, S. R. (2000, 10). Polynucleotide phosphorylase functions both as a 3' right-arrow 5' exonuclease and a poly(A) polymerase in Escherichia coli. *Proceedings of the National Academy of Sciences of the United States of America*, *97*(22), 11966–11971. Retrieved from https://pubmed.ncbi.nlm.nih.gov/11035800/ doi: 10.1073/PNAS.220295997

Mohanty, B. K., & Kushner, S. R. (2007, 12). Ribonuclease P processes polycistronic tRNA transcripts in Escherichia coli independent of ribonuclease E. *Nucleic Acids Research*, *35*(22), 7614–7625. Retrieved from https://dx.doi.org/10.1093/nar/gkm917 doi: 10.1093/NAR/GKM917

Mohanty, B. K., & Kushner, S. R. (2010). Processing of the Escherichia coli leuX tRNA transcript, encoding tRNA Leu5 , requires either the 3 0 !5 0 exoribonuclease polynucleotide phosphorylase or RNase P to remove the Rho-independent transcription terminator. *Nucleic Acids Research*, *28*(2), 597–607. doi: 10.1093/nar/gkp997

Moore, S. D., & Sauer, R. T. (2007). The tmRNA system for translational surveillance and ribosome rescue. *Annual Review of Biochemistry*, *76*, 101–124. doi: 10.1146/ANNUREV.BIOCHEM.75.103004.142733

Moreillon, P., Tomasz, A., & Tomasz, A. (1988, 6). Penicillin Resistance and Defective Lysis in Clinical Isolates of Pneumococci: Evidence for Two Kinds of Antibiotic Pressure Operating in the Clinical Environment. *The Journal of Infectious Diseases*, *157*(6), 1150–1157. Retrieved from https://dx.doi.org/10.1093/infdis/157.6.1150 doi: 10.1093/INFDIS/157.6.1150

Morris, R. P., Nguyen, L., Gatfield, J., Visconti, K., Nguyen, K., Schnappinger, D., ... Thompson, C. J. (2005, 8). Ancestral antibiotic resistance in Mycobacterium tuberculosis. *Proceedings of the National Academy of Sciences of the United States of America*, *102*(34), 12200–12205. Retrieved from https://pubmed.ncbi.nlm.nih.gov/16103351/ doi: 10.1073/PNAS.0505446102

Morscher, R. J., Ducker, G. S., Li, S. H. J., Mayer, J. A., Gitai, Z., Sperl, W., & Rabinowitz, J. D. (2018, 1). Mitochondrial translation requires folate-dependent tRNA methylation. *Nature 2018 554:7690*, *554*(7690), 128–132. Retrieved from https://www.nature.com/articles/nature25460 doi: 10.1038/nature25460

Motta, I., Boeree, M., Chesov, D., Dheda, K., Günther, G., Horsburgh, C. R., ... Guglielmetti, L. (2023, 7). Recent advances in the treatment of tuberculosis. *Clinical Microbiology and Infection*. doi: 10.1016/J.CMI.2023.07.013

Mouton, J. M., Helaine, S., Holden, D. W., & Sampson, S. L. (2016, 6). Elucidating population-wide mycobacterial replication dynamics at the single-cell level. *Microbiology*, *162*(6), 966. Retrieved from /pmc/articles/PMC5042079//pmc/articles/PMC5042079/?report=abstracthttps://www.ncbi.nlm.nih.gov/pmc/articles/PMC5042079/ doi: 10.1099/MIC.0.000288

Moyed, H. S., & Bertrand, K. P. (1983). hipA, a newly recognized gene of Escherichia coli K-12 that affects frequency of persistence after inhibition of murein synthesis. *Journal of Bacteriology*, *155*(2), 768–775. doi: 10.1128/jb.155.2.768-775.1983

Mulcahy, L. R., Burns, J. L., Lory, S., & Lewis, K. (2010, 12). Emergence of Pseudomonas aeruginosa strains producing high levels of persister cells in patients with cystic fibrosis. *Journal of Bacteriology*, *192*(23), 6191–6199. Retrieved from http://www.ncbi.nlm.nih.gov/pubmed/20935098http://www.pubmedcentral.nih.gov/articlerender.fcgi?artid=PMC2981199 doi: 10.1128/JB.01651-09

Murphy, K. C., Papavinasasundaram, K., & Sassetti, C. M. (2015). Mycobacterial recombineering. *Methods in molecular biology (Clifton, N.J.)*, *1285*, 177–199. Retrieved from https://pubmed.ncbi.nlm.nih.gov/25779316/ doi: 10.1007/978-1-4939-2450-9{_}10

Murray, C. J., Ikuta, K. S., Sharara, F., Swetschinski, L., Robles Aguilar, G., Gray, A., ... Naghavi, M. (2022, 2). Global burden of bacterial antimicrobial resistance in 2019: a systematic analysis. *The Lancet*, *399*(10325), 629–655. doi: 10.1016/S0140-6736(21)02724-0

Nash, K. A., Brown-Elliott, A. B., & Wallace, R. J. (2009, 4). A novel gene, erm(41), confers inducible macrolide resistance to clinical isolates of Mycobacterium abscessus but is absent from Mycobacterium chelonae. *Antimicrobial agents and chemotherapy*, *53*(4), 1367–1376. Retrieved from https://pubmed.ncbi.nlm.nih.gov/19171799/ doi: 10.1128/AAC.01275-08

Nedialkova, D. D., & Leidel, S. A. (2015, 6). Optimization of Codon Translation Rates via tRNA Modifications Maintains Proteome Integrity. *Cell*, *161*(7), 1606–1618. doi: 10.1016/

J.CELL.2015.05.022

Nguyen, D., Joshi-Datar, A., Lepine, F., Bauerle, E., Olakanmi, O., Beer, K., ... Singh, P. K. (2011, 11). Active starvation responses mediate antibiotic tolerance in biofilms and nutrient-limited bacteria. *Science (New York, N.Y.)*, *334*(6058), 982–986. Retrieved from https://pubmed.ncbi.nlm.nih.gov/22096200/ doi: 10.1126/SCIENCE.1211037

Nguyen, G. T., Green, E. R., & Mecsas, J. (2017, 8). Neutrophils to the ROScue: Mechanisms of NADPH Oxidase Activation and Bacterial Resistance. *Frontiers in cellular and infection microbiology*, *7*(AUG). Retrieved from https://pubmed.ncbi.nlm.nih.gov/28890882/ doi: 10.3389/FCIMB.2017.00373

O'Garra, A., Redford, P. S., McNab, F. W., Bloom, C. I., Wilkinson, R. J., & Berry, M. P. (2013). The Immune Response in Tuberculosis. *Annual Review of Immunology*, *31*(1), 475–527. doi: 10.1146/annurev-immunol-032712-095939

O'Neill, J. (2014). *Antimicrobial Resistance: Tackling a crisis for the health and wealth of nations* (Tech. Rep.). Wellcome Collection. Retrieved from https://wellcomecollection.org/works/rdpck35v

Ozanick, S. G., Wang, X., Costanzo, M., Brost, R. L., Boone, C., & Anderson, J. T. (2009, 1). Rex1p deficiency leads to accumulation of precursor initiator tRNAMet and polyadenylation of substrate RNAs in Saccharomyces cerevisiae. *Nucleic Acids Research*, *37*(1), 298–308. Retrieved from https://academic.oup.com/nar/article/37/1/298/1027231 doi: 10.1093/NAR/GKN925

Pai, M., Behr, M. A., Dowdy, D., Dheda, K., Divangahi, M., Boehme, C. C., ... Raviglione, M. (2016, 10). Tuberculosis. *Nature Reviews Disease Primers 2016 2:1*, *2*(1), 1–23. Retrieved from https://www.nature.com/articles/nrdp201676 doi: 10.1038/nrdp.2016.76

Patterson, B., & Wood, R. (2019, 7). Is cough really necessary for TB transmission? *Tuberculosis (Edinburgh, Scotland)*, *117*, 31. Retrieved from /pmc/articles/PMC6688829//pmc/articles/PMC6688829/?report=abstracthttps://www.ncbi.nlm.nih.gov/pmc/articles/PMC6688829/ doi: 10.1016/J.TUBE.2019.05.003

Personne, Y., & Parish, T. (2014, 1). Mycobacterium tuberculosis possesses an unusual tmRNA rescue system. *Tuberculosis*, *94*(1), 34–42. doi: 10.1016/J.TUBE.2013.09.007

Peyron, P., Vaubourgeix, J., Poquet, Y., Levillain, F., Botanch, C., Bardou, F., ... Altare, F. (2008). Foamy Macrophages from Tuberculous Patients' Granulomas Constitute a Nutrient-Rich Reservoir for M. tuberculosis Persistence. *PLOS Pathogens*, *4*(11),

e1000204. doi: 10.1371/JOURNAL.PPAT.1000204

Pisu, D., Huang, L., Grenier, J. K., & Russell, D. G. (2020). Dual RNA-Seq of Mtb-Infected Macrophages In Vivo Reveals Ontologically Distinct Host-Pathogen Interactions. *Cell Reports*, *30*(2), 335–350. Retrieved from https://doi.org/10.1016/j.celrep.2019.12.033 doi: 10.1016/j.celrep.2019.12.033

Płociński, P., MacIos, M., Houghton, J., Niemiec, E., Płocińska, R., Brzostek, A., ... Dziembowski, A. (2019, 6). Proteomic and transcriptomic experiments reveal an essential role of RNA degradosome complexes in shaping the transcriptome of Mycobacterium tuberculosis. *Nucleic Acids Research*, *47*(11), 5892. Retrieved from /pmc/articles/PMC6582357//pmc/articles/PMC6582357/?report=abstracthttps://www.ncbi.nlm.nih.gov/pmc/articles/PMC6582357/ doi: 10.1093/NAR/GKZ251

Pontes, M. H., & Groisman, E. A. (2019, 7). Slow growth determines nonheritable antibiotic resistance in Salmonella enterica. *Science Signaling*, *12*(592), 3938. doi: 10.1126/scisignal.aax3938

Poulton, N. C., DeJesus, M. A., Munsamy-Govender, V., Roberts, C. G., Azadian, Z. A., Bosch, B., ... Rock, J. M. (2023, 6). Beyond antibiotic resistance: the whiB7 transcription factor coordinates an adaptive response to alanine starvation in mycobacteria. *bioRxiv : the preprint server for biology*. Retrieved from https://pubmed.ncbi.nlm.nih.gov/37333137/http://www.pubmedcentral.nih.gov/articlerender.fcgi?artid=PMC10274678 doi: 10.1101/2023.06.02.543512

Prossliner, T., Agrawal, S., Heidemann, D. F., Sørensen, M. A., & Svenningsen, S. L. (2023, 1). tRNAs Are Stable After All: Pitfalls in Quantification of tRNA from Starved Escherichia coli Cultures Exposed by Validation of RNA Purification Methods. *mBio*, *14*(1). Retrieved from https://pubmed.ncbi.nlm.nih.gov/36598190/ doi: 10.1128/MBIO.02805-22

Prusa, J., Zhu, D. X., & Stallings, C. L. (2018, 7). The stringent response and Mycobacterium tuberculosis pathogenesis. *Pathogens and disease*, *76*(5). Retrieved from https://pubmed.ncbi.nlm.nih.gov/29947752/ doi: 10.1093/FEMSPD/FTY054

Quendera, A. P., Pinto, S. N., Pobre, V., Antunes, W., Bonifácio, V. D., Arraiano, C. M., & Andrade, J. M. (2023, 12). The ribonuclease PNPase is a key regulator of biofilm formation in Listeria monocytogenes and af-

fects invasion of host cells. *NPJ Biofilms and Microbiomes*, *9*(1). Retrieved from /pmc/articles/PMC10247797//pmc/articles/PMC10247797/?report=abstracthttps://www.ncbi.nlm.nih.gov/pmc/articles/PMC10247797/ doi: 10.1038/S41522-023-00397-1

Radzikowski, J. L., Vedelaar, S., Siegel, D., Ortega, D., Schmidt, A., & Heinemann, M. (2016, 9). Bacterial persistence is an active σS stress response to metabolic flux limitation. *Molecular Systems Biology*, *12*(9), 882. Retrieved from /pmc/articles/PMC5043093//pmc/articles/PMC5043093/?report=abstracthttps://www.ncbi.nlm.nih.gov/pmc/articles/PMC5043093/ doi: 10.15252/MSB.20166998

Ramadoss, N. S., Alumasa, J. N., Cheng, L., Wang, Y., Li, S., Chambers, B. S., ... Keiler, K. C. (2013, 6). Small molecule inhibitors of trans-translation have broad-spectrum antibiotic activity. *Proceedings of the National Academy of Sciences of the United States of America*, *110*(25), 10282–10287. Retrieved from /pmc/articles/PMC3690859//pmc/articles/PMC3690859/?report=abstracthttps://www.ncbi.nlm.nih.gov/pmc/articles/PMC3690859/ doi: 10.1073/PNAS.1302816110/-/DCSUPPLEMENTAL

Ramón-García, S., Ng, C., Jensen, P. R., Dosanjh, M., Burian, J., Morris, R. P., ... Thompson, C. J. (2013, 11). WhiB7, an Fe-S-dependent Transcription Factor That Activates Species-specific Repertoires of Drug Resistance Determinants in Actinobacteria. *The Journal of Biological Chemistry*, *288*(48), 34514. Retrieved from /pmc/articles/PMC3843066//pmc/articles/PMC3843066/?report=abstracthttps://www.ncbi.nlm.nih.gov/pmc/articles/PMC3843066/ doi: 10.1074/JBC.M113.516385

Reeves, A. Z., Campbell, P. J., Sultana, R., Malik, S., Murray, M., Plikaytis, B. B., ... Posey, J. E. (2013, 4). Aminoglycoside cross-resistance in Mycobacterium tuberculosis due to mutations in the 5 untranslated region of whiB7. *Antimicrobial Agents and Chemotherapy*, *57*(4), 1857–1865. Retrieved from https://journals.asm.org/doi/10.1128/aac.02191-12 doi: 10.1128/AAC.02191-12/SUPPL{_}FILE/ZAC999101731SO1.PDF

Rhen, M. (2019, 4). Salmonella and Reactive Oxygen Species: A Love-Hate Relationship. *Journal of innate immunity*, *11*(3), 216–226. Retrieved from https://pubmed.ncbi.nlm.nih.gov/30943492/ doi: 10.1159/000496370

Rittershaus, E. S., Baek, S. H., & Sassetti, C. M. (2013, 6). *The normalcy of dormancy: Common themes in microbial quiescence* (Vol. 13) (No. 6). Cell Press. doi: 10.1016/j.chom.2013.05.012

Riva, M. A. (2014, 8). From milk to rifampicin and back again: history of failures and successes in the treatment for tuberculosis. *The Journal of Antibiotics 2014 67:9*, *67*(9), 661–665. Retrieved from https://www.nature.com/articles/ja2014108 doi: 10.1038/ja.2014.108

Robson, J., McKenzie, J. L., Cursons, R., Cook, G. M., & Arcus, V. L. (2009, 7). The vapBC Operon from Mycobacterium smegmatis Is An Autoregulated Toxin–Antitoxin Module That Controls Growth via Inhibition of Translation. *Journal of Molecular Biology*, *390*(3), 353–367. doi: 10.1016/J.JMB.2009.05.006

Rojas, A. M., Ehrenberg, M., Andersson, S. G., & Kurland, C. G. (1984, 10). ppGpp inhibition of elongation factors Tu, G and Ts during polypeptide synthesis. *Molecular & general genetics : MGG*, *197*(1), 36–45. Retrieved from https://pubmed.ncbi.nlm.nih.gov/6392824/ doi: 10.1007/BF00327920

Ronneau, S., & Helaine, S. (2019, 8). *Clarifying the Link between Toxin–Antitoxin Modules and Bacterial Persistence* (Vol. 431) (No. 18). Academic Press. doi: 10.1016/j.jmb.2019.03.019

Ronneau, S., Michaux, C., & Helaine, S. (2023, 6). Decline in nitrosative stress drives antibiotic persister regrowth during infection. *Cell Host & Microbe*, *31*(6), 993–1006. doi: 10.1016/J.CHOM.2023.05.002

Rowe, S. E., Wagner, N. J., Li, L., Beam, J. E., Wilkinson, A. D., Radlinski, L. C., ... Conlon, B. P. (2020, 2). Reactive oxygen species induce antibiotic tolerance during systemic Staphylococcus aureus infection. *Nature microbiology*, *5*(2), 282. Retrieved from /pmc/articles/PMC6992501//pmc/articles/PMC6992501/?report=abstracthttps://www.ncbi.nlm.nih.gov/pmc/articles/PMC6992501/ doi: 10.1038/S41564-019-0627-Y

Rustad, T. R., Harrell, M. I., Liao, R., & Sherman, D. R. (2008, 1). The enduring hypoxic response of Mycobacterium tuberculosis. *PloS one*, *3*(1). Retrieved from https://pubmed.ncbi.nlm.nih.gov/18231589/ doi: 10.1371/JOURNAL.PONE.0001502

Safi, H., Gopal, P., Lingaraju, S., Ma, S., Levine, C., Dartois, V., ... Alland, D. (2019, 9). Phase variation in Mycobacterium tuberculosis glpK produces transiently heritable

drug tolerance. *Proceedings of the National Academy of Sciences of the United States of America*, *116*(39), 19665–19674. Retrieved from https://pubmed.ncbi.nlm.nih.gov/31488707/ doi: 10.1073/PNAS.1907631116

Saikia, M., Fu, Y. E., Pavon-Eternod, M., He, C., & Pan, T. (2010). Genome wide analysis of N 1-methyl-adenosine modification in human tRNAs. *RNA*, *16*(7), 1317–1327. doi: 10.1261/rna.2057810

Sala, A., Bordes, P., & Genevaux, P. (2014, 3). Multiple Toxin-Antitoxin Systems in Mycobacterium tuberculosis. *Toxins*, *6*(3), 1002. Retrieved from /pmc/articles/PMC3968373//pmc/articles/PMC3968373/?report=abstracthttps://www.ncbi.nlm.nih.gov/pmc/articles/PMC3968373/ doi: 10.3390/TOXINS6031002

Salzer, A., & Wolz, C. (2023, 1). Role of (p)ppGpp in antibiotic resistance, tolerance, persistence and survival in Firmicutes. *microLife*, *4*, 1–12. Retrieved from https://dx.doi.org/10.1093/femsml/uqad009 doi: 10.1093/FEMSML/UQAD009

Sassetti, C. M., Boyd, D. H., & Rubin, E. J. (2003, 4). Genes required for mycobacterial growth defined by high density mutagenesis. *Molecular microbiology*, *48*(1), 77–84. Retrieved from https://pubmed.ncbi.nlm.nih.gov/12657046/ doi: 10.1046/J.1365-2958.2003.03425.X

Sawyer, E. B., Grabowska, A. D., & Cortes, T. (2018). Survey and summary: Translational regulation in mycobacteria and its implications for pathogenicity. *Nucleic Acids Research*, *46*(14), 6950–6961. doi: 10.1093/nar/gky574

Schaffer, A. E., Pinkard, O., & Coller, J. M. (2019, 8). tRNA Metabolism and Neurodevelopmental Disorders. *https://doi.org/10.1146/annurev-genom-083118-015334*, *20*, 359–387. Retrieved from https://www.annualreviews.org/doi/abs/10.1146/annurev-genom-083118-015334 doi: 10.1146/ANNUREV-GENOM-083118-015334

Scherrer, R., & Moyed, H. S. (1988). Conditional impairment of cell division and altered lethality in hipA mutants of Escherichia coli K-12. *Journal of Bacteriology*, *170*(8), 3321. Retrieved from /pmc/articles/PMC211297/?report=abstracthttps://www.ncbi.nlm.nih.gov/pmc/articles/PMC211297/ doi: 10.1128/JB.170.8.3321-3326.1988

Schnappinger, D., Ehrt, S., Voskuil, M. I., Liu, Y., Mangan, J. A., Monahan, I. M., ... Schoolnik, G. K. (2003). Transcriptional Adaptation of Mycobacterium tuberculosis within Macrophages: Insights into the Phagosomal Environment. *The Journal of Experimental Medicine J. Exp. Med. The*, *198*(5), 693–704. Retrieved from http://www.jem.org/

cgi/doi/10.1084/jem.20030846 doi: 10.1084/jem.20030846

Schrader, S. M., Botella, H., Jansen, R., Ehrt, S., Rhee, K., Nathan, C., & Vaubourgeix, J. (2021, 8). Multiform antimicrobial resistance from a metabolic mutation. *Science Advances*, *7*(35), eabh2037. Retrieved from https://advances.sciencemag.org/lookup/doi/10.1126/sciadv.abh2037 doi: 10.1126/SCIADV.ABH2037

Schrader, S. M., Botella, H., & Vaubourgeix, J. (2023, 4). Reframing antimicrobial resistance as a continuous spectrum of manifestations. *Current Opinion in Microbiology*, *72*, 102259. doi: 10.1016/J.MIB.2022.102259

Schrader, S. M., Vaubourgeix, J., & Nathan, C. (2020, 6). Biology of antimicrobial resistance and approaches to combat it. *Science translational medicine*, *12*(549). Retrieved from /pmc/articles/PMC8177555//pmc/articles/PMC8177555/?report=abstracthttps://www.ncbi.nlm.nih.gov/pmc/articles/PMC8177555/ doi: 10.1126/SCITRANSLMED.AAZ6992

Schumacher, M. A., Piro, K. M., Xu, W., Hansen, S., Lewis, K., & Brennan, R. G. (2009, 1). Molecular Mechanisms of HipA Mediated Multidrug Tolerance and its Neutralization by HipB. *Science (New York, N.Y.)*, *323*(5912), 396. Retrieved from /pmc/articles/PMC2764309//pmc/articles/PMC2764309/?report=abstracthttps://www.ncbi.nlm.nih.gov/pmc/articles/PMC2764309/ doi: 10.1126/SCIENCE.1163806

Sebastian, J., Swaminath, S., Nair, R. R., Jakkala, K., Pradhan, A., & Ajitkumar, P. (2017, 2). De novo emergence of genetically resistant mutants of Mycobacterium tuberculosis from the persistence phase cells formed against antituberculosis drugs in vitro. *Antimicrobial Agents and Chemotherapy*, *61*(2). doi: 10.1128/AAC.01343-16

Siegfried, N. A., Busan, S., Rice, G. M., Nelson, J. A., & Weeks, K. M. (2014, 9). RNA motif discovery by SHAPE and mutational profiling (SHAPE-MaP). *Nature methods*, *11*(9), 959. Retrieved from /pmc/articles/PMC4259394//pmc/articles/PMC4259394/?report=abstracthttps://www.ncbi.nlm.nih.gov/pmc/articles/PMC4259394/ doi: 10.1038/NMETH.3029

Sim, S., & Wolin, S. L. (2018, 7). Bacterial Y RNAs: Gates, Tethers and tRNA Mimics. *Microbiology spectrum*, *6*(4). Retrieved from /pmc/articles/PMC6047535//pmc/articles/PMC6047535/?report=abstracthttps://www.ncbi.nlm.nih.gov/pmc/articles/PMC6047535/ doi: 10.1128/MICROBIOLSPEC.RWR-0023-2018

Sinha, P., Gupta, A., Prakash, P., Anupurba, S., Tripathi, R., & Srivastava, G. N. (2016, 12). Differentiation of Mycobacterium tuberculosis complex from non-tubercular mycobacteria by nested multiplex PCR targeting IS6110, MTP40 and 32kD alpha antigen encoding gene fragments. *BMC Infectious Diseases*, *16*(1), 123. Retrieved from http://www.biomedcentral.com/1471-2334/16/123 doi: 10.1186/s12879-016-1450-1

Skinner, R., Cundliffe, E., & Schmidt, F. J. (1983, 10). Site of action of a ribosomal RNA methylase responsible for resistance to erythromycin and other antibiotics. *Journal of Biological Chemistry*, *258*(20), 12702–12706. doi: 10.1016/S0021-9258(17)44232-3

Slattery, A., Victorsen, A. H., Brown, A., Hillman, K., & Phillips, G. J. (2013, 2). Isolation of highly persistent mutants of Salmonella enterica serovar typhimurium reveals a new toxin-antitoxin module. *Journal of bacteriology*, *195*(4), 647–657. Retrieved from https://pubmed.ncbi.nlm.nih.gov/23204462/ doi: 10.1128/JB.01397-12

Smith, B. A., Gupta, N., Denny, K., & Culver, G. M. (2018, 6). Characterization of 16S rRNA Processing with Pre-30S Subunit Assembly Intermediates from E. coli. *Journal of Molecular Biology*, *430*(12), 1745–1759. doi: 10.1016/J.JMB.2018.04.009

Sparks, I. L., Derbyshire, K. M., Jacobs, W. R., & Morita, Y. S. (2023, 1). Mycobacterium smegmatis: The Vanguard of Mycobacterial Research. *Journal of Bacteriology*, *205*(1). Retrieved from /pmc/articles/PMC9879119//pmc/articles/PMC9879119/?report=abstracthttps://www.ncbi.nlm.nih.gov/pmc/articles/PMC9879119/ doi: 10.1128/JB.00337-22

Stapels, D. A. C., Hill, P. W. S., Westermann, A. J., Fisher, R. A., Thurston, T. L., Saliba, A.-E., ... Helaine, S. (2018, 12). Salmonella persisters undermine host immune defenses during antibiotic treatment. *Science (New York, N.Y.)*, *362*(6419), 1156–1160. Retrieved from http://www.ncbi.nlm.nih.gov/pubmed/30523110 doi: 10.1126/science.aat7148

Stein, A. J., Fuchs, G., Fu, C., Wolin, S. L., & Reinisch, K. M. (2005, 5). Structural insights into RNA quality control: The Ro autoantigen binds misfolded RNAs via its central cavity. *Cell*, *121*(4), 529. Retrieved from /pmc/articles/PMC1769319//pmc/articles/PMC1769319/?report=abstracthttps://www.ncbi.nlm.nih.gov/pmc/articles/PMC1769319/ doi: 10.1016/J.CELL.2005.03.009

Stekel, D. (2018, 10). First report of antimicrobial resistance pre-dates penicillin. *Nature*, *562*(7726), 192. doi: 10.1038/D41586-018-06983-0

Stepanyan, K., Wenseleers, T., Duéñez-Guzmán, E. A., Muratori, F., Van Den Bergh,

B., Verstraeten, N., ... Michiels, J. (2015, 4). Fitness trade-offs explain low levels of persister cells in the opportunistic pathogen Pseudomonas aeruginosa. *Molecular Ecology*, *24*(7), 1572–1583. Retrieved from https://onlinelibrary.wiley.com/doi/full/10.1111/mec.13127https://onlinelibrary.wiley.com/doi/abs/10.1111/mec.13127https://onlinelibrary.wiley.com/doi/10.1111/mec.13127 doi: 10.1111/MEC.13127

Stokes, J. M., Lopatkin, A. J., Lobritz, M. A., & Collins, J. J. (2019, 8). Bacterial Metabolism and Antibiotic Efficacy. *Cell Metabolism*, *30*(2), 251. Retrieved from /pmc/articles/PMC6990394//pmc/articles/PMC6990394/?report=abstracthttps://www.ncbi.nlm.nih.gov/pmc/articles/PMC6990394/ doi: 10.1016/J.CMET.2019.06.009

Stsiapanava, A., & Selmer, M. (2019, 12). Crystal structure of ErmE - 23S rRNA methyltransferase in macrolide resistance. *Scientific reports*, *9*(1). Retrieved from https://pubmed.ncbi.nlm.nih.gov/31601908/ doi: 10.1038/S41598-019-51174-0

Sulaiman, J. E., & Lam, H. (2021, 2). Evolution of Bacterial Tolerance Under Antibiotic Treatment and Its Implications on the Development of Resistance. *Frontiers in microbiology*, *12*. Retrieved from https://pubmed.ncbi.nlm.nih.gov/33717007/ doi: 10.3389/FMICB.2021.617412

Tejada-Arranz, A., de Crécy-Lagard, V., & de Reuse, H. (2020, 1). Bacterial RNA Degradosomes: Molecular Machines under Tight Control. *Trends in Biochemical Sciences*, *45*(1), 42–57. doi: 10.1016/J.TIBS.2019.10.002

Tenson, T., Lovmar, M., & Ehrenberg, M. (2003, 7). The mechanism of action of macrolides, lincosamides and streptogramin B reveals the nascent peptide exit path in the ribosome. *Journal of Molecular Biology*, *330*(5), 1005–1014. Retrieved from https://pubmed.ncbi.nlm.nih.gov/12860123/ doi: 10.1016/S0022-2836(03)00662-4

Tomasz, A., Albino, A., & Zanati, E. (1970). Multiple Antibiotic Resistance in a Bacterium with Suppressed Autolytic System. *Nature 1970 227:5254*, *227*(5254), 138–140. Retrieved from https://www.nature.com/articles/227138a0 doi: 10.1038/227138a0

Toprak, E., Veres, A., Michel, J. B., Chait, R., Hartl, D. L., & Kishony, R. (2011, 12). Evolutionary paths to antibiotic resistance under dynamically sustained drug selection. *Nature Genetics 2011 44:1*, *44*(1), 101–105. Retrieved from https://www.nature.com/articles/ng.1034 doi: 10.1038/ng.1034

Torrey, H. L., Keren, I., Via, L. E., Lee, J. S., & Lewis, K. (2016, 5). High Persister Mutants in Mycobacterium tuberculosis. *PLoS ONE*, *11*(5). Retrieved from /pmc/articles/PMC4866775//pmc/articles/PMC4866775/?report=abstracthttps://www.ncbi.nlm.nih.gov/pmc/articles/PMC4866775/ doi: 10.1371/JOURNAL.PONE.0155127

Treatment of Pulmonary Tuberculosis with Streptomycin and Para-Amino-Salicylic Acid: A Medical Research Council Investigation. (1950, 11). *British Medical Journal*, *2*(4688), 1073. Retrieved from https://www.ncbi.nlm.nih.gov/pmc/articles/PMC2039351/ doi: 10.1136/bmj.2.4688.1073

Tripathi, A., Dewan, P. C., Siddique, S. A., & Varadarajan, R. (2014, 2). MazF-induced growth inhibition and persister generation in escherichia coli. *Journal of Biological Chemistry*, *289*(7), 4191–4205. Retrieved from http://www.jbc.org/article/S0021925820442036/fulltexthttp://www.jbc.org/article/S0021925820442036/abstracthttps://www.jbc.org/article/S0021-9258(20)44203-6/abstract doi: 10.1074/jbc.M113.510511

Tuomanen, E., Cozens, R., Tosch, W., Zak, O., & Tomasz, A. (1986). The rate of killing of Escherichia coli by β-lactam antibiotics is strictly proportional to the rate of bacterial growth. *Journal of General Microbiology*, *132*(5), 1297–1304. doi: 10.1099/00221287-132-5-1297

Ude, S., Lassak, J., Starosta, A. L., Kraxenberger, T., Wilson, D. N., & Jung, K. (2013, 1). Translation elongation factor EF-P alleviates ribosome stalling at polyproline stretches. *Science*, *339*(6115), 82–85. Retrieved from https://www.science.org/doi/10.1126/science.1228985 doi: 10.1126/SCIENCE.1228985/SUPPL{_}FILE/UDE.SM.PDF

Van Acker, H., Sass, A., Bazzini, S., De Roy, K., Udine, C., Messiaen, T., ... Coenye, T. (2013, 3). Biofilm-Grown Burkholderia cepacia Complex Cells Survive Antibiotic Treatment by Avoiding Production of Reactive Oxygen Species. *PLOS ONE*, *8*(3), e58943. Retrieved from https://journals.plos.org/plosone/article?id=10.1371/journal.pone.0058943 doi: 10.1371/JOURNAL.PONE.0058943

van den Bergh, B., Fauvart, M., & Michiels, J. (2017, 5). Formation, physiology, ecology, evolution and clinical importance of bacterial persisters. *FEMS Microbiology Reviews*, *41*(3), 219–251. Retrieved from https://dx.doi.org/10.1093/femsre/fux001 doi: 10.1093/FEMSRE/FUX001

Van Den Bergh, B., Michiels, J. E., Wenseleers, T., Windels, E. M., Boer, P. V., Kestemont, D., ... Michiels, J. (2016, 3). Frequency of antibiotic application drives rapid evolutionary adaptation of Escherichia coli persistence. *Nature microbiology*, *1*(5). Retrieved from https://pubmed.ncbi.nlm.nih.gov/27572640/ doi: 10.1038/NMICROBIOL.2016.20

Vani, B. R., Ramakrishnan, T., Taya, Y., Noguchi, S., Yamaizumi, Z., & Nishimura, S. (1979). Occurrence of 1-methyladenosine and absence of ribothymidine in transfer ribonucleic acid of Mycobacterium smegmatis. *Journal of Bacteriology*, *137*(3), 1084. Retrieved from /pmc/articles/PMC218285/?report=abstracthttps://www.ncbi.nlm.nih.gov/pmc/articles/PMC218285/ doi: 10.1128/JB.137.3.1084-1087.1979

Various combinations of isoniazid with streptomycin or with P.A.S. in the treatment of pulmonary tuberculosis; seventh report to the Medical Research Council by their Tuberculosis Chemotherapy Trials Committee. (1955, 2). *British medical journal*, *1*(4911), 435–45. Retrieved from http://www.ncbi.nlm.nih.gov/pubmed/13230514http://www.pubmedcentral.nih.gov/articlerender.fcgi?artid=PMC2061210http://www.ncbi.nlm.nih.gov/pubmed/13230514%0Ahttp://www.pubmedcentral.nih.gov/articlerender.fcgi?artid=PMC2061210

Varshney, U., Lee, C. P., & RajBhandary, U. L. (1991, 12). Direct analysis of aminoacylation levels of tRNAs in vivo. Application to studying recognition of Escherichia coli initiator tRNA mutants by glutaminyl-tRNA synthetase. *Journal of Biological Chemistry*, *266*(36), 24712–24718. doi: 10.1016/S0021-9258(18)54288-5

Varshney, U., Ramesh, V., Madabushi, A., Gaur, R., Subramanya, H. S., & RajBhandary, U. L. (2004). Mycobacterium tuberculosis Rv2118c codes for a single-component homotetrameric m1A58 tRNA methyltransferase. *Nucleic Acids Research*, *32*(3), 1018. Retrieved from /pmc/articles/PMC373377//pmc/articles/PMC373377/?report=abstracthttps://www.ncbi.nlm.nih.gov/pmc/articles/PMC373377/ doi: 10.1093/NAR/GKH207

Verstraete, L., Van den Bergh, B., Verstraeten, N., & Michiels, J. (2022, 5). Ecology and evolution of antibiotic persistence. *Trends in Microbiology*, *30*(5), 466–479. doi: 10.1016/J.TIM.2021.10.001

Verstraeten, N., Gkekas, S., Kint, C. I., Deckers, B., Van den Bergh, B., Herpels, P., ... Versées, W. (2019, 11). Biochemical determinants of ObgE-mediated persistence. *Molecular Microbiology*, *112*(5), 1593–1608. Retrieved from https://onlinelibrary.wiley.com/

doi/abs/10.1111/mmi.14382 doi: 10.1111/mmi.14382

Verstraeten, N., Knapen, W. J., Kint, C. I., Liebens, V., Van den Bergh, B., Dewachter, L., ... Michiels, J. (2015, 7). Obg and Membrane Depolarization Are Part of a Microbial Bet-Hedging Strategy that Leads to Antibiotic Tolerance. *Molecular Cell*, *59*(1), 9–21. doi: 10.1016/J.MOLCEL.2015.05.011

Viducic, D., Ono, T., Murakami, K., Susilowati, H., Kayama, S., Hirota, K., & Miyake, Y. (2006). Functional analysis of spoT, relA and dksA genes on quinolone tolerance in Pseudomonas aeruginosa under nongrowing condition. *Microbiology and immunology*, *50*(4), 349–357. Retrieved from https://pubmed.ncbi.nlm.nih.gov/16625057/ doi: 10.1111/J.1348-0421.2006.TB03793.X

Vinogradova, D. S., Zegarra, V., Maksimova, E., Nakamoto, J. A., Kasatsky, P., Paleskava, A., ... Milón, P. (2020). How the initiating ribosome copes with ppGpp to translate mRNAs. *PLOS Biology*, *18*(1), e3000593. doi: 10.1371/JOURNAL.PBIO.3000593

Vogel, J., Argaman, L., Wagner, E. G. H., & Altuvia, S. (2004, 12). The small RNA IstR inhibits synthesis of an SOS-induced toxic peptide. *Current biology : CB*, *14*(24), 2271–2276. Retrieved from https://pubmed.ncbi.nlm.nih.gov/15620655/ doi: 10.1016/J.CUB.2004.12.003

Vynnycky, E., & Fine, P. E. (1997, 10). The natural history of tuberculosis: the implications of age-dependent risks of disease and the role of reinfection. *Epidemiology and infection*, *119*(2), 183–201. Retrieved from https://pubmed.ncbi.nlm.nih.gov/9363017/https://pubmed.ncbi.nlm.nih.gov/9363017/?dopt=Abstract doi: 10.1017/S0950268897007917

Wakamoto, Y., Dhar, N., Chait, R., Schneider, K., Signorino-Gelo, F., Leibler, S., & McKinney, J. D. (2013, 1). Dynamic persistence of antibiotic-stressed mycobacteria. *Science*, *339*(6115), 91–95. doi: 10.1126/science.1229858

Wang, T., El Meouche, I., & Dunlop, M. J. (2017, 3). Bacterial persistence induced by salicylate via reactive oxygen species. *Scientific reports*, *7*. Retrieved from https://pubmed.ncbi.nlm.nih.gov/28281556/ doi: 10.1038/SREP43839

Warit, S., Phunpruch, S., Jityam, C., Jaitrong, S., Billamas, P., Chaiprasert, A., ... Prammananan, T. (2015, 12). Genetic characterisation of a whiB7 mutant of a Mycobacterium tuberculosis clinical strain. *Journal of Global Antimicrobial Resistance*, *3*(4), 262–266. doi: 10.1016/J.JGAR.2015.07.004

Watanabe, K., Shinma, M., Oshima, T., & Nishimura, S. (1976, 10). Heat-induced stability of tRNA from an extreme thermophile, Thermus thermophilus. *Biochemical and biophysical research communications*, *72*(3), 1137–1144. Retrieved from https://pubmed.ncbi.nlm.nih.gov/985514/ doi: 10.1016/S0006-291X(76)80250-1

WHO. (2022). *Global Tuberculosis Report 2022.* Retrieved from https://www.who.int/teams/global-tuberculosis-programme/tb-reports

WHO. (2023, 11). *Global Tuberculosis Report 2023.* Retrieved from https://www.who.int/teams/global-tuberculosis-programme/tb-reports/global-tuberculosis-report-2023

Willenborg, J., Willms, D., Bertram, R., Goethe, R., & Valentin-Weigand, P. (2014, 5). Characterization of multi-drug tolerant persister cells in Streptococcus suis. *BMC microbiology*, *14*(1). Retrieved from https://pubmed.ncbi.nlm.nih.gov/24885389/ doi: 10.1186/1471-2180-14-120

Wilmaerts, D., Focant, C., Matthay, P., & Michiels, J. (2022). Transcription-coupled DNA repair underlies variation in persister awakening and the emergence of resistance Graphical abstract. *CellReports*, *38*, 110427. Retrieved from https://doi.org/10.1016/j.celrep.2022.110427 doi: 10.1016/j.celrep.2022.110427

Windels, E. M., Michiels, J. E., Fauvart, M., Wenseleers, T., Bram Van Den Bergh, & Michiels, J. (2019). Bacterial persistence promotes the evolution of antibiotic resistance by increasing survival and mutation rates. *The ISME Journal*, *13*, 1239–1251. Retrieved from https://doi.org/10.1038/s41396-019-0344-9 doi: 10.1038/s41396-019-0344-9

Windels, E. M., Van Den Bergh, B., & Michiels, J. (2020, 5). Bacteria under antibiotic attack: Different strategies for evolutionary adaptation. *PLoS Pathogens*, *16*(5). Retrieved from /pmc/articles/PMC7205213//pmc/articles/PMC7205213/?report=abstracthttps://www.ncbi.nlm.nih.gov/pmc/articles/PMC7205213/ doi: 10.1371/JOURNAL.PPAT.1008431

Winther, K. S., & Gerdes, K. (2011, 5). Enteric virulence associated protein VapC inhibits translation by cleavage of initiator tRNA. *Proceedings of the National Academy of Sciences of the United States of America*, *108*(18), 7403–7407. Retrieved from https://www.pnas.org/doi/abs/10.1073/pnas.1019587108 doi: 10.1073/PNAS.1019587108/SUPPL{_}FILE/PNAS.1019587108{_}SI.PDF

Wolf, A. J., Desvignes, L., Linas, B., Banaiee, N., Tamura, T., Takatsu, K., & Ernst, J. D. (2008,

1). Initiation of the adaptive immune response to Mycobacterium tuberculosis depends on antigen production in the local lymph node, not the lungs. *Journal of Experimental Medicine*, *205*(1), 105–115. doi: 10.1084/jem.20071367

Wu, J., Jiang, Z., Liu, M., Gong, X., Wu, S., Burns, C. M., & Li, Z. (2009, 3). Polynucleotide phosphorylase protects escherichia coli against oxidative stress. *Biochemistry*, *48*(9), 2012–2020. Retrieved from https://pubs.acs.org/doi/abs/10.1021/bi801752p doi: 10.1021/BI801752P/ASSET/IMAGES/MEDIUM/BI-2008-01752P{_}0001.GIF

Wu, Y., Vulić, M., Keren, I., & Lewis, K. (2012, 9). Role of oxidative stress in persister tolerance. *Antimicrobial agents and chemotherapy*, *56*(9), 4922–4926. Retrieved from https://pubmed.ncbi.nlm.nih.gov/22777047/ doi: 10.1128/AAC.00921-12

Yamagami, R., Sieg, J. P., Assmann, S. M., & Bevilacqua, P. C. (2022, 6). Genome-wide analysis of the in vivo tRNA structurome reveals RNA structural and modification dynamics under heat stress. *Proceedings of the National Academy of Sciences of the United States of America*, *119*(25), e2201237119. Retrieved from https://www.pnas.org/doi/abs/10.1073/pnas.2201237119 doi: 10.1073/PNAS.2201237119/SUPPL{_}FILE/PNAS.2201237119.SD02.XLSX

Yang, Z., Zeng, X., & Tsui, S. K. W. (2019, 5). Investigating function roles of hypothetical proteins encoded by the Mycobacterium tuberculosis H37Rv genome. *BMC genomics*, *20*(1). Retrieved from https://pubmed.ncbi.nlm.nih.gov/31113361/ doi: 10.1186/S12864-019-5746-6

Yokoyama, S., Watanabe, K., & Miyazawa, T. (1987). Dynamic structures and functions of transfer ribonucleic acids from extreme thermophiles. *Advances in biophysics*, *23*(C), 115–147. Retrieved from https://pubmed.ncbi.nlm.nih.gov/2449804/ doi: 10.1016/0065-227X(87)90006-2

Zaffiri, L., Gardner, J., & Toledo-Pereyra, L. H. (2012, 4). History of Antibiotics. From Salvarsan to Cephalosporins. *http://dx.doi.org/10.3109/08941939.2012.664099*, *25*(2), 67–77. Retrieved from https://www.tandfonline.com/doi/abs/10.3109/08941939.2012.664099 doi: 10.3109/08941939.2012.664099

Zhang, Q., Lambert, G., Liao, D., Kim, H., Robin, K., Tung, C. K., ... Austin, R. H. (2011, 10). Acceleration of emergence of bacterial antibiotic resistance in connected microenvironments. *Science*, *333*(6050), 1764–1767. Retrieved from https://www.science.org/doi/10.1126/science.1208747 doi: 10.1126/SCIENCE.1208747/SUPPL{_}FILE/

ZHANG.SOM.PDF

Zhang, Y., Zborníková, E., Rejman, D., & Gerdes, K. (2018, 3). Novel (p)ppGpp Binding and Metabolizing Proteins of Escherichia coli. *mBio*, *9*(2). Retrieved from `https://pubmed.ncbi.nlm.nih.gov/29511080/` doi: 10.1128/MBIO.02188-17

Zheng, E. J., Andrews, I. W., Grote, A. T., Manson, A. L., Alcantar, M. A., Earl, A. M., & Collins, J. J. (2022, 5). Modulating the evolutionary trajectory of tolerance using antibiotics with different metabolic dependencies. *Nature Communications 2022 13:1*, *13*(1), 1–11. Retrieved from `https://www.nature.com/articles/s41467-022-30272-0` doi: 10.1038/s41467-022-30272-0

Zheng, E. J., Stokes, J. M., & Collins, J. J. (2020, 12). Eradicating Bacterial Persisters with Combinations of Strongly and Weakly Metabolism-Dependent Antibiotics. *Cell Chemical Biology*, *27*(12), 1544–1552. Retrieved from `http://www.cell.com/article/S2451945620303378/fulltexthttp://www.cell.com/article/S2451945620303378/abstracthttps://www.cell.com/cell-chemical-biology/abstract/S2451-9456(20)30337-8` doi: 10.1016/j.chembiol.2020.08.015

Zhu, J., Liu, Y. J., & Fortune, S. M. (2023, 4). Spatiotemporal perspectives on tuberculosis chemotherapy. *Current Opinion in Microbiology*, *72*, 102266. doi: 10.1016/J.MIB.2023.102266

Appendix

A Plasmids, primers, and strains used in this study

Table 6.1: Primers used in this study. F=forward, R=reverse

ID	Name	Nucleotide sequence (5' to 3')	F/R	Purpose
1	M13-F	GTAAAACGACGGCCAG	F	sequencing entry plasmids
2	seq-pGMCK-1	GGTTCCGCGCACATTTC	R	sequencing
3	1834	TTCCTGTGAAGAGCCAT TGATAATG	F	sequencing CRISPRi plasmid pLJR962
4	attB2_NP_MS3906_F	GGGGACAGCTTTCTTGT ACAAAGTGGCCGGTCG ATGGCGCGGAACCGGT ACAG	F	complementation
5	attB2_SD1a_MS3906_F	GGGGACAGCTTTCTTG TACAAAGTGGATCCAG GAGGTATCTCCGTGGC AGGAAACAGACCGACC GGGCCGTTC	F	complementation
6	attB3_MS3906_R	GGGGACAACTTTGTAT AATAAAGTTGCTAGAT CCCGCCGCCGATCTGAC	R	complementation
7	MS3906_G128S_F	TCGGCCCTGAGAGCAG CGTGACGTCC	F	internal primers for overlap extension mutagenesis
8	MS3906_G128S_R	AGGACGTCACGCTGCT CTCAGGGCCG	R	internal primers for overlap extension mutagenesis

Table 6.1 continued from previous page

9	clo-MS3906-HU-attB4	GGGGACAACTTTGTAT AGAAAAGTTGCCACGG CGTAGAACTTCATC	F	*mstrmI* KO
10	clo-MS3906-HU-attB1	GGGGACTGCTTTTTTG TACAAACTTGTCGGGC AATCCGATCACGTC	R	*mstrmI* KO
11	clo-MS3906-HD-attB3	GGGGACAACTTTGTAT AATAAAGTTGCCGAAT CGCAGTCCTGAGTG	R	*mstrmI* KO
12	clo-MS3906-HD-attB2	GGGGACAGCTTTCTTG TACAAAGTGGGCGTCG CAAACGTCAGATCG	F	*mstrmI* KO
13	Verif_MS3906_F	CTGGATGGCCTTCCAG ATCG	F	*mstrmI* KO verification
14	Verif_MS3906_R	CCGGTTGGCAGATCTC GAAG	R	*mstrmI* KO verification
15	Verif_MS3906_mid_F	GCGTCGTCAAGTCCAC CAAC	F	*mstrmI* KO verification
16	Verif_MS3906_mid_R	GTGGCGACGTAGATCA TCAG	R	*mstrmI* KO verification
17	attB3_MS3906_HA_R	GGGGACAACTTTGTAT AATAAAGTTGCTAGGC ATAGTCCGGGACGTCA TACGGATAGATCCCGC CGCCGATCTGAC	R	3' HA tag
18	clo-MS1953-HU-attB4	GGGGACAACTTTGTAT AGAAAAGTTGGATCGT GCCAAAACCGCAGG	F	*whiB7* KO
19	clo-MS1953-HU-attB1	GGGGACTGCTTTTTTG TACAAACTTGGTGTTT TTCCCCCTGCATCT	R	*whiB7* KO
20	clo-MS1953-HD-attB2	GGGGACAGCTTTCTTG TACAAAGTGGTCGACC GCCCCGTCAACGGA	F	*whiB7* KO
21	clo-MS1953-HD-attB3	GGGGACAACTTTGTAT AATAAAGTTGGGTGGA TTCCCGACCTCGCT	R	*whiB7* KO
22	clo-MS3513-HU-attB4	GGGGACAACTTTGTAT AGAAAAGTTGTTTCCC GACGACATGTTGCG	F	*eis* KO

Table 6.1 continued from previous page

23	clo-MS3513-HU-attB1	GGGGACTGCTTTTTTG TACAAACTTGAGATCT CGAATGTGCCAGAG	R	*eis* KO
24	clo-MS3513-HD-attB2	GGGGACAGCTTTCTTG TACAAAGTGGCGACGT GCTCGGCGGTCTCT	F	*eis* KO
25	clo-MS3513-HD-attB3	GGGGACAACTTTGTAT AATAAAGTTGTGCCTC GTCGAGCACGAGTT	R	*eis* KO
26	clo-MS3513-B3	GGGGACAACTTTGTAT AATAAAGTTGTCAGAA TCCGTATCCCAGCT	R	complementation
27	clo-MS3513-NP-B2	GGGGACAGCTTTCTTG TACAAAGTGGGAGAC CACCGGCTGGCAGCA	F	complementation
28	clo-NP-MS1953-800-B2	GGGGACAGCTTTCTTG TACAAAGTGGACGCGG CACTGTCCACCCCG	F	complementation
29	clo-MS1953-B3	GGGGACAACTTTGTAT AATAAAGTTGTCAGGC GGCGGCCGGGTTGC	R	complementation
30	seq-zeoR-1	GGCCTACTGTCCTCGT TGATCC	F	sequencing
31	seq-pUC-1	TGCGGCATCAGAGCA GATTG	F	sequencing
32	seq-pUC-2	TTCCGGCTCGTATGTT GTG	F	sequencing
33	verif-MS1953-F	TCACGGACACCACGC TGATG	F	*whiB7* KO verification
34	verif-MS1953-R	GCATCCCGGAAACTT CATGC	R	*whiB7* KO verification
35	verif-MS1953-mid-F	TGACATGCGAGACG CGACTG	F	*whiB7* KO verification
36	verif-MS1953-mid-R	GTTGCCGCCGGAATC CTTAC	R	*whiB7* KO verification
37	verif-MS3513-F	CCTCACGGGAACATT CTTGG	F	*eis* KO verification
38	veriif-MS3513-R	AACCACATCGGCTGC AACTC	R	*eis* KO verification
39	verif-MS3513-mid-F	CGAACCCGAACAGAC ACAGG	F	*eis* KO verification

Table 6.1 continued from previous page

40	verif-MS3513-mid-R	TGATGCGGATCCACA AATCG	R	*eis* KO verification
41	Verif_hygR_R	TCCTGGTCGTTCCGCA GGCTC	R	hyg cassette verification
42	Verif_hygR_F	TGAAAGGCCCTGGCA TCCTC	F	hyg cassette verification
43	Verif_hygR_R	TCCTGGTCGTTCCGCA GGCTC	R	hyg cassette verification
44	Verif_hygR_F	TGAAAGGCCCTGGCA TCCTC	F	hyg cassette verification
45	Verif-KO-R	GTACAATCTGCTCTCT GATGCC	R	hyg/zeo cassette verification
46	Verif-KO-F	CGAGCCGGAAGCATA AAGT	F	hyg/zeo cassette verification
47	qPCR_MS3906_F	ACACCCATCGCGGCA TCATC	R	qPCR *mstrmI*
48	qPCR_MS3906_R	GCCGCAACACCAGGA ACT	F	qPCR *mstrmI*
49	qPCR_MSsigA_F	ATGGCGTTCCTCGACC TCATC	F	qPCR *sigA*
50	qPCR_MSsigA_R	GCCCTTGGTGTAGTCG AACTTCT	R	qPCR *sigA*
51	clo-Rv2118cHU-B4_F	GGGGACAACTTTGTAT AGAAAAGTTGGGCGG CGCCTTGCCAGTCTTG	F	Rv2118c KO
52	clo-Rv2118cHU-B1_R	GGGGACTGCTTTTTTG TACAAACTTGACGTTC GCCGATGCTGAATG	R	Rv2118c KO
53	clo-Rv2118cHD-B2_F	GGGGACAGCTTTCTTG TACAAAGTGGCTAGGT CGTAAGCGCGAGGG	F	Rv2118c KO
54	clo-Rv2118cHD-B3_R	GGGGACAACTTTGTAT AATAAAGTTGACCCGA AGCCCTGATCGATG	R	Rv2118c KO
55	Oligo-Rv2118cHU-F	ACGTCAATGCGGTCGA TGTAG	F	Rv2118c KO
56	Oligo-Rv2118cHD-R	ACTGCGTGACGGGAG CTACTTG	R	Rv2118c KO
57	Verif_Rv2118c_F	GGCCGTCGGCCAGAT AGATG	F	Rv2118c KO verification
58	Verif_Rv2118c_R	GATGCGCCGAAACAT CCGTG	R	Rv2118c KO verification

Table 6.1 continued from previous page

59	Verif_midRv2118c_F	AAGATGCGGCCCAGA TCGTG	F	Rv2118c KO verification
60	Verif_midRv2118c_R	TGACGACCAGTCGCC AGTTG	R	Rv2118c KO verification
61	attB2_NP_Rv2118c_F	GGGGACAGCTTTCTTG TACAAAGTGGGAAACC GGTATAGCAGCGGGC ATT	F	complementation
62	attB3_Rv2118c_R	GGGGACAACTTTGTAT AATAAAGTTGCTACCC GTCGCGTCCCTCGCG	R	complementation
63	G128A_F	GCCCTGAGGCCAGCGT GACGTCCTAC	F	internal primers for overlap extension mutagenesis
64	G128A_R	GTAGGACGTCACGCTG GCCTCAGGG	R	internal primers for overlap extension mutagenesis
65	G128D_F	CCCTGAGGACAGCGTG ACGTCCTAC	F	internal primers for overlap extension mutagenesis
66	G128D_R	GTAGGACGTCACGCTG TCCTCAGGG	R	internal primers for overlap extension mutagenesis
67	attB2_NP_MS2656_F	GGGGACAGCTTTCTTG TACAAAGTGGCGACAG TTCACGGTTTGCGTCGA GAATG	F	complementation
68	attB2_SD1a_MS2656_F	GGGGACAGCTTTCTTGT ACAAAGTGGATCCAGG AGGTATCTCCATGTCTG TAGTCGAACTTGAAGA	F	complementation
69	attB3_MS2656_R	GGGGACAACTTTGTATA ATAAAGTTGTCAGGCCT CGGCCGGCGTGACATCG	R	complementation
70	seq_MS2656_F_1	AAAGAGGCCACTGGAC	F	pnpase sequencing
71	seq_MS2656_F_2	TCATCAAGGCGCTGTG	F	pnpase sequencing
72	seq_MS2656_F_3	CGGGACCAAGGACTTC	F	pnpase sequencing
73	seq_MS2656_R_1	CAGCGCCTTGATGAAC	R	pnpase sequencing
74	seq_MS2656_R_2	CACCGGCGAGCACCTG	R	pnpase sequencing

Table 6.1 continued from previous page

75	attB2_NP_MS1712	GGGGACAGCTTTCTTGT ACAAAGTGGGAAATCC ACGCCGATGACGTACTT CGG	F	complementation
76	B2_SD1a_MS1712_F	GGGGACAGCTTTCTTGT ACAAAGTGGATCCAGG AGGTATCTCCGTGAGG AAGATGTTTGCTGCGG CGATCGG	F	complementation
77	attB3_MS1712_R	GGGGACAACTTTGTATA ATAAAGTTGTCAGTACT GACGGTTCGGCAGAGC	R	sequencing
78	seq_MS1712_F	CCGAAATCCACGCCGAT GAC	F	sequencing
79	seq_MS1712_R	GCGCTCCCACCCTCCG	R	sequencing
80	sgRNA_smpB_2_F	AGGGACGATCCCGGCC TCGTAGGTGT	F	CRISPRi sgRNA smpB
81	sgRNA_smpB_2_R	AAACACACCTACGAGG CCGGGATCGT	R	CRISPRi sgRNA smpB
82	qPCR_smpB_F	CGCAAGCAGATCGACA ACCT	F	qPCR *smpB*
83	qPCR_smpB_R	TTGCCGTCGGTGAAGT AGA	R	qPCR *smpB*
84	clo_MS2656_HD_B2_F	GGGGACAGCTTTCTTG TACAAAGTGGGCGCTG CCGCCGATGTCACG	F	*pnpase* KO
85	clo_MS2656_HD_B3_R	GGGGACAACTTTGTAT AATAAAGTTGCCGGCG TGTAGCGCCGGACGTGG	R	*pnpase* KO
86	clo_MS2656_HU_B1_R	GGGGACTGCTTTTTTGT ACAAACTTGTCGTACAC ACCGTCTTCAAGT	R	*pnpase* KO
87	clo_MS2656_HU_B4_F	GGGGACAACTTTGTATA GAAAAGTTGGATGCATG AATGTCGACCCGG	F	*pnpase* KO
88	rec_oligo_MS2656_F	GCACCGGCAACGGGTC ACAGAG	F	*pnpase* KO final oligo
89	rec_oligo_MS2656_R	TCCGAGATGGACTCGA TACTG	R	*pnpase* KO final oligo
90	clo_*yrlAB*_HU_B4_F	GGGGACAACTTTGTAT AGAAAAGTTGCCCGAA TCGGCGTCGCGGACC	F	*yrlAB* KO

Table 6.1 continued from previous page

91	clo_*yrlAB*_HU_B1_R	GGGGACTGCTTTTTTGT ACAAACTTGAACCGATC GACGTCCGGCTCAC	R	*yrlAB* KO
92	clo_*yrlAB*_HD_B2_F	GGGGACAGCTTTCTTGT ACAAAGTGGCCGGTTGG CACCTCACACGCTC	F	*yrlAB* KO
93	clo_*yrlAB*_HD_B3_R	GGGGACAACTTTGTATA ATAAAGTTGTGCTCGAC GTAACCGGCGAAC	R	*yrlAB* KO
94	clo_*rsr*_HD_attB2_F	GGGGACAGCTTTCTTGT ACAAAGTGGCCGACTCT GCTCGCCGATTTC	F	*rsr* KO
95	clo_*rsr*_HD_attB3_R	GGGGACAACTTTGTATA ATAAAGTTGGGTGCCGG AGTGCCGCTCGTC	R	*rsr* KO
96	clo_*rsr*_HU_attB1_R	GGGGACTGCTTTTTTGTA CAAACTTGTGCGGCGTCT GACGCAGGCGAA	R	*rsr* KO
97	clo_*rsr*_HU_attB4_F	GGGGACAACTTTGTATAG AAAAGTTGCGTGCCGGCC ATGCGTGATTG	F	*rsr* KO
98	rec_oligo_*rsr*_F	TGCCGATAAATCGGTAG CG	F	*rsr* KO final oligo
99	rec_oligo_*rsr*_R	CCGCCGTGGCGGCTGCA GG	R	*rsr* KO final oligo
100	rec_oligo_*yrlAB*_F	TCACCTCCGCGGGCGCG AC	F	*yrlAB* KO final oligo
101	rec_oligo_*yrlAB*_R	CAGCGCGGCCAGCGCGG CAC	R	*yrlAB* KO final oligo
102	attB2_NP_*yrlAB*_F	GGGGACAGCTTTCTTGTA CAAAGTGGTAGCGCAGC AAATCCC	F	complementation
103	attB2_SD1a_*rsr*_F	GGGGACAGCTTTCTTGTA CAAAGTGGATCCAGGAG GTATCTCCGTGGACATCC TCAAGACC	F	complementation
104	attB2_SD1a_*yrlAB*_F	GGGGACAGCTTTCTTGTA CAAAGTGGATCCAGGAG GTATCTCCCGCTTGGTGA TGTGAG	F	complementation

Table 6.1 continued from previous page

105	attB3_*rsr*_R	GGGGACAACTTTGTATAA TAAAGTTGCTAGATGTCG CCGCGTGAG	R	complementation
106	attB3_*yrlAB*_R	GGGGACAACTTTGTATAA TAAAGTTGCAGGGGCCG CGAGCGTGTGAG	R	complementation
107	seq_*rsr*_F	TGTTCGCCGGTTACGTC	F	sequencing
108	seq_*rsr*_R	CCAGCCGCAGCATGTC	R	sequencing
109	qPCR_MS2656_F_2	GCGCAACGAGATCCAG GT	F	qPCR *pnpase*
110	qPCR_MS2656_R_2	GAGCACGTCGTACAGA TCCT	R	qPCR *pnpase*

Table 6.2: **Bacterial strains used in this study**. Primers ID is based on Table 6.1.

ID	Species	Strain name	Parent ID	Resistance	Primers
1	*Msm*	mc2155 (WT)	-	-	
2	*Msm*	AG	1	-	
3	*Msm*	GS	1	-	
4	*Msm*	AG::NP *mstrmI*	2	STREP	4, 6
5	*Msm*	AG::TetON *mstrmI*	2	STREP	5, 6
6	*Msm*	GS::NP *mstrmI*	3	STREP	4, 6
7	*Msm*	GS::TetON *mstrmI*	3	STREP	5, 6
8	*Msm*	WT::TetON G128S *mstrmI*	1	STREP	5, 6, 7, 8
9	*Msm*	AG::TetON *mstrmI*-HA	2	STREP	4, 17
10	*Msm*	GS::TetON *mstrmI*-HA	3	STREP	4, 17
11	*Msm*	AG::TetON G128S *mstrmI*-HA	2	STREP	4, 17, 7, 8
12	*Msm*	AG::TetON G128A *mstrmI*-HA	2	STREP	4, 17, 63, 64
13	*Msm*	AG::TetON G128D *mstrmI*-HA	2	STREP	4, 17, 65, 66
14	*Msm*	GS::TetON G128S *mstrmI*-HA	3	STREP	4, 17
15	*Msm*	GS::TetON G128A *mstrmI*-HA	3	STREP	4, 17, 63, 64
16	*Msm*	GS::TetON G128D *mstrmI*-HA	3	STREP	4, 17, 65, 66
17	*Msm*	Δ*mstrmI_pnpase*A167D	1	HYG	9, 10, 11, 12, 13,14, 15, 16
18	*Msm*	Δ*mstrmI_pnpase*A167D ::TetON *mstrmI*	17	HYG, STREP	5, 6
19	*Msm*	Δ*mstrmI_pnpase*A167D ::TetON *pnpase*	17	HYG, ZEO	68, 69
20	*Msm*	Δ*mstrmI_pnpase*A167D ::NP *pnpase*	17	HYG, ZEO	67, 69
21	*Msm*	Δ*mstrmI_pnpase*A167D ::TetON *MSMEG_1712*	17	HYG, ZEO	75, 77
22	*Msm*	Δ*mstrmI_pnpase*A167D ::NP *MSMEG_1712*	17	HYG, ZEO	76, 77
23	*Msm*	WT::NP *MSMEG_1712*	1	ZEO	76, 77
24	*Msm*	WT::NP *pnpase*	1	ZEO	67, 69
25	*Msm*	Δ*mstrmI_pnpase*A167D ::NP *pnpase*::NP *mstrmI*	17	HYG, ZEO, STREP	67, 69, 4, 6
26	*Msm*	Δ*mstrmI_pnpase*delNP	1	HYG	9, 10, 11, 12, 13, 14, 15, 16
27	*Msm*	Δ*mstrmI_pnpase*delNP ::NP *pnpase*	26	HYG, ZEO	67, 69
28	*Msm*	Δ*mstrmI_pnpase*delNP ::NP *pnpase*::NP *mstrmI*	26	HYG, ZEO, STREP	67, 69, 4, 6
29	*Msm*	WT::TetON *pnpase*	1	ZEO	68, 69

Table 6.2 continued from previous page

30	*Msm*	Δ*pnpase*::TetON *pnpase*	1	HYG, ZEO	68, 69
31	*Msm*	AG::TetON *pnpase*	2	ZEO	68, 69
32	*Msm*	AG Δ*pnpase*::TetON *pnpase*	31	HYG, ZEO	68, 69
33	*Mtb*	H37Rv (WT)	-	-	-
34	*Mtb*	ΔmttrmI (Rv2118c)	33	HYG	51, 52, 53, 54, 55, 56, 57, 58, 59, 60
35	*Mtb*	ΔmttrmI::NP mttrmI	33	HYG, STREP	61, 62
36	*Msm*	Δ*whiB7*	1	HYG	18, 19, 20, 21
37	*Msm*	AG Δ*whiB7*	2	ZEO	18, 19, 20, 21
38	*Msm*	GS Δ*whiB7*	3	ZEO	18, 19, 20, 21
39	*Msm*	Δ*whiB7*::NP *whiB7*	36	HYG, STREP	28, 29
40	*Msm*	AG Δ*whiB7*::NP *whiB7*	37	ZEO, STREP	28, 29
41	*Msm*	GS Δ*whiB7*::NP *whiB7*	38	ZEO, STREP	28, 29
42	*Msm*	AG Δ*eis*	2	ZEO	22, 23, 24, 25
43	*Msm*	GS Δ*eis*	3	ZEO	22, 23, 24, 25
44	*Msm*	AG Δ*eis*::NP *eis*	42	ZEO, STREP	26, 27
45	*Msm*	GS Δ*eis*::NP *eis*	43	ZEO, STREP	26, 27
46	*Msm*	WT::NP *whiB7*	1	STREP	28, 29
47	*Msm*	WT::NP *eis*	1	STREP	26, 27
48	*Msm*	Δ*rsr*	1	ZEO	93, 94, 95, 96, 97, 98, 99
49	*Msm*	Δ*yrlAB*	1	ZEO	90, 91, 92, 93, 94,100, 101
50	*Msm*	Δ*rsr*::TetON *rsr*	48	ZEO, STREP	103, 105
51	*Msm*	Δ*yrlAB*::TetON *yrlAB*	49	ZEO, STREP	104, 106
52	*Msm*	AG Δ*rsr*	2	ZEO	93, 94, 95, 96, 97, 98, 99
53	*Msm*	AG Δ*yrlAB*	2	ZEO	90, 91, 92, 93, 94, 100, 101
54	*Msm*	AG Δ*rsr*::TetON *rsr*	52	ZEO, STREP	103, 105
55	*Msm*	AG Δ*yrlAB*::TetON *yrlAB*	53	ZEO, STREP	104, 106
56	*Msm*	WT::TetON *rsr*	1	STREP	103, 105
57	*Msm*	WT::TetON *yrlAB*	1	STREP	104, 106
58	*Msm*	WT smpBKD	1	KAN	80, 81
59	*Msm*	AG smpBKD	2	KAN	80, 81
60	*Msm*	Δ*whiB7*::NP uORF *whiB7* GCG>GCC	36	HYG, STREP	28, 29
61	*Msm*	Δ*whiB7*::NP uORF *whiB7* GCG>GCA	36	HYG, STREP	28, 29
62	*Msm*	Δ*whiB7*::NP uORF *whiB7* GCG>CAC	36	HYG, STREP	28, 29

Table 6.2 continued from previous page

63	*Msm*	AG Δ*whiB7*::NP uORF *whiB7* GCG>GCC	40	ZEO, STREP	28, 29
64	*Msm*	AG Δ*whiB7*::NP uORF *whiB7* GCG>GCA	40	ZEO, STREP	28, 29
65	*Msm*	AG Δ*whiB7*::NP uORF *whiB7* GCG>CAC	40	ZEO, STREP	28, 29

Table 6.3: **Plasmids used in this study.** Z=zeocin, S=streptomycin, H=hygromycin, K=kanamycin.

ID	Plasmid abbreviation	Plasmid name	R	Purpose
1	NP *mstrmI*	pGMCS T02 AgeI NP *mstrmI*	S	*mstrmI* complementation
2	TetON *mstrmI*	pGMCS T10MP1 SD1a *mstrmI*	S	*mstrmI* complementation
3	TetON G128S *mstrmI*	pGMCS T10MP1 SD1a G128S *mstrmI*	S	*mstrmI* complementation
4	TetON *mstrmI*-HA	pGMCS T10MP1 SD1a *mstrmI*-HA	S	pull down of *mstrmI*
5	TetON G128S *mstrmI*-HA	pGMCS T10MP1 SD1a G128S *mstrmI*-HA	S	G128S *mstrmI* expression
6	TetON G128A *mstrmI*-HA	pGMCS T10MP1 SD1a G128A *mstrmI*-HA	S	G128A *mstrmI* expression
7	TetON G128D *mstrmI*-HA	pGMCS T10MP1 SD1a G128D *mstrmI*-HA	S	G128D *mstrmI* expression
8	TetON pnpase	pGMCgZ T10MP1 SD1a pnpase	Z	pnpase complementation
9	NP pnpase	pGMCgZ T02 AgeI NP pnpase	Z	pnpase complementation
10	TetOn *MSMEG_1712*	pGMCgZ T10MP1 SD1a *MSMEG_1712*	Z	*MSMEG_1712* expression
11	NP *MSMEG_1712*	pGMCgZ T02 AgeI NP *MSMEG_1712*	Z	*MSMEG_1712* expression
12	NP mttrmI	pGMCS T02 AgeI NP mttrmI	S	mttrmI complementation
13	NP *whiB7*	pGMCS T02 AgeI NP *whiB7*	S	*whiB7* complementation
14	NP *eis*	pGMCS T02 AgeI NP *eis*	S	*eis* complementation
15	TetON rsr	pGMCS T10MP1 SD1a rsr	S	rsr complementation
16	TetON yrlAB	pGMCS T10MP1 SD1a yrlAB	S	yrlAB complementation
17	TetON yrlAB rsr	pGMCS T10MP1 SD1a yrlAB rsr	S	yrlAB rsr complementation
18	/	pXSTS HU Hyg HD *mstrmI*	S, H	KO *mstrmI*
19	/	pXSTS HU Hyg HD *whiB7*	S, H	KO *whiB7*

Table 6.3 continued from previous page

ID	Plasmid abbreviation	Plasmid name	R	Purpose
20	/	pXSTS HU Zeo HD *whiB7*	S, Z	KO *whiB7*
21	/	pXSTS HU Zeo HD *eis*	S, Z	KO *eis*
22	/	pGMCgS HU Hyg HD rsr	S, H	KO rsr
23	/	pGMCgS HU Hyg HD yrlAB	S, H	KO yrlAB
24	/	pLJR962	K	empty plasmid for KD
25	*smpBKD*	pLJR962 smpB	K	KD smpB
26	P*whiB7*_mScarlet	pGMCgZ T02 AgeI *whiB7*_uORF mScarlet	Z	measure *whiB7* activity

B *Mtb* clinical isolates harbour mutations in *mttrmI*

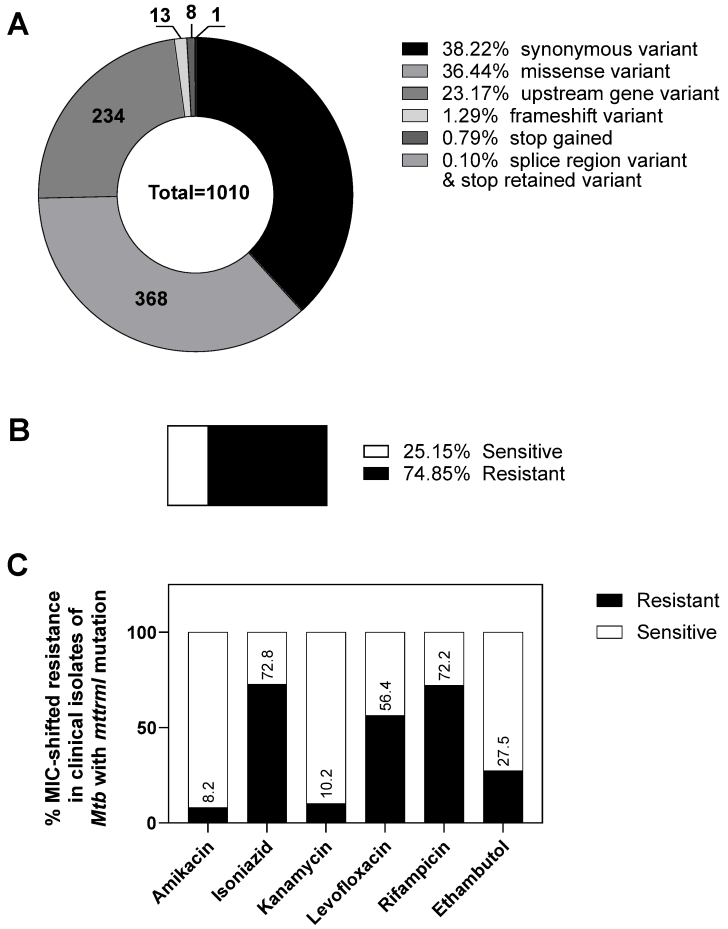


Figure 6.1: **Mutations in *mttrmI* are found in *Mtb* clinical isolates.** Data from (Crook et al., 2022) were analysed for mutations in *Rv2118c*, encoding an MtTrmI. The graphs indicate (A) the types and percentages of the mutations found within *Rv2118c*, (B) the percentage of sensitive or resistant isolates, and (C) the percentages of resistant strains with resistance to indicated antibiotics.